FRAGMENT-BASED APPROACHES TO TARGETING

ETHR FROM MYCOBACTERIUM TUBERCULOSIS

by

Brendan Neil McConnell

Wolfson College

University of Cambridge

*This dissertation is submitted to the University of Cambridge in partial fulfilment of requirements for the degree of **Doctor of Philosophy***

August 2018

This dissertation is the result of my own work and includes nothing which is the outcome of work done in collaboration except as declared in the Preface and specified in the text.

It is not substantially the same as any that I have submitted, or, is being concurrently submitted for a degree or diploma or other qualification at the University of Cambridge or any other University or similar institution except as declared in the Preface and specified in the text. I further state that no substantial part of my dissertation has already been submitted, or, is being concurrently submitted for any such degree, diploma or other qualification at the University of Cambridge or any other University of similar institution except as declared in the Preface and specified in the text.

It does not exceed the prescribed word limit for the relevant Degree Committee.

28 January 2019

Brendan Neil McConnell   Date

To my family, who have supported me throughout this work and in my decision to travel so far to accomplish my dream.

Look up at the stars and not down at your feet.
Try to make sense of what you see,
and wonder about what makes the universe exist.
Be curious.

– Professor Stephen Hawking

Abstract

Tuberculosis affects millions of people worldwide every year. The current treatment for TB is divided into a regimen of both first- and second-line drugs, where first-line treatments are more tolerated and require shorter treatment lengths. With rising levels of resistance, alternative treatment regimes are urgently needed to fight this disease.

Ethionamide, a second-line drug is administered as a prodrug which is activated *in vivo* by the enzyme EthA, which is in turn regulated by EthR. The disruption of the action of EthR could lead to novel therapeutics which could enhance the efficacy of ethionamide, and raise it to a first-line treatment.

The work reported in this thesis examines the elaboration of three chemical scaffolds using fragment-based approaches to develop novel inhibitors capable of disrupting the EthR-DNA interaction. The first scaffold, 5-(furan-2-yl)isoxazole was investigated by fragment-merging approaches and produced compounds with the best of these having a K_D of 7.4 μM. The second scaffold, an aryl sulfone was elaborated using fragment-merging strategies. This led to several modifications of the fragment, leading to several variants with K_Ds around 20 μM. With both of these series the affinity could not be improved below 10 μM and due to the synthetic complexity a further scaffold was prioritised.

The third scaffold was explored was a 4-(4-(trifluoromethyl)phenyl)piperazine using fragment-growing from the NH of the piperazine to probe deeper into the EthR binding pocket. In addition to this, SAR around the 4-(trifluoromethyl)phenyl group was assessed to explore the interactions with EthR. These modifications led to compounds with nanomolar IC_{50}s. A range of compounds were then screened by REMAssay to determine the boosting effect on ethionamide, and this identified compounds with up to 30 times boosting in the ethionamide MIC.

The final chapter examines a concept where compounds were designed to exploit the dimeric nature of EthR by linking two chemical warheads with a flexible linker. These compounds are examined using mass spectrometry to investigate the stoichiometry of the interaction to provide insight into the binding of these extended compounds and exploring an alternative strategy to inhibit EthR.

The work in this thesis demonstrated the successful use of fragment-based approaches for development of novel EthR inhibitors which showed significant ethionamide boosting effects.

Acknowledgements

No man is an island, entire of itself   *– John Donne*

Table of Contents

Abbreviations

°C = degree(s) centigrade

Å = angstrom(s)

acetone-d_6 = deuterated acetone

ATR = attenuated total reflectance

Asn = asparagine

BCG = Bacille Calmette-Guerin

BMS = borane dimethylsulfide

bp = base pair

br. = broad

$CDCl_3$ = deuterochloroform

cm^{-1} = per centimeter (equivalent to wavenumber)

COMU = (1-Cyano-2-ethoxy-2-oxoethylidenaminooxy)dimethylamino-morpholino-carbenium hexafluorophosphate

d = doublet

DCM = dichlormethane

DIPEA = diisopropylethylamine

DMAP = 4-dimethylaminopyridine

DMF =N,N'-dimethylformamide

DMSO = dimethylsulfoxide

DMSO-d_6 = hexadeuterated dimethylsulfoxide

dRFU = 1st derivative of response fluorescence units

DSF = differential scanning fluorimetry

EDC = N-(3-dimethylaminopropyl)-N'-ethylcarbodiimide hydrochloride

ETH = ethionamide

FBDD/FBLD = fragment-based drug (lead) design

g = gram(s)

HRMS = high-resolution mass-spectrometry

Hz = hertz

IC_{50} = 50% inhibitory concentration

INH = isoniazid

IR = infrared

ITC = isothermal titration calorimetry

J = coupling constant (NMR)

K_D = dissociation constant

LCMS = liquid-chromatography mass-spectrometry

LE = ligand efficiency

LHMDS = lithium hexamethyldisilylamide / lithium bis(trimethylsilyl)amide

ln = natural logarithm

m = multiplet (NMR)

m = medium (IR)

M = molar

MeCN = acetonitrile

MeCN-d_3 = deuterated acetonitrile

MeOD = deuteromethanol

MES-Na = sodium 2-(morpholino)ethanesulfonate

Met = methionine

mg = milligram(s)

MHz = megahertz

MIC = minimum inhibitory concentration

min = minute(s)

mL = millilitre(s)

mM = millimolar

mmol = millimole(s)

M.tb. = Mycobacterium tuberculosis

N = normal

NMP = N-methyl-2-pyrrolidone

NMR = nuclear magnetic resonance

Phe = phenylalanine

R = gas constant

r.f. = retention factor

r.t. = retention time

REMA = resazurin microtiter assay

RFU = response fluorescence units

RuPhos = 2-Dicyclohexylphosphino-2′,6′-diisopropoxybiphenyl

s = singlet (NMR)

s = strong (IR)

SAR = structure-activity relationship

SPR = surface plasmon resonance

T = temperature (Kelvin)

t = triplet

TB = tuberculosis

TFA = trifluoroacetic acid

Thr = threonine

TLC = thin layer chromatography

T_M = melting (denaturation) temperature

Trp = tryptophan

Tyr = tyrosine

w = weak

X-Phos = 2-Dicyclohexylphosphino-2′,4′,6′-triisopropylbiphenyl

$\Delta G_{binding}$ = change in Gibbs free energy upon binding

ΔT_M = change in melting temperature

δ ppm = shift in parts per million from tetramethylsilane (NMR)

λ = wavelength

μL = microliter(s)

μM = micromolar

= number

1.0 Introduction

1.1 Tuberculosis

Despite worldwide efforts, tuberculosis (TB) remains a major public health concern and "a leading cause of death worldwide".[1-3] Known since ancient times,[2,4-6] tuberculosis is caused by the bacterium *Mycobacterium tuberculosis* (*M.tb.*).[5,7-10] Currently, the preferred preventative method for TB is performed using the Bacillus Calmette-Guerin vaccine (BCG). This was identified in the early 20th century by the French scientists Albert Calmette and Camille Guerin and first administered in 1921.[2,6] This live, attenuated strain of *Mycobacterium bovis* [5,7,11] provides some resistance to *M.tb.*, although the effect can be variable.[4,5,7]

Tuberculosis is acquired primarily by inhalation of bacilli, aspirated from an infected patient, which lodge in the upper respiratory tract [10,12,13] and here, they invade the macrophages.[2,4,13] While the lungs remain the most prominent locale, *M.tb.* can infect almost any organ or joint in the body, including the spine, brain, and heart,[7,12,14] and can activate or reactivate months or years after the initial infection.[4,5,9,13]

It is believed that around one-third of the world's population carry the bacterium,[10,12,15,16] with over 90% of infected individuals asymptomatic carriers of latent infection.[7,11-13] The remaining 10% who develop active TB show a wide range of symptoms, ranging from fever, headache, malaise or cough to blindness, paraplegia, coma or death.[11,12,14,15] The World Health Organisation (WHO) estimates that 1.8 million people died as a result of tuberculosis in 2015, although the number of annual fatalities is gradually decreasing.[1]

Treatment for tuberculosis generally uses a combination of several drugs, which include the first-line drugs isoniazid **1**, rifampicin **2**, pyrazinamide **3**, ethambutol **4** and streptomycin **5** (Figure 1), in two phases of treatment.[7-9,14,17] These treatment regimens typically run for six to twelve months, and are well tolerated.[1,14] Unfortunately, due to low patient compliance and poor completion of the treatment courses, drug-resistant strains have developed, and these continue to be a major impediment to treatments.[13,18-20] Where resistance is found against both rifampicin and isoniazid, the infection is classified as multiple-drug-resistant TB (MDR-TB).[1,6] Management of this form of infection requires further treatment with second-line drugs, which include ethionamide **6**, cycloserine **7**, fluoroquinolones (e.g. levofloxacin **8**), aminoglycosides (other than streptomycin) and polypeptides (e.g. capreomycin **9**). These drugs are more expensive and less well tolerated than first-line drugs,[17,21,22] and the treatment regimen runs from 20 months to

as long as four years,[1,9,20,23] which further contributes to low compliance and incomplete courses of treatment. Where resistance to a second-line drug is found in addition to isoniazid and rifampicin, the bacterium is considered to be extensively drug-resistant (XDR-TB),[1] and can be extremely difficult to treat.[9]

First-line drugs:
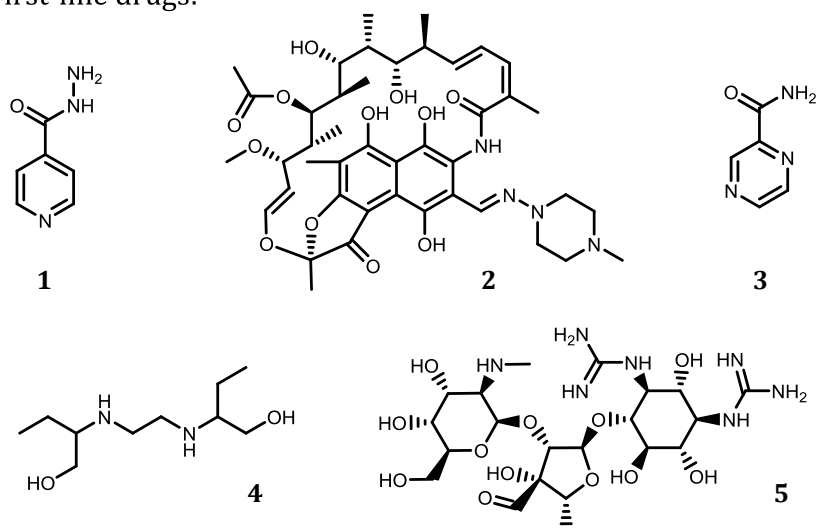
Second-line drugs:
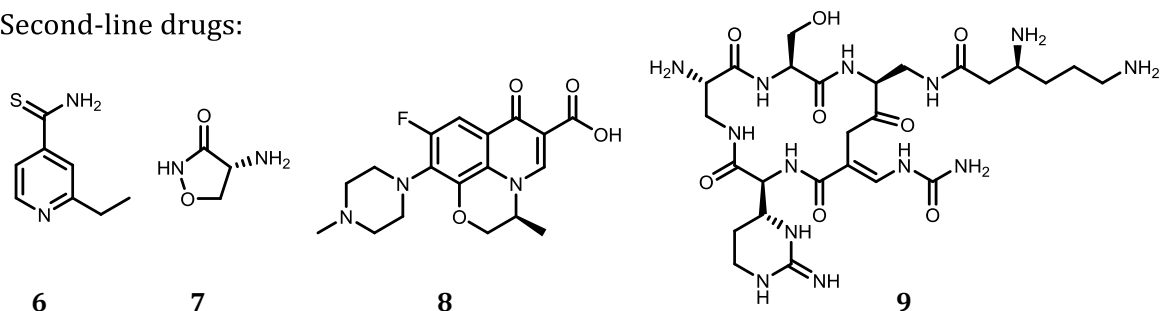
Figure 1: Structures of first and second line TB drugs; Isoniazid **1**, rifampicin **2**, pyrazinamide **3**, ethambutol **4**, streptomycin **5**, ethionamide **6**, cycloserine **7**, levofloxacin **8**, capreomycin **9**.

The emergence of resistant strains of *M.tb.* makes it essential to identify new targets for drug discovery to enhance or replace the current treatment regimens.[8,9,13,24]

1.2   EthR

1.2.1   Cell Wall and Mycolic Acid Biosynthesis

The mycobacterial cell wall in *M.tb.* is composed of five layers (Figure 2). The first is a lipid bilayer to contain the cytosol, which is covered on the extracellular side by a layer of peptidoglycan.[24,25] This is a common feature of many cell types made of a series of alternating sugars, crosslinked by a short peptide sequence.[10,24,25] Although normally consisting of N-acetylglucosamine and N-acetylmuramic acid, in mycobacteria (except *M. leprae*) the N-acetylmuramic acid is replaced by N-glycolylmuramic acid.[10,24,26] These sugars are further crosslinked by a pentapeptide unit.[10,26] Building from the N-glycolylmuramic acid, the pentapeptide sequence consists of L-alanine, D-glutamic acid, meso-diaminopimelic acid (meso-DAP), D-alanine, D-alanine. The crosslinking occurs from the meso-DAP to an adjacent meso-DAP or D-alanine of an adjacent pentapeptide.[10,26]
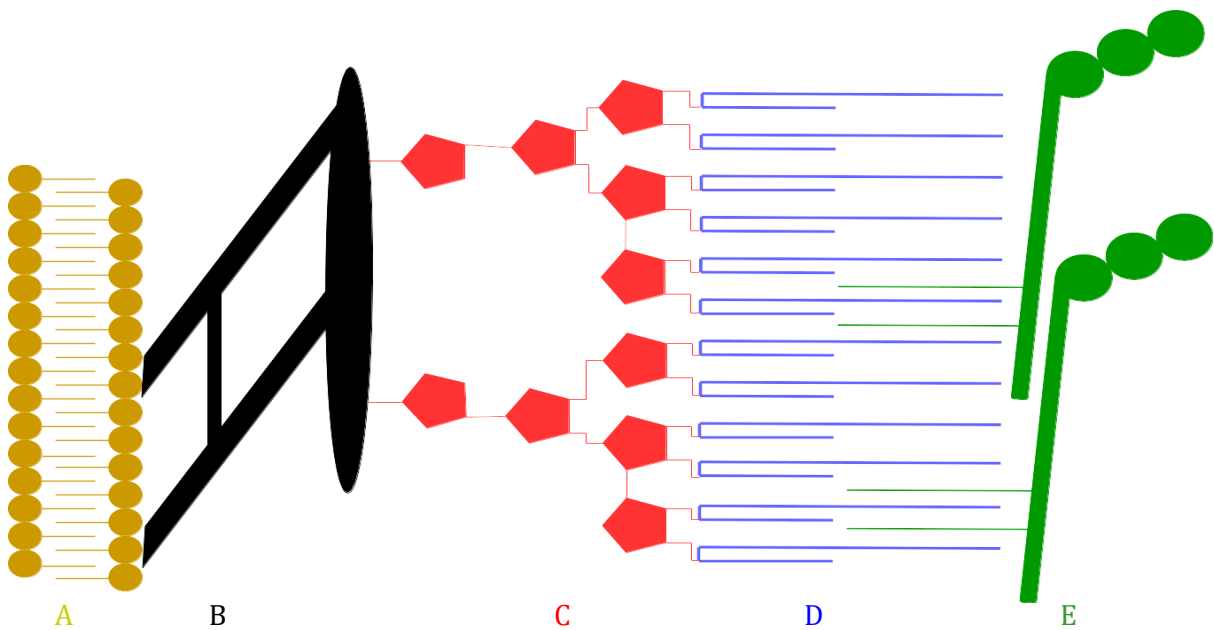
Figure 2: Structure of the mycobacterial cell wall in *M.tb*. A: lipid bilayer. The lipid bilayer contains the cytosol by forming a hydrophobic barrier; B: peptidoglycan. A network of crosslinked peptides capped with a layer of N-acetylglucosamine and N-acetylmuriamic acid; C: arabinogalactan. A series of arabinose and galactose sugars which provide an anchor for the mycolic acids; D: mycolic acids. Waxy esters which influence cell permeability and oxidative stress in mycobacteria; E: mycosides. Outer layer of the mycobacterial cell wall, consisting of peptidoglycolipids and phenolic glycolipid dimycocerates.

Outside this peptidoglycan layer is another sugar layer, formed of arabinogalactan.[10,25] Mycobacteria produce an additional, waxy layer composed primarily of mycolic acids beyond this (Figure 2).[25,27-31] These mycolic acids consist of a β-hydroxy fatty acids of 54-63 carbons attached to another chain of 22-24 carbons in length.[22,27,28,30] The longer of these two chains typically has one of three substitution patterns, termed α-, keto- and methoxymycolates.[27,28,30,31] The keto- and methoxy- forms are both produced as *cis* and *trans* isomers, generating five basic mycolic acids (Figure 3), which are linked to the arabinogalactan layer.[27] Approximately 70% of the mycolic acids present are of the α-type, with a further 10-15% each of the keto- and methoxy- forms.[27] It is believed that these fatty acids are responsible for preventing damage to the bacterium, in addition to regulating permeability.[25,31]
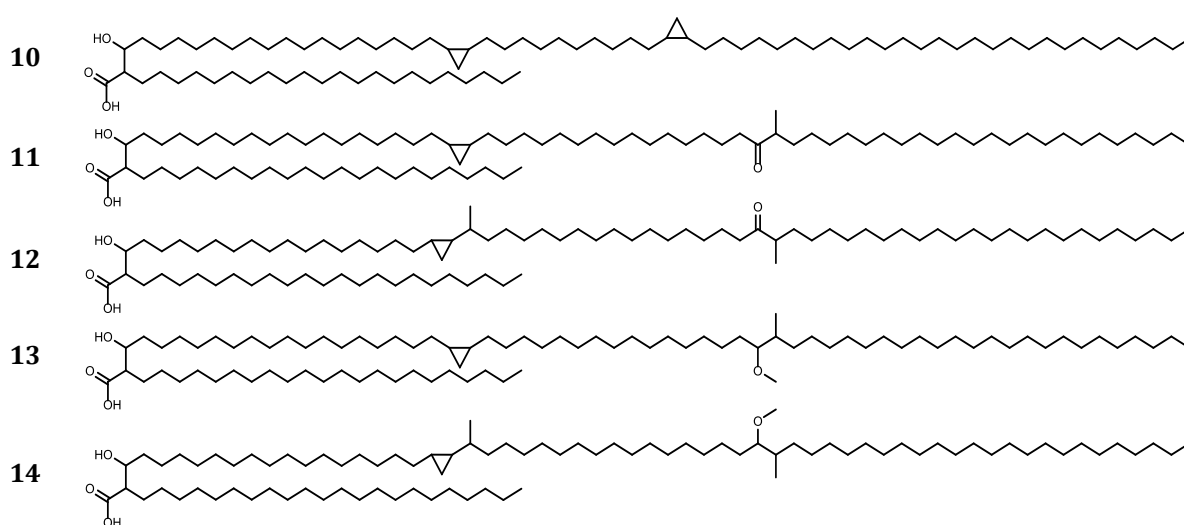
Figure 3: Structure of mycolic acids (from top) α-mycolic acid **10**, keto-(cis)-mycolic acid **11**, keto-(trans)-mycolic acid **12**, methoxy-(cis)-mycolic acid **13**, methoxy-(trans)-mycolic acid **14**.

Beyond this layer resides the final layer of the cell wall, the mycosides (Figure 2).[25] These consist of a series of peptidoglycolipids and phenolic glycolipid dimycocerates.[25]

The mycolic acids are produced in two parts by two biosynthetic pathways; Fatty Acid Synthase I (FAS-I) and Fatty Acid Synthase II (FAS-II). The shorter chain (known as the α-branch) is produced by the FAS-I pathway. In contrast to the FAS-II pathway, FAS-I utilises CoA rather than the acyl carrier protein from mycobacterium (AcpM).[31]
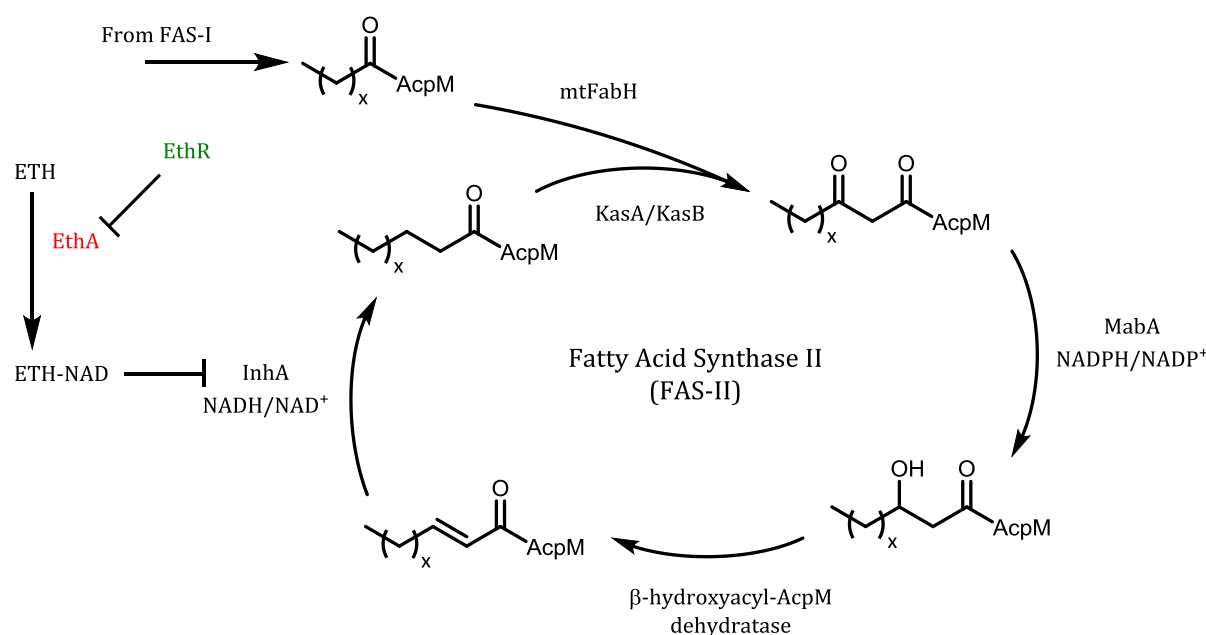
Figure 4: FAS-II cycle in *M.tb*. FAS-II catalyses the extension of shorter fatty acids from FAS-I into the longer meromycolates necessary for mycolic acid production. EthR regulates the expression of EthA, which is responsible for activating ethionamide – an inhibitor of InhA, preventing the successful production of mycolic acids by FAS-II.

The longer chain (meromycolate) is produced by the FAS-II pathway (Figure 4). Part of the meromycolate is produced by the FAS-I cycle and incorporated as the alkyl terminus of the growing meromycolate, as the FAS-II system (unlike FAS-I) is unable to perform de-novo fatty acid synthesis.[31] The CoA ester produced is converted to C_{16}-AcpM by a β-keto AcpM synthase (mtFabH) using malonyl-AcpM as the additional unit to enter the FAS-II cycle. This alkyl-AcpM compound is then elongated by two carbons via the β-ketoacyl AcpM synthase KasA/KasB complex. The ketoacyl intermediate is subsequently reduced by MabA (a β-keto AcpM reductase) with NADPH and dehydrated by β-hydroxyacyl AcpM dehydratase to the enoyl-AcpM compound. This compound is then reduced by InhA (enoyl AcpM reductase), consuming NADH to complete one round of the elongation cycle.[27,28,31] After modification, the two chains (the meromycolate from FAS-II and the α-branch from FAS-I) are condensed by Pks13 (poly-ketide synthase) to form the finished mycolic acid.[28]

1.2.2 ETH and EthA Activity

Ethionamide, like the structurally similar Isoniazid is administered as a prodrug, requiring modification into its active form.[25,32-34] Despite their similarities, these drugs are activated by different enzymes in *M.tb*. Isoniazid is activated by KatG, a catalase/peroxidase, while ethionamide (ETH) is activated by EthA, a Bayer-Villager monooxidase.[29,32,35-37] These different mechanisms of activation for both drugs function by inhibiting the same enzyme – InhA, a member of the FAS-II pathway.[25,29,35]

Ethionamide activation involves a series of intermediates. The initial activating step is recognised to be the oxidation of the thioamide functionality (ETH-SO) **15**,[22] while the active product is thought to be the ETH-NAD adduct **16** (Figure 5).[22,23,33] The exact sequence of intermediates is not known, but it is thought that ETH is oxidised to the amidopyridine[20] or the methanol form,[29] possibly via a radical intermediate.[3,22]
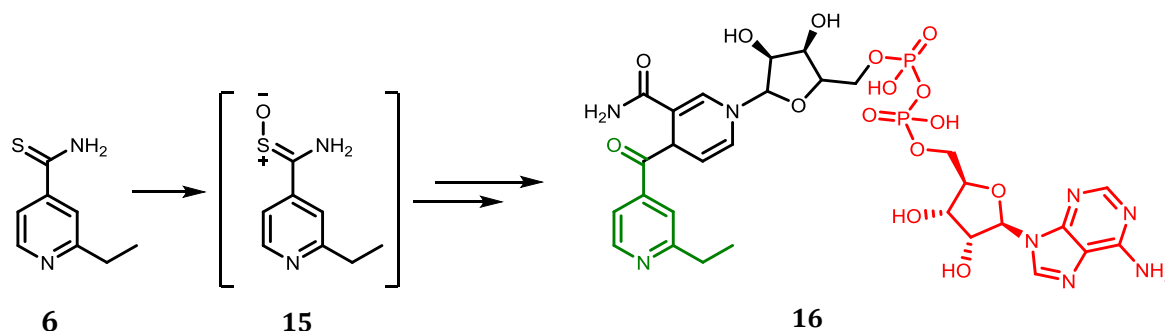
Figure 5: Structures of (L-R) ETH **6**, ETH-SO **15** and ETH-NAD **16**. ETH is initially oxidised to the S-oxide form, which is then converted to the ETH-NAD adduct, which inhibits InhA in the FAS-II pathway, preventing the synthesis of the mycolic acids, which are essential components of the mycobacterial cell wall. No intermediates between the S-oxide and the ETH-NAD adduct have been isolated.

1.2.3 EthR

EthA expression is regulated by the transcriptional repressor EthR which is a 216 amino acid protein of the TetR family.[32-34,37-39] Composed entirely of helices, EthR has two domains, a helix-turn-helix DNA-binding domain, and a ligand-binding domain (Figure 7). In solution, this dimerizes, and is reported to form an octamer[35,37,38] upon binding to its 55 bp operator, situated in the intergenic region between the ethR and ethA genes (Figure 6).[35,37,38] A recent paper by Chan *et al.* (2017) however, indicates that EthR binds to its operator as a hexamer instead.[40]
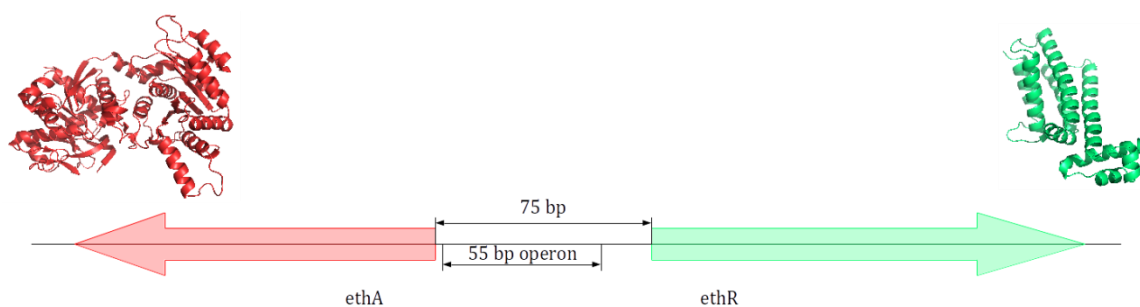
Figure 6: Construction of the ethA-R intergenic region. The ethA and ethR genes are expressed in opposing directions with 75 base pair intergenic region containing the 55 base pair EthR operon between.

EthR has been considered a validated target for some time.[22] Bacteria overexpressing EthR were shown to be hypersensitive for ETH by both DeBarber *et al.*[29] and Baulard *et al.*[41] while examining the activation process for ETH.[22,29,37,41] Meanwhile, EthA knockdown models have proven to be ETH resistant.[36] Despite this, no direct evidence for a natural role for EthA has been forthcoming,[34,36,37] although the present theory is that it plays a role in oxidation of meromycolates or the catabolism of mycolic acids to maintain appropriate levels in the cell wall.[36]
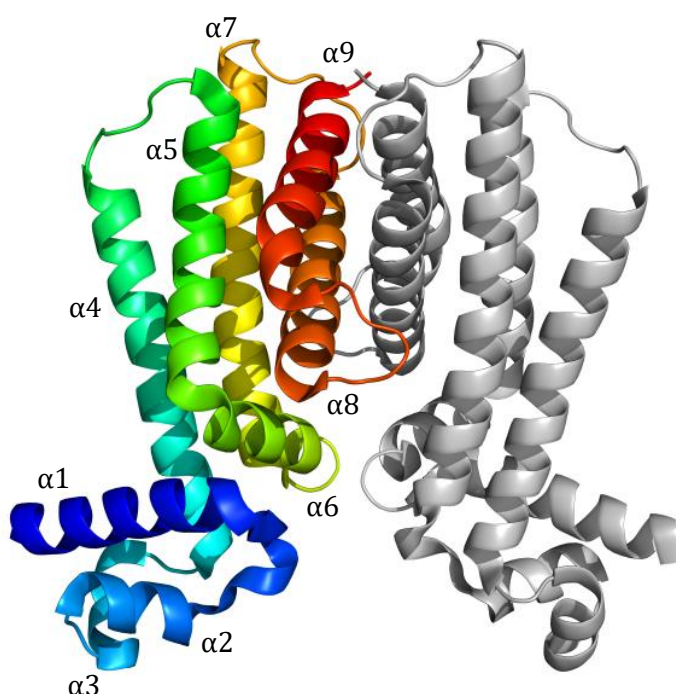
Figure 7: Structure of the EthR dimer (PDB: 1T56). Helices are numbered from the N-C terminal. Helices α1-3 form the helix-turn-helix DNA-binding domain, while helices α4-9 form the drug-binding domain, with helices α8-9 forming the dimerization interface.[35]

The binding domain of EthR (Figure 7) is located between helices 4-9 in an 'L' shape, with the main pocket paralleling helices 4, 5, 7 and 8, while an additional binding region can be observed running parallel to helix α6 under the side chain of Trp138.[32,33,37,42,43] Amino acids lining this pocket are largely hydrophobic, aromatic residues resulting in a long greasy surface available for ligands.[35,37] This is reinforced by the presence of the "natural ligand", hexadecyloctanoate **17**, as reported by Frenois *et al.*[32,43] and Willand *et al.*[44] (Figure 8).
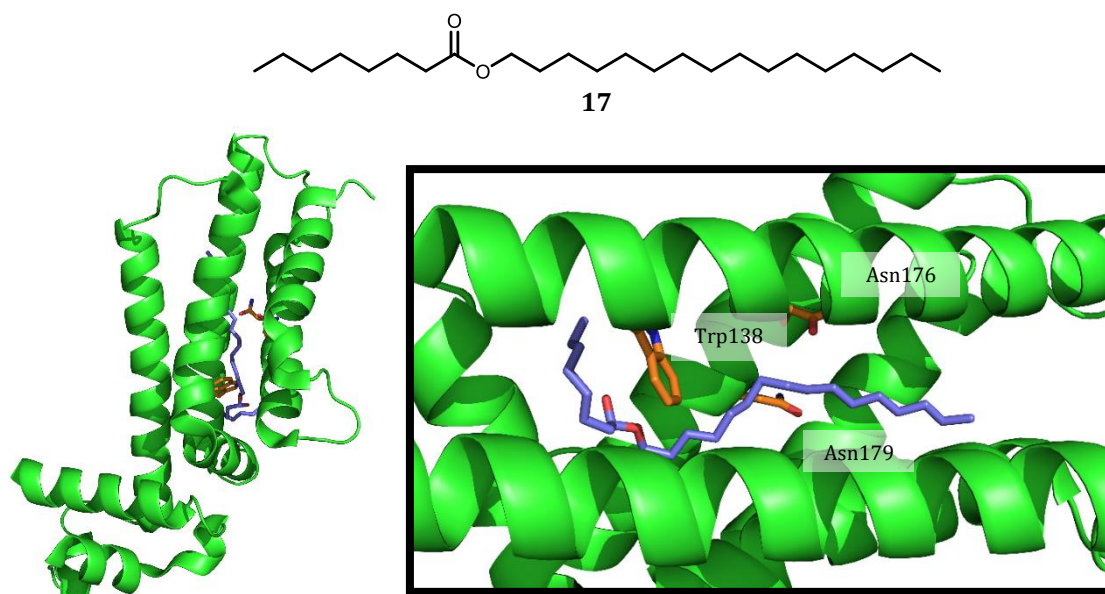
Figure 8: EthR bound to hexadecyloctanoate **17** (purple), with key binding site residues (orange) (only the monomer is shown, PDB: 1U9N).[43]

The binding site of EthR is accessible only by a small opening, situated at the opposing end of the protein to the DNA-binding domain that leads to a pocket of approximately 20 Å in length.[35,37] Within the binding site, several amino acids of interest have been identified. The Trp138 provides a border between the regions of the binding site, forming the 'L' shape, while Asn176 and Asn179 provide a polar region within the centre of the pocket.[16,22,33,39] In addition, two Phe residues have been shown adopt differing orientations (Phe184 and Phe114).[16,22,39]

The distance between the binding domains of the dimer is altered upon binding of the ligand.[32,43] Frenois, Baulard and Villeret have shown that upon binding of the natural ligand, the two binding domains increase in separation from 37 Å to 48-52 Å when compared with

analogous TetR family transcriptional repressors (Figure 9A and Figure 9B), resulting in the loss of DNA binding capability (Figure 9C and Figure 9D).[32,43]
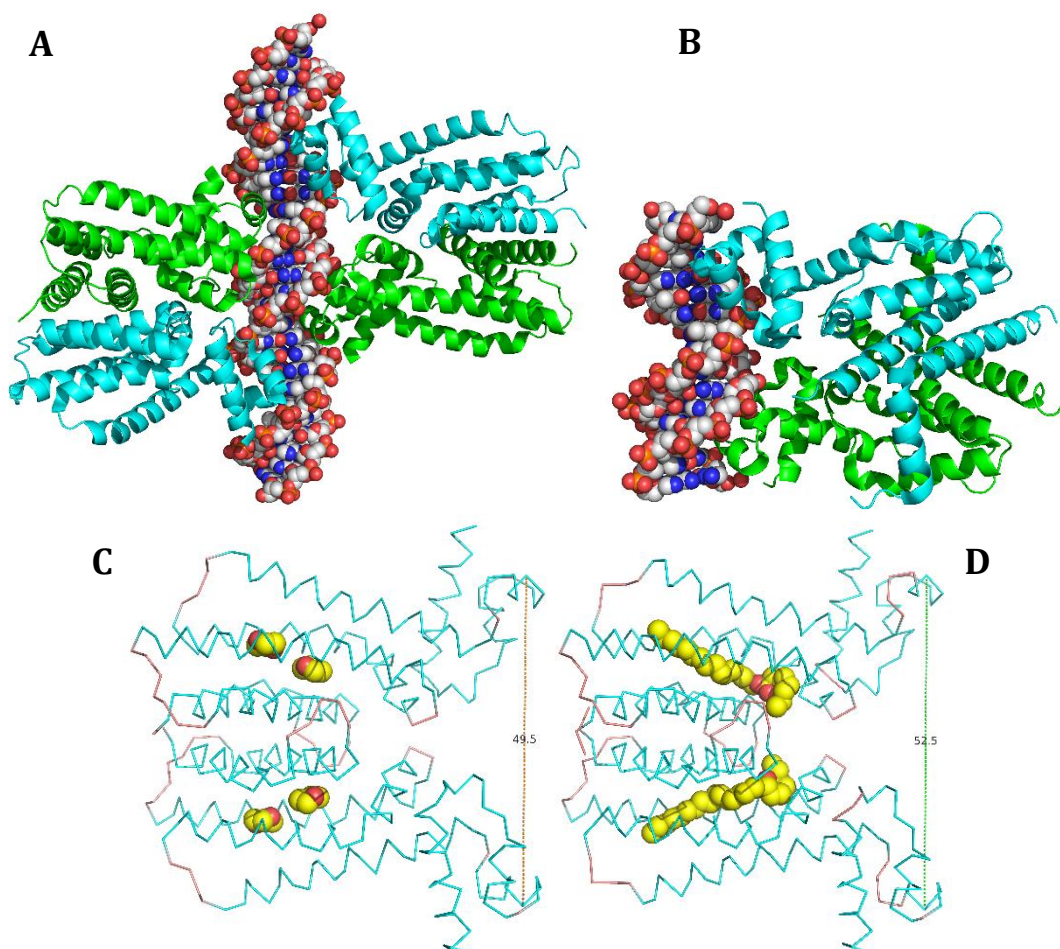
Figure 9: (A) - DNA-bound structures of TetR family member QacR (PDB: 1JT0) 38.7 Å (Gly37Cα-Gly37'Cα); (B) – DNA-bound structure of TetR (PDB: 1QPI) 31.1 Å (Pro39Cα-Pro39'Cα); (C) – DNA binding domain distance for EthR binding dioxane (PDB: 1T56) 49.5 Å (Thr60Cα-Thr60'Cα); (D) – DNA binding domain distance for EthR binding hexadecyloctanoate (PDB: 1U9N) 52.5 Å (Thr60Cα-Thr60'Cα); Figures A and B adapted from Schumacher *et al.* (2002),[45] figures C and D adapted from Willand *et al.* (2009).[44]

1.3   FBDD

1.3.1   *What is FBDD?*

Fragment-based Drug Discovery (FBDD), also known as Fragment-based Lead Discovery (FBLD) is an approach that has gained favour among drug design scientists in both academia and industry.[46] Pioneered by companies such as Astex Pharmaceuticals and Abbott Pharmaceuticals

in the mid-1990s,[47-53] this relies on a cascade of biophysical assays to quantify binding of small molecules (or fragments) to known targets.[53,54]

This method employs screening of libraries of small molecules, typically less than 250 Da molecular weight, and ranging in size from around a few hundred to around 10,000 molecules,[47,51,55-57] to identify molecules which can efficiently bind to target proteins. Many companies are now incorporating fragment-based approaches into their drug discovery programs.[50,58]

To date, there have been three fragment-derived drugs approved for use by the FDA, and there are a number currently in Phase I, II, and III clinical trials.[51,53,54,59] The first drug approved which was derived from a fragment-based approach was Vemurafenib, developed by Plexxicon and Roche to treat advanced skin cancers.[46,60] The initial fragment hit 7-azaindole **18**, showed an IC_{50} >200 μM against the PIM1 (used as a surrogate for B-Raf),[61] and this fragment was developed into the final drug **23**, which exhibited an IC_{50} of 0.031 μM against the target B-Raf^{V600E} (Figure 10).[51,60-64] The FDA approved Vemurafenib in August 2011,[60] taking just six years from the start of development.[51]
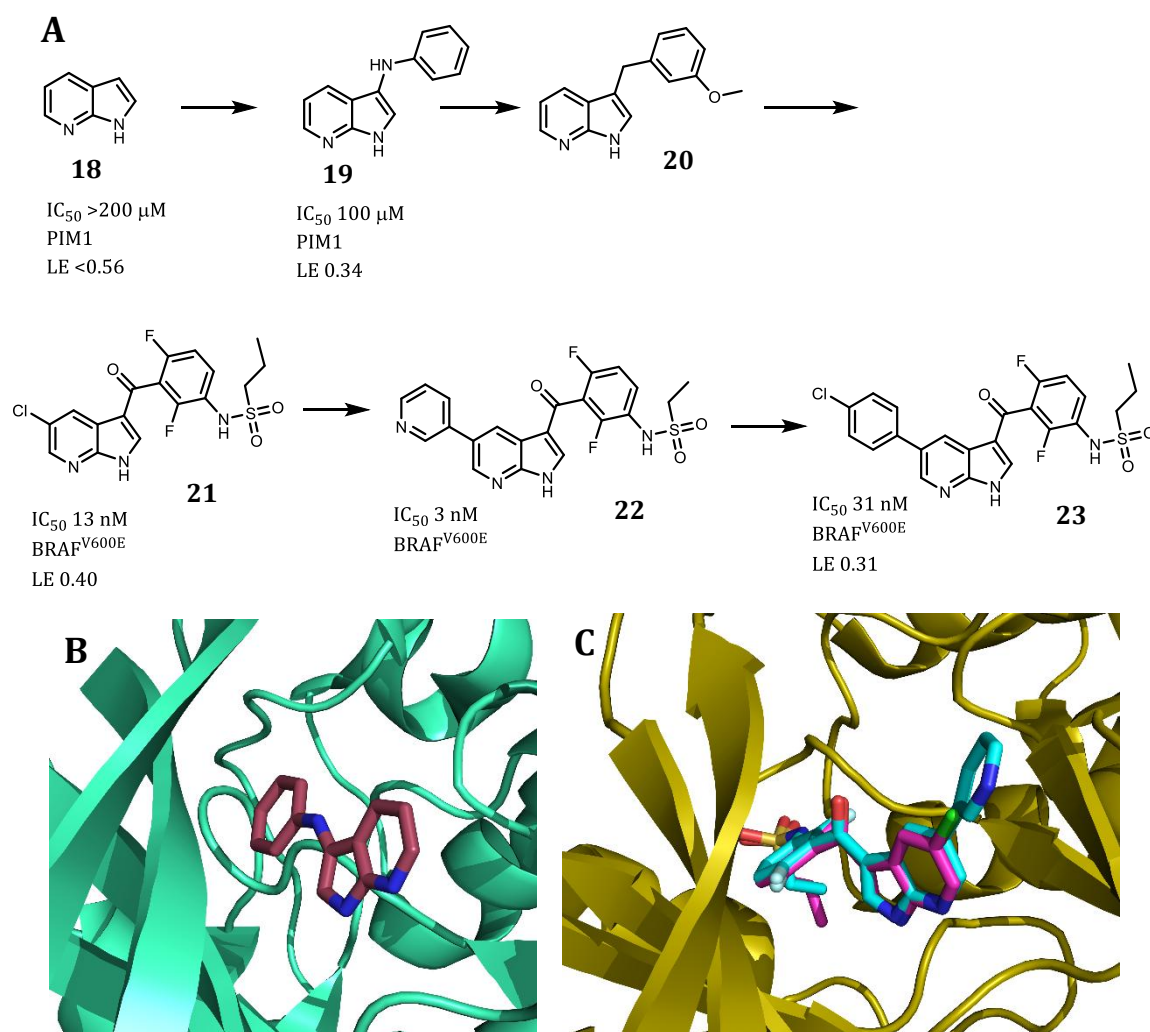
Figure 10: (A) - Development of Vemurafenib **23**. The fragment 7-azaindole **18** was identified and elaborated by fragment growing strategies; (B) – X-ray crystal structure of elaborated fragment **19** bound to PIM1 (PDB: 3C4E); (C) – Overlaid X-ray crystal structures of compounds **21** (pink; PDB: 3C4C) and **22** (blue; PDB: 4FK3) bound to BRAF[V600E].[62]

In April 2016, the second drug derived from a fragment-based approach was approved by the FDA, Venetoclax **28** (Scheme 1) and is used for the treatment of chronic lymphocytic leukemia [46,51,53,65] and was developed by AbbVie and Genentech as a result of over 20 years of research on this target.[51] With a molecular weight of 865 Da, this would suggest that this would be inappropriate for an orally administered drug according to Lipinski's rules.[66] Despite this, Venetoclax has been formulated as an oral drug,[67] and shows excellent activity and selectivity against its target Bcl-2.[51,54]
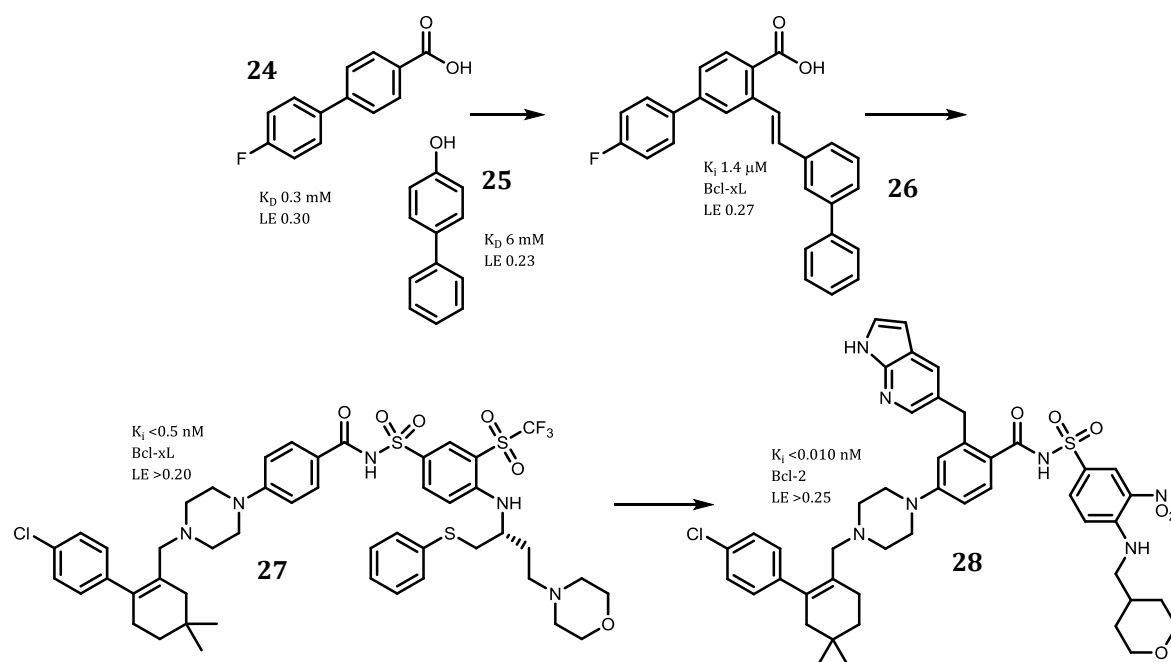
Scheme 1: Development of Venetoclax **28**. Two fragments (**24**, **25**) were identified and linked to form compound **26**, then elaborated to produce compound **27** (Navitoclax) and finally Venetoclax (**28**) with a K_i of <0.01 nM.[51,54]

The latest fragment-derived drug to receive approval is ribociclib from Astex Pharmaceuticals in conjunction with Novartis. As a treatment for breast cancer, ribociclib is a Cyclin-Dependent Kinase 4 and 6 inhibitor, and is used with an aromatase inhibitor.[68]

1.3.2   FBDD in comparison to HTS

Traditionally, pharmaceutical companies have used high-throughput screening (HTS) as the basis of their drug discovery programmes. This consists of screening libraries that typically contain upwards of 10^5 compounds.[53]

Estimates of the size of "drug-like" chemical space predict that there may be as many as 10^{63} individual molecules with 30 or fewer heavy atoms.[57,58,69-71] In 2013, Polishchuk, Madzhidov and Varnek predicted that compounds of ≤500 Da (approximately 36 heavy atoms – C, N, O, S, Halogens) and following the Lipinski rule of 5 could comprise as much as 10^{33} compounds.[66,72] When restricted to 17 heavy atoms (C, H or N), this space is reduced to around 10^{11} molecules.[51,72] While estimates of chemical space vary greatly, it is clear that molecules with a lower molecular weight encompass a smaller amount chemical space, thus allowing the same number of molecules to cover a much larger portion of that space.[57,58,69,73] This allows fragment

libraries to be smaller in size while still covering the same or a larger portion of chemical space than HTS libraries.[74]

In addition, fragment-based approaches allow for selection of molecules that can have better physical properties than larger HTS-type molecules. Fragments tend to be more polar than molecules found in a HTS library, often giving a starting point with better pharmacological properties.[51,58,75] The smaller size of fragment libraries (typically 1000-5000 compounds) mean fewer compounds are screened and subsequently less material such as protein is required. The nature of fragments also means that binding affinities are weaker than HTS hits (in the order of 0.1 to 10 mM), however these interactions tend to be of higher quality than those gained from HTS.[55,56,59,69,73,75] Lead-like molecules derived from high-throughput screening may not be flexible enough to achieve optimal binding orientations within the protein of interest, while fragments, by nature of their small size and limited functionality, can better arrange themselves for higher quality interactions (Figure 11).[69]

Fragment hit   HTS hit
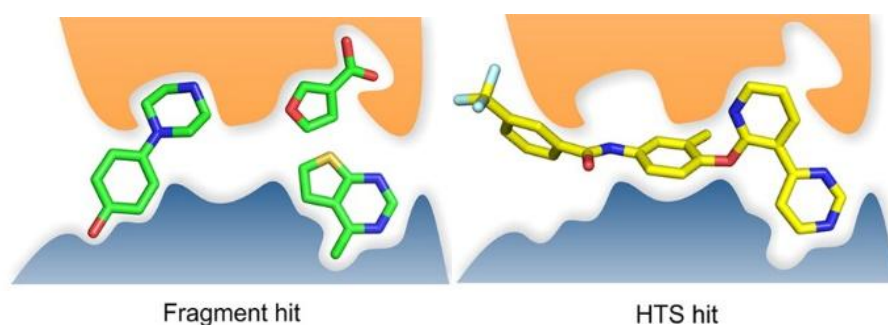
Figure 11: Fragment hits v HTS hits. While each fragment hit constitutes a small binding energy, the interactions are generally better quality than those from HTS, which have higher affinity, but may not possess optimal functionality or flexibility. Figure taken from Scott *et al.* (2012).[49]

1.3.3 Fragment Elaboration Strategies

Once a fragment hit has been obtained, there are a number of methods that can be used to elaborate the compounds to high affinity inhibitors. These strategies have been classed as fragment merging, fragment linking and fragment growing. [49,51,73,75,76]

1.3.3.1 Fragment Merging

Fragment merging is perhaps conceptually the simplest of methods, although in practice, this may not necessarily be true (Figure 12). In the event that library screening identifies molecules which are found to overlap as determined using X-ray crystallography, the fragments can be

merged into a single molecule in order to exploit the binding characteristics of both fragments.[49,51,69]
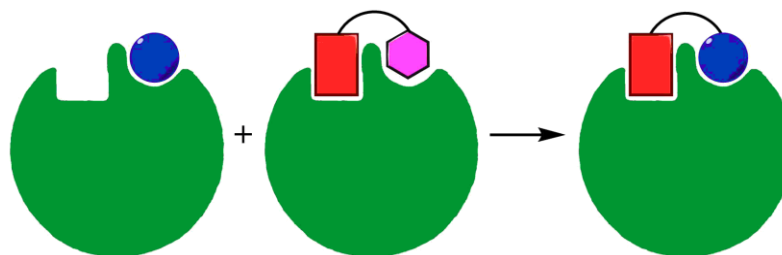
Figure 12: Fragment merging. When multiple fragments bind in overlapping fashion, fragment merging takes the best structural components of each fragment and combines them into a single molecule.

Hudson *et al.*[77] examined a fragment-based approach to targeting cytochrome P450 121 (CYP121) from *M.tb*. A fragment library of 668 fragments was screened against CYP121 using a fluorescence-based thermal shift assay which was used as a primary screen followed by ligand-based nuclear magnetic resonance (NMR) and isothermal titration calorimetry (ITC). Sixty-six fragment hits were identified and four X-ray crystal structures were obtained. These four fragments could be divided into two classes; the haem binders (**29** and **30**), and the non-haem binding fragments (**32** and **33**) and the K_{DS} of these fragments were found to range from 400 μM – 3 mM.[77] When the X-ray crystal structures of these fragments were overlaid together, a number of fragment merging strategies were possible.

The first strategy involved the overlay of fragments **29** and **30**, where there is clear overlap between the aniline ring of **29** and the aromatic ring of **30**. The synthesis of the merged compound **31** gave an increase in affinity to 28 μM while maintaining ligand efficiency (LE = $-\Delta G_{binding}/\#_{non\text{-}hydrogen\ atoms}$ = $-RT\ln K_D/\#_{non\text{-}hydrogen\ atoms}$)[78] (Figure 13). When the NH_2 of the aromatic amine was removed, the affinity significantly decreased as this is the key metal binding group for the haem iron.[77]
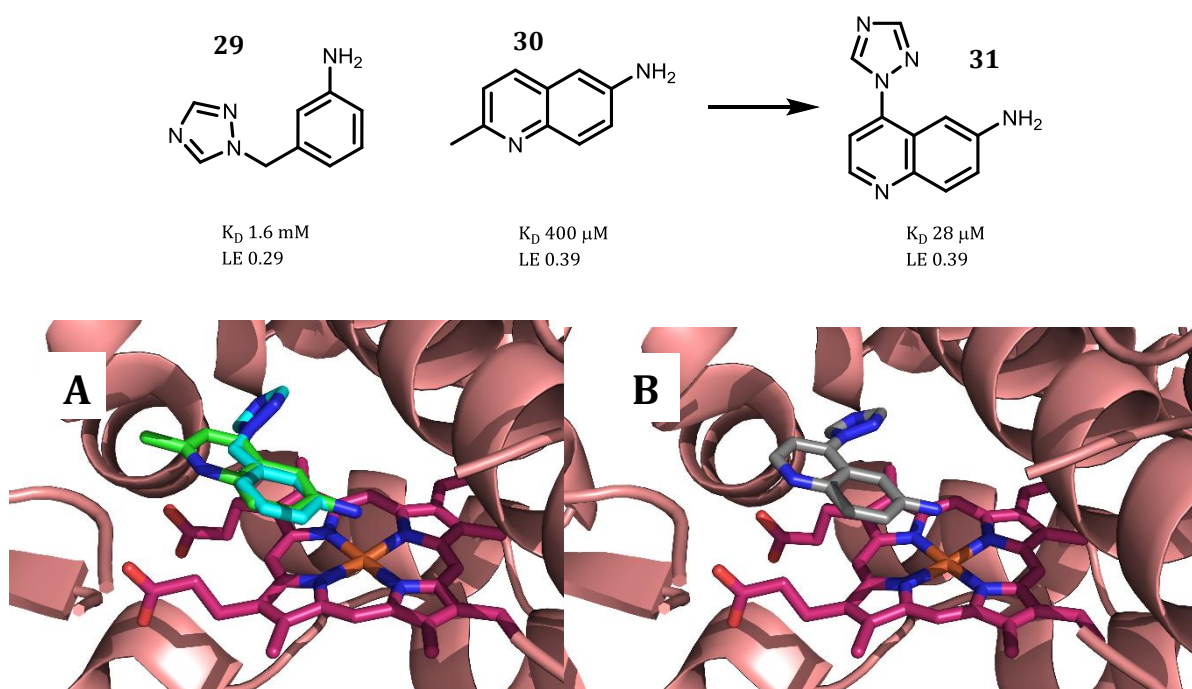
Figure 13: Fragment merging strategy for CYP121. Fragments **29** and **30** were merged which led to the development of compound **31**; A - Overlaid X-ray crystal structures of **29** (blue) and **30** (green) (PDB: 4G44, 4G45); B - X-ray crystal structure of merged compound **31** (PDB: 4G1X).[77]

A second fragment merging strategy involved the merging of fragments **32** and **33** (Figure 14), however the merged structures (**34**, **35**) were not observed to bind to CYP121.[77]
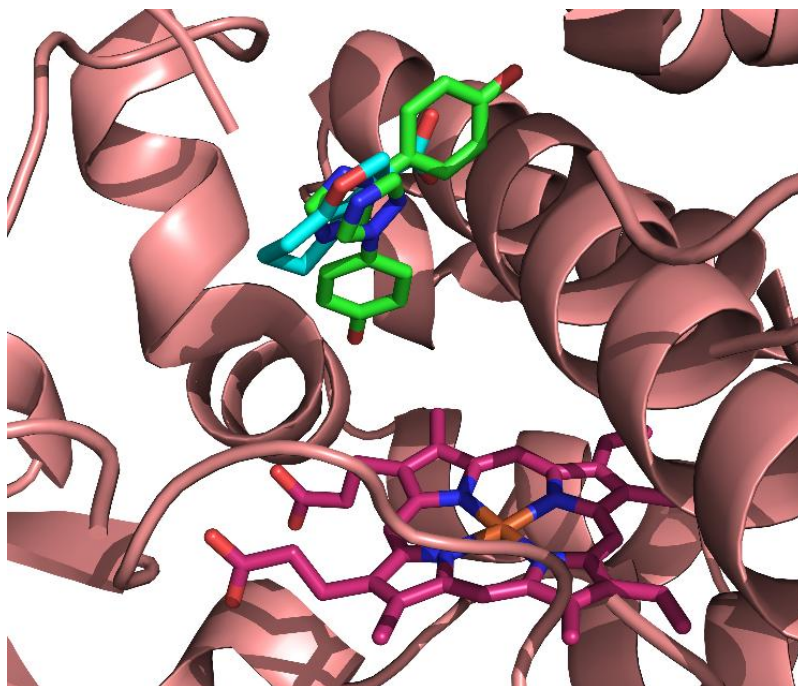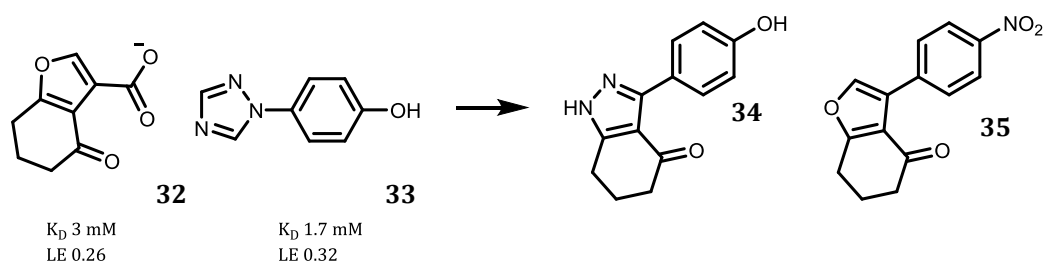
Figure 14: Fragment merging strategy for CYP121. Fragments **32** and **33** were merged to give compounds **34** and **35**, however neither of these were observed to bind. X-ray crystal structures of **32** (blue, PDB: 4G46) and **33** (green, PDB: 4G47). **33** binds in two orientations.[77]

Interestingly, in the X-ray crystal structure of fragment **33**, this was observed to bind in two orientations, and merging of these led to the development of a series of compounds (**36-40**) with K_Ds from 500 µM - 4 mM (Figure 15).[77] However, no significant improvement in affinity was observed. When the 1,2,3-triazole ring was changed to a pyrazole ring only a small increase in affinity was observed. Introduction of an amino group onto the pyrazole resulted in compound **41**, where an increase in affinity to 40 µM was observed. Substituting the amine group with a phenol ring **42** again increased potency to a K_D of 15 µM.[77] Further work by Kavanagh *et al.*[79] in optimisation of this fragment merged series resulted in compound **43** which had an affinity of 15 nM. The key to the increase in affinity of this compound was to build towards the haem iron using an aniline, which was discovered in the original fragment series.

36

K_D 2.8 mM

37

K_D 4 mM

38

K_D 1.2 mM

39

K_D 2.2 mM

40

K_D 500 μM
LE 0.24

41

K_D 40 μM
LE 0.30

42

K_D 15 μM
LE 0.25

43
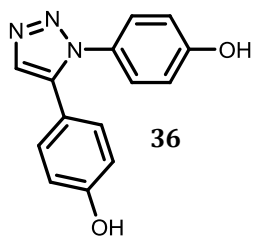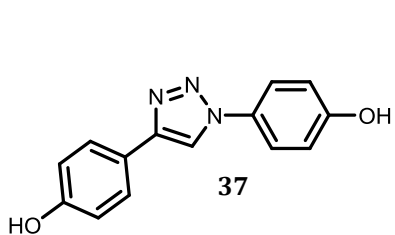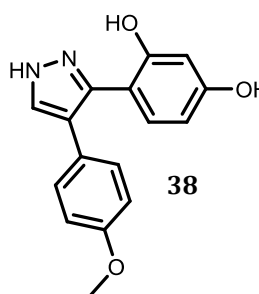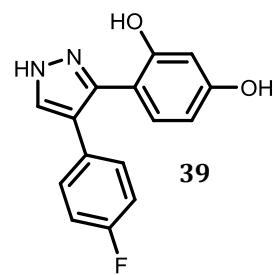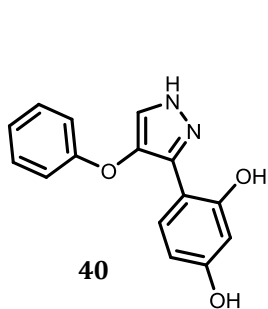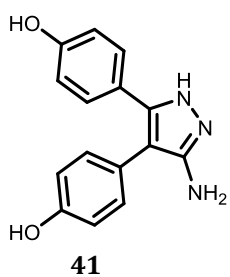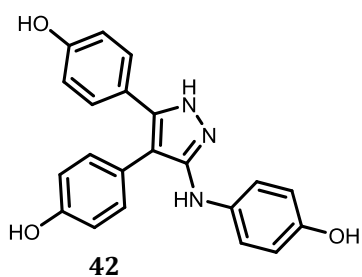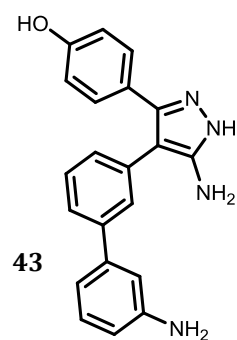
K_D 15 nM
LE [N/A]
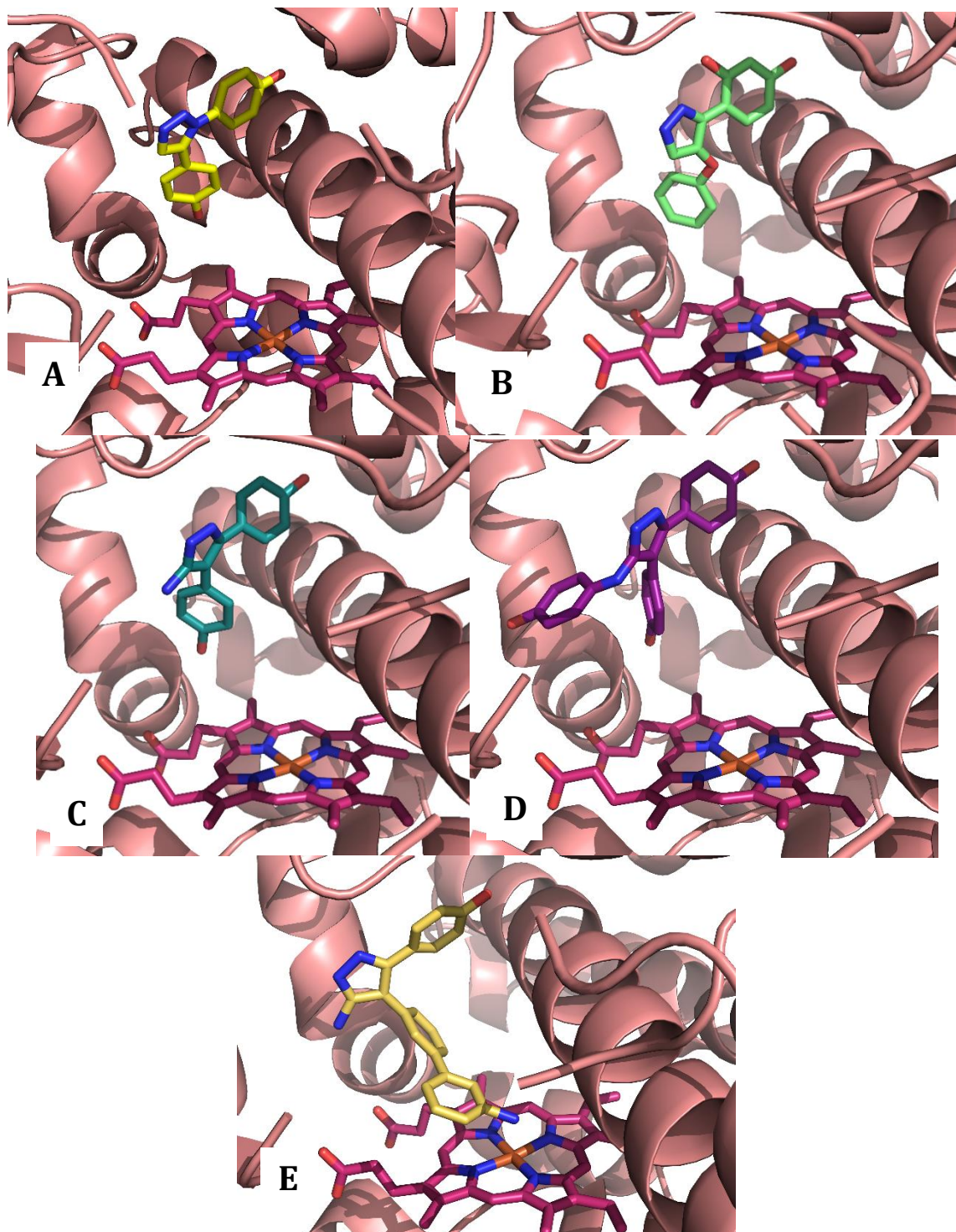
Figure 15: Structures of compounds **36-43** bound to CYP121; (A) - X-ray crystal structure of **36** (PDB: 4G2G);[77] (B) - X-ray crystal structure of **40** (PDB: 4G48);[77] (C) - X-ray crystal structure of compound **41** (PDB: 4KTF);[76] (D) - X-ray crystal structure of compound **42** (PDB: 4KTL);[76] (E) - X-ray crystal structure of compound **43** (PDB: 5IBE).[79]

1.3.3.2   Fragment Linking

Fragment linking may be thought of as 'chaining' two fragments together. These may be fragments that bind in different sites or even different parts of the same pocket, or they may be different compounds that result in different but not overlapping positions on the target (Figure 16).[49,51,69,73] An interesting effect may be observed when fragment linking approaches are used, and that is super-additivity.[80,81] This relates to the amount of energy necessary to overcome the entropic loss on binding the ligand to the protein – the rigid body entropy. In a linked compound, there is only one rigid body entropy term to overcome, as opposed to two terms in the non-linked fragments, therefore raising the potential for a linked fragment to have a greater binding affinity than the sum of the two fragment affinities would suggest.[49,61,82] The major difficulty that can arise in this strategy is trying to identify the optimum linker.[51,54,61]
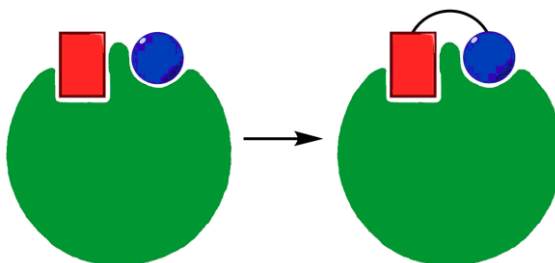
Figure 16: Fragment linking. Where two fragments bind in close but non-overlapping positions, these separate fragments can be connected to create one compound, which retains the binding of both fragments. This linked compound may show binding greater than the sum of the two fragments, since there will only be one rigid body entropic penalty to be overcome when binding to the target.

Pelz *et al.*[83] examined linking strategies for Mcl-1 inhibitors. Using a known ligand **44** to bind in the P2 site, seven fragments were identified which bound within the nearby P4 subpocket (Scheme 2). Of the seven fragment hits identified, compound **51** was reported as being the most potent, with a K_D of 1.5 mM.[83]
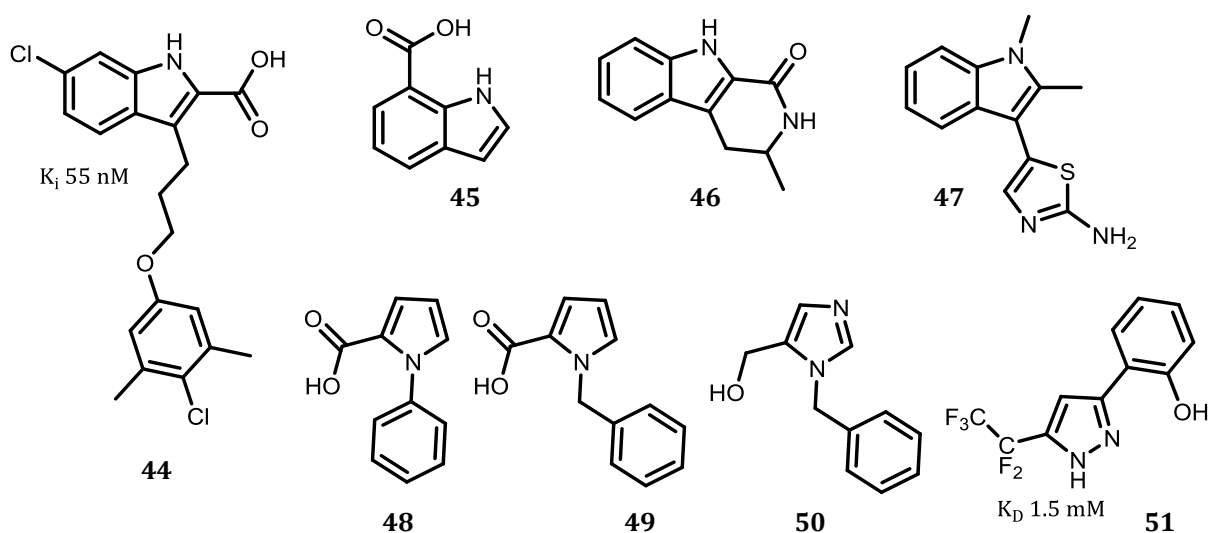
Scheme 2: Structures of compound **44**, and fragments **45**-**51**. Taken from Pelz *et al.*[83]

Compound **52** was synthesised whereby the acid functionality of **44** was replaced with an acylsulfonamide to retain important interactions with R263, however a drop in affinity was observed in comparison to the original compound **44** (Figure 17).

The authors then proceeded to link the fragments to compound **52**, resulting in compounds **53** and **54**, with K_is of 278 and 308 nM respectively. From here, the authors continued to optimise the compounds until they produced compound **55**, with a K_i of 1 nM.[83]
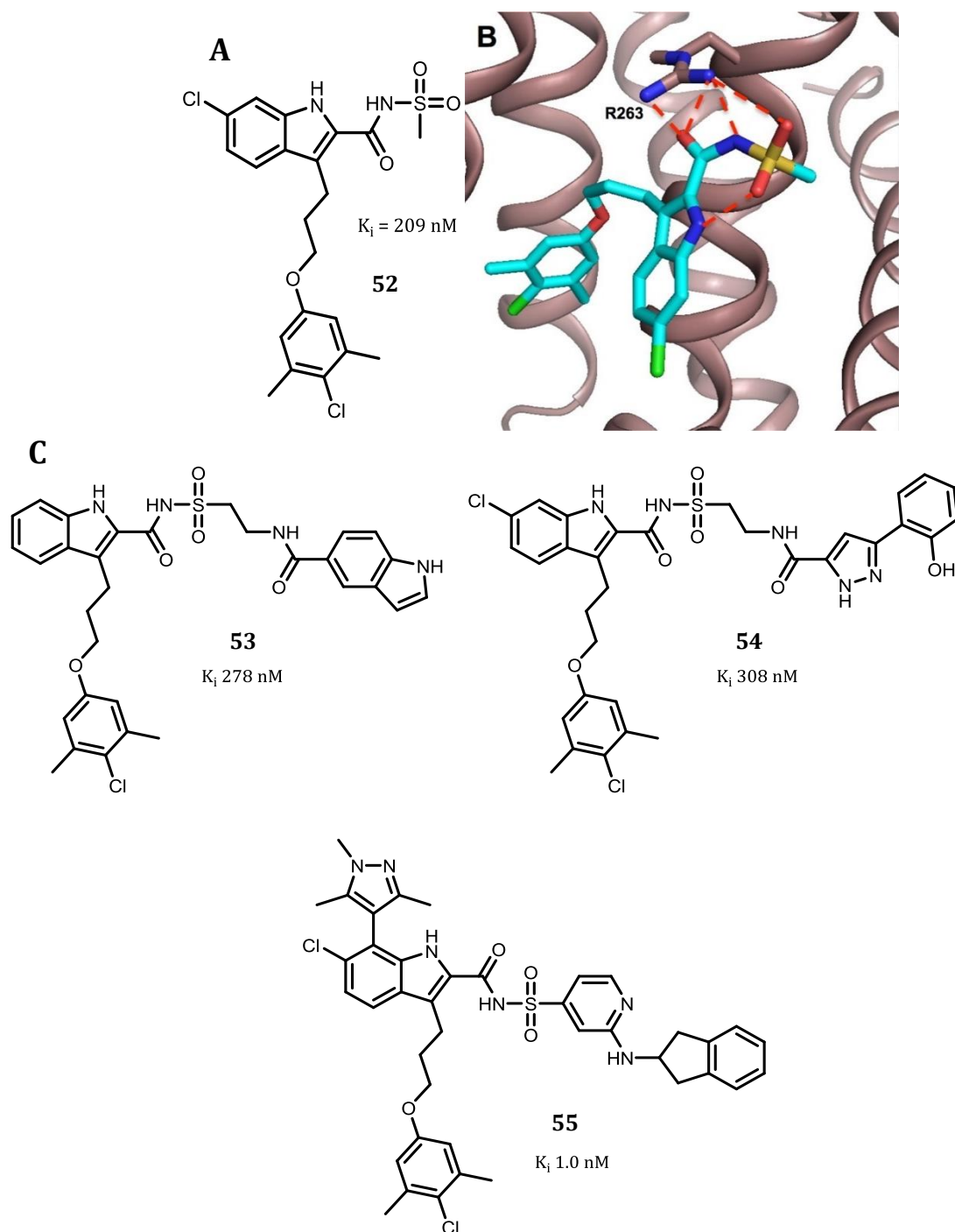
Figure 17: A - structure of compound **52**; B - X-ray crystal structure of **52** bound to Mcl-1 showing important interactions. Figure taken from Pelz *et al.* (2016).[83]; C - Structures of compounds **53**-**55** which were shown to bind to Mcl-1.[83]

1.3.3.3   Fragment Growing

Fragment growing allows the greatest degree of freedom in design of new molecules. This requires the synthesis of larger molecules to probe the space near the fragment (Figure 18).[51,69]
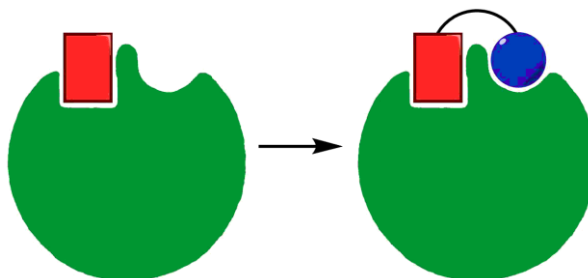
Figure 18: Fragment growing. When one fragment is bound in the binding pocket, potential nearby interactions may be probed by building new functionality onto the existing fragment.

An example of the use of fragment growing was reported by Wyatt *et al.*[84] in their development of the cyclin-dependant kinase (CDK) inhibitor AT7519 (Scheme 3). The initial fragment hit indazole **56**, was grown from the 3-position, and guided by X-ray crystallography (Figure 19), additional H-bonding interactions were obtained which led to the development of compound **57**. This subsequently had the sulfonamide group removed (**58**) to simplify synthesis, and this did not lead to a loss in ligand efficiency from **57**. The introduction of two fluorine atoms at the 2 and 6 positions of the phenyl group and addition of an amide as a hydrogen-bond acceptor led to compound **59**, with an improved ligand efficiency and a 100-fold improvement in activity over compound **52**.[84]
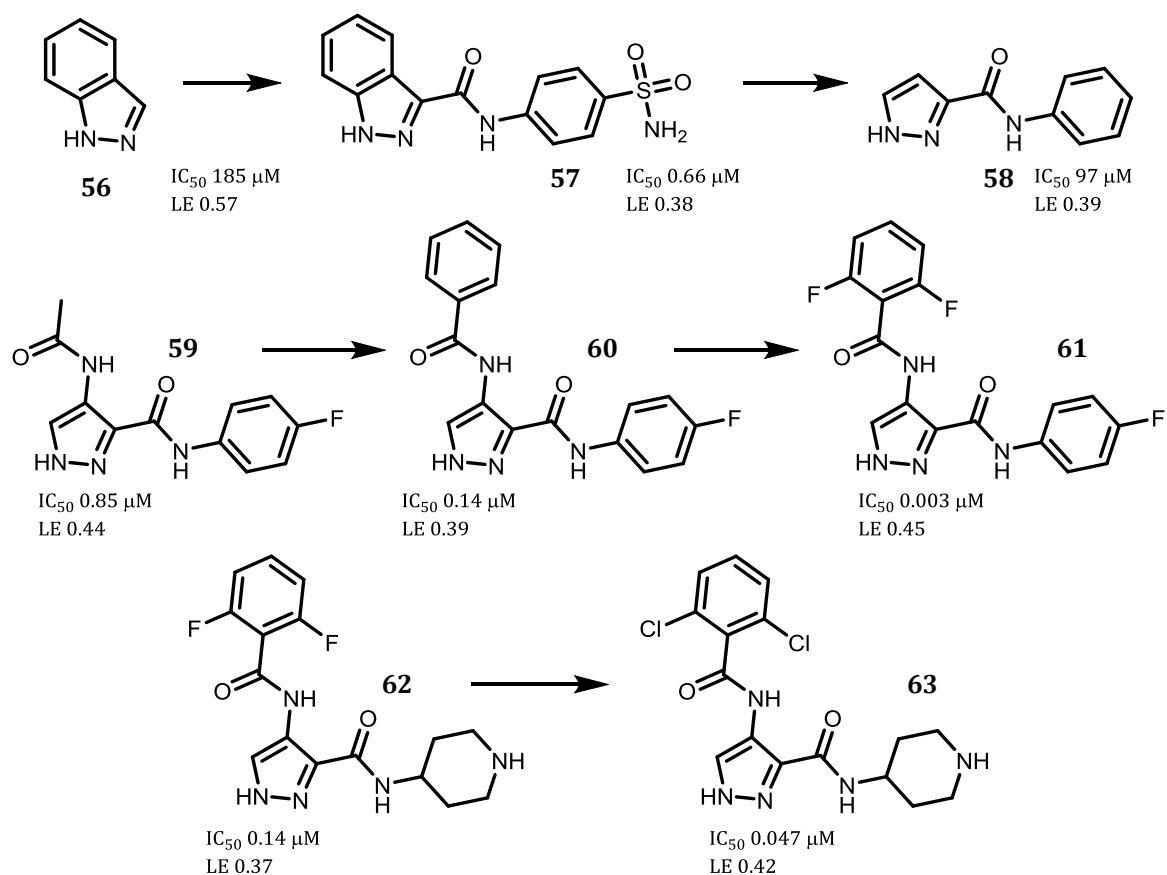
Scheme 3: Development of CDK inhibitor **63** (AT7519).[84] Indazole **56** was developed by fragment growing strategies into compound **63**, which has an improvement in IC_{50} of almost 4000 times over compound **56**, while still maintaining a ligand efficiency >0.4.[84]

Figure 19: A – Overlay of X-ray crystal structures of **56** (green, PDB: 2VTA), **57** (pink, PDB: 2VTI) and **58** (orange, PDB: 2VTL) with CDK; B - Overlaid X-ray crystal structures of **59** (pink, PDB: 2VTN), **60** (grey, PDB: 2VTO) and **61** (orange, PDB: 2VTP); C – X-ray crystal structure of **59** (PDB: 2VTN) with measurements. Nitrogen shown in dark blue, fluorine in light blue, oxygen in red and sulfur in yellow.[84]
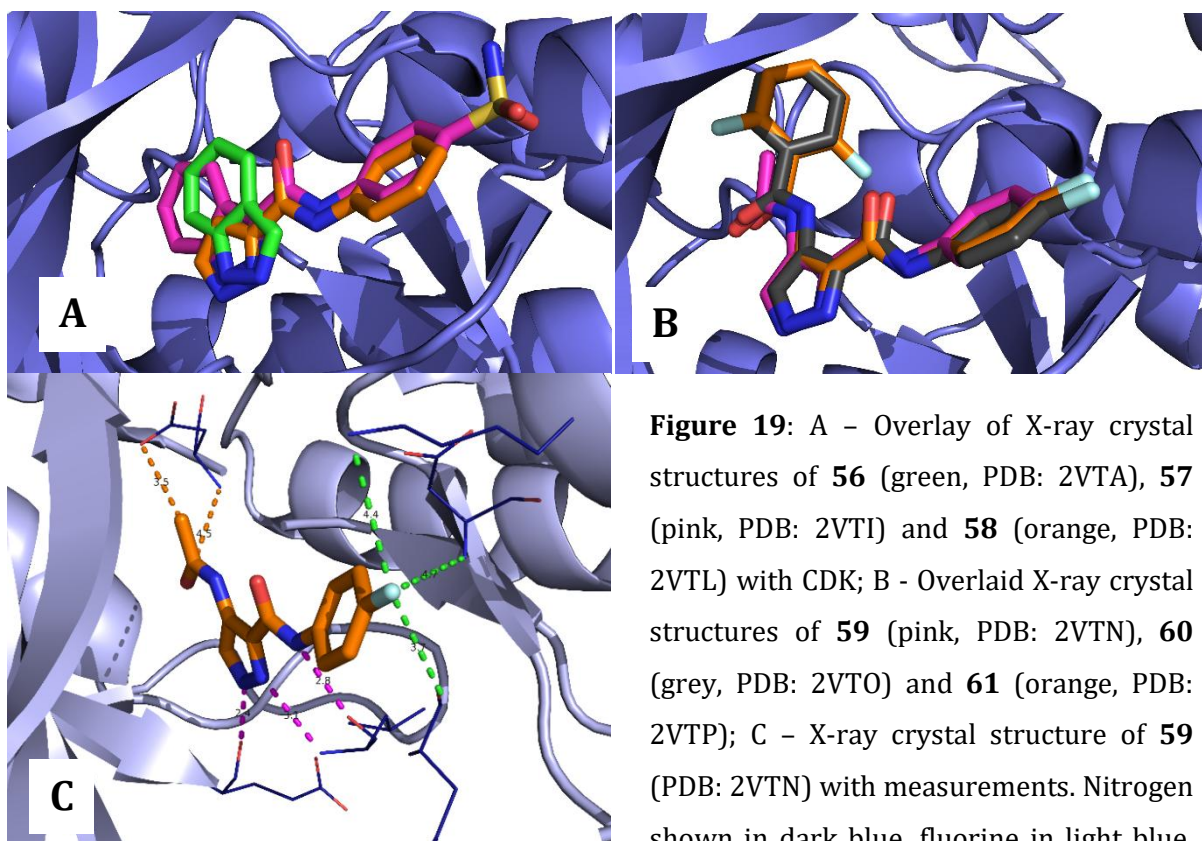
Modification of the amide with a phenyl ring, **60**, resulted in an improvement in activity (IC$_{50}$ 0.14 µM), at the expense of torsional strain of the phenyl ring. The introduction of a 2,6-disubstitution (**61**) increased both activity and ligand efficiency. Replacing the opposing 4-fluorophenyl group with piperidine for improved hydrophilicity led to **62**, after which the two fluorines in the 2 and 6 positions were swapped with chlorines (**63**) to better fill the binding pocket (Figure 20), with the end result being a compound of higher activity (IC$_{50}$ = 0.047 µM) and ligand efficiency (0.42) when compared to compound **62**.[84]
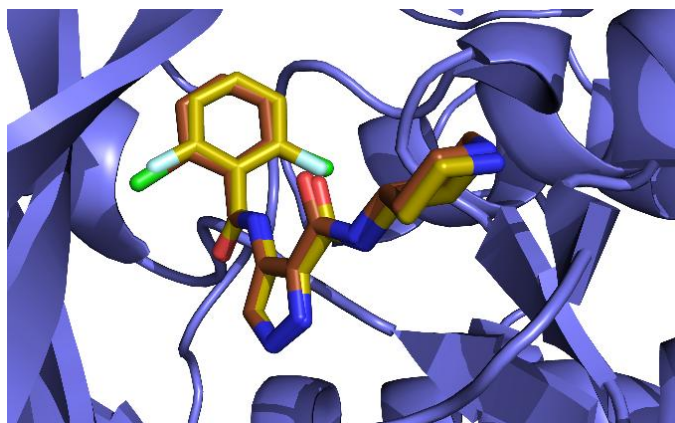
Figure 20: X-ray crystal structure overlay of **62** (yellow, PDB: 2VTQ) and **63** (orange, PDB: 2VU3) bound to CDK. Nitrogen shown in dark blue, oxygen in red, chlorine in green and fluorine in light blue.[84]

1.3.4   Biophysical Screening Techniques

Fragment-based drug discovery approaches rely on a suite of biophysical data to provide information on the binding nature of fragments to the protein target.[50,51] These are usually used as a cascade of screening techniques (Figure 21) designed to enrich the fragment hits through successive rounds of biophysical screening.[53] Each technique provides different information about the binding interaction under investigation,[53] so multiple techniques should be used in parallel to confirm the binding to the protein and lead to an enrichment of the fragment hits.[53,59,74]
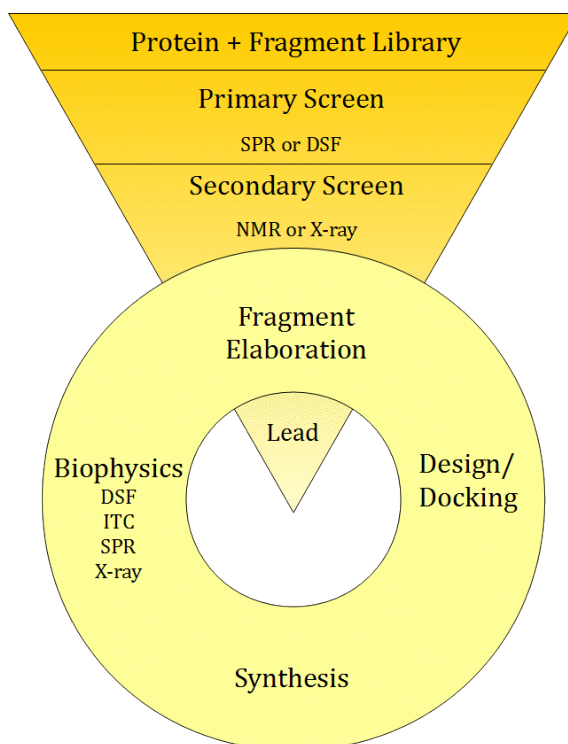
Figure 21: Fragment screening cascade. The primary screen identifies fragment hits from the fragment library, which are validated in the secondary screen. Validated fragments are then iteratively examined through a cycle of design, synthesis and biophysical analysis to improve the compound properties towards a lead candidate.

1.3.4.1 Surface Plasmon Resonance

Surface plasmon resonance (SPR) is a functional assay, where the binding of the protein of interest to its target is assessed in the presence of the ligand. SPR uses the change in refractive index to determine changes to the material under investigation,[51,53,54,85] without the requirement for labelled materials or additional fluorescent substrates,[85] with the exception of the immobilised component.[50,51,59]

SPR relies on the total internal reflection of the IR light beam by the gold-coated surface of a chip.[85] When the free component binds to its immobilised partner, the sample changes refractive index, causing a change in the total internal reflection angle, which can be recorded as a change in intensity of the reflected signal.[51] SPR can be used to measure several parameters about the binding interaction, including IC_{50}, binding stoichiometry, specificity, and kinetic parameters (e.g. K_D, association and dissociation rate constants).[53,85]

1.3.4.2   Differential Scanning Fluorimetry

Differential Scanning Fluorimetry (DSF or Thermal Shift) is a technique used as a first-line screening technique due to its high-throughput nature.[51,52] The technique involves heating the samples of protein with or without ligand at a fixed rate in the presence of a fluorescent dye such as SYPRO® Orange, which fluoresces upon binding to hydrophobic surfaces[51-53] as the protein unfolds. As this happens, more of the internal hydrophobic surface is exposed, and the change in fluorescence in recorded (Figure 22A). The first derivative of the fluorescence curve (Figure 22B) is obtained, from which the change in melting temperature (ΔT_M) between the control and ligands/fragments can be calculated.[51]
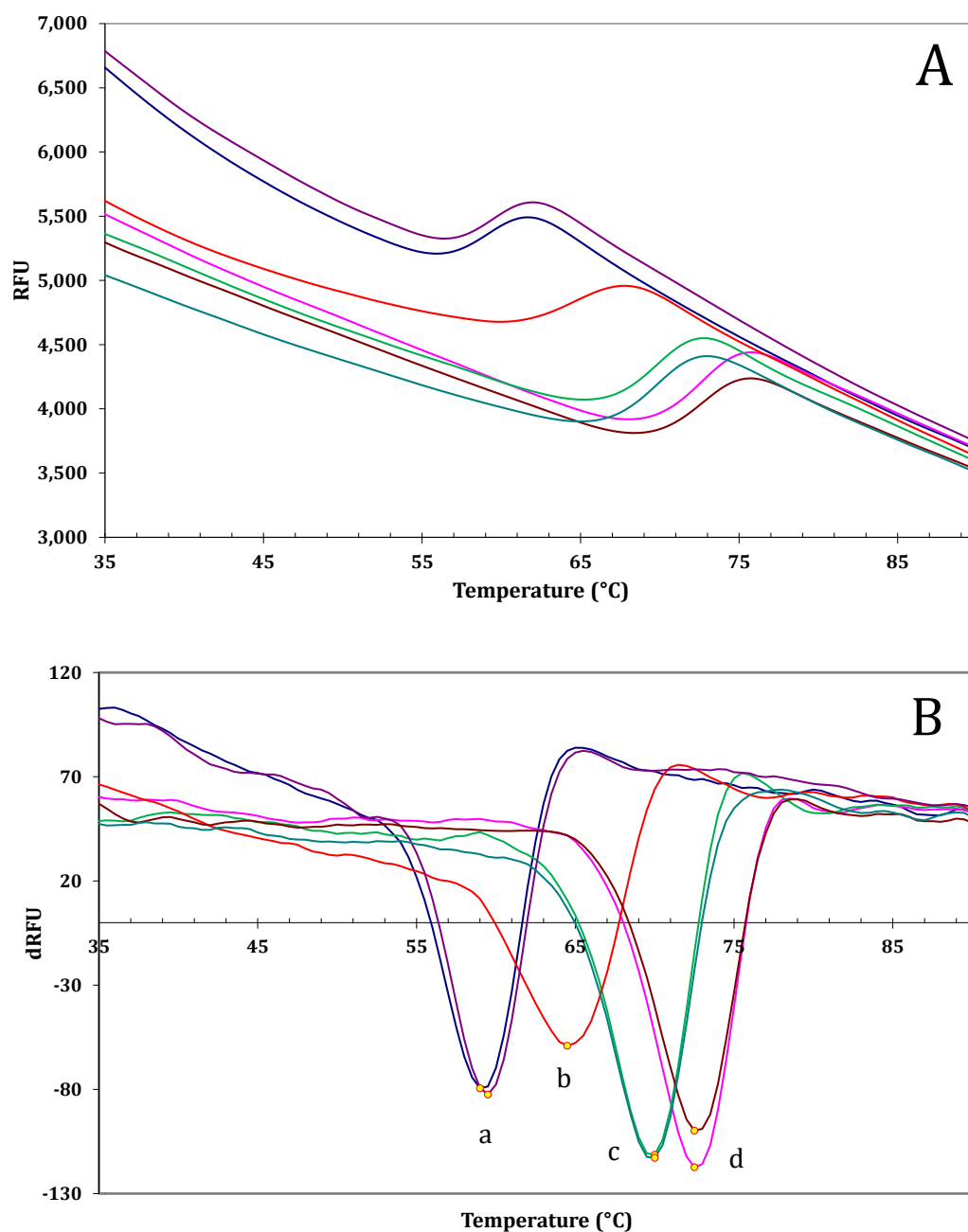
Figure 22: DSF plots for thermal denaturation of a protein in the presence of varying concentrations of ligand. (**A**) - RFU (response fluorescence units)/temperature; (**B**) - dRFU (1st derivative response fluorescence units)/temperature, where minima represent T_M. a) DMSO control T_M, b-d) sample T_Ms at increasing concentrations of compound added (b = 0.01 mM; c = 0.1 mM; d = 1 mM).

1.3.4.3 Ligand-observed NMR

Ligand-observed NMR utilises the phenomenon of magnetisation transfer to investigate the binding of the ligand to the macromolecule.[53,59] Three different experiments are commonly used, saturation transfer difference (STD), water-ligand observed by gradient spectroscopy (WaterLOGSY) and Carr-Purcell-Meiboom-Gill (CPMG) spin-lock relaxation edited experiments (Figure 23).[69,75,86]

STD is performed by irradiating the methyl groups on the protein, and observing the transfer of magnetisation to the ligand signals.[75,86] The technique is performed in two parts; an ON- and OFF-resonance, which are combined to generate a difference spectrum.[69,75,86,87] Ligand peaks are only observed when nOe is transferred from the irradiated protein to bound ligands, therefore the presence of ligand peaks in the difference spectrum is indicative of ligand binding.[69,86,87] Since the intensity of the observed signal is dependent upon the rotational properties of the protein-ligand complex, larger (and therefore slower rotating complexes) will be able to transfer more magnetisation, generating stronger signals and greater sensitivity in the spectrum.[78]

WaterLOGSY observes the change in nOe of the ligand after irradiation of the bulk water.[69,75,86,87] The ligands receive the transferred magnetisation from water while bound to the protein, causing a build-up of nOe of opposite sign to that of free ligand. Tris (which does not generally bind to proteins) can be used as an internal reference when present in the buffer to phase the spectrum to a negative signal, meaning signals from ligands in the bound state present as positive (or less negative) signals, while free ligands appear as negative signals.[86,88]

CPMG relies on the difference in transverse relaxation time between the slow-moving proteins (giving rise to broad signals and fast relaxation) and fast moving ligands (resulting in sharp signals and slow relaxation). The experiment eliminates the protein and protein-ligand complex signals by delaying the acquisition for a few hundred milliseconds, allowing the slow tumbling molecules to relax before acquisition begins. Comparison of the signals to an equivalent sample without protein can be used to identify ligands binding to the target.[69,86]
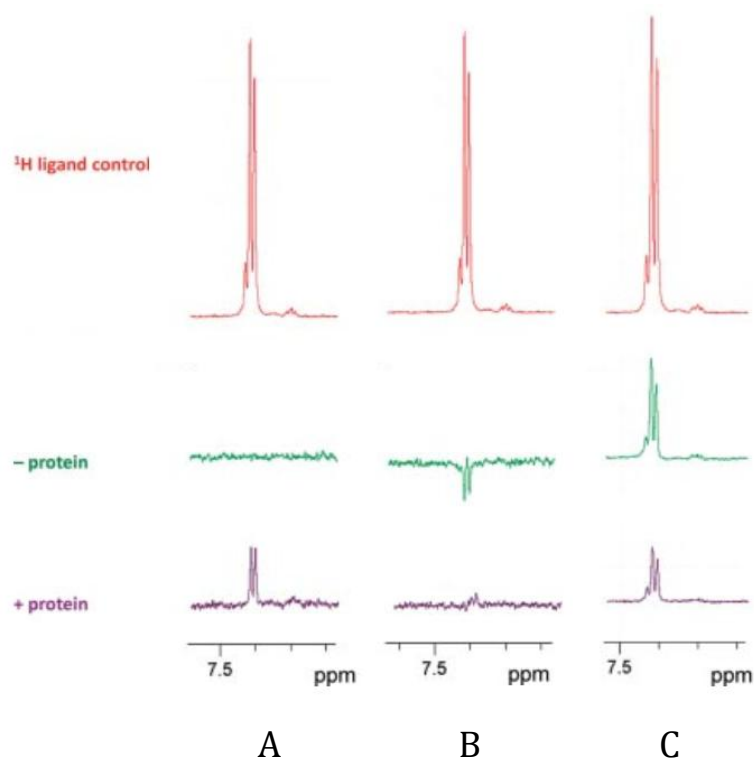
Figure 23: Ligand-observed NMR. (A) – STD difference spectra. Ligands will produce a signal only in the presence of the protein if binding. Non-binding ligands will not be observed; (B) – WaterLOGSY spectra. In the presence of the protein, the ligand has a signal which is less negative than the spectrum without protein, indicating binding; (C) – CPMG spectra. The change in intensity of the ligand signal is indicative of binding. Figure adapted from Sledz, Abell and Ciulli (2012).[86]

1.3.4.4 X-Ray Crystallography

X-ray crystallography is considered the gold standard for the identification of fragments that bind to the protein of interest.[52,53,59] Protein crystals are grown and can be soaked with solutions of the desired ligand, and the resulting protein-ligand complex structure determined by X-ray analysis.[54,59,75,89] In some cases, where soaking does not produce suitable results, co-crystallisation can be used, whereby both protein and ligand are crystallised together before X-ray analysis.[75,89] Key considerations in the use of X-ray crystallography for drug design include the ability to produce diffraction quality crystals, which are sufficiently stable for soaking and X-ray data generation, and generate sufficient diffraction.[74]

1.3.4.5   Computational Docking

Computational docking, although useful in some respects, can be difficult when working with fragments due to the small energies involved in binding, small size of the molecules and the design of programs which favour larger molecules.[59,73,75] It has been reported that computational docking accurately predicts binding mode between 40 and 70% of the time.[73,90] Docking is performed by loading a protein model and ligand structure(s), and the program generates one or more binding poses for the ligand and searches for an energy minima with the protein, with constraints on the available binding site.[91] Docking is useful for gaining insight into possible binding motifs and molecules, and can be used to assist in directing synthesis.[49]

1.3.4.6   Isothermal Titration Calorimetry

Isothermal Titration Calorimetry (ITC) can be used to measure the binding energy (as heat) released or absorbed upon binding of the ligand molecules to the protein of interest.[49,52,53] The technique is performed by titrating one component of the system into the other, where this is typically the ligand being titrated into the protein.[53,92] As each aliquot of ligand is injected into the mixing cell, the change in heat is recorded by comparison to a reference cell which maintains a constant energy input for a stable temperature.[93,94] Upon completion, the heat profile is integrated and fitted to a sigmoidal curve model.[94]

Isothermal titration calorimetry is typically used as a second-line screen due to the low throughput nature of the technique.[53] The ITC experiments (Figure 24) can provide measurement of several important thermodynamic properties of the binding, most importantly the Gibbs free energy and association constant (K_A), which is inversely proportional to the dissociation constant (K_D) in addition to giving an indication as to the stoichiometry of the interaction (N value).[53,54,92,93]
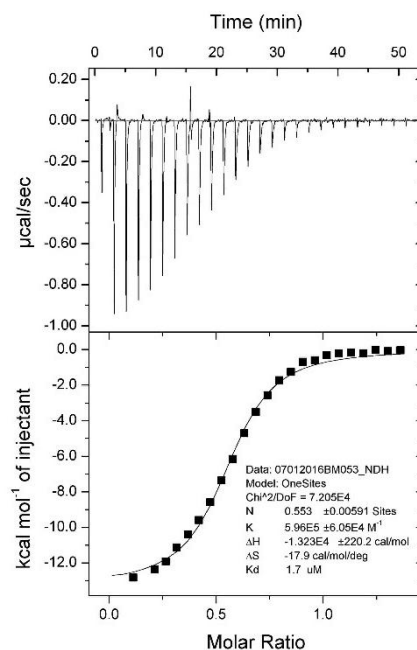
Figure 24: ITC Trace. Top – Heat profile. This is the change in heat measured during the experiment plotted against the experiment time; Bottom - integrated heat profile (binding isotherm) measured against molar ratio of the two components, fitted to a single site binding model.

1.4   Research Focus

The focus of this thesis will be to examine the use of fragment-based drug discovery to target the mycobacterial transcriptional repressor EthR. Three fragment scaffolds (Figure 25) will be explored using a combination of fragment merging, growing and linking. Chapter 2 will investigate two scaffolds, the first is based on 1-(3-(furan-2-yl)-1,2,4-oxadiazol-5-yl)-*N*-methylmethanamine **64** and examines fragment linking strategies. The second scaffold based on 2-((4-chlorophenyl)sulfonyl)ethanethioamide **65** will be investigated using fragment merging strategies.

Chapter 3 examines (5-trifluoromethyl)pyridin-2-yl)piperazine **66** through fragment growing, producing a series of compounds which show strong affinity for EthR. Results of a resazurin microtiter assay (REMAssay) are reported to demonstrate the effectiveness of these molecules in boosting the efficacy of ethionamide.

Chapter 4 will examine the synthesis of linked molecules designed to stabilise the dimeric form of EthR in an inactive conformation.

64   **65**   **66**
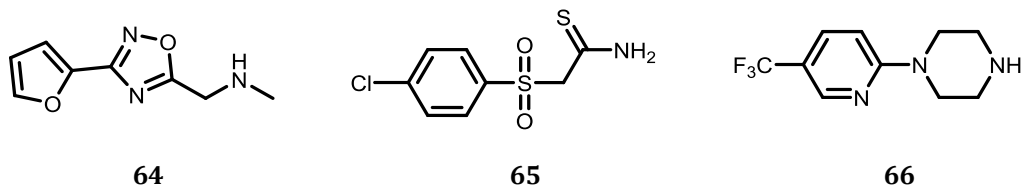
Figure 25: Fragments **64-66**. These fragments form the scaffolds examined in chapters 2 and 3, while chapter 4 examines linking strategies using compounds based on fragment **66** developed in chapter 4.

2.0 Fragment merging and growing approaches for targeting EthR

2.1 Oxadiazoles and sulfones in drug design

This chapter will describe fragment growing and merging approaches to targeting EthR. The first strategy employs a 1,2,4-oxadiazole fragment as a starting point for elaboration. A second strategy will examine fragment merging and growing employing an aryl-sulfone fragment.

Oxadiazoles have been used in a variety of applications in the medicinal and materials chemistry fields.[95-97] These 5-membered heterocycles have been shown to be important scaffolds in drug design [98,99] due to their increased lipophilicity when compared with other isomers such as the 1,3,4-oxadiazole.[96,97] The 1,2,4-oxadiazole scaffold (Figure 26) has gained interest as bioactive molecules for a variety of conditions ranging from anti-asthmatic and anti-diabetic agents, to apoptosis promoters and immuno-suppressants due to their synthetic tractability, altered H-bonding capacity and high metabolic turnover. They have also shown promise in antimicrobials, with a particular focus on anti-tuberculosis medicines.[95,97]
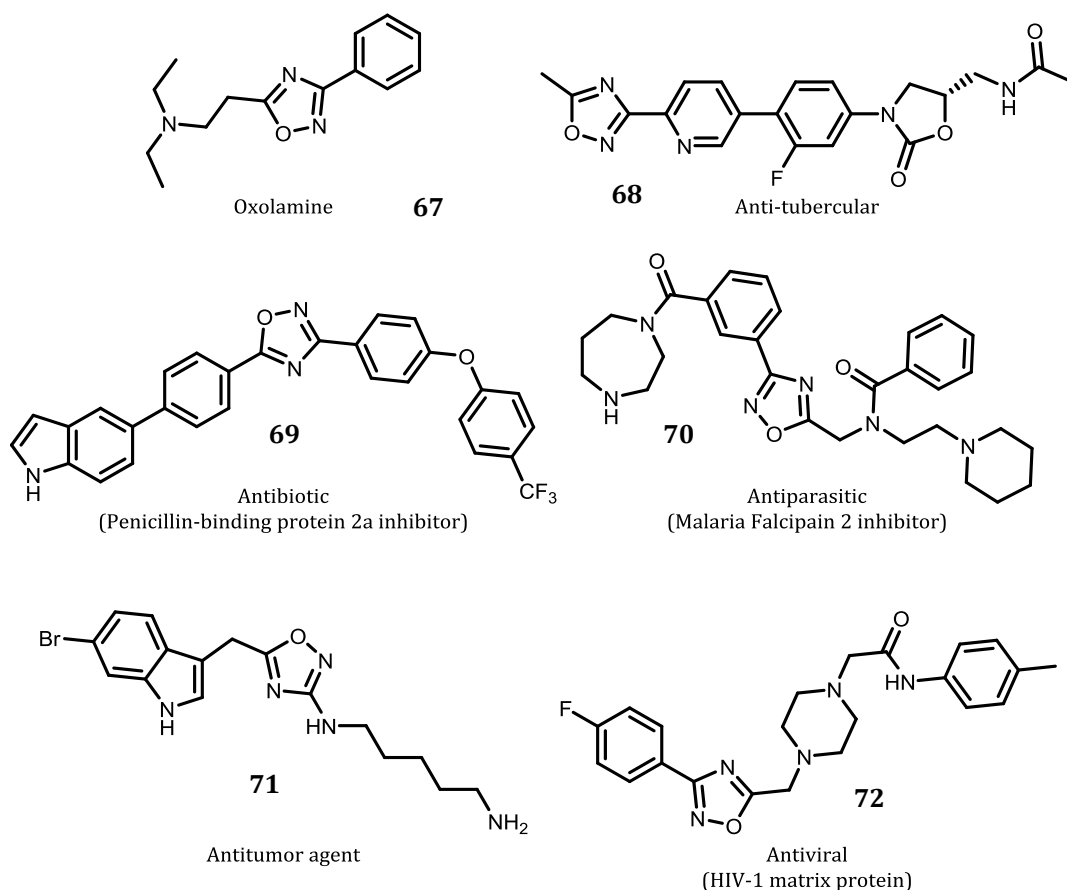
Figure 26: Selected examples of 1,2,4-oxadiazole-containing bioactive molecules.[95,97]

The use of fragment-merging strategies with sulfur-containing fragments was utilised by Goswami *et al.* where they described the use of the technique with a sulfonamide-containing compound to develop inhibitors of matriptase.[100] A targeted library of benzamidine analogue fragments were screened and fragments **73** and **74** were observed to bind to matriptase with K_is of 79 μM and 81 μM respectively. As these compounds were binding in overlapping binding sites P1/P4 and P1/P1', a fragment linking strategy was employed. Compound **75** (*S*-isomer) gave a K_i of 7.4 μM, while the *R*-isomer was shown to be less active than the original fragment hits, with a K_i of 99 μM (Figure 27).[100]
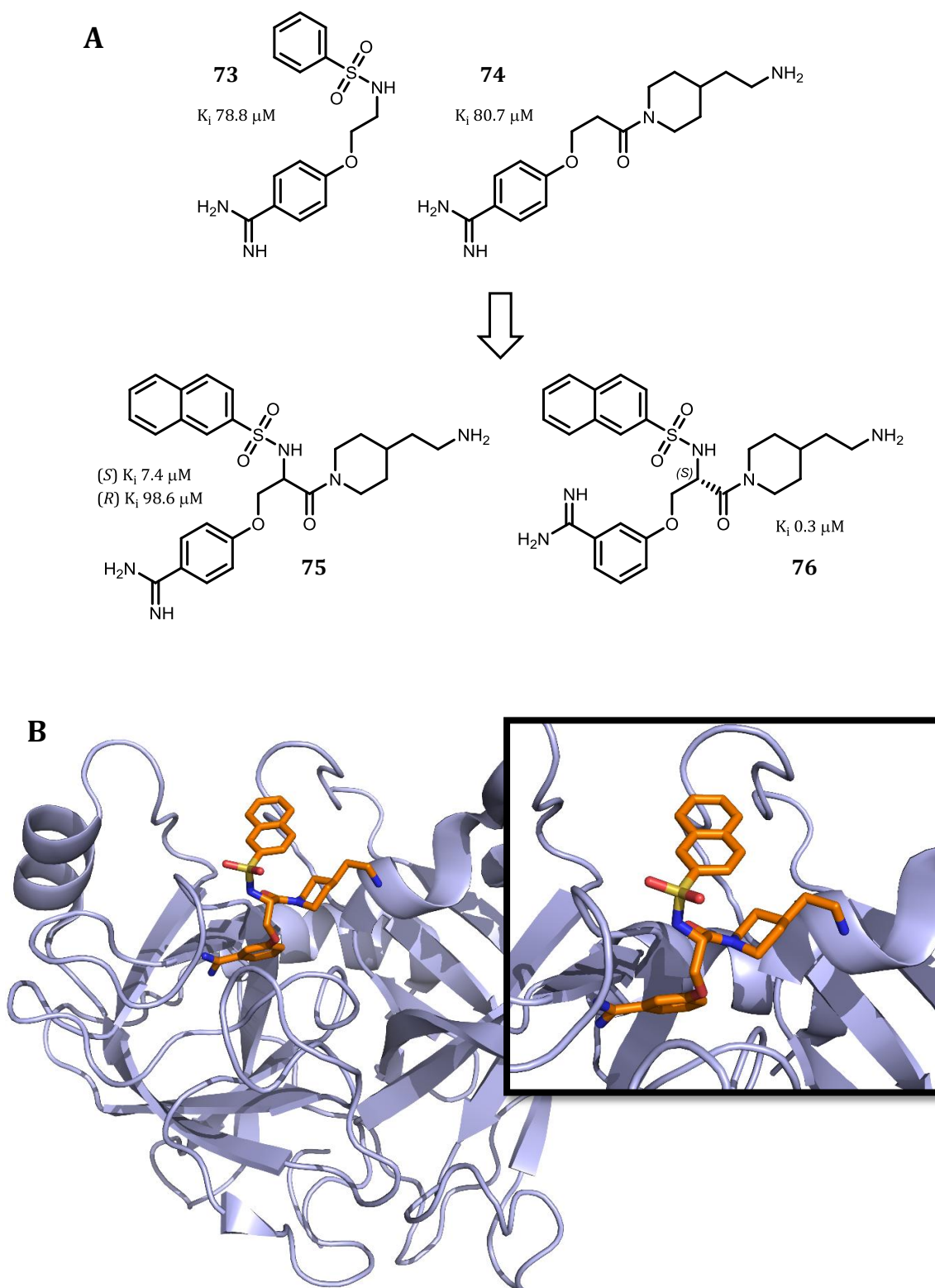
Figure 27: (A) - Structures of compounds **73-76**. Compounds **73** and **74** were identified by a fragment screen, and subsequently merged to form compound **75**. Moving the imidamine group to the *meta*-position (compound **76**), a sub-micromolar K_i was obtained against matriptase;[100] (B) - X-ray crystal structure of matriptase with compound **76** bound (orange, PDB: 4R0I). Inset – close-up of compound **76** in the binding pocket of matriptase.[100]

When the imidamine group on compound **75** was moved from the *para-* to the *meta*-position (compound **76**) the K_i improved to 0.3 μM which was a result of a change in the binding mode. The replacement of the naphthalene ring with a sterically bulky 2,4,6-triisopropylbenzene ring yielded the strongest binding inhibitor with a K_i of 0.1 μM.[100] This demonstrates a successful fragment merging strategy resulting in an over 700-fold improvement in K_i.

The scaffolds investigated in this chapter rely upon fragment-merging strategies as the primary technique for elaborating the fragment hits, containing 5-membered heterocycles and sulfones as core functionalities.

2.2 Fragment merging strategies to target EthR

The fragment **64** was identified previously from a fragment screen against EthR, and a ΔT_M of +6.9 °C [10 mM] was measured (Narin Hengrung, Dept. of Biochemistry). The X-ray crystal structure (Sachin Surade, Dept. of Biochemistry) showed that two molecules of **64** bind in opposing directions and in close proximity (Figure 28A, '1' and '2'), with the NH of molecule 1 situated 1.4 Å from the CH_2 of molecule 2. This suggests the merging of these two binding positions through an amine or amide bond as a possible strategy for elaboration.
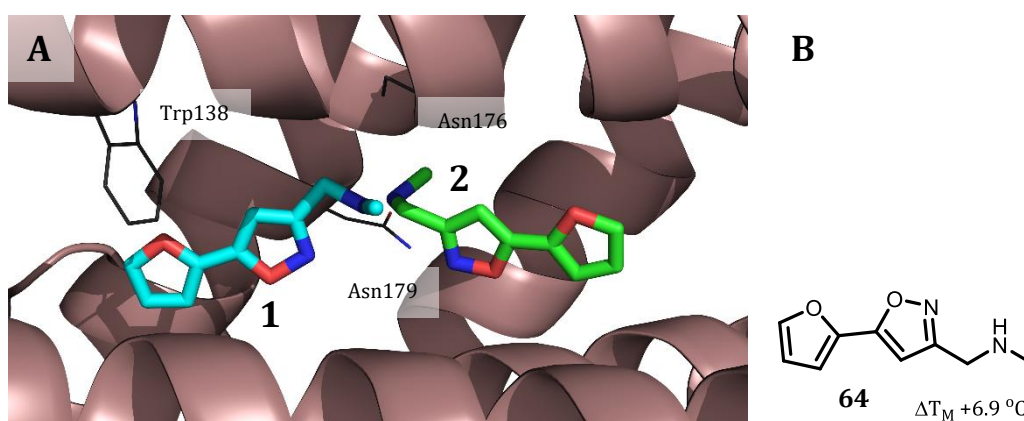
Figure 28: (A) - X-ray crystal structure of fragment **64** (blue and green), bound twice to EthR. The NH of 1 (blue) is 1.4 Å from the CH_2 of 2 (green); (B) - Structure of fragment **64**.

2.2.1   5-(Furan-2-yl)-isoxazole fragment-linking approach

A fragment linking strategy, guided by X-ray crystallography was applied by linking fragments (5-(furan-2-yl)isoxazol-3-yl)methanamine (**77**) and 5-(furan-2-yl)isoxazole-3-carboxylic acid (**78**). This was achieved in an amide bond forming reaction, using COMU to obtain the compound **79** in 74% yield (Scheme 4).
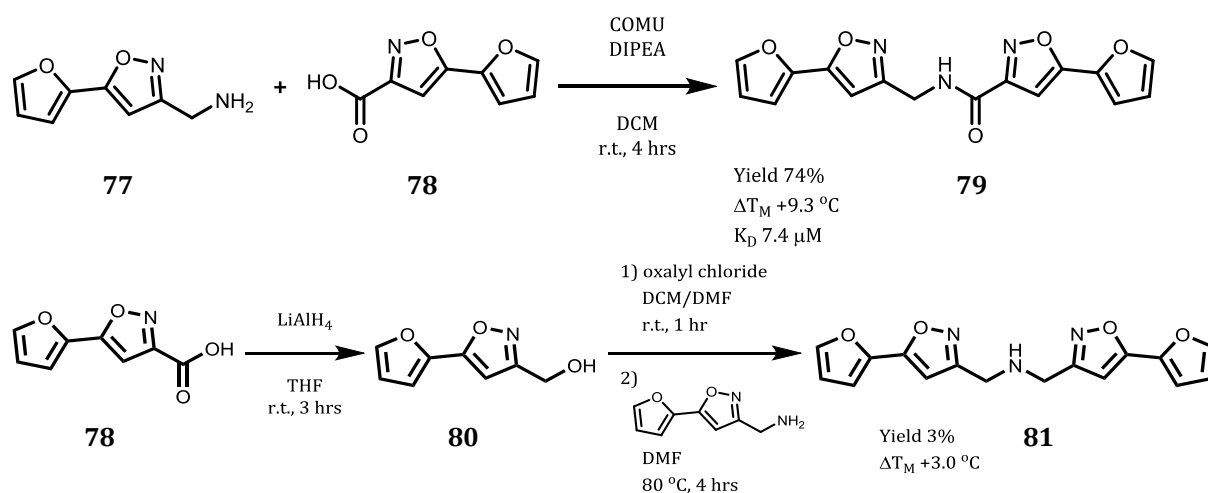
Scheme 4: Synthesis of compounds **79** and **81**. Compound **79** was synthesised by coupling the amine **77** and acid **78** using COMU. Acid **78** was reduced to the alcohol **80** with LiAlH$_4$, then coupled to the amine **77** via the alkyl chloride to form compound **81**.

In order to obtain the symmetrical molecule (**81**), the acid (**78**) was reduced using LiAlH$_4$ to the alcohol (**80**). The acyl chloride was synthesised using oxalyl chloride and the amine (**77**) was coupled to yield the compound (**81**).

Compounds **79** and **81** were examined by differential scanning fluorimetry (DSF), and ΔT_{MS} [1 mM] of +9.3 and +3.0 °C were measured respectively. Compound **79** was examined by isothermal titration calorimetry (ITC), where a K_D of 7.4 μM was measured. These results demonstrate a significant improvement in binding affinity over the starting fragment **64**.

## 2.2.2   1,2,4-Oxadiazole fragment-linking approach

In order to allow for potential modification of the terminal furan ring of fragment **64**, a synthetic strategy was selected using a 1,2,4-oxadiazole heterocyclic ring to synthesise the molecules, allowing the compounds to be treated as modular in nature. Willand *et al.* showed that 1,2,4-oxadiazoles were tolerated as scaffolds that can bind in the EthR-binding pocket.[44] The synthesis of these heterocyclic rings can be achieved where the starting materials are prepared from commercially available carboxylic acids combined with amidoximes which are synthesised from the corresponding nitriles. Benzonitrile was utilised as the starting nitrile to provide a simplified aromatic functionality.

Benzonitrile (**82**) was converted to benzamidoxime (**83**) through heating with hydroxylamine hydrochloride in the presence of diisopropylethylamine (DIPEA). The product was obtained in 76% yield. This was reacted with Boc-glycine and HBTU in the presence of DIPEA to synthesise the Boc-protected compound. This was deprotected with HCl to yield compound **85** in 42% yield (Scheme 5). The benzamidoxime (**83**) was coupled with ethyloxalyl chloride at 0 °C in the presence of pyridine to yield the ester (**87**) in 25% yield, in order to synthesise the carboxylic acid for the linking strategy. The hydrolysis of this ester was attempted with sodium hydroxide, however the acid was not obtained due to decarboxylation which was observed by MS and NMR. An attempt to synthesise the amide directly from the ester **87** and amine **85** was also unsuccessful, as was synthesising the *tert*-butyl ester with deprotection by TFA.
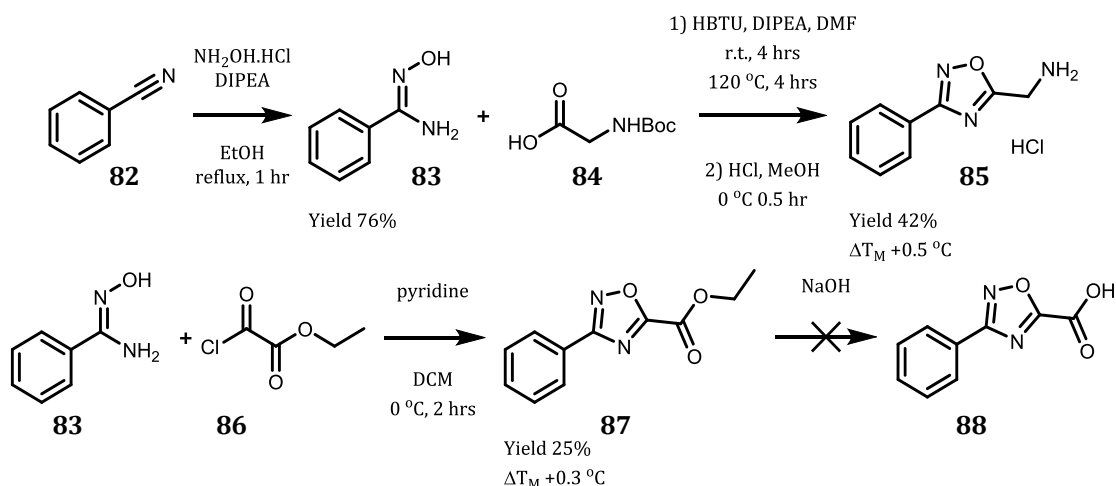
Scheme 5: Synthesis of compounds **83**-**87**. The amidoxime **83** was synthesised from benzonitrile (**82**) with hydroxylamine hydrochloride. This was used to synthesise compound **85** from Boc-glycine (**84**) followed by deprotection of the amine with HCl. The amidoxime (**83**) was also used to synthesise compound **87** from ethyloxayl chloride (**86**).

As the carboxylic acid **88** proved difficult to synthesise, an alternative strategy was employed where an amine linked compound (**93**) was proposed. This was synthesised using a one-pot strategy from glycine (**89**) and isobutyl chloroformate (**90**) at 0 °C with triethylamine (TEA) and activated 4 Å molecular sieves. This was followed by the addition of benzamidoxime and heating the reaction to reflux where compound **91** was isolated in 86% yield. The carbonate (**91**) was treated with sodium hydroxide to yield the alcohol (**92**) (Scheme 6).
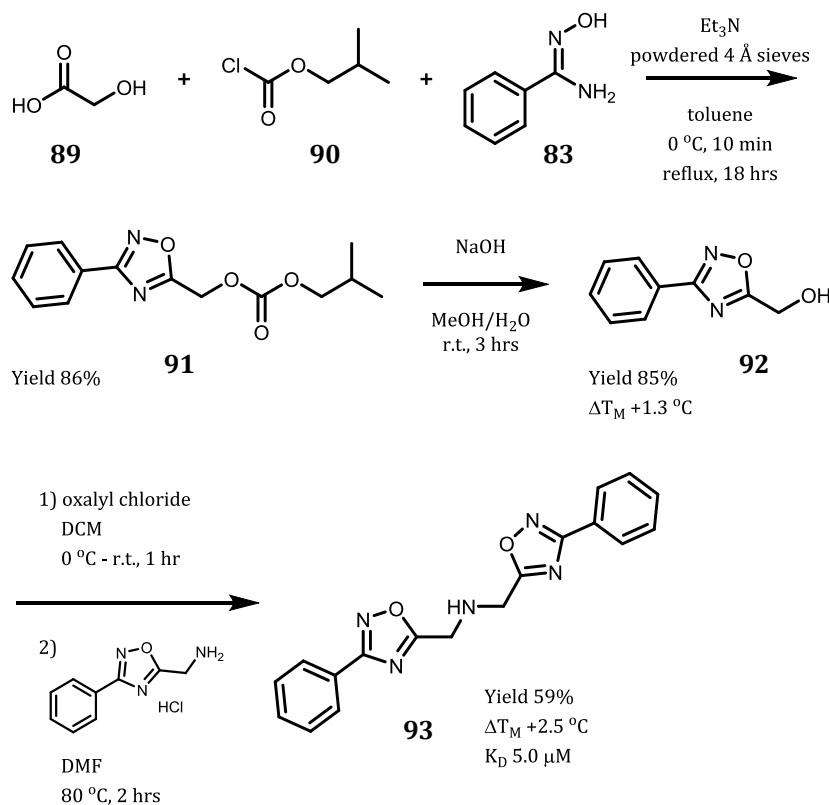
Scheme 6: Synthesis of compounds **91-93**.

Compounds **92** and **85** were used to synthesise the linked compound **93** by treatment of **92** with oxalyl chloride followed by addition of the amine **85** and heating to 80 °C, to yield **93** in 59% yield (Scheme 6).

During the course of this work, Huguet *et al.* reported that the treatment of 1,2,4-oxadiazole-5-carboxylate esters with base results in the decarboxylation of the starting material rather than the hydrolysis of the ester.[101] In light of this, the oxadiazole strategy was changed to use a 5-aryl-1,2,4-oxadiazole as the starting scaffold. As proof of concept, compound **97** was synthesised by reacting **95** with benzoyl chloride (**94**) in DCM with pyridine at room temperature, followed by heating in DMF to promote the ring closure to the oxadiazole

(Scheme 7) and this yielded the ester **96** in 80% yield. The ester product was hydrolysed with lithium hydroxide to yield the corresponding acid **97** in 62% yield.
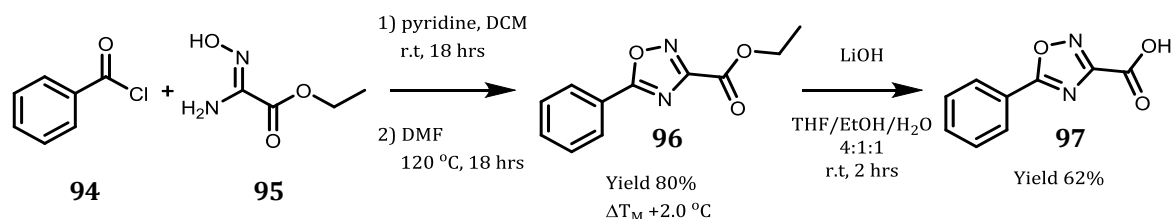
Scheme 7: Synthesis of compounds **96** and **97**.

The ester (**96**) was screened by DSF, where a ΔT_M of +2.0 °C [1 mM] was observed. Due to the difficulties in synthesising the desired 1,2,4-oxadiazole compounds, and solubility difficulties with this series of compounds this series was discontinued in favour of other fragments which were more synthetically tractable.

2.3   Sulfone fragment merging strategies
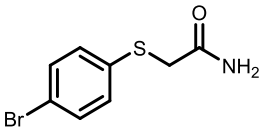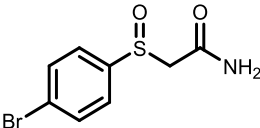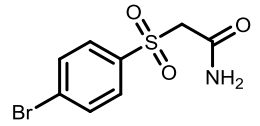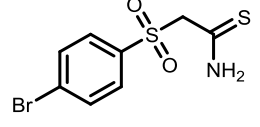
Fragment **65** (Scheme 8) was identified from the fragment screen as having a ΔT_M of +4.5 °C, and a K_D of 36 µM suggesting that this is a good starting point for fragment elaboration. X-ray crystallography (Sachin Surade, Department of Biochemistry) showed that fragment **65** bound twice within the EthR binding pocket. The first molecule (Scheme 8a) is located in the centre of the binding pocket, making interactions between the sulfonyl oxygens and the side-chain nitrogen of Asn179, while the thioamide nitrogen H-bonded with the side-chain carbonyl of Asn176. The second molecule of **65** (Scheme 8b) was shown to bind at the solvent exposed end of the EthR binding pocket, lying across the entrance making a H-bonding interaction with the hydroxyl of Tyr148.
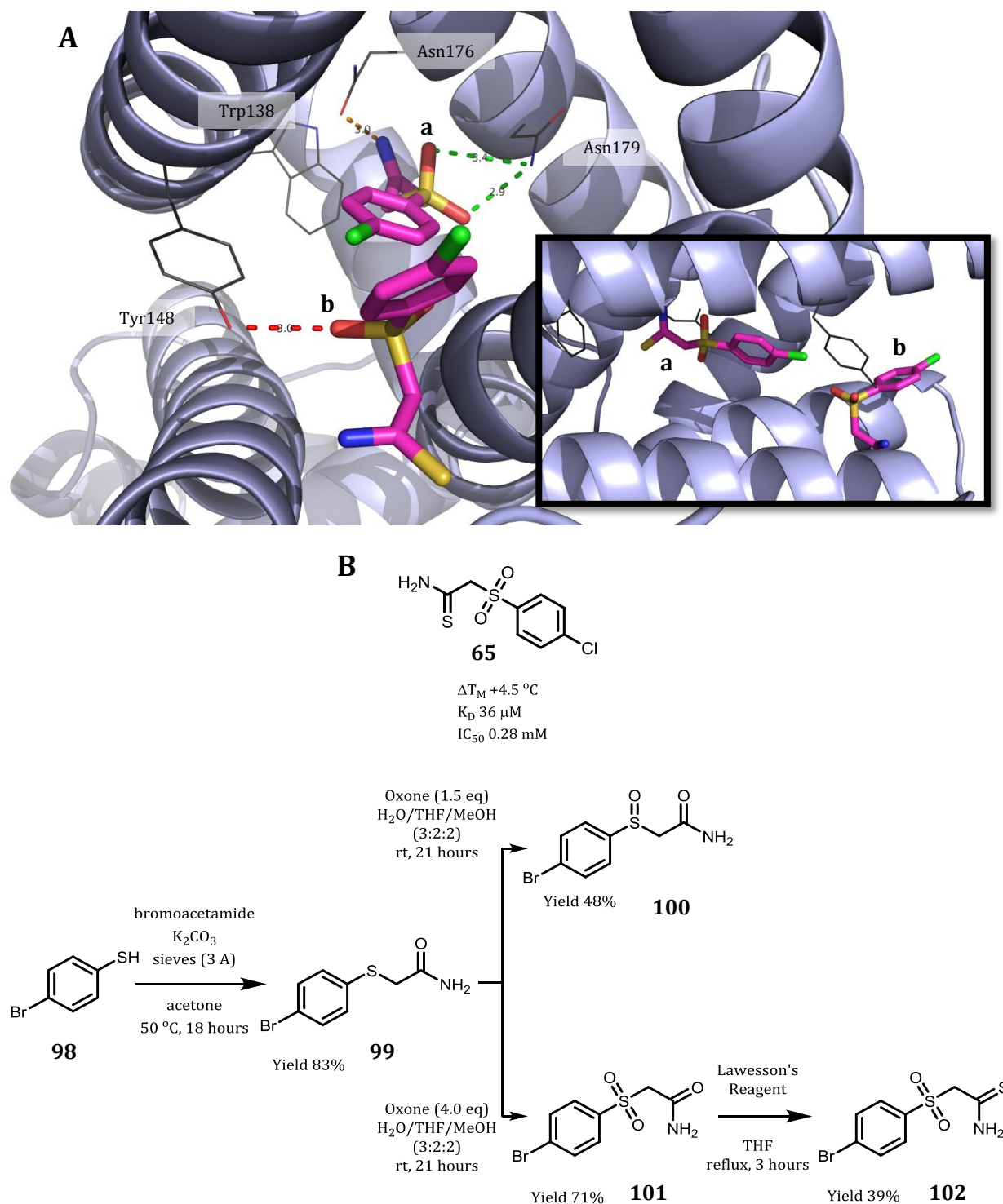
Scheme 8: (A) - X-ray crystal structure of **65** showing H-bonding interactions. The oxygens of the sulfonyl of 'a' is able to interact with the N of Asn179 at distances of 2.9 and 3.2 Å (green dashed lines), while the nitrogen of the thioamide sits at 3.0 Å from the oxygen of Asn176 (orange dashed line). One oxygen of the sulfonyl of 'b' rests at 3.0 Å from the hydroxyl of Tyr148 (red dashed line); (B) - Structure of **65**; (C) - Synthesis of compounds **99**-**102**.

The synthesis of the thioether **99** was carried out where the thiol of 4-bromothiophenol (**98**) was alkylated with bromoacetamide in the presence of potassium carbonate in 83% yield (Scheme 8). The sulfur was oxidised using Oxone™, controlling the quantity of Oxone™ at 1.5 (sulfoxide) and 4 (sulfone) equivalents to produce a hydrogen-bond donor near the Asn179 side-chain nitrogen of EthR. When these compounds (**99** and **100**) were screened by DSF against EthR, they showed no indication that they stabilised EthR, while the sulfone compound **101** produced a K_D of 43 µM by ITC. The thioamide (compound **102**) was synthesised from compound **101** using Lawesson's reagent in 39% yield. This compound gave a K_D of 17 µM as measured by ITC, an improvement by a factor of two over fragment **65** (Table 1).

Table 1: DSF and ITC results for compounds **99-102**. DSF solutions: 1, 2.5 or 5 mM fragment, 20 mM EthR, 150 mM NaCl, 20 mM Tris-HCl (pH 8.0), 2.5x SYPRO® Orange, 100 µL final volume. ITC conditions: buffer 300 mM NaCl, 20 mM Tris-HCl (pH 8.0), glycerol (matched to EthR stock). Compounds (100 mM in DMSO) were diluted to 0.75 mM in buffer. EthR (75 µM) prepared in buffer with 10% DMSO.

#		ΔT_M (°C)	K_D (µM)
99		0.3 [1 mM]	-
100		-0.3 [2.5 mM]	-
101		-1.0 [5 mM]	43
102		0.5 [1 mM]	17

An overlay of the X-ray crystal structures of fragments **103** and **65** (Figure 29) led to the development of merged compound **104** (Scheme 9). The synthesis employed a method similar to those described by Curti *et al.*[102] where the sodium sulfinate intermediate was synthesised,

followed by oxidative addition of bromoacetamide in the presence of pyridine. The amide **107** was converted to the thioamide using Lawesson's reagent in 53% yield. This compound (**104**) was shown to bind to EthR when screened by DSF (ΔT_M +4.2 °C [1 mM]), ITC (K_D 21 µM), and SPR (IC_{50} 20 µM) (Table 2).
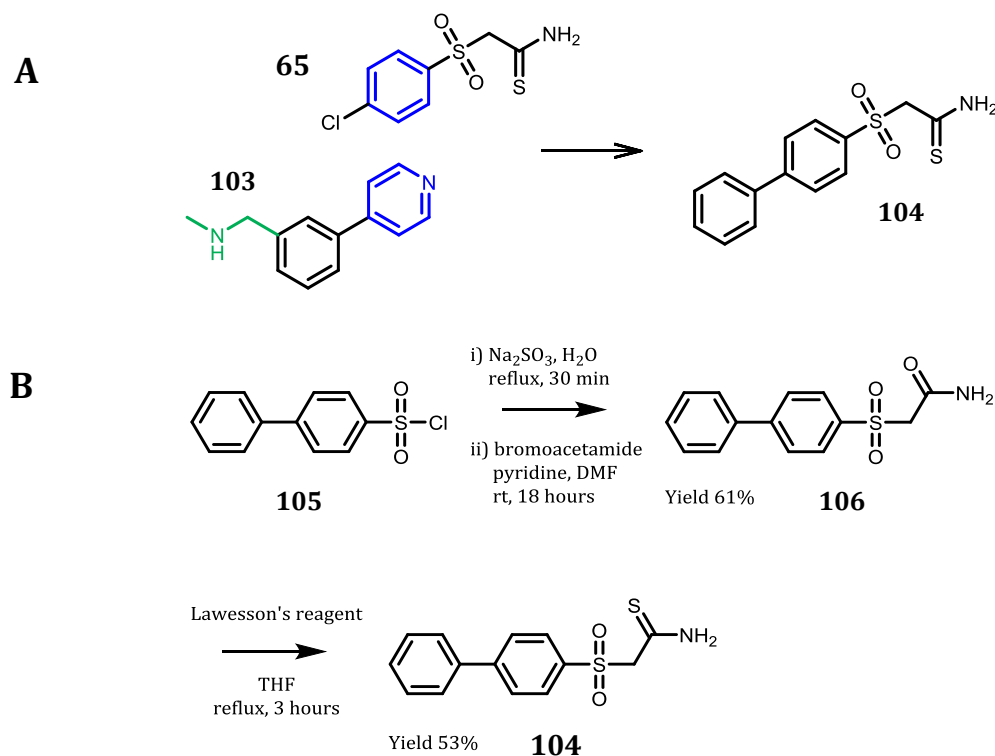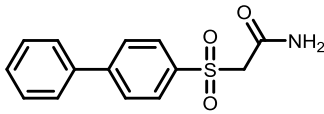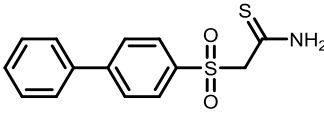
Scheme 9: (A) – Fragment merging strategy of fragments **65** and **103**. Overlap (blue) of the phenyl ring of **65** with the pyridine ring of **103** led to compound **104**; (B) – Synthesis of compounds **104** and **106**.
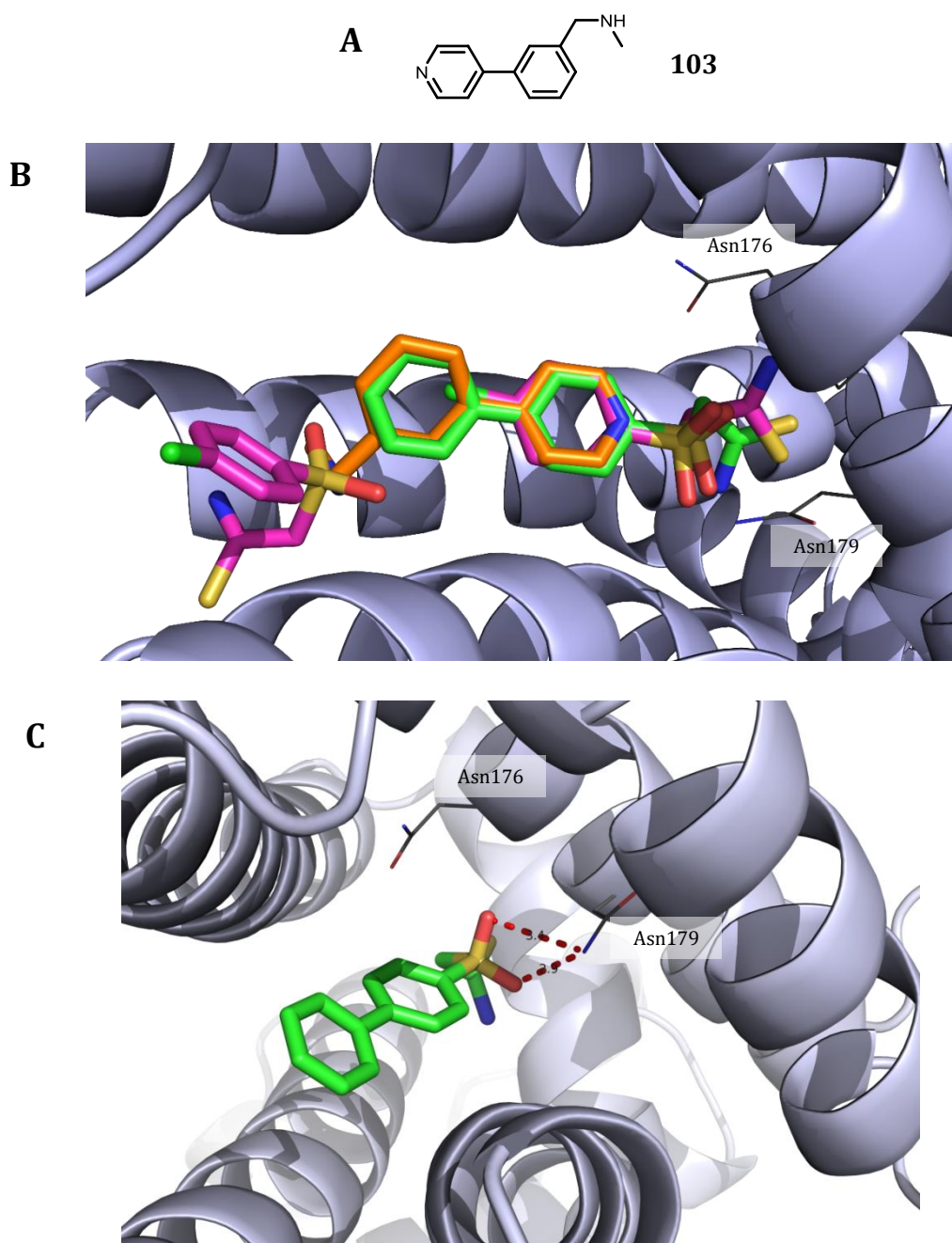
Figure 29: (A) – Structure of compound **103**; (B) - Overlay of X-ray crystal structures of **65** (pink) and **103** (orange) bound to EthR (Sachin Surade) with compound **104** (green, Michal Blaszczyk). This overlay led to the merged fragment series containing the biphenylsulfonyl scaffold; (C) - X-ray crystal structure of **104** showing the H-bonding interactions between the compound and Asn179. The oxygens of the sulfonyl group are able to interact with the side-chain NH_2 of Asn179 at 3.4 and 2.9 Å (red dashed lines). The thioamide orientation changes in comparison to **65**, where it no longer makes an interaction with Asn176.

Table 2: Biophysical screening results for compounds **106** and **104**. DSF solutions: 1 or 5 mM fragment, 20 mM EthR, 150 mM NaCl, 20 mM Tris-HCl (pH 8.0), 2.5x SYPRO® Orange, 50 µL final volume. ITC conditions: buffer 300 mM NaCl, 20 mM Tris-HCl (pH 8.0), glycerol (matched to EthR stock). Compounds (100 mM in DMSO) were diluted to 0.75 mM in buffer. EthR (75 µM) prepared in buffer with 10% DMSO. SPR solutions: running buffer 2 mM $MgCl_2$, 10 mM Tris-HCl (pH 7.5), 0.1 mM EDTA, 200 mM NaCl, 2% DMSO. EthR prepared as 2 µM in running buffer. Compounds were prepared at varying concentrations in running buffer.

#		ΔT_M (°C)	K_D (µM)	IC_{50} (µM)
106		12.5 [5 mM]	25	>100
104		4.2 [1 mM]	21	20.0

2.4 Fragment growing by modification of the thioamide group

Modification of the thioamide functionality of compound **104** (section 2.3) was explored where this was incorporated into a thiazole ring to investigate the necessity of the amide NH_2 hydrogen-bond donating group, while providing a potential handle for fragment-growing into the deeper region of the EthR binding pocket. The first compound synthesised was a thiazole (**110**) which was synthesised by reacting sodium sulfate with the 2-(bromomethyl)thiazole, produced from 2-(hydroxymethyl)thiazole with phosphorous tribromide (Scheme 10). The second compound, a thiophene (**111**) was synthesised using the same method, where 2-(hydroxymethyl)thiophene was used as the starting material. The thiazole **110** gave a ΔT_M of +5.0 °C [1 mM], and subsequent SPR testing recorded an IC_{50} of 11 µM. The thiophene **111** produced a stronger thermal stabilisation with a ΔT_M of +9.0 °C [1 mM], in addition to a K_D of 12 µM by ITC and IC_{50} of 9 µM suggesting that the nitrogen is not essential for the activity of the molecule.
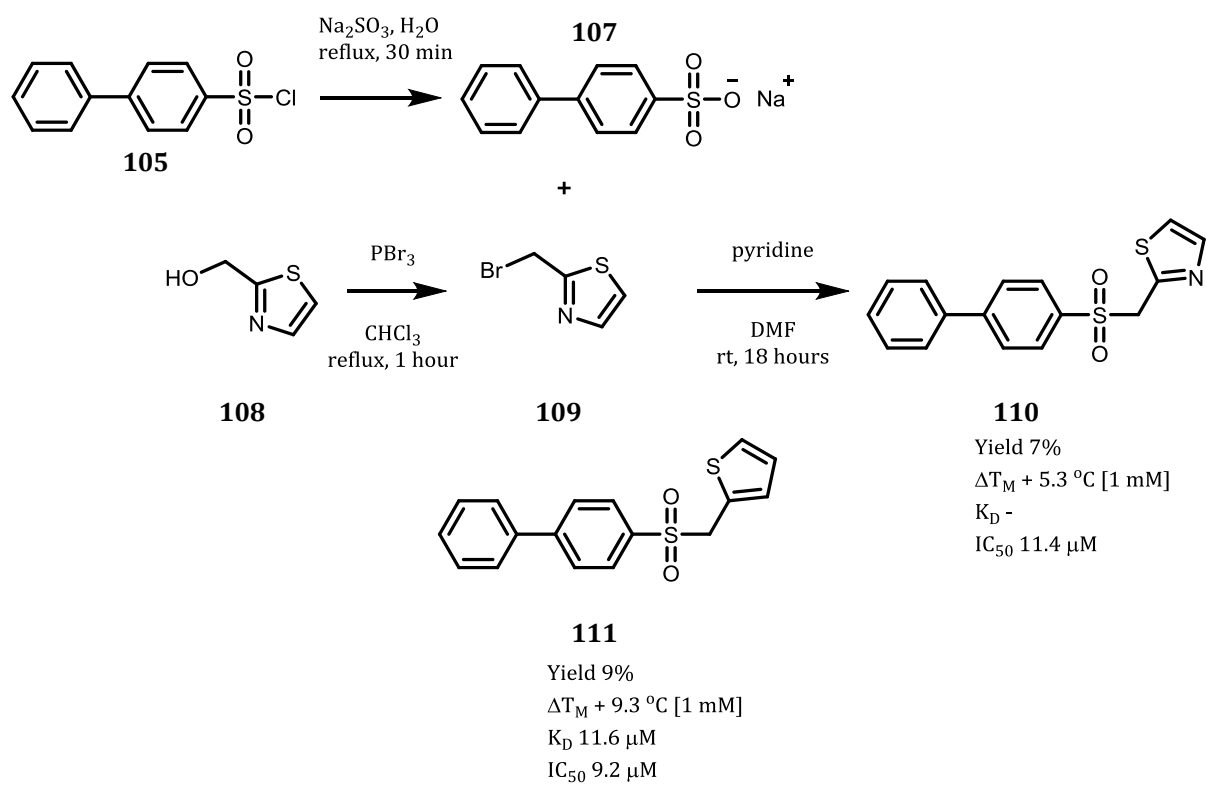
Scheme 10: Synthesis of compounds **107-111**.

107

+

108 → PBr$_3$, CHCl$_3$ reflux, 1 hour → **109** → pyridine, DMF, rt, 18 hours → **110**

110
Yield 7%
ΔT_M + 5.3 °C [1 mM]
K_D -
IC$_{50}$ 11.4 μM

111
Yield 9%
ΔT_M + 9.3 °C [1 mM]
K_D 11.6 μM
IC$_{50}$ 9.2 μM

Na$_2$SO$_3$, H$_2$O
reflux, 30 min

105
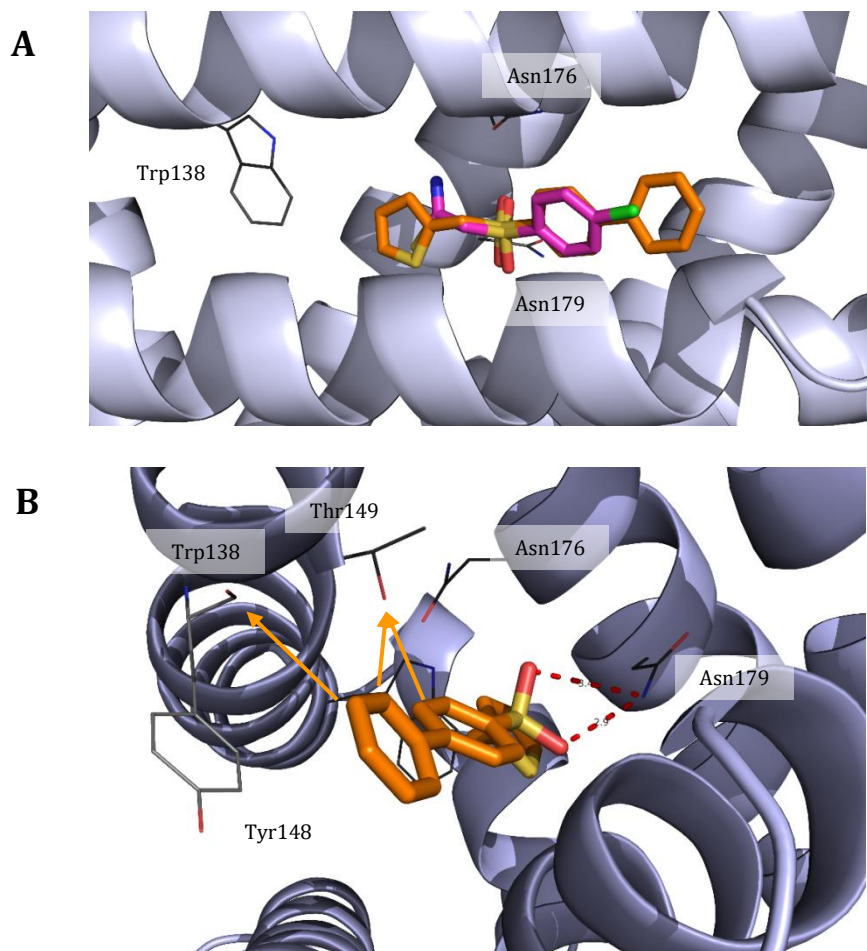
Figure 30: (A) – Overlay of X-ray crystal structures of **65** (pink) and **111** (orange); (B) - H-bonding interactions between the sulfonyl oxygens of **111** and Asn179 of EthR at distances of 2.9 and 3.4 Å (red dashed lines). Potential interactions with the amide carbonyl of Tyr148, and with the hydroxyl of Thr149 (orange arrows) shown.

Three potential interactions of compound **111** were identified from the X-ray crystal structure (Figure 30). The *meta*-carbon of the phenyl ring is 4.1 Å from the amide carbonyl Tyr148, while the carbons *ortho* to the biphenyl linkage is 3.2 and 3.7 Å from the hydroxyl of Thr149. In order to exploit the potential Tyr148 interaction, compound **114** was synthesised (Scheme 11). Although the K_D of **114** was found to be 8 μM, this improvement in affinity was not supported by an improvement in IC_{50} of 15 μM over that of **111**. This suggests that the improvement in binding affinity was not translated into an improved functional interaction. The synthesis of compounds with a 2-pyridyl ring in place of the 3-pyridyl ring of **111** was attempted, however due to the de-boronation of 2-pyridylboronic acids under Suzuki conditions, and the failure of 2-pyridylboronate-MIDA esters,[103-105] neither of these proved successful *via* the methods employed.

Previous work by Frenois *et al.*[43] has shown that hexadecyloxtanoate resides deeper in the binding pocket of EthR than the fragments thus far examined. In an attempt to probe deeper into the EthR binding pocket, compound **120** was synthesised (Scheme 11), providing an extended, flexible hydrophobic group. Screening of compounds **119** and **120** produced ΔT_M values of +3.8 and +1.8 °C [1 mM] respectively, with a IC_{50} of 12 μM for compound **120** (Sherine Thomas). This suggests that this is a potential means for extending the compounds from the thioamide nitrogen while still maintaining potency.
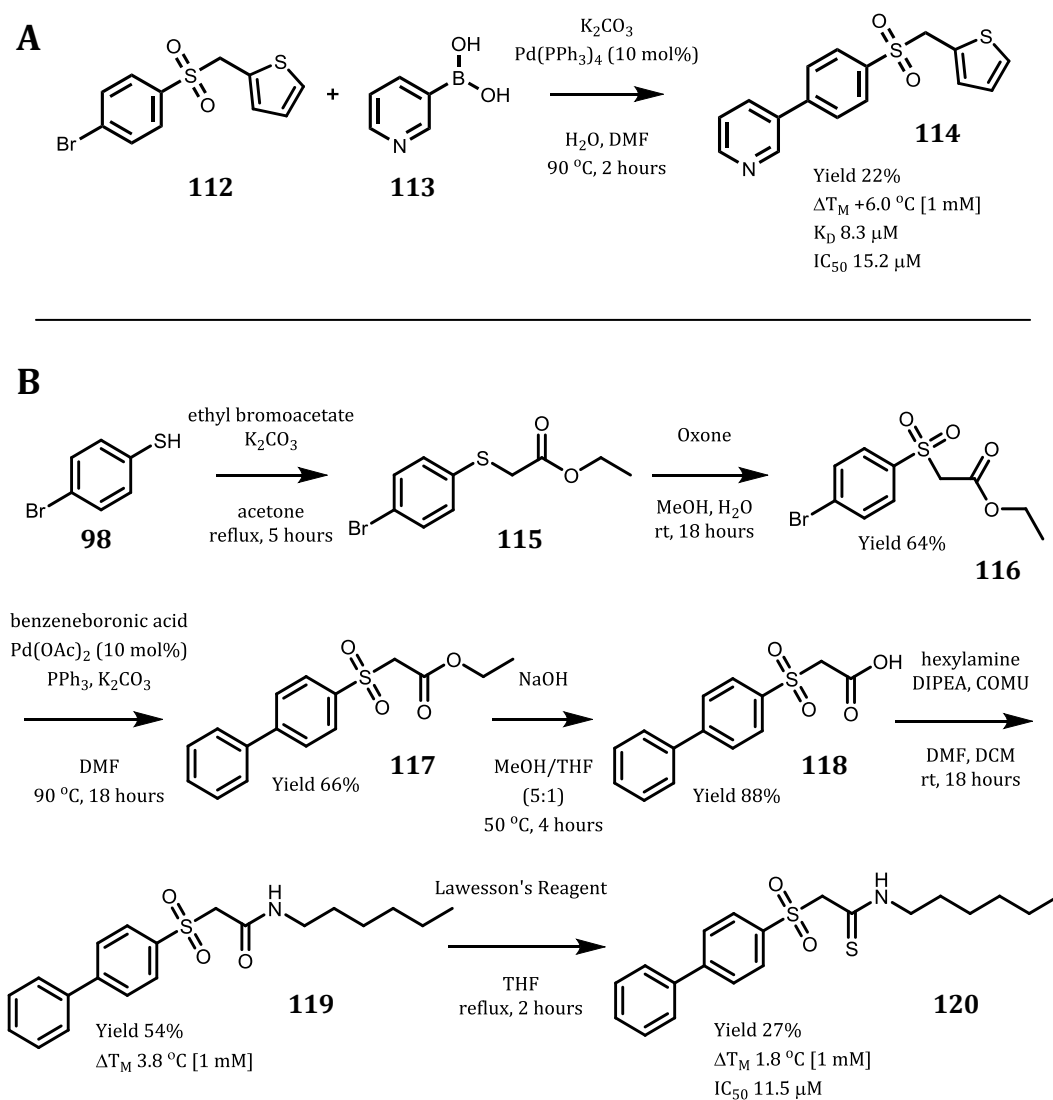
Scheme 11: (A) Synthesis of compound **114**; (B) Synthesis of **120**, the thiol (**98**) was acylated with ethyl bromoacetate, then the thioester (**115**) oxidised to the sulfone (**116**) using Oxone™. Suzuki cross-coupling chemistry was used to add the second benzene ring before the ester was hydrolysed to the acid (**118**). Hexylamine was added by COMU coupling and the amide converted to the thioamide **120** with Lawesson's reagent.

2.5   Conclusions

The use of both fragment merging and growing strategies has been applied to two fragments previously identified through a fragment screen against EthR. The first fragment (**64**) was elaborated using a fragment merging approach where the use of structural biology was key in the development of novel compounds. The best compound in this series was compound **79**, which had a K_D of 7.4 μM, however due to the synthetic complexity of this series, they were discontinued.

The second fragment (**65**) examined contained an aryl-sulfone core, and was elaborated by fragment-merging strategies with fragment **103**. This led to compound **104** with a K_D of 21 μM and an IC_{50} of 20 μM. The oxidation states of the sulfur were explored and this indicated that only the sulfone was beneficial to binding, confirming the importance of the sulfone interaction with Asn179 seen in the X-ray crystal structure (Scheme 8).

On changing of the thioamide into a thiazole ring (compound **110**) the IC_{50} decreased to 11 μM, while the corresponding thiophene (compound **111**) demonstrated an IC_{50} of 9 μM. The thiazole and thiophene rings provided greater stability against oxidation for the sulfur group compared to the thioamide, without compromising the functional activity of the scaffold. On substituting the biphenyl ring system with a 4-(pyridine-3-yl)benzene group (compound **114**), this did not provide an improvement in affinity.

This chapter has explored the linking of adjacent fragments within the EthR binding pocket, in addition to the use of sulfone-containing compounds to provide an anchor through the interaction with Asn179 of EthR to allow for growth into the EthR binding pocket. The thioamide was further investigated, and by fixing the sulfur into a 5-membered ring generated a compound which was more stable and offered further vectors for elaboration. While both of the fragment series discussed in this chapter offered increased affinity upon elaboration, these were not explored further as other fragment growing strategies were prioritised, and these will be discussed in chapters 3 and 4.

3.0   Fragment growing strategies for targeting EthR

3.1   Piperazines as a privileged structure in drug discovery

This chapter will discuss fragment-growing strategies to target EthR. A piperazine scaffold derived from a fragment hit **66** provides the focus of the fragment-growing strategy where growth is achieved in the EthR binding pocket by the addition of a linker to the piperazine NH and modification of the 5-(trifluoromethyl)pyridine group (Figure 31). This resulted in compounds which are shown to provide a boosting of the effectiveness of ethionamide against *M.tb*.
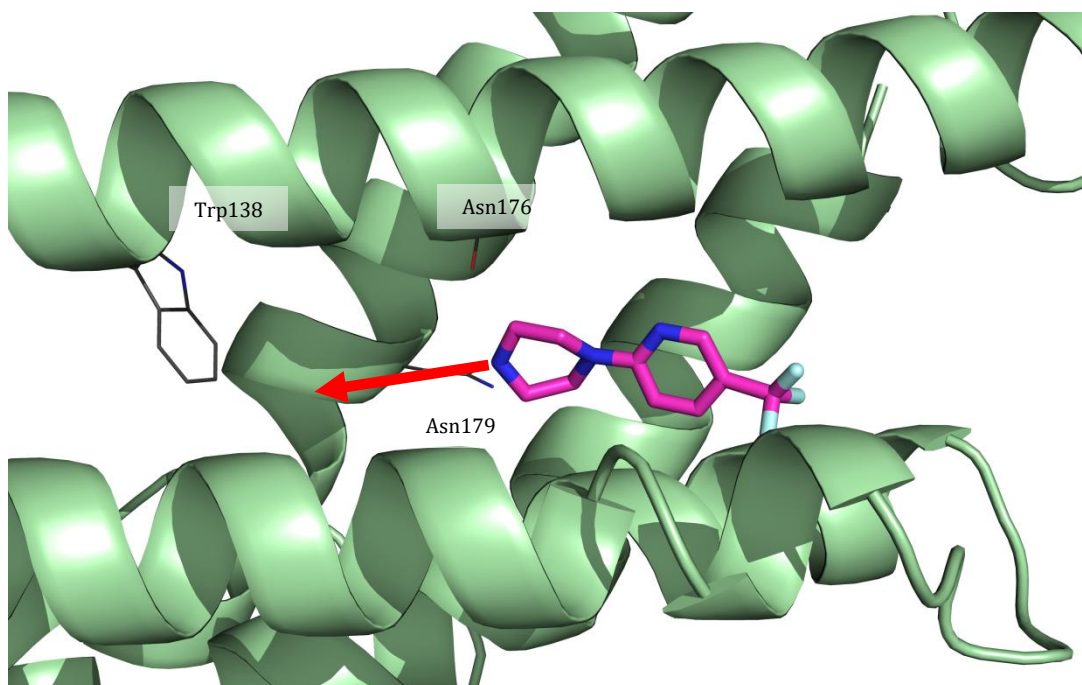
Figure 31: Fragment **66** bound to EthR. This fragment hit was used as the basis for the fragment-growing strategies. Arrow indicates the direction of the primary growth vector examined, extending from the NH of the piperazine.

The piperazine heterocyclic ring is widely utilised in drug discovery as it provides a useful synthetic handle for elaboration from both nitrogens. It has been found to improve the solubility of drugs while providing additional H-bond acceptors.[106] Several drugs containing the piperazine scaffold are known for their psychoactive effects, others have become well known

such as Viagra (Sildenafil, **121**), and in the treatment of a variety of conditions ranging from depression and anxiety to hypertension, malaria and epilepsy (Figure 32).[107]

121

Sildenafil
(vasodilator for erectile dysfunction)

122

para-fluorophenylpiperazine
(psychodelic/euphoric)

123

Buspirone (antidepressant)

124

Cetirizine (antihistamine)

125

Fluphenazine (antipsychotic)
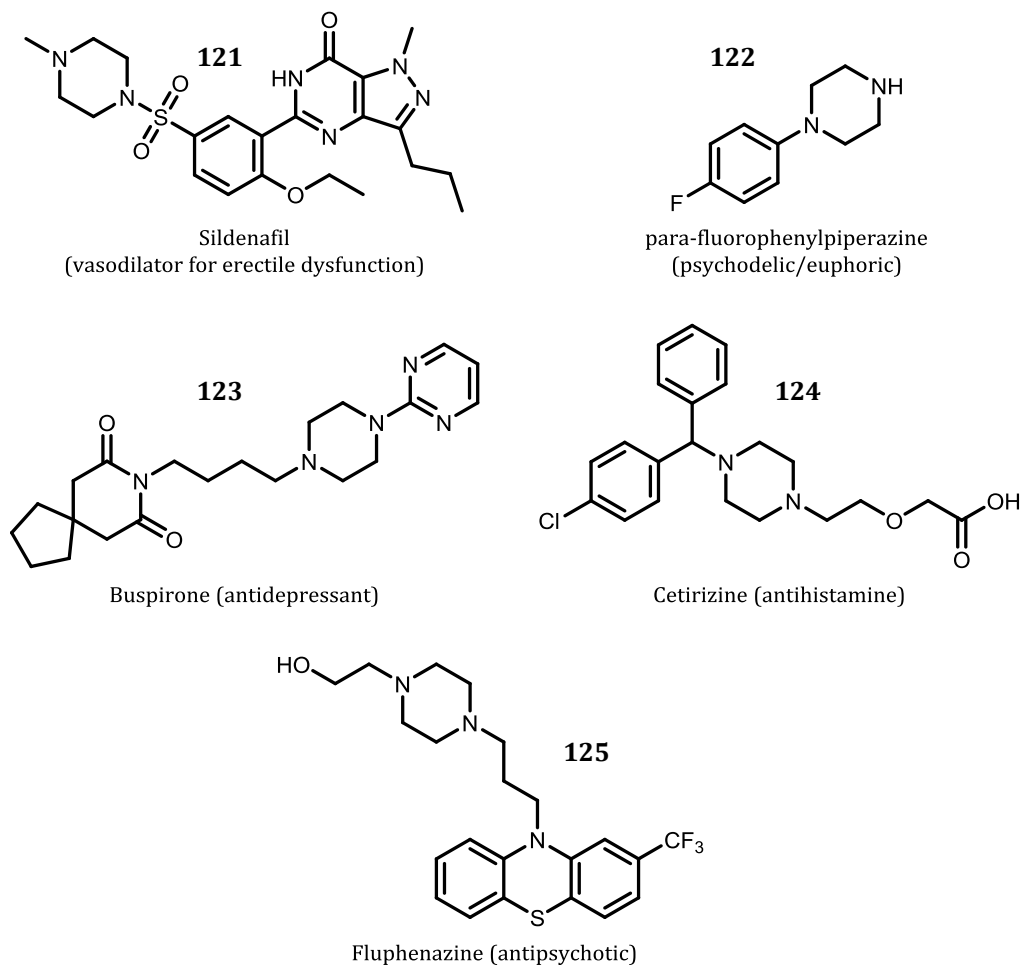
Figure 32: Structures of drugs that contain a piperazine scaffold.

Christopher *et al.*[108] examined the use of fragment-based approaches for targeting the β_1-Adrenergic Receptor (β_1AR) where SPR was used to identify fragments **126** and **127** containing a piperazine ring. The binding pocket of β_1AR is lined by hydrophobic residues (tryptophan, phenylalanine, tyrosine, valine and alanine) with a polar region at the bottom of the pocket. A library of 650 fragments was screened against both β_1AR and Adenosine A_{2A} receptor. Fragments **126** and **127** were identified which were selective for β_1AR, and K_Ds of 16 μM and 6 μM were measured respectively by SPR. Structure-activity relationships were explored to evaluate changes to the aromatic group, and compound **128** showed the greatest K_i by their assay at 68 nM. Protein X-ray crystallography of this compound with β_1AR indicated that the indole was forming a H-bonding interaction with Ser211, while the NH of the piperazine forms interactions with Asn329 and Asp121 (Figure 33).[108]
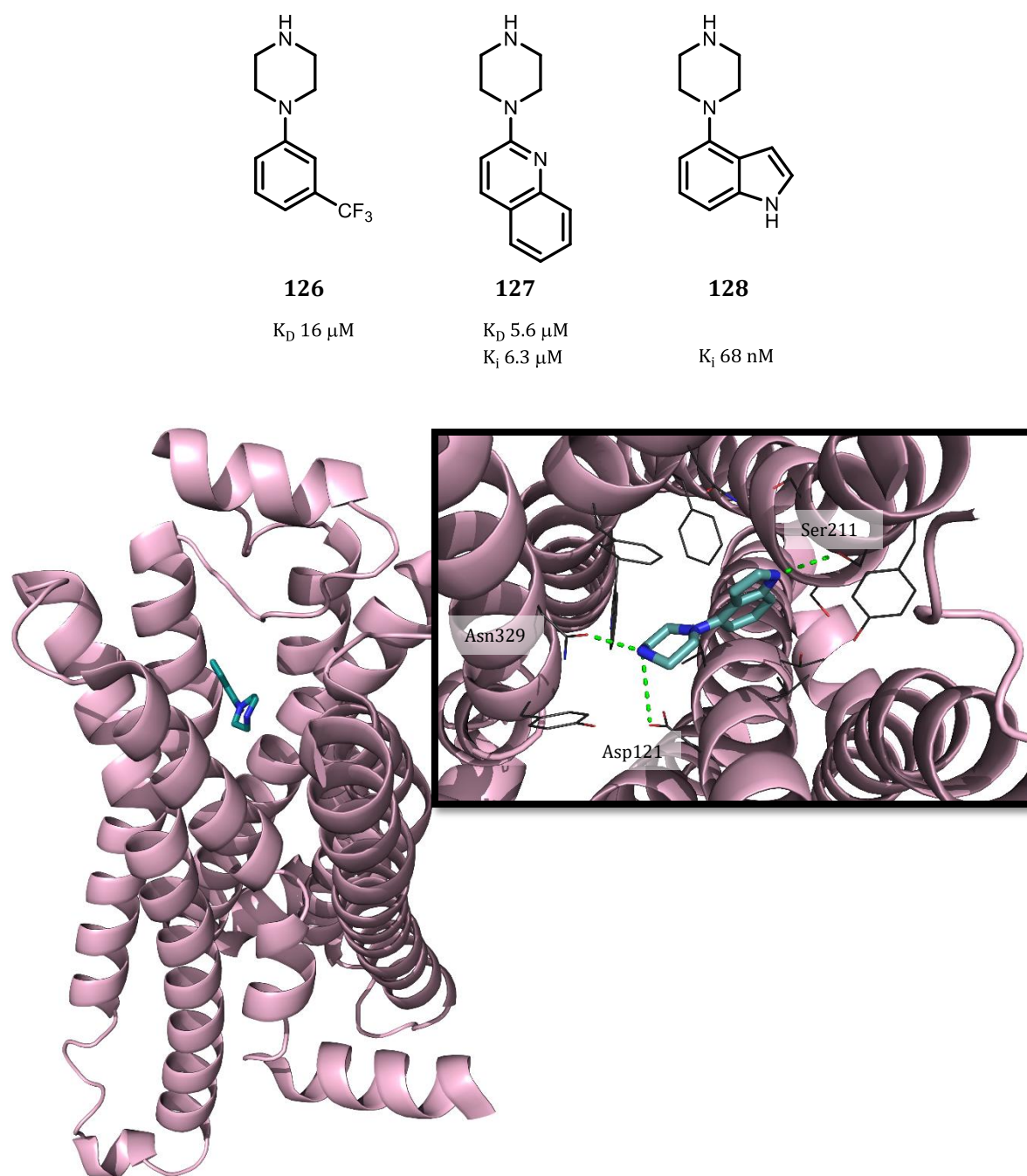
Figure 33: Structures of fragments **126**-**128**. Compound **128** bound to β₁-Adrenergic Receptor (PDB: 3ZPQ). Only the monomer is shown. Inset – compound **128** bound to β$_1$AR showing residues near the fragment and H-bonding interactions (green dashed lines).[108]

The strategies described in this chapter use a piperazine scaffold to provide dual vectors for fragment growth oriented along the EthR binding pocket, allowing fragments to be grown deeper and shallower within the binding site.

3.2   Fragment identification and merging

Fragment **66** was previously identified in a fragment screen against EthR and shown by X-ray crystallography (Dr Vitor Mendes) to bind in two orientations (Figure 34). The two orientations overlap at the piperazine ring, with the 5-trifluoromethylpyridine rings facing either deeper into the pocket, or towards the solvent exposed end of the binding pocket (Figure 34). This fragment gave a ΔT_M of +4.3 °C as determined by differential scanning fluorimetry (DSF), and an affinity (K_D) of 35 µM with EthR by ITC.
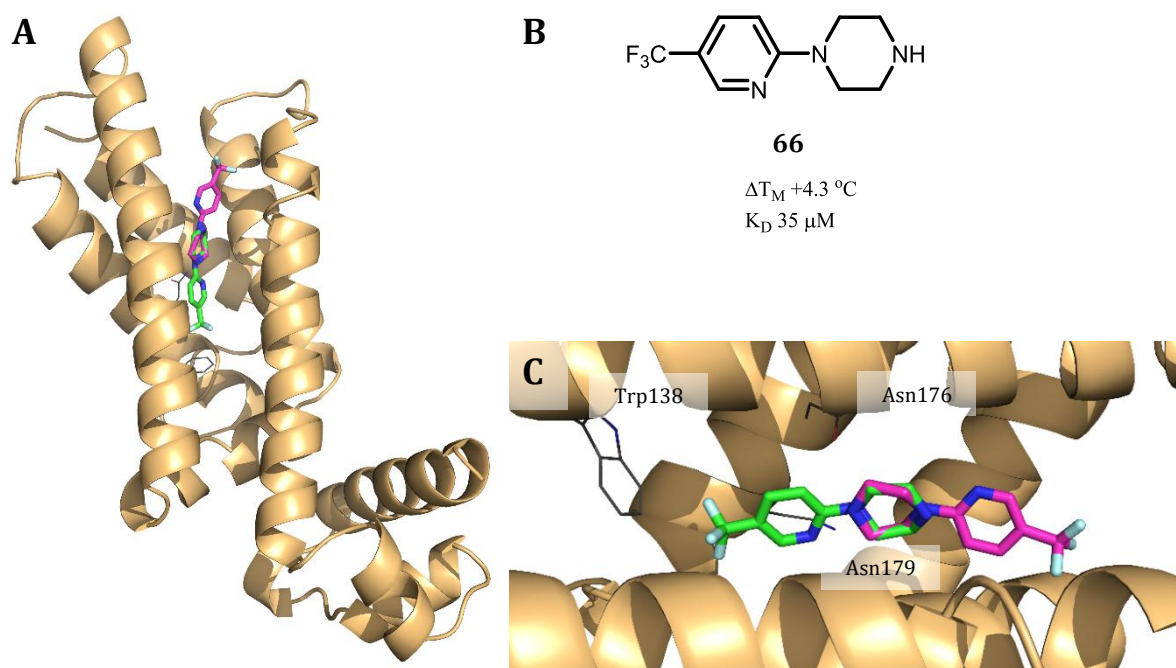
**Figure 34**: (A) - X-ray crystal structure of compound **66** bound to EthR. Only the monomer is shown; (B) - Structure of compound **66**; (C) - X-ray crystal structure of compound **66** (green and pink) bound to EthR showing the two binding poses where the CF$_3$ group faces into the pocket (green) and out of the pocket (pink). In both orientations, the piperazine ring occupies the same position.

In order to examine the dual binding mode of **66**, compound **130** was synthesised (Scheme 12) by alkylation of the NH of compound **66** with 2-bromo-5-trifluoromethylpyridine. A ΔT_M of +7.3 °C [1 mM] was determined by DSF and an IC$_{50}$ of 2.2 µM was measured by SPR. This fragment merging strategy shows that building from both nitrogens of the piperazine can provide compounds with increased affinity and could be used as a strategy to develop novel inhibitors of EthR.
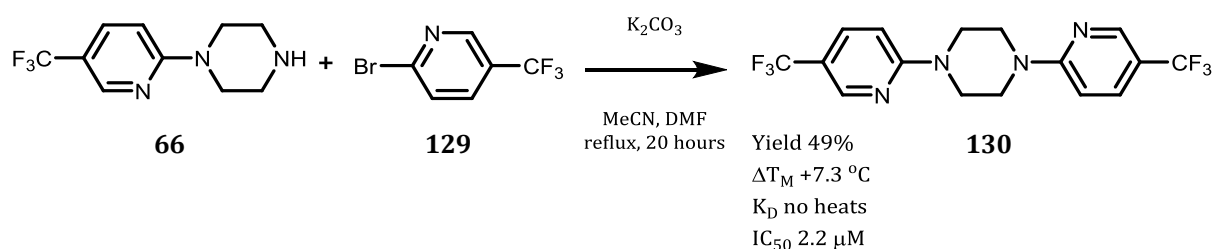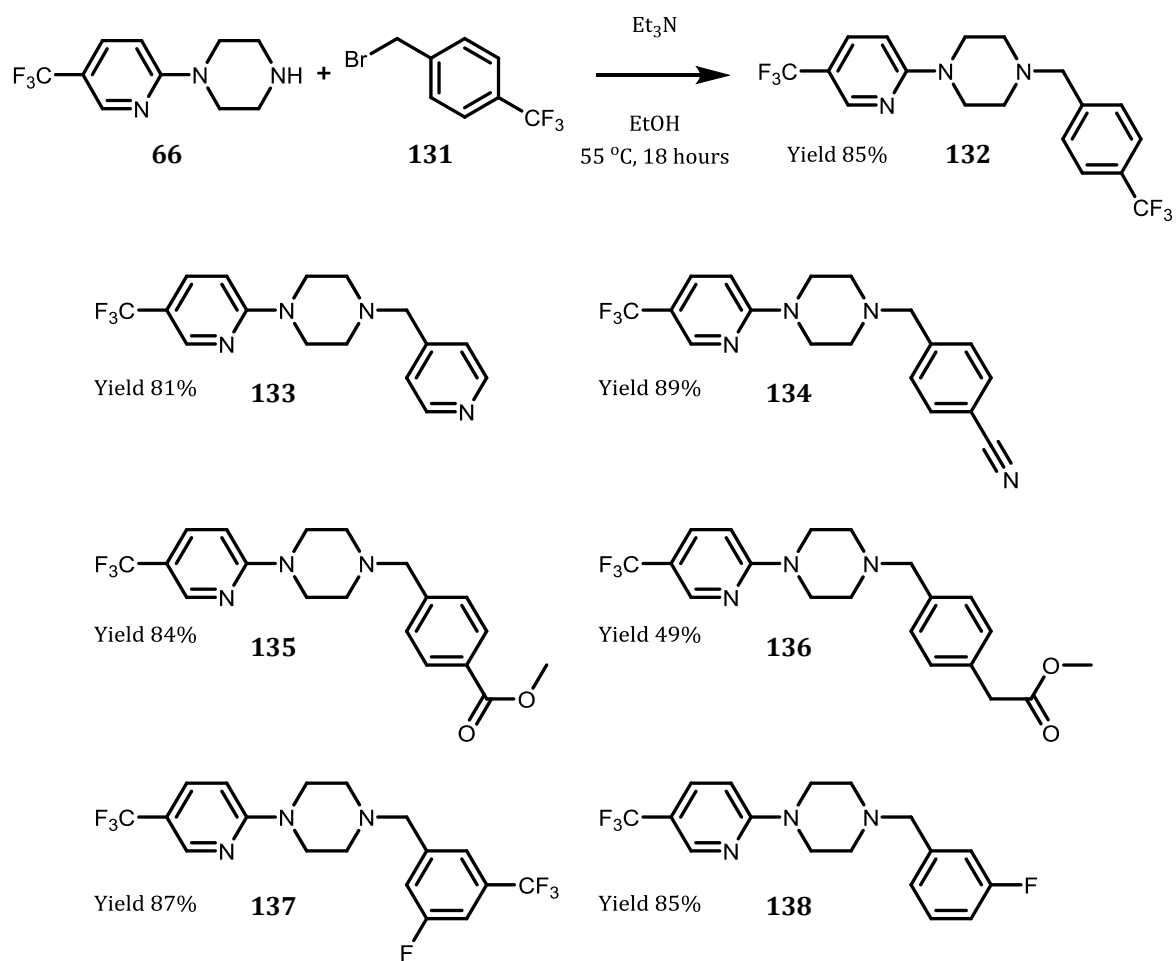
Scheme 12: Synthesis of compound **130**. Fragment **66** was merged with 2-bromo-5-trifluoromethylpyridine (**129**) to yield the merged compound **130**, which retains elements of both binding poses from fragment **66**.

3.3   Fragment growing strategy

3.3.1   Amine linkers
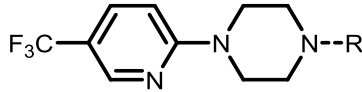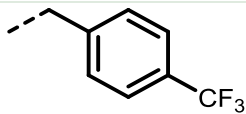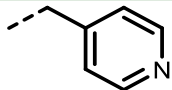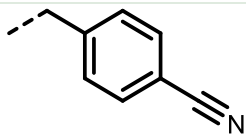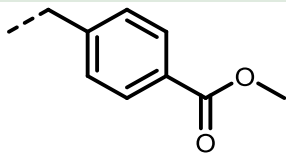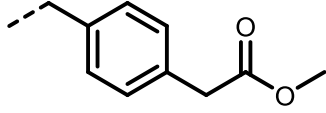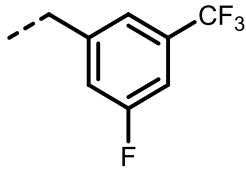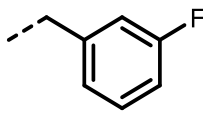
With the knowledge that the binding site of EthR is largely hydrophobic,[35,37] a series of compounds were synthesised based on the piperazine fragment hit **66** (Scheme 13) to investigate the possibility of growing the fragment from the NH of the piperazine ring. A benzyl group with various substitutions at the *meta* or *para* positions or 4-methylpyridine ring was added in this position by N-alkylation with appropriate aryl methylbromides in the presence of Et_3N. These reactions proceeded with yields of 49-89%.

These compounds were examined using DSF and showed only a slight increase in melting temperature (T_M), with a maximum increase of +3.8 °C for compound **137** [2 mM] and +2.5 °C for compound **134** [1 mM]. Compound **137** was examined by ITC, and a K_D of 24 μM was determined, with only a slight improvement over **66** (35 μM). The IC_{50} of this compound (Dr Michal Blaszczyk) against DNA-bound EthR was measured by SPR at 66 μM, while compounds **132**, **134** and **135** gave IC_{50}s >100 μM (Table 3).

Scheme 13: Synthesis of compounds **132-138**. Fragment **66** was coupled to various aryl methylbromides in the presence of triethylamine with mild heating.

Table 3: Table of DSF, ITC, and SPR results for compounds **132-138**. DSF of fragment **66** performed by Narin Hengrung, Department of Biochemistry. DSF solutions: 1,2, or 10 mM fragment, 20 mM EthR, 150 mM NaCl, 20 mM Tris-HCl (pH 8.0), 2.5x SYPRO® Orange, 50 µL final volume. ITC conditions: buffer 300 mM NaCl, 20 mM Tris-HCl (pH 8.0), glycerol (matched to EthR stock). Compounds (100 mM in DMSO) were diluted to 0.75 mM in buffer. EthR (75 µM) prepared in buffer with 10% DMSO. SPR solutions: running buffer 2 mM $MgCl_2$, 10 mM Tris-HCl (pH 7.5), 0.1 mM EDTA, 200 mM NaCl, 2% DMSO. EthR prepared as 2 µM in running buffer. Compounds were prepared at varying concentrations in running buffer.

#	R =	ΔT_M (°C)	K_D (µM)	IC_{50} (µM)
66	---H	+4.3 [10 mM]	35.0	-
132	(4-CF3-benzyl)	+1.3 [1 mM]	-	> 100
133	(4-pyridylmethyl)	+0.2 [1 mM]	-	-
134	(4-cyanobenzyl)	+2.5 [1 mM]	-	> 100
135	(methyl 4-benzoate)	+1.1 [1 mM]	-	> 100
136	(methyl 4-phenylacetate)	+2.1 [1 mM]	-	-
137	(3-CF3-5-F-benzyl)	+3.8 [2 mM]	24.3	66.2
138	(3-F-benzyl)	+2.8 [2 mM]	-	-

Two compounds (**140** and **141**) were synthesised where the linker between the piperazine and aromatic rings was extended by a methylene group (Scheme 14). These compounds were docked into EthR using GOLD (Figure 35) to attempt to predict possible binding interactions, before further biophysical analysis was performed. DSF indicated that both **137** and **141** had a greater increase in melting temperature, with compound **141** producing a ΔT_M of +3.0 °C [1 mM], and a K_D of 1.3 μM with EthR (Table **4**). Observing that both **138** and **137** possess an *m*-fluorobenzene, and compound **137** also had a *m*-trifluoromethyl substituent, a number of compounds were synthesised where the *meta* groups were modified (**142**, **143** and **146**, Scheme 14).
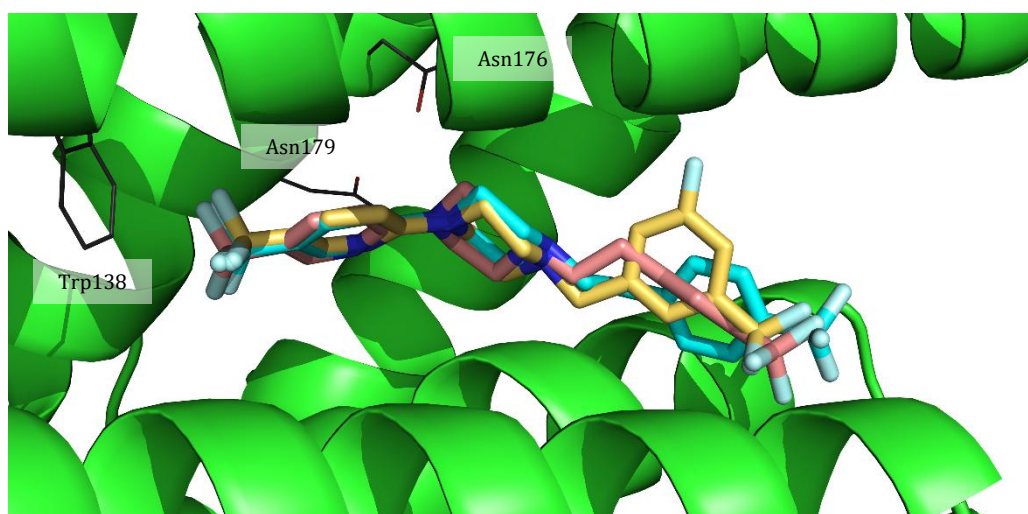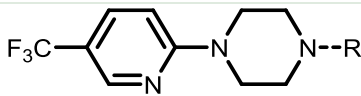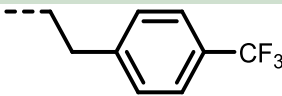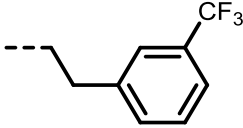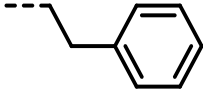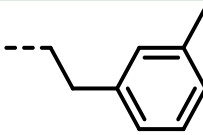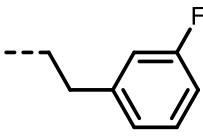
Figure 35: Docked structures of compounds **140** (blue), **141** (pink), and **137** (yellow) overlaid in the EthR binding pocket showing the similarities in the position of the docked CF_3 groups.
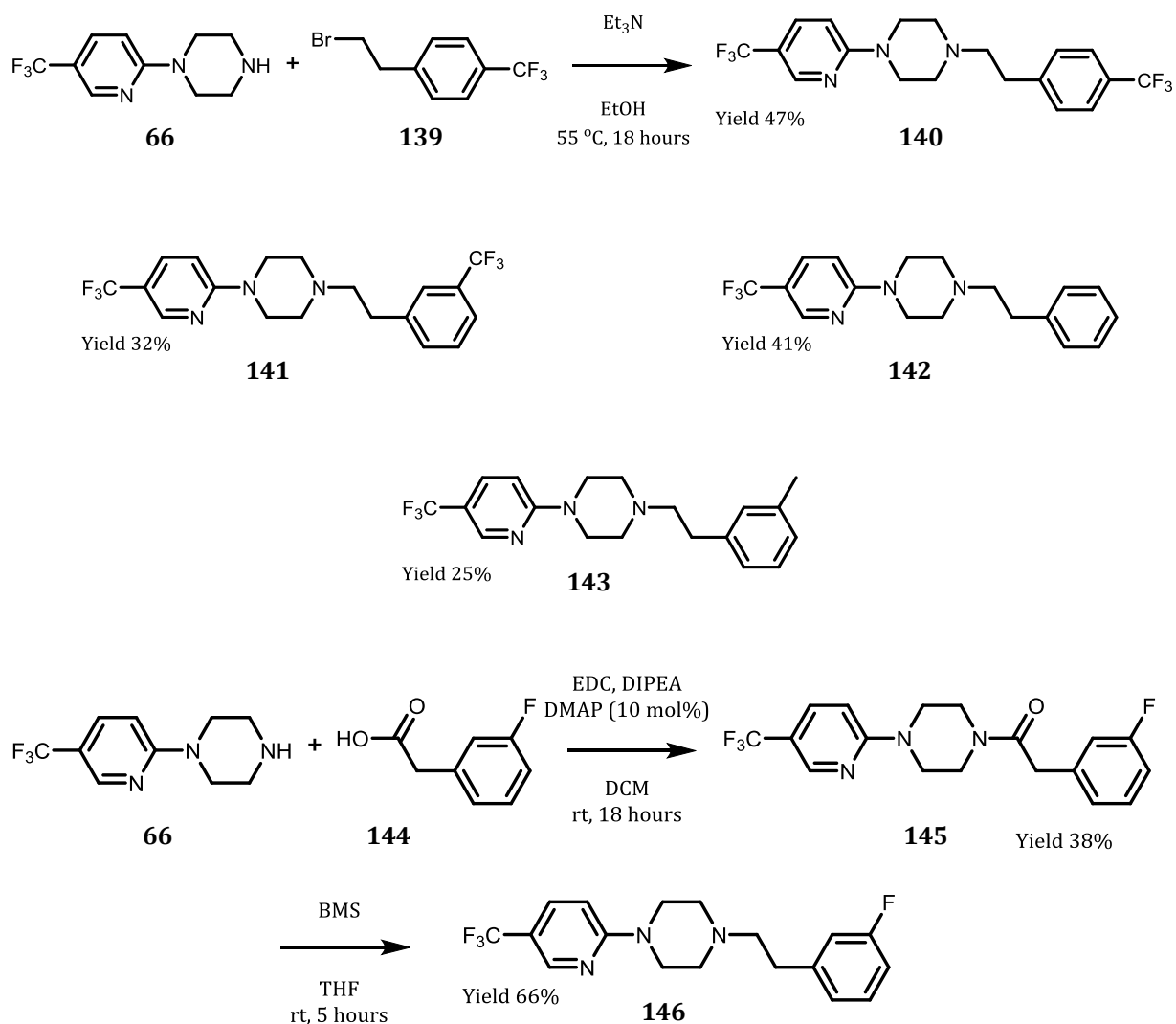
Scheme 14: Synthesis of **140-143**, **145** and **146**. Compounds **140-143** were synthesised with appropriate aryl ethyl bromides under basic conditions, while compound **146** was synthesised by EDC-mediated coupling of 2-(3-fluorophenyl)acetic acid (**144**) to fragment **66** to produce the intermediate amide **145**, followed by reduction to the amine with borane-dimethyl sulfide (BMS).

Table 4: Biophysical results for compounds **140-143**, **146**. DSF solutions: 1 or 2 mM fragment, 20 mM EthR, 150 mM NaCl, 20 mM Tris-HCl (pH 8.0), 2.5x SYPRO® Orange, 50 μL final volume. ITC conditions: buffer 300 mM NaCl, 20 mM Tris-HCl (pH 8.0), glycerol (matched to EthR stock). Compounds (100 mM in DMSO) were diluted to 1 mM in buffer. EthR (50 μM) prepared in buffer with 10% DMSO. SPR solutions: running buffer 2 mM $MgCl_2$, 10 mM Tris-HCl (pH 7.5), 0.1 mM EDTA, 200 mM NaCl, 2% DMSO. EthR prepared as 2 μM in running buffer. Compounds were prepared at varying concentrations in running buffer.

#	R =	ΔT_M (°C)	K_D (μM)	IC_{50} (μM)
140	4-CF₃ benzyl	+0.9 [1 mM]	-	-
141	3-CF₃ benzyl	+3.0 [1 mM]	1.3	> 100
142	benzyl	+2.8 [2 mM]	-	-
143	3-methyl benzyl	+1.8 [2 mM]	-	-
146	3-fluoro benzyl	+2.0 [2 mM]	-	92.9

3.3.2 Amide linkers
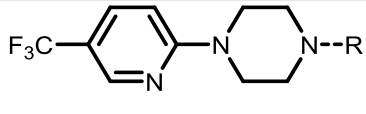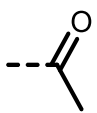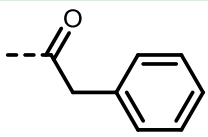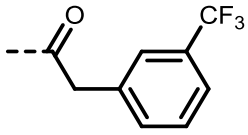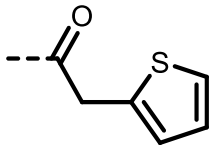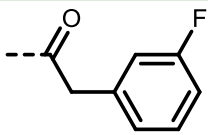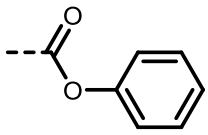
The results of DSF screening of compound **145**, which was synthesised as an intermediate to the synthesis of **146**, suggested that an amide linker in place of the amine would be tolerated, with compound **145** giving a ΔT_M of +8.5 °C [2 mM]. A methyl amide (compound **147**) was synthesised using acetyl chloride to determine if the amide alone would be tolerated. Screening of this compound by DSF gave a ΔT_M of +3.3 °C [1 mM] with an IC_{50} of 31.4 μM by SPR. Three additional compounds incorporating an amide (**148**-**150**) were synthesised (Scheme 15) in order to allow a comparison of the SAR upon inclusion of the amide carbonyl. The yields ranged from 40% to 98%.

A comparison of the amides with their corresponding amines (e.g. compound **141** and compound **149**) shows a trend towards an increase in ΔT_M for the amides, while the carbamate **151** appears to be less well tolerated when compared to its equivalent amide **148** (Table 5). Compound **150** had a ΔT_M of +12.8 °C, and when screened by SPR, had an IC_{50} below the threshold of the assay, with 58% inhibition at the minimum concentration (0.3 μM).
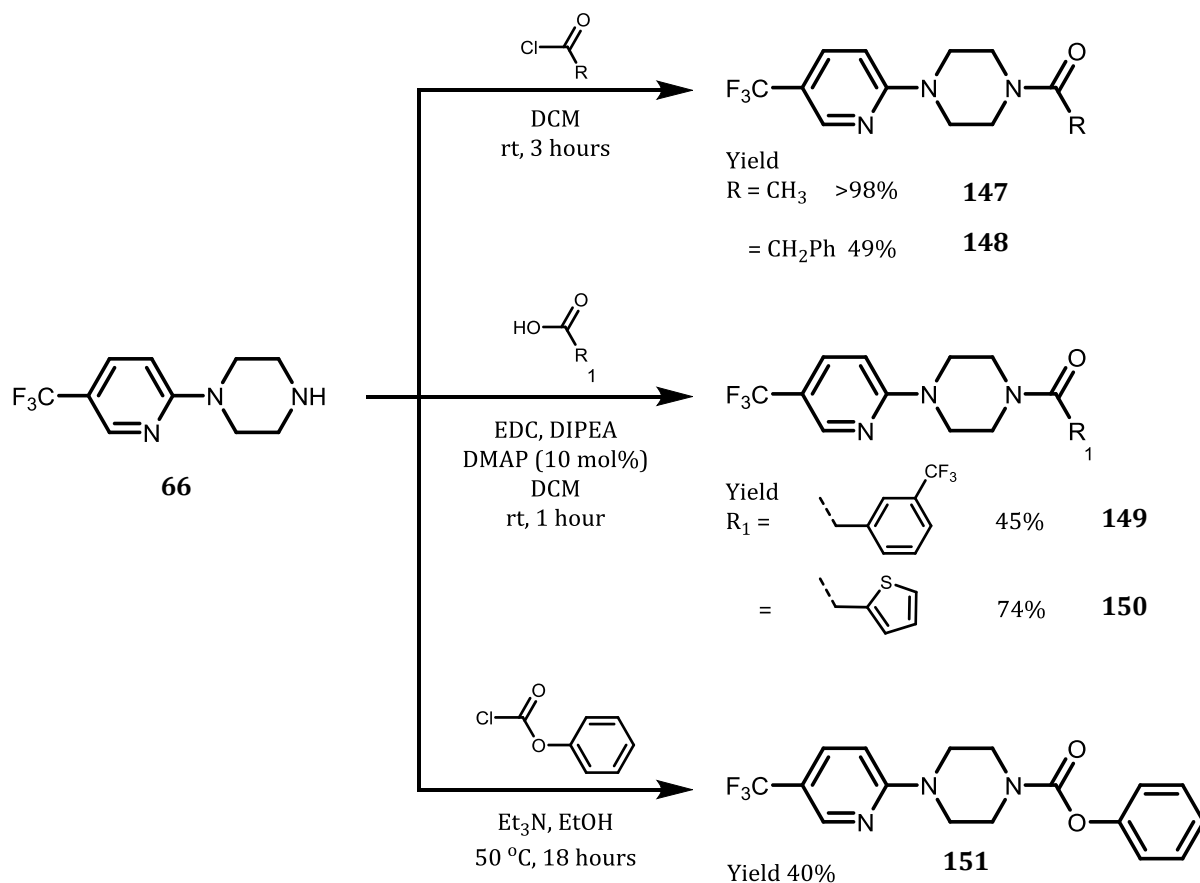
Scheme 15: Synthesis of compounds **147**-**151**. Synthesis of compounds **147** and **148** was performed by coupling the acid chlorides to fragment **66**, while compounds **149** and **150** were synthesised by EDC-mediated coupling of appropriate acids to fragment **66**. Synthesis of compound **151** was completed by coupling phenylchloroformate to fragment **66** in the presence of triethylamine and mild heating.

Table 5: Table of DSF, ITC and SPR results for compounds **145**, **147**-**151**. DSF solutions: 1 or 2 mM fragment, 20 mM EthR, 150 mM NaCl, 20 mM Tris-HCl (pH 8.0), 2.5x SYPRO® Orange, 50 μL final volume. ITC conditions: buffer 300 mM NaCl, 20 mM Tris-HCl (pH 8.0), glycerol (matched to EthR stock). Compounds (100 mM in DMSO) were diluted to 0.75 mM in buffer. EthR (75 μM) prepared in buffer with 10% DMSO. IC_{50} was unable to be determined for compound **150**, therefore percent inhibition at the lowest assay concentration is reported. SPR solutions: running buffer 2 mM $MgCl_2$, 10 mM Tris-HCl (pH 7.5), 0.1 mM EDTA, 200 mM NaCl, 2% DMSO. EthR prepared as 2 μM in running buffer. Compounds were prepared at varying concentrations in running buffer.

#	R =	ΔT_M (°C)	K_D (μM)	IC_{50} (μM)
147		+3.3 [1 mM]	-	31.4
148		+8.3 [2 mM]	6.1	7.2
149		+6.5 [2 mM]	27.2	51.1
150		+12.8 [1 mM]	9.6	58% (0.3 μM)
145		+8.5 [2 mM]	48.3	3.4
151		+5.5 [2 mM]	18.0	-

X-ray crystal structures of compounds **148** and **150** were solved and these show that the molecules bind in the opposite orientation to that proposed by the docking. The X-ray crystal structures show the trifluoromethyl group is directed towards the solvent-exposed end of the pocket, and a H-bond is formed between the amide carbonyl group and the NH of Asn179, similar to that observed for the sulfone compounds (Figure 36).
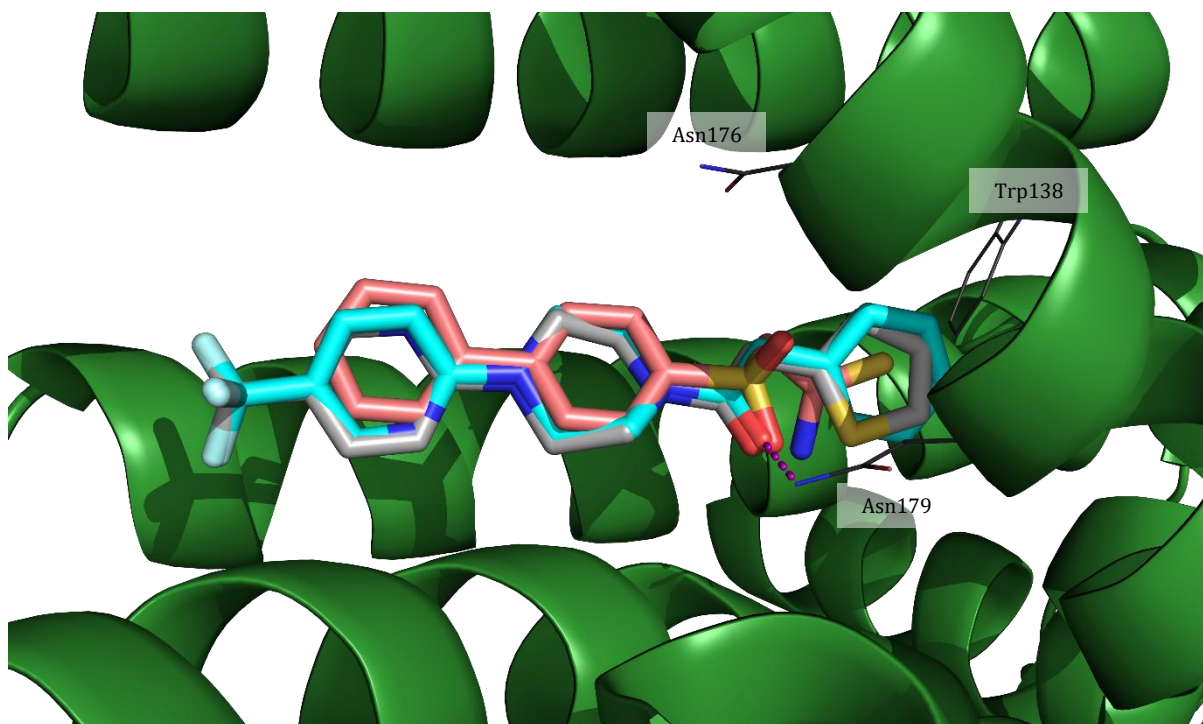
Figure 36: X-ray crystal structure of **104** (pink) **148** (blue) and **150** (grey), showing the H-bonding interaction between Asn179 and the amide carbonyl/sulfone (purple dashed line). This interaction is highly conserved with this chemical series and provides a key anchor point for compound design.

A series of compounds were synthesised where the amide linker was extended by an additional methylene group (Scheme 16) in order to allow greater flexibility. These compounds were synthesised using either EDC coupling of the appropriate carboxylic acids or by heating the acid chloride or chloroformate in the presence of triethylamine with the corresponding amine. DSF indicated strong thermal stabilisation by these compounds (**152**-**155**), with compound **155** generating the highest ΔT_M of +12.8 °C [1 mM].
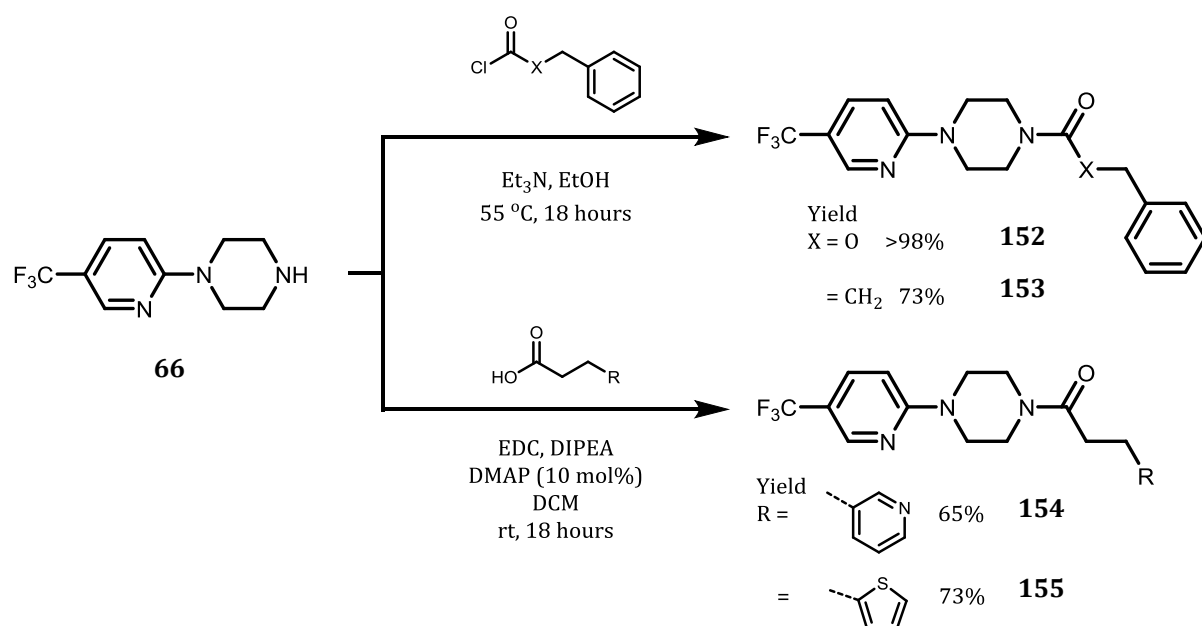
#	R =	ΔT$_M$ (°C)	K$_D$ (µM)	IC$_{50}$ (µM)
152		+7.0 [2 mM]	14.7	42.9
153		+9.3 [2 mM]	3.1	4.3
154		+9.8 [1 mM]	5.0	1.3
155		+12.8 [1 mM]	0.9	73% (0.3 µM)

Scheme 16: Synthesis of compounds **152-155**. Compounds **152** and **153** were synthesised either by coupling of fragment **66** with 3-phenylpropanoyl chloride or benzyl chloroformate in the presence of triethylamine with mild heating. Compounds **154** and **155** were synthesised from fragment **66** and appropriate arylpropionic acids by EDC-mediated coupling. Table of results (DSF, ITC and SPR) for compounds **152-155**; DSF solutions: 1 or 2 mM fragment, 20 mM

EthR, 150 mM NaCl, 20 mM Tris-HCl (pH 8.0), 2.5x SYPRO® Orange, 50 μL final volume. ITC conditions: buffer 300 mM NaCl, 20 mM Tris-HCl (pH 8.0), glycerol (matched to EthR stock). Compounds (100 mM in DMSO) were diluted to 0.75 mM in buffer. EthR (75 μM) prepared in buffer with 10% DMSO. Where IC_{50}s were below the assay threshold, percent inhibition is reported at the lowest assay concentration. SPR solutions: running buffer 2 mM $MgCl_2$, 10 mM Tris-HCl (pH 7.5), 0.1 mM EDTA, 200 mM NaCl, 2% DMSO. EthR prepared as 2 μM in running buffer. Compounds were prepared at varying concentrations in running buffer.
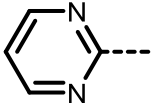
The IC_{50}s were measured for compounds **152**, **155** and **120** using SPR, and these ranged from 42.9 μM for compound **152** to <0.3 μM for compound **155** (73% inhibition at 0.3 μM). This suggests that the carbamate **152** is less well tolerated in comparison to the equivalent amide **153** (4.3 μM), while the presence of a pyridine or thiophene ring terminating the flexible linker was preferred, with compound **154** containing a pyridine ring having an IC_{50} of 1.3 μM and compound **155** possessing a thiophene having an IC_{50} of <0.3 μM.

3.3.3   *Examination of the CF₃ position on the pyridine ring as a vector for elaboration*

A further potential site for optimisation was the pyridine ring, and modification of this region would allow for a growth vector directed towards the top of the binding pocket. Compounds **161** and **163** were synthesised so as to determine the importance of the CF_3 and pyridine nitrogen respectively. The aryl-piperazines were coupled to 2-thiophenepropionic acid using EDC in yields from 73-86%. As 1-(pyridin-2-yl)piperazine was not available at the time from commercial sources, compound **161** was prepared by coupling 2-thiophenepropionic acid to *N*-Boc-piperazine, followed by deprotection and alkylation with 2-fluoropyridine under mild basic conditions (Scheme 17).

Removal of the CF_3 group from the pyridne ring of compound **155** was shown to be not detrimental to the binding of the compound as evidenced by the SPR results of compound **161** (63% inhibition at 0.3 μM) compared to **155** (73% inhibition at 0.3 μM), while removal of the pyridine nitrogen reduced the IC_{50} of compound **163** to 0.8 μM when compared to **155**. When the pyridine ring was replaced with a phenyl ring (**164**), the IC_{50} (0.7 μM) was similar to compound **163**, suggesting that the nitrogen is important for binding which is in agreement with the previous reports.[39]

156 + **157** → EDC, DIPEA, DMAP (10 mol%) / DCM, rt, 18 hours → **158** Yield 89%

TFA / DCM, rt, 3 hours → **159** + **160** → K$_2$CO$_3$ / toluene, reflux, 48 hours → **161** Yield 80%

_____

162 + **157** → EDC, DIPEA, DMAP (10 mol%) / DCM, rt, 18 hours → **163** Yield 86%

Yield 80% **164**

Yield 73% **165**

#	R' =	ΔT_M (°C)	K_D (µM)	IC_{50} (µM)
161	(pyridin-2-yl)	+13.3 [1 mM]	2.3	63% (0.3 µM)
163	F$_3$C–C$_6$H$_4$–	+9.5 [1 mM]	14.8	0.8
164	(phenyl)	+10.8 [1 mM]	2.4	0.7
165	(pyrimidin-2-yl)	+12.8 [1 mM]	1.7	61% (0.3 µM)

Scheme 17: Synthesis of compounds **158**-**165** to determine the importance of the trifluoromethylpyridine group and its potential as a growth vector. Biophysical data for compou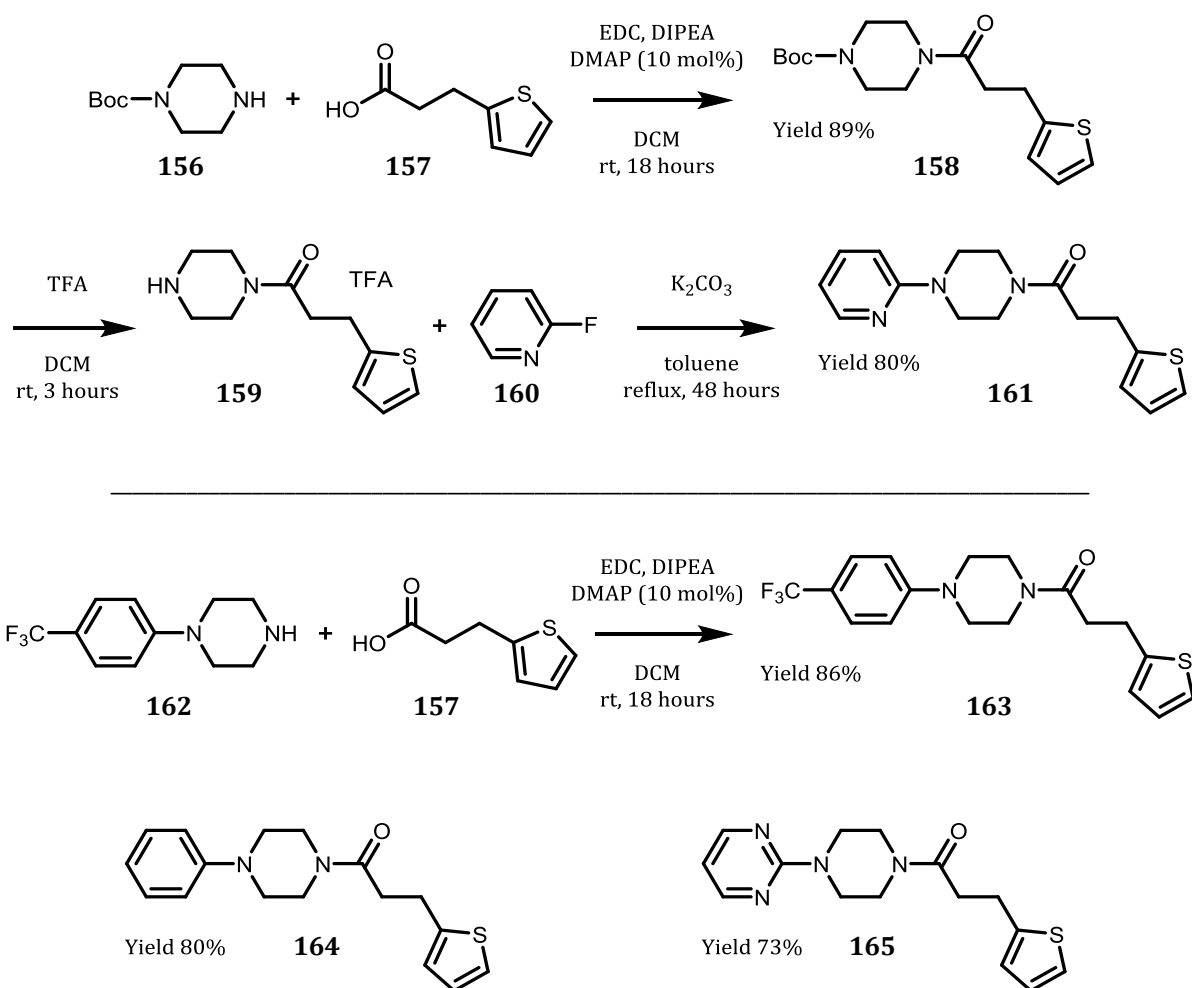nds **161**, **163**-**165**. DSF solutions: 1 mM fragment, 20 mM EthR, 150 mM NaCl, 20 mM Tris-HCl (pH 8.0), 2.5x SYPRO® Orange, 50 μL final volume. ITC conditions: buffer 300 mM NaCl, 20 mM Tris-HCl (pH 8.0), glycerol (matched to EthR stock). Compounds (100 mM in DMSO) were diluted to 0.75 mM in buffer. EthR (75 μM) prepared in buffer with 10% DMSO. Where IC_{50}s were below the assay threshold, percent inhibition at the lowest assay concentration are reported. SPR solutions: running buffer 2 mM $MgCl_2$, 10 mM Tris-HCl (pH 7.5), 0.1 mM EDTA, 200 mM NaCl, 2% DMSO. EthR prepared as 2 μM in running buffer. Compounds were prepared at varying concentrations in running buffer.
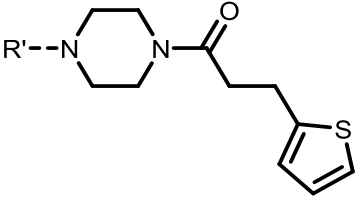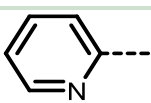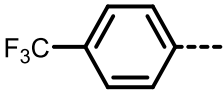
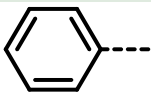The introduction of a pyrimidine ring as a replacement of the pyridine ring (**165**, Scheme 17) revealed that this additional heteroatom did not produce any significant change in the percent inhibition compared to **161** (61% versus 63% inhibition).

An X-ray crystal structure of **161** revealed potential H-bonding interactions with the backbone carbonyl groups of Met102, Trp103, Tyr148 or Thr 149 (Figure 37). This prompted the synthesis of compounds **167**-**171** (Scheme 18), in an attempt to probe the possible interaction through H-bonding by the addition of an NH functionality. Compound **169** was synthesised using a Pd-mediated Buchwald-Hartwig coupling of 5-bromo-7-azaindole (**166**), with *N*-Boc-piperazine (**156**), followed by removal of the Boc protecting group and EDC coupling of the resulting salt with 2-thiophenepropionic acid (**157**). Compounds **170** and **171** were synthesised by an analogous method with appropriate bromoindoles, giving the compounds **169**, **170** and **171** in yields ranging from 37-52% over the final 2 steps.
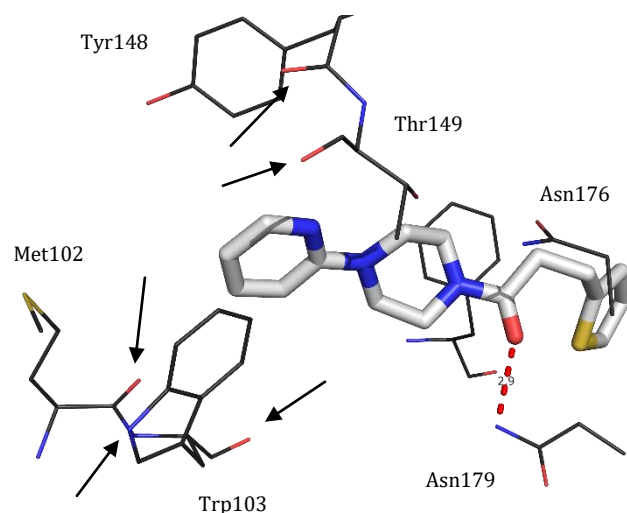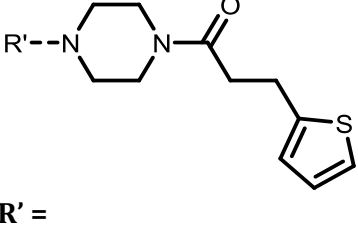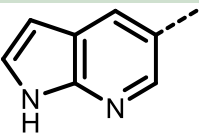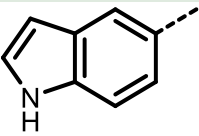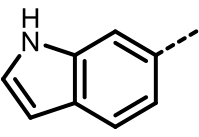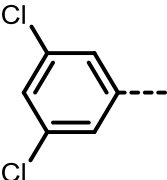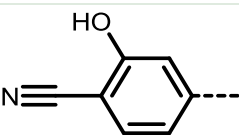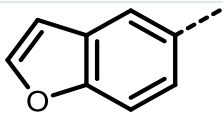
Figure 37: X-ray crystal structure of **161** showing nearby residues. Arrows indicate possible locations for H-bonding interactions with EthR.

The three compounds showed a decrease in ΔT_M compared to compound **161**, as well as poorer K_Ds (14-20 μM) (Table 6, Figure 38). The IC_{50}s for the indole compounds **170** and **171**, measured by SPR, were between 6 and 7 μM, while the azaindole **169** was 19 μM (Table 6).
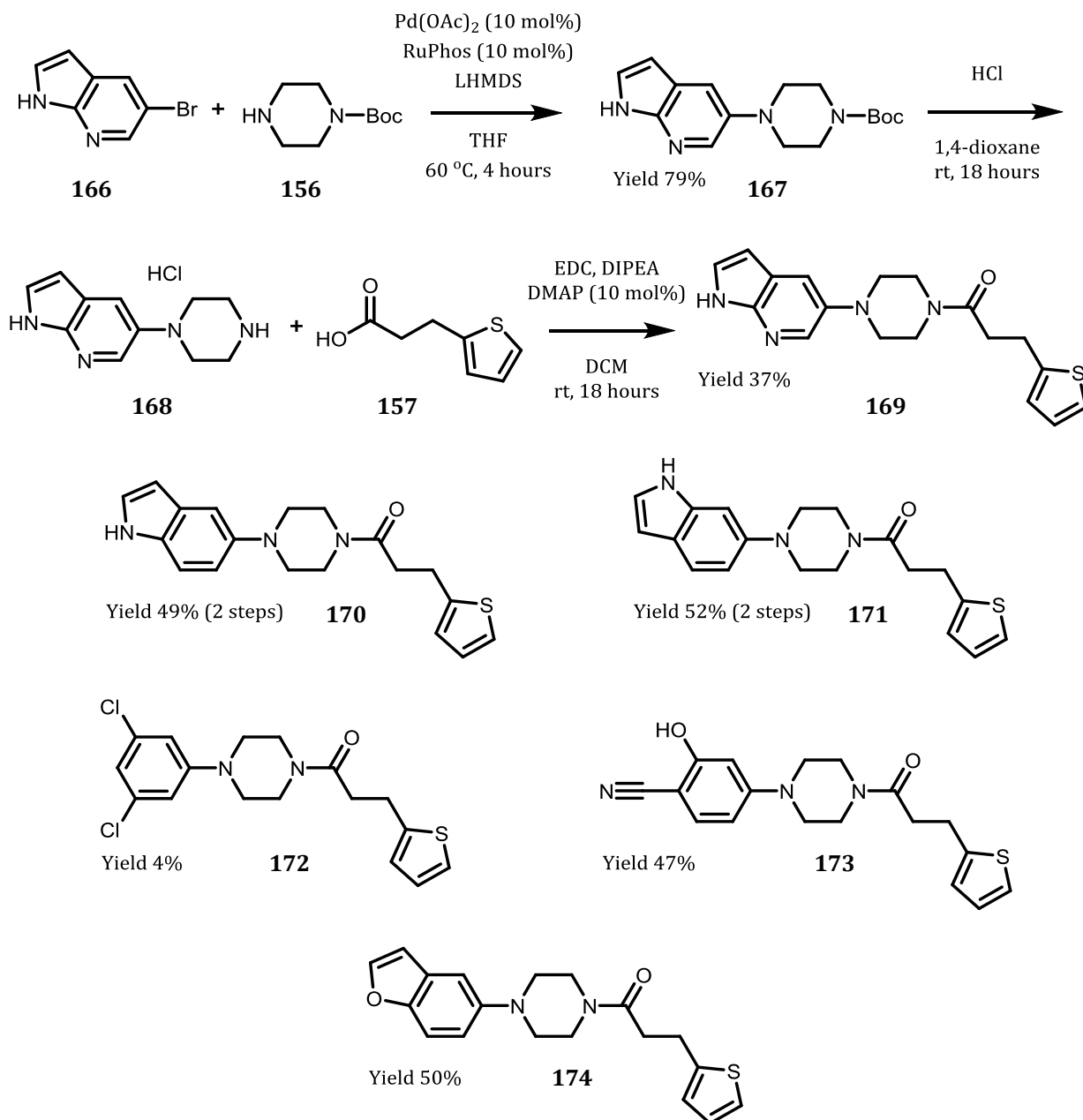
Scheme 18: Synthesis of compounds **167-174**. These compounds were synthesised from arylbromide starting materials, coupled via Buchwald-Hartwig chemistry to N-Boc-piperazine (**156**). The resulting Boc amines were deprotected under acidic conditions and coupled to 2-thiophenepropionic acid (**157**) using EDC.

Table 6: Table of DSF, ITC, and SPR results for compounds **169-174**. DSF solutions: 1 mM fragment, 20 mM EthR, 150 mM NaCl, 20 mM Tris-HCl (pH 8.0), 2.5x SYPRO® Orange, 50 μL final volume. ITC conditions: buffer 300 mM NaCl, 20 mM Tris-HCl (pH 8.0), glycerol (matched to EthR stock). Compounds (100 mM in DMSO) were diluted to 0.75 mM in buffer. EthR (75 μM) prepared in buffer with 10% DMSO. SPR solutions: running buffer 2 mM $MgCl_2$, 10 mM Tris-HCl (pH 7.5), 0.1 mM EDTA, 200 mM NaCl, 2% DMSO. EthR prepared as 2 μM in running buffer. Compounds were prepared at varying concentrations in running buffer.

#	R' =	ΔT_M (°C)	K_D (μM)	IC_{50} (μM)
169		+5.8 [1 mM]	20.3	18.9
170		+7.5 [1 mM]	14.0	6.4
171		+7.5 [1 mM]	15.6	6.9
172		+8.8 [1 mM]	No binding	12.9
173		+4.0 [1 mM]	No binding	48.0
174		+11.8 [1 mM]	3.0	2.1
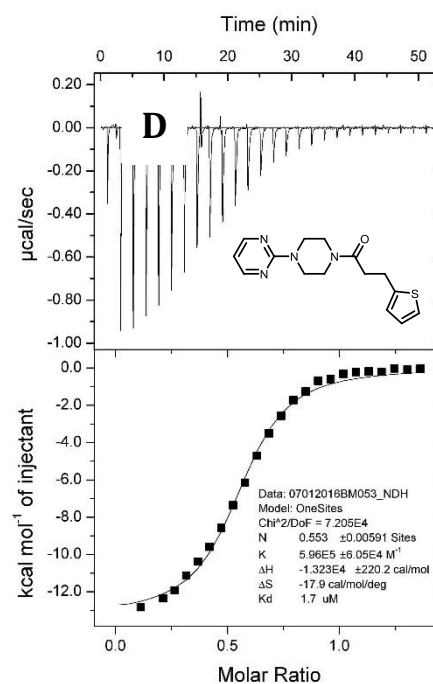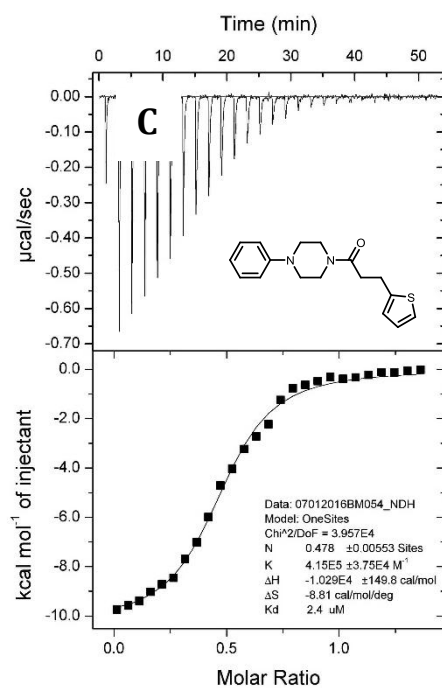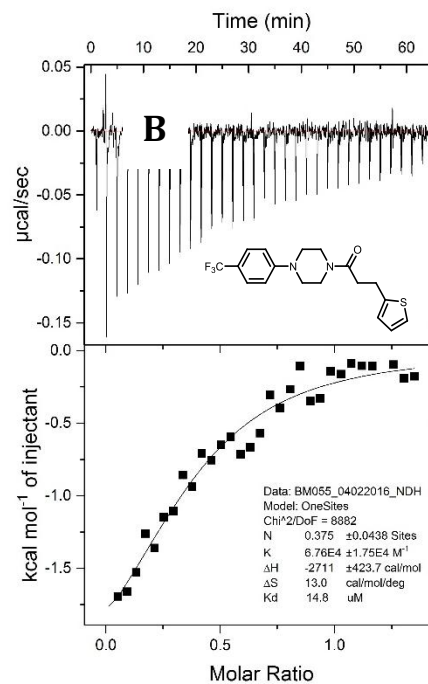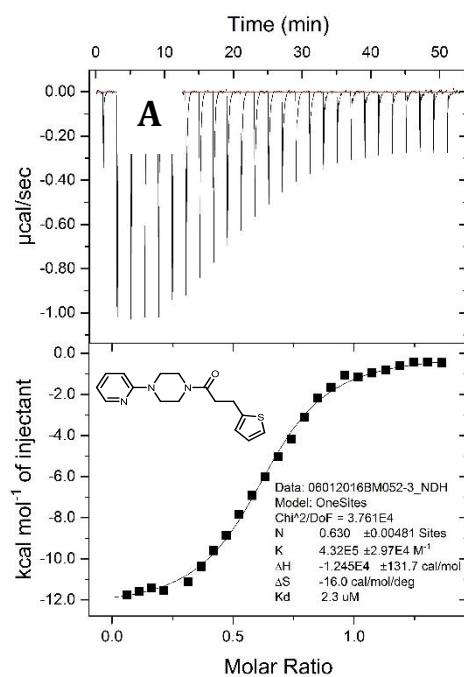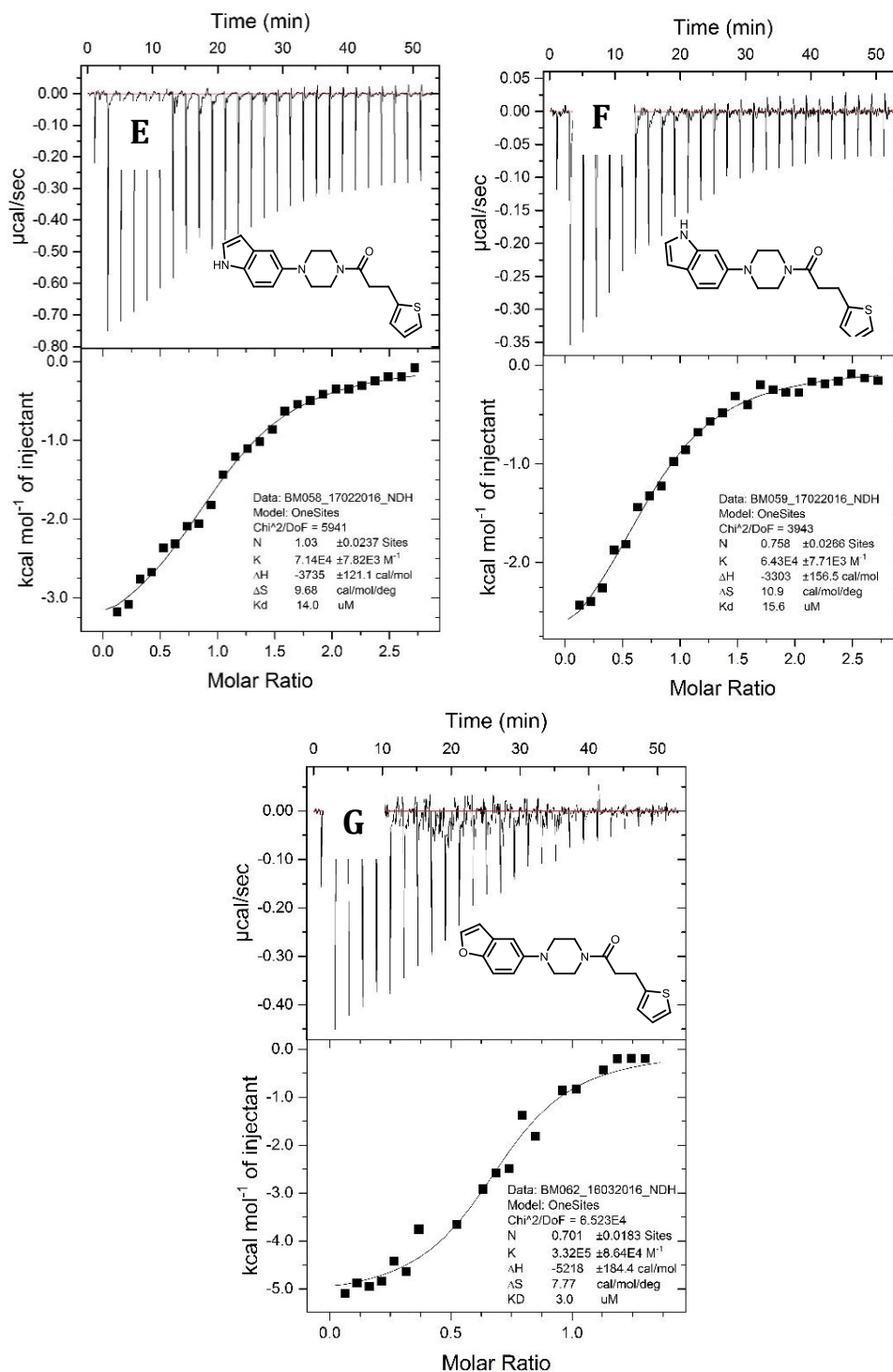
Figure 38: ITC traces of compounds (A) - **161**; (B) - **163**; (C) - **164**; (D) - **165**; (E) - **170**; (F) - **171**; (G) – **174**.

The K_Ds for the azaindole and indole compounds **169-171** (K_Ds 20.3, 14.0 and 15.6 μM) showed a decrease in binding affinity when compared with compounds **161** (K_D 2.3 μM) and **164** (K_D 2.4 μM). Compounds **172-174** were synthesised to investigate the effect of reversing the

hydrogen bonding potential by substituting a benzofuran for the indole, and changing the electronics of the ring by addition of electron-withdrawing groups. Compounds **172** and **174** were synthesised using the same route as compounds **169**-**171** (Scheme 18) to investigate the potential for H-bonding with the main-chain NH of Trp103 (compounds **173** and **174**) and the effect of electron-withdrawing groups on the benzene ring (compound **172**). These compounds produced ΔT_Ms of +8.8 °C [1 mM] and +11.8 °C [1 mM] respectively. When tested by ITC, compound **172** did not produce any heats of binding (Table 6), while **174** gave a K_D of 3 µM. Despite this, compound **172** yielded an IC_{50} of 12.9 µM and compound **174** gave an IC_{50} of 2.1 µM by SPR. This suggested that the presence of the hydrogen bond acceptor of compound **174** is preferred to the electron withdrawing groups of compound **172** or the hydrogen bond donors of compounds **169**-**171**.

Compound **173** was synthesised to contain a benzisoxazole however, this was found to be unstable towards the reaction conditions employed and resulted in ring opening to form the hydroxybenzonitrile. The compound still provided interesting functionality in the hydroxyl and nitrile groups, however the DSF indicated a ΔT_M of only +4 °C [1 mM], with SPR recording an IC_{50} of 48 µM.

3.4   Ethionamide boosting assay
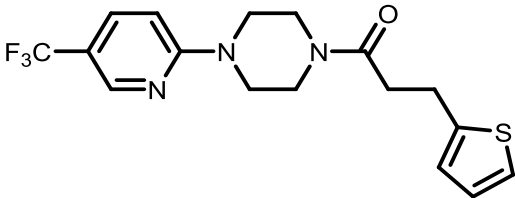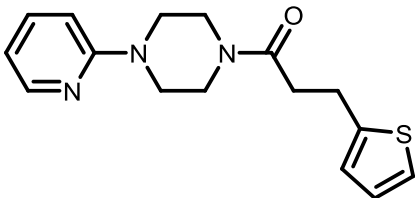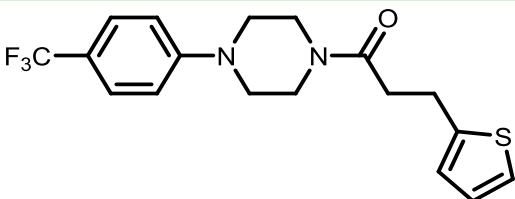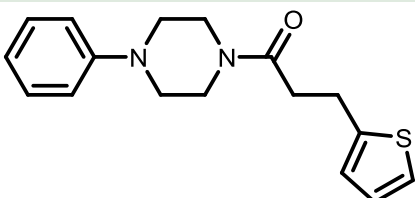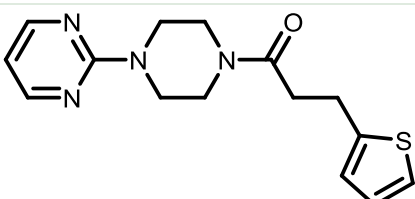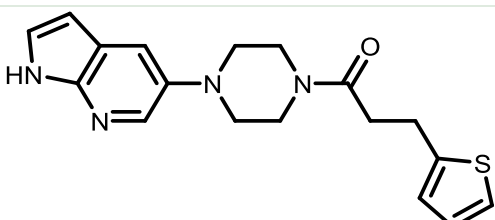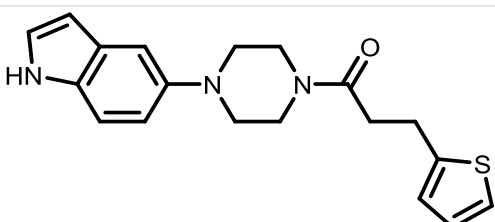
A number of compounds were screened using the resazurin microtiter assay (REMAssay) (Professor Stuart Cole Laboratory, EPFL). The compounds were screened alone and in combination with ethionamide (ETH) at a fixed concentration of 1 µM, with varying concentrations of ETH to determine if the compounds would boost ethionamide activity (testing carried out by Anthony Vocat, EPFL). Cell viability was measured by fluorometric analysis of resorufin, produced as a metabolite of resazurin in viable cells.

The results indicated that the indole and azaindole compounds **169**-**171** did not boost ETH efficacy, with MIC results in the range of 25-26 µM (Figure 39). Compound **165**, containing the pyrimidine had an MIC of 6.4 µM. Contrary to the K_D values, the presence of the pyridine nitrogen had little effect, with compound **163** giving an MIC of 1.7 µM, the same as compound **155**. Meanwhile the removal of the CF_3 group in addition to the pyridine nitrogen lowered the MIC of compound **164** to 1.1 µM. The benzoxazole compound **174** also had an MIC of 1.1 µM, making **164** and **174** the most potent boosters of ethionamide screened.
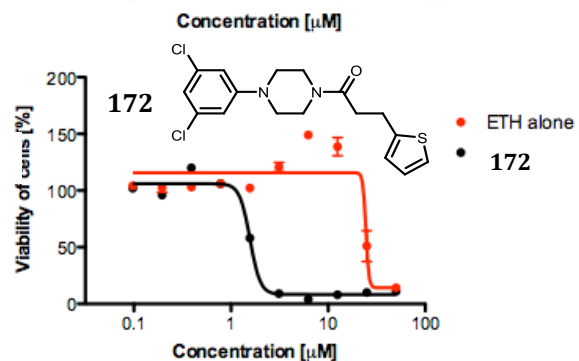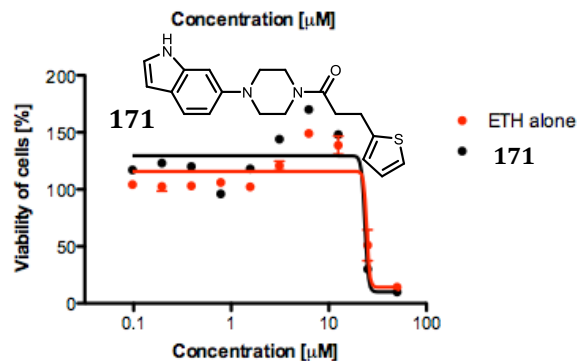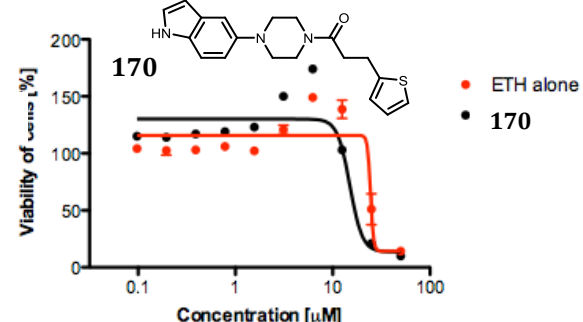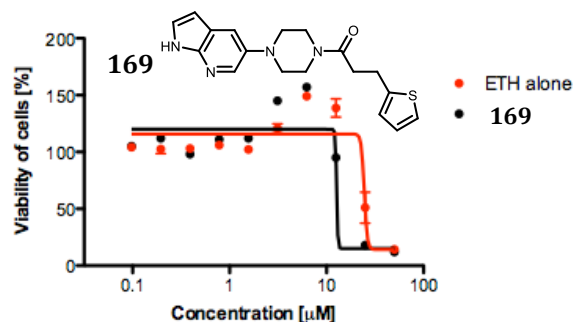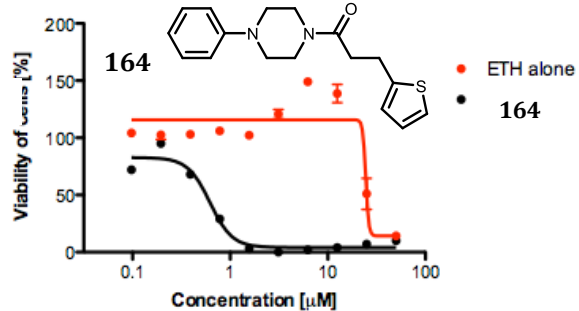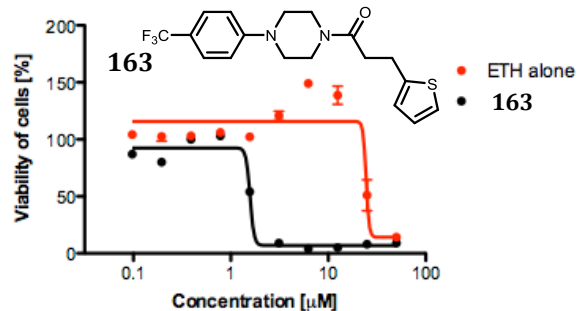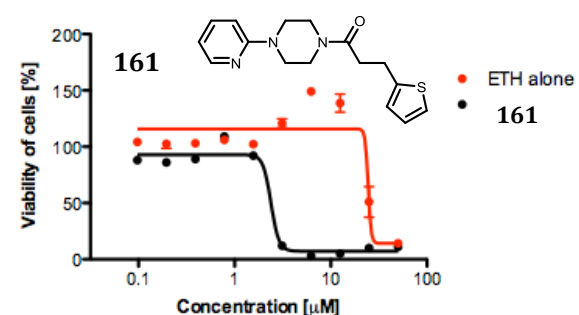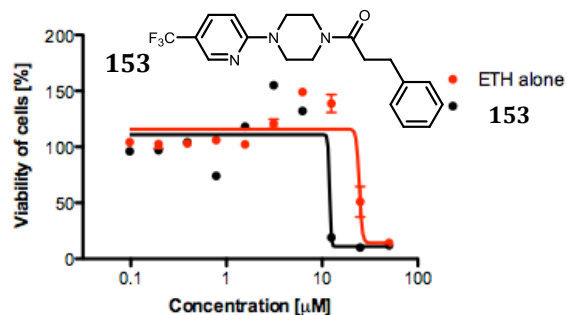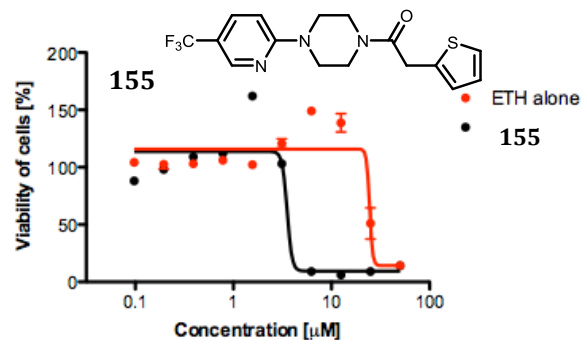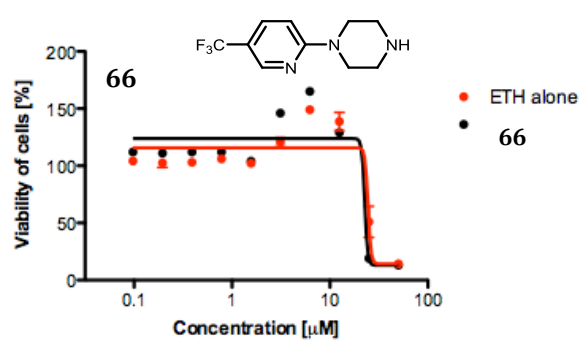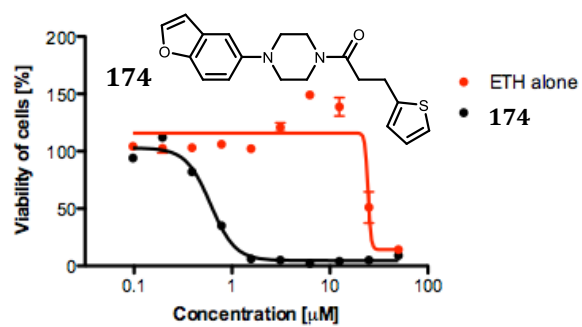
#	Structure	IC$_{50}$ (μM) [REMAssay]	MIC (μM) [REMAssay]
6		24.5	30.3
66		22.7	25
148		21.2	23.6
152		11.6	13.3
150		3.5	5.2
153		12	12.7
154		18.4	25

155		1.5	1.7
161		2.4	3
163		1.6	1.7
164		0.6	1.1
165		3.7	6.4
169		12.7	25
170		15	25.2

171		23.4	25.7
172		1.6	1.7
173		13.5	25
174		0.6	1.1

Figure 39: REMAssay MIC plots (provided by Anthony Vocat, EPFL). Red lines indicate fitting to ETH only control curve, black lines indicate cell viability in the presence of 1 μM test compound at varying concentrations of ETH. Movement of the inflection point of the black line to the left of the red line indicates ETH boosting. Table of IC_{50} and MIC values calculated from the REMAssay. Values are the average of two replicates. REMAssay solutions: *M.tb.* (H37Rv) was prepared at an OD of 0.0001 in 7H9 broth with 10% albumin-dextrose-catalase, 0.2% glycerol and 0.05% Tween-20. Ethionamide was diluted with the above solution at 2-fold dilutions and test compounds added at 1 μM. After incubation, 0.025% resazurin was added and the metabolite resorufin fluorescence read (λ_{ex-em} 560-590 nm) after overnight incubation.

The REMAssay results show that through a fragment growing strategy from the original fragment hit **66**, compounds **164** and **174** were synthesised which each gave a 30 fold boosting effect of the ethionamide MIC.

3.5   Conclusions

The elaboration of fragment hit **66** with an IC_{50} of 35 μM to a compound with an IC_{50} of < 0.3 μM (compound **155**) was described using fragment growing strategies. X-ray crystallography was key in guiding the development of these compounds. The elaboration strategies were achieved through two vectors on the original fragment hit **66**. The free NH of fragment **66** was used as a synthetic handle for extending the molecule deeper into the EthR binding pocket, while the (trifluoromethyl)pyridine was replaced with several alternative motifs to improve the H-bonding capacity of this region of the molecule.

It was found that the addition of a linker containing an amide bond to the piperazine proved beneficial, where compound **153** gave a K_D of 3.1 μM with EthR. X-ray crystallography suggests that this improvement was primarily through the introduction of a hydrogen bond between the amide carbonyl and Asn179 of EthR. The aryl group at the termination of the linker was examined, resulting in a 2-thiophene group (compound **155**) providing an affinity for EthR of 0.9 μM.

Removal of the trifluoromethyl group produced a minor decrease in affinity, with compound **161** yielding a K_D of 2.3 μM compared to compound **155** with a K_D of 0.9 μM. By replacing the 5-(trifluoromethyl)pyridine group with a 7-azaindole (**169**), or indole (compounds **170** and **171**), the IC_{50} was reduced from < 0.3 μM (compound **155**) to 18.9 μM (**169**), 6.4 μM (**170**) and 6.9 μM (**171**). When the 5-(trifluoromethyl)pyridine group was replaced with a benzofuran (compound **174**), an IC_{50} of 2.1 μM was obtained.

The screening of these compounds in the REMAssay to examine the ethionamide boosting ability identified that the benzofuran compound (**174**) yielded an MIC of 1.1 μM, along with the benzene derivative (**164**), while the 5-(trifluoromethyl)pyridine compound (**155**) gave an MIC of 1.7 μM, all boosting the efficacy ethionamide by approximately 30 times.

This work provides a starting point for the development of efficient small molecule therapeutics which, co-administered with ethionamide could boost the efficacy of this second line anti-tubercular drug by interacting with both available binding sites of the EthR dimer and inhibiting the ability of this repressor to bind to its DNA target. There remains further scope for growing and linking strategies to reach deeper into the EthR binding pocket.

4.0 Extended and bivalent molecules for stabilising the EthR dimer in a non-active conformation

4.1   Bifunctional molecules in drug discovery

This chapter describes the strategy of linking two molecules of compound **155** described previously (section 3.3.3) with linkers to bridge the two binding pockets of the dimeric EthR structure. The hypothesis is that this could allow the dimer to be stabilised in the non-active conformation. This approach has been examined previously in proteins such as transthyretin (TTR),[109] bromodomains and extraterminal bromodomain (BET),[110] and for the drug isoniazid (INH) [111] where researchers looked to improve clearance and bioavailability.

Bifunctional molecules have been examined for improving the plasma clearance of the amyloidogenic protein transthyretin. Transthyretin is a homotetrameric protein where a build-up of this can lead to systemic amyloidosis, a condition that can prove fatal. Mangione *et al.*[109] proposed that by linking two TTR homotetramers, the body would recognise the abnormal structure and improve the clearance of TTR. The small molecule 2-((3,5-dichlorophenyl)amino)benzoic acid, was used as the active warhead, which was linked by polyproline or polypiperidine linker to form palindromic compounds (Figure 40A and B). Mass spectrometry indicated that the compounds were successful in forming stable, crosslinked complexes with over 95% of TTR complexed.[109] The authors proposed that two possible structures existed for the protein-ligand complex – a barbell-type structure where two tetramers are linked linearly by one drug molecule (Figure 40C), and a bracelet-type structure, where the two tetramers are linked with two drug molecules into a ring (Figure 40D).
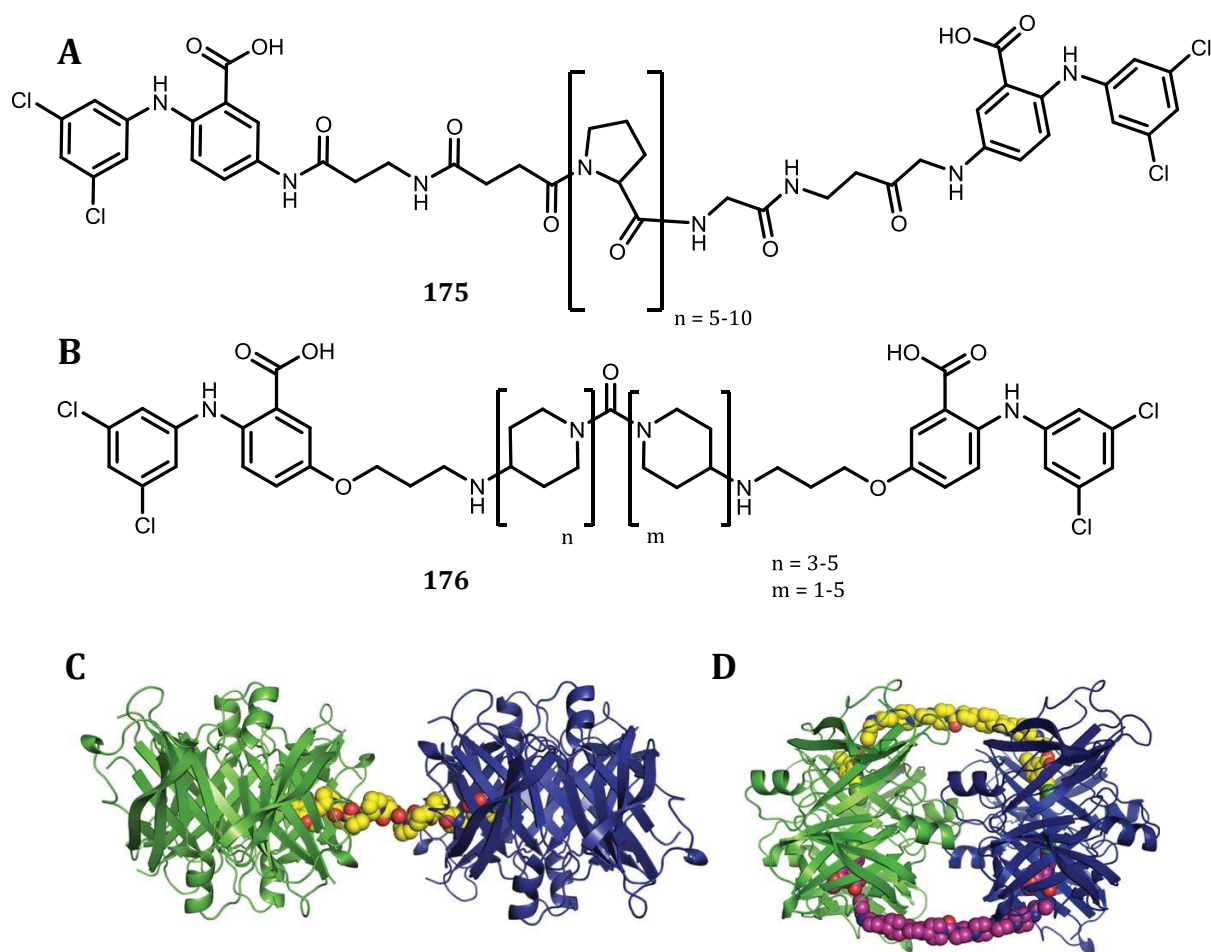
Figure 40: (A) – Structure of the polyproline linked ligand; (B) – Structure of the polypiperidine linked ligand; (C) – Proposed docked 'barbell-like' structure of the octameric transthyretin complex, linked by one polyproline linker (n = 9). The rigidity of this linker prevents the cyclisation of the complex; (D) – Proposed 'bracelet-like' structure of the octameric transthyretin complex, linked by two polypiperidine linker compounds (n = 4, m = 4), forming a ring.[109]

Despite successfully forming the octameric complex as observed by mass spectroscopy, it was found that plasma clearance was not improved in the complexes when compared to tetrameric transthyretin.[109]

Tanaka *et al.* utilised bifunctional ligands to improve the affinity of molecules targeting the BET transcriptional coactivators.[110] Three possible orientations for linking compound **177** to the polyethylene glycol (PEG) linker were proposed, generating two palindromic 'homodimers' (**178** and **179**) and one 'heterodimer' (**180**) (Figure 41).[110]
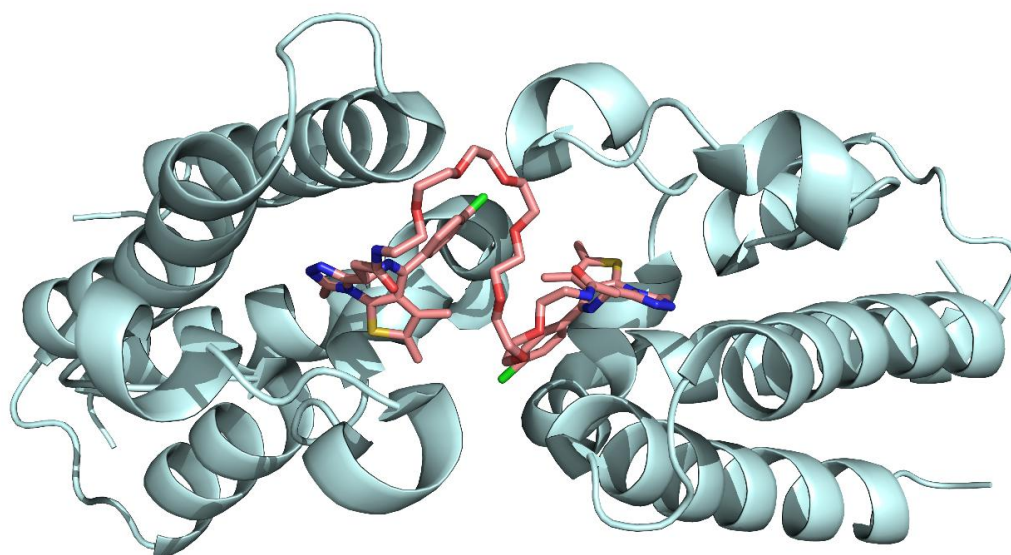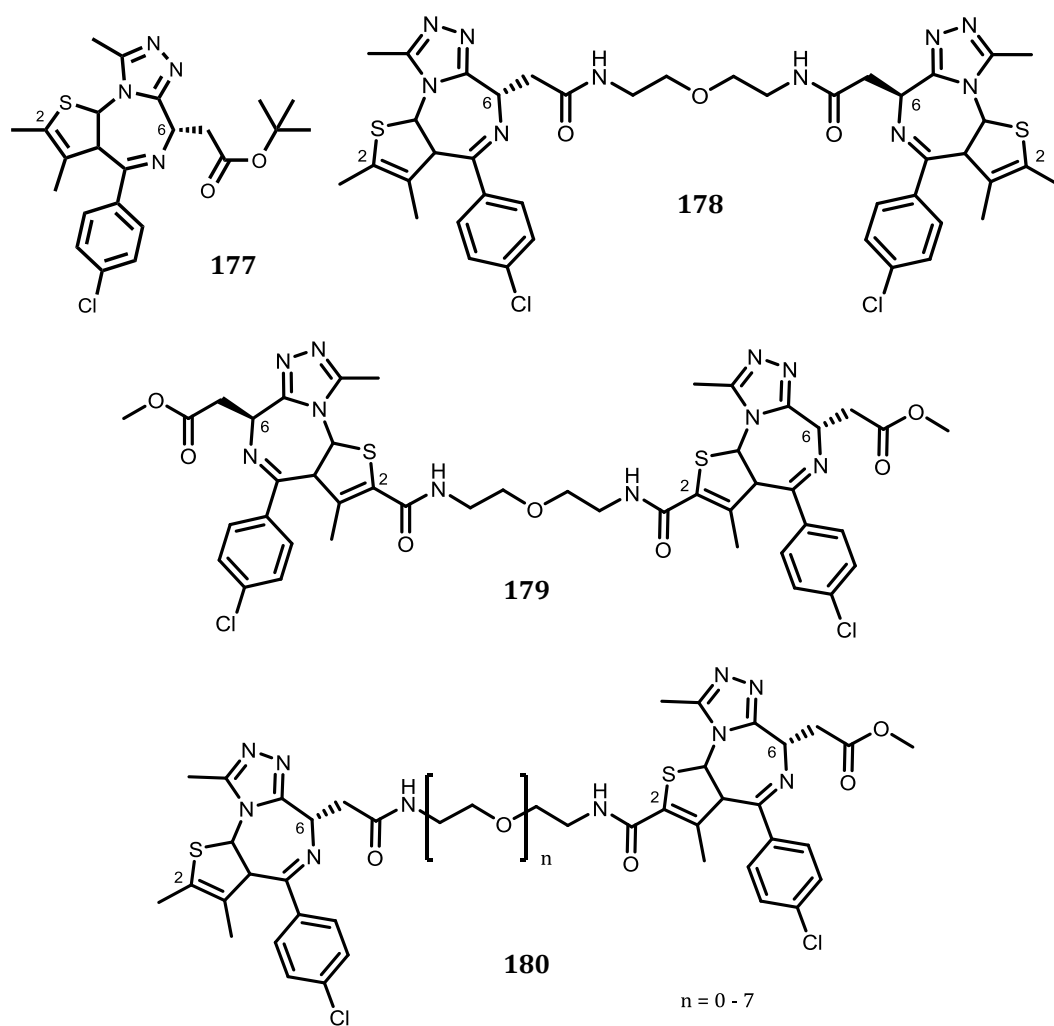
Figure 41: Structure of compound **177** and linked compounds **178**, **179** and **180**. Compound **177** was known to bind to BET. Compound **180** (heterodimer) was synthesised to examine the potential for PEG-linked compounds to bind multiple BET domains simultaneously. X-ray crystal structure of **178** (n = 7) bound to two BET monomers (PDB: 5JWM).[110]

The homodimers **178** and **179** failed to show an increase in activity in both the biochemical (IC$_{50}$ **177** = 21 nM, **178** = 158 nM, **179** = 1 nM) and cellular assays (IC$_{50}$ **177** = 72 nM, **178** = 42 nM, **179** = 24 nM). The heterodimer **180** (*6S,2R* and *6R,2S*; n = 1) was therefore utilised for further study, in addition to a monofunctional **177**-PEG (*2S*) molecule and a bifunctional compound with *6S,2S* stereochemistry. Size exclusion chromatography indicated that compound **180** (n = 1; *6S,2S*) was dimerising BET by showing a decrease in the elution volume corresponding to a larger compound size, while **180** (n = 1; *6R,2R*) and single warhead (**177**) did not alter the elution volume of BET indicating no change in volume of the compound. These results were supported by ITC, where compound **180** (n = 1, *6S,2S*) was shown to bind BET with a 1:2 stoichiometry (K$_D$ 17 nM), while compound **177** bound with a 1:1 ratio (K$_D$ 40 nM).[110]

A further series of compounds were synthesised with various linker lengths up to 7 PEG units where the warheads were attached in various combinations by either the 6' position of the ester of the diazepine or the 2' position of the thiophene. It was determined that the PEG7 linker with both warheads attached at the ester functional group (**178**; *6S,6S*) had comparable activity (IC$_{50}$ 3 nM, biochemical assay) to the previous heterodimer **180** derivatives, however this had better pharmacokinetic properties. An X-ray crystal structure of compound **178** (n = 7; *6S,6S*) was obtained (Figure 41), showing that it bound to two BET molecules while retaining the binding mode of **177**.[110]

A further exploration of bivalent molecules was the use of PEGylated Isoniazid for delivery into *M.tb.*, which was examined by Kakkar *et al.*[111] Two INH moieties linked by a PEG linker with 4, 11 or 14 repeated units (Figure 42), were examined to see whether the cytotoxicity, which is noted with Isoniazid use, can be reduced. PEG was selected for the linker due to its structural simplicity and low toxicity and excretion profiles.[111]

181	INH	t$_{1/2}$ = 50 min
	n = 4	t$_{1/2}$ = 72 min
	n = 11	t$_{1/2}$ = 1.3 hr
	n = 14	t$_{1/2}$ = 2.1 hr
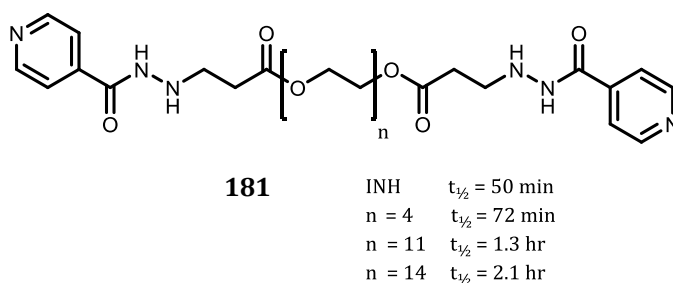
Figure 42: Structure of the bis-Isoniazid-PEG conjugate showing the clearance times with the increasing PEG chain length.[111]

It was demonstrated that the INH-PEG conjugates showed improved cytotoxicity, although compound **181** variants gave a minimum inhibitory concentration (MIC) of 0.6 nM compared to 0.9 nM for INH alone. The bis-INH compounds were shown to have longer half-lives in blood, $t_{1/2}$ 2.1 hr (**181**; n = 14) compared to $t_{1/2}$ 50 min (INH). The increase in the half-lives of the compounds also corresponded to an increase in molecular weight. Furthermore, the PEG-INH conjugates were shown to have greater uptake by infected tissue than INH alone.[111]

Looking at the utilisation of bifunctional molecules in the above strategies, the goal was to see whether this novel inhibition strategy could be applied to EthR. The aim was to explore whether binding to both pockets of the EthR dimer could result in increased inhibition of the EthR-DNA interaction, resulting in an increase in ethionamide efficacy.

4.2 Replacement of the CF₃ group to facilitate growth towards the solvent-exposed end of the binding pocket of EthR

Compound **155**, which was previously discussed in section 3.3, was selected as the starting point to examine the potential for building extended molecules. The strategy involves replacement of the CF₃ group and addition of alkyl and PEG chains to extend the molecule towards the open end of the binding pocket. This approach will be used to link the two binding pockets of the EthR dimer, to establish whether EthR can be stabilised in a non-active, ligand-bound conformation.

ΔT_M +12.8 °C
K_D 0.9 μM
IC_{50} 73% inhibition [0.3 μM]
MIC 1.7 μM
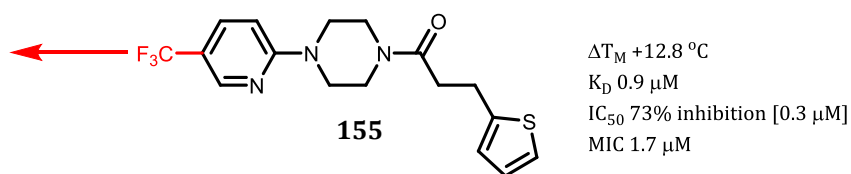
Figure 43: Structure of compound **155** showing the vector for linking the two EthR monomers.

Having determined that the CF₃ component of the piperazine-series compounds such as **155** could be removed with little or no detriment to activity (section 3.3.3, compound **155** 73% inhibition at 0.3 μM, compound **161** 63% inhibition at 0.3 μM), the replacement of this with alternative functional groups designed to grow out of the binding pocket was developed.

A hexylamine group was introduced onto the pyridine ring in the 5-position (Figure 44) to determine if a linear hydrophobic group would be tolerated. This compound was synthesised in

four synthetic steps where EDC coupling of the acid was followed by removal of the Boc protecting group with TFA and addition of the 5-bromo-2-fluoropyridine under basic conditions gave the core scaffold. The hexylamine group was introduced using Buchwald chemistry and the product **183** was isolated in a yield of 7%.
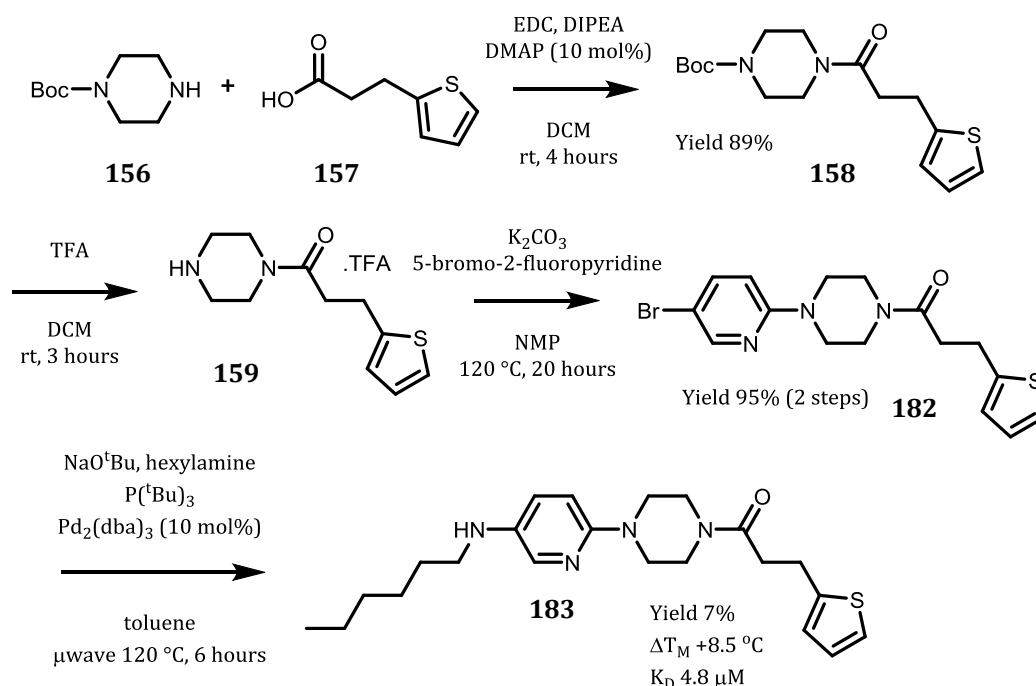
Figure 44: Synthesis of compounds **182** and **183**. N-Boc-piperazine (**156**) was coupled to 2-thiophenepropionic acid (**157**) with EDC, then the Boc protecting group removed with TFA. 5-bromo-2-fluoropyridine was aminated with the TFA salt (**159**), then hexylamine added via palladium-catalysed Buchwald chemistry.

Upon screening using DSF, compound **183** was found to give a ΔT_M of +8.5 °C [1 mM], with a K_D of 4.8 μM determined by ITC. X-ray crystallography (Dr Michal Blaszczyk) confirmed that the hexylamine was oriented towards the solvent exposed end of the pocket (Scheme 19A), showing that the strategy of building towards the solvent exposed end of the pocket is possible.

In order to explore whether other linkers were tolerated, and to simplify the chemistry, compounds **187**-**189** were synthesised (Scheme 19B) where a carboxylic acid was introduced (**188**) to provide a more convenient synthetic handle. Compounds **187** and **189**, when measured by DSF gave a ΔT_M of +13.3 °C [1 mM] and +11.0 °C [1 mM] respectively, while compound **188** gave a ΔT_M of +9.3 °C [1 mM]. Upon examination by ITC against EthR,

compounds **187** and **189** gave K_Ds of 4.8 and 3.9 μM respectively, however no heats of binding to EthR were detected for compound **188**. The IC_{50}s of these compounds against EthR bound to immobilised promoter DNA were determined by SPR (Sherine Thomas) and this showed that compound **188** was not as potent as compounds **187** and **189** with values of 11.3, 0.5 and 0.6 μM respectively. These compounds served as useful starting points in order to develop the bivalent ligands.

Scheme 19: (A) - X-ray crystal structure of compound **183** (purple) bound to EthR, with Arg159 shown (orange) (Dr Michal Blaszczyk); (B) - Synthetic scheme showing the introduction of an amide on the 5-position of the pyridine ring. Methyl 6-bromonicotinate (**184**) was aminated with N-Boc-piperazine (**156**), which was then deprotected with HCl. The salt (**186**) was coupled to 2-thiophenepropionic acid with EDC, before the ester (**187**) was cleaved to the acid (**188**) with LiOH. The acid was reacted with methanolic ammonia with EDC to produce the amide **189**.

As compounds **187**-**189** showed good affinities in SPR and ITC, they were screened to determine whether they boosted the ethionamide effect. The compounds were screened against TB (H37Rv) using the REMAssay (Anthony Vocat, EPFL) and compound **188** gave an MIC of 25 μM, compound **189** 15.8 μM and compound **187** showed the greatest boosting activity at 5.2 μM (Table 7). The compounds were tested at 1 μM against *M.tb.* grown in supplemented 7H9 broth with ethionamide at varying concentrations. After 6 days of incubation at 37 °C, resazurin was added, and incubated overnight, at which time the fluorescence of the resazurin metabolite resorufin is recorded.

Table 7: Biophysical results for compounds **187**-**189**. DSF solutions: 1 mM fragment, 20 mM EthR, 150 mM NaCl, 20 mM Tris-HCl (pH 8.0), 2.5x SYPRO® Orange, 50 μL final volume. ITC conditions: buffer 300 mM NaCl, 20 mM Tris-HCl (pH 8.0), glycerol (matched to EthR stock). Compounds (100 mM in DMSO) were diluted to 0.75 mM in buffer. EthR (75 μM) prepared in buffer with 10% DMSO. SPR performed by Sherine Thomas. SPR solutions: running buffer 2 mM MgCl$_2$, 10 mM Tris-HCl (pH 7.5), 0.1 mM EDTA, 200 mM NaCl, 2% DMSO. EthR prepared as 2 μM in running buffer. Compounds were prepared at varying concentrations in running buffer. REMAssay performed by Anthony Vocat (EPFL). REMAssay solutions: *M.tb.* (H37Rv) was prepared at an OD of 0.0001 in 7H9 broth with 10% albumin-dextrose-catalase, 0.2% glycerol and 0.05% Tween-20. Ethionamide was diluted with the above solution at 2-fold dilutions and test compounds added at 1 μM. After incubation, 0.025% resazurin was added and the metabolite resorufin fluorescence read (λ_{ex-em} 560-590 nm) after overnight incubation.
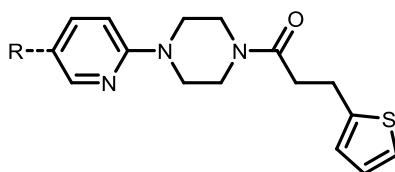
#	R =	ΔT_M (°C)	K_D (ITC) (μM)	IC_{50} (SPR) (μM)	IC_{50} (REMAssay) (μM)	MIC (REMAssay) (μM)
187		+ 13.3 [1 mM]	4.8	0.5	4.2	5.2
188		+ 9.3 [1 mM]	no heats	11.3	19.3	25
189		+ 11.0 [1 mM]	3.9	0.6	13	15.8

In order to further extend the molecules towards the top of the binding pocket, the X-ray crystal structure of compound **183** was examined for potential interactions (Scheme 19A). The residue Arg159, which is located at the top of helix 7, could offer the possibility for a π-cation interaction with an aromatic ring.[112] Utilising the acid functional group of compound **188** and with the knowledge that both the ester (compound **187**) and amide (compound **189**) had sub-micromolar IC_{50} values (Table 7), compounds **190** and **191** were synthesised (Scheme 20).

Compound **190** was synthesised by formation of an activated ester of compound **188** with 2,4,6-trichlorobenzyl chloride followed by transesterification with 2-(2-(benzyloxy)ethoxy)ethan-1-ol which gave the product **190** in 14% yield. Compound **191** was synthesised by EDC coupling of compound **188** with 4-phenylbutan-1-amine where the product **191** was isolated in a 14% yield.
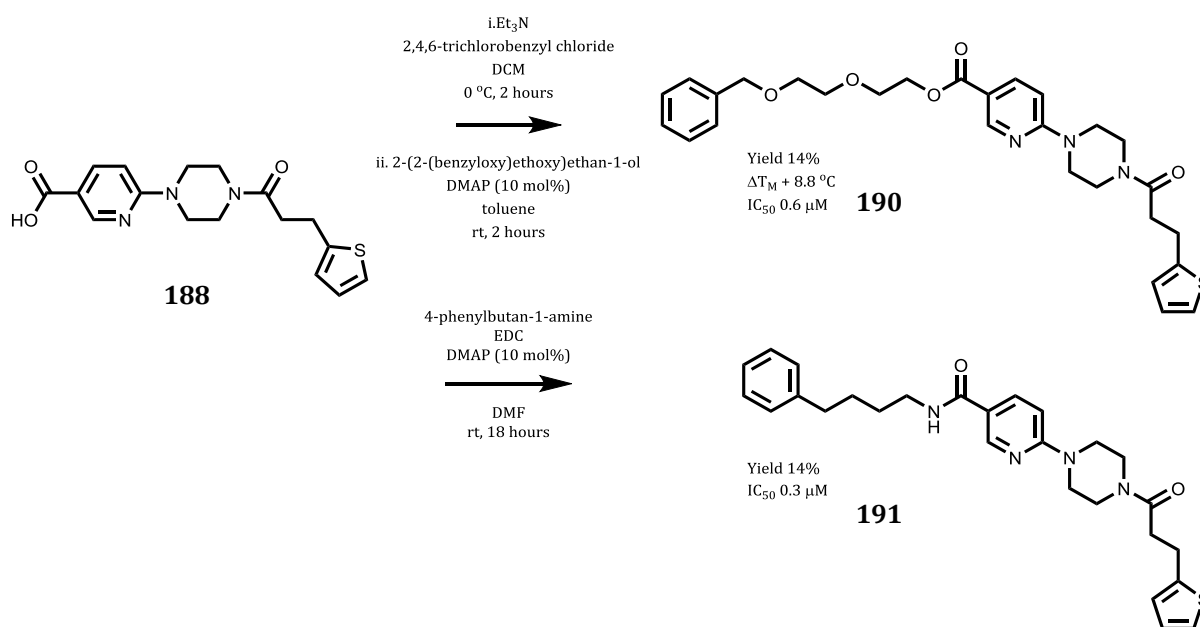
Scheme 20: Synthesis of **190** and **191**. These compounds aimed to exploit the presence of an asparagine residue at the solvent-exposed end of the EthR binding pocket. Both compounds were synthesised from the acid **188**, with compound **190** proceeding via the activated ester formed with 2,4,6-trichlorobenzyl chloride, with subsequent transesterification with 2-(2-(benzyloxy)ethoxy)ethanol. Compound **191** was synthesised by EDC coupling with 4-phenylbutanamine.

Screening of compound **190** against EthR by DSF was found to give a ΔT_M of +8.8 °C [1 mM], while compound **191** did not produce a measurable ΔT_M curve. Despite this, sub-micromolar IC_{50}s were determined by SPR (Sherine Thomas), where compound **190** gave an IC_{50} of 0.6 µM and compound **191** an IC_{50} of 0.3 µM, some of the strongest binding compounds developed during the course of this work.

4.3   Stabilisation of the dimeric form of EthR

It was previously established that the binding of small molecules within the binding cavity of EthR induces a conformational change, which inhibits the binding of EthR.[32] As the protein forms a dimer in solution in the absence of the target DNA,[38] compounds were envisioned which would be able to link the binding sites of two EthR monomers to stabilise the dimeric structure in an inactive conformation.

From consideration of the X-ray crystal structure of compound **183** bound to EthR, the distance between the two binding sites (Figure 45) was measured to be approximately 71-78 Å. This suggests that a polyethylene glycol (PEG) linker of approximately 900-1000 Da (20-22 PEG units) would be appropriate to link the two binding sites. Three PEG linkers were obtained – PEG-600 (13 PEG units, 47 Å), PEG-1000 (22 PEG units, 79 Å), and PEG-1500 (34 PEG units, 122 Å), in addition to block polymer Jeffamine-ED900 (**192**). The PEG-1500 was selected to provide a linker which would have additional flexibility, while the PEG-600 was chosen to produce a compound which would be too short to reach both binding sites. The synthesis of the PEG-linked molecules was attempted by two routes. The first was the conversion of the carboxylic acid to the acid chloride followed by displacement with the PEG alcohol. The second involved the formation of the activated ester with 2,4,6-trichlorobenzylchloride and attempted transesterification with the PEG alcohol. Both of these routes proved unsuccessful, however the Jeffamine-linked compound **193** was synthesised by COMU coupling. Upon examination of this compound by DSF, a ΔT_M of +6.5 °C [1 mM] was measured, and an IC_{50} of 11.8 µM was measured by SPR. These results indicate that these molecules disrupt the EthR-DNA interaction.
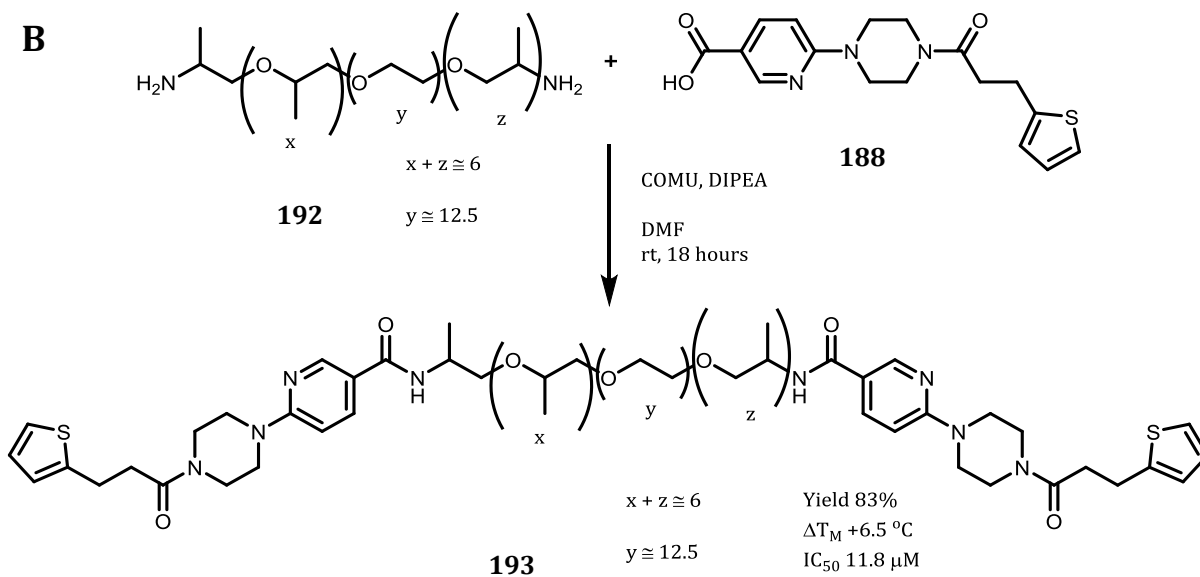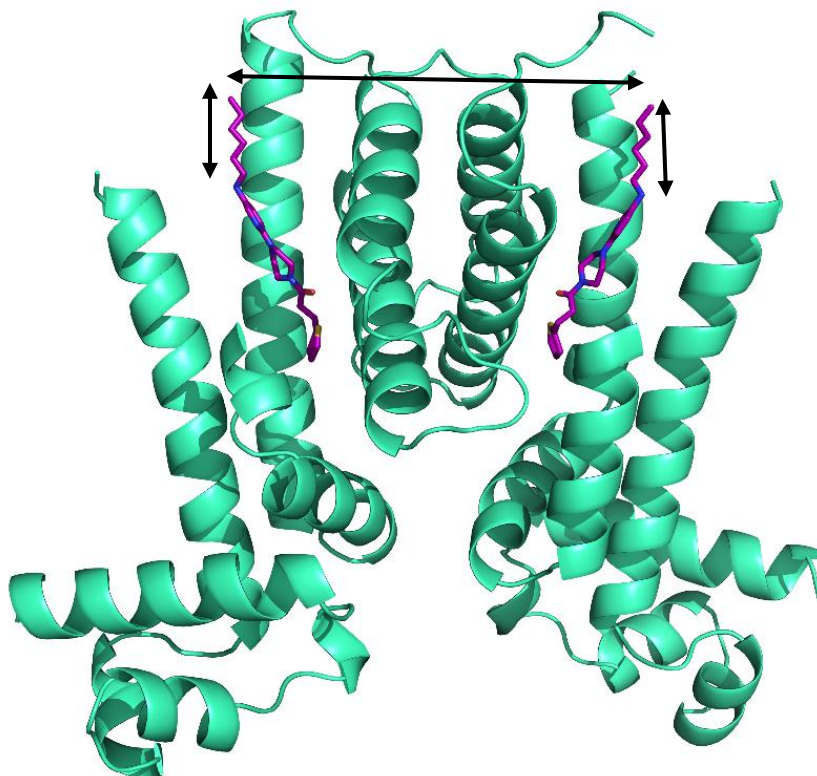
Figure 45: (A) - Structure of the EthR dimer showing two molecules of compound **183** (purple), indicating the separation of the two substrate binding sites. The black arrows indicate the distance measured from the amine of one molecule of **183** to the amine of the second molecule of **183** as the desired position for joining of the linker. (B) - Synthesis of compound **193**. Jeffamine ED-900 was coupled to compound **188** with COMU to yield compound **193**.

The Jeffamine-linked compound **193** was examined by mass spectrometry (Daniel Chan, Department of Chemistry) in order to determine how **193** was binding to the EthR dimer. The results indicated that compound **193** was able to bind one or two units per dimer, while some tetrameric species were also observed in the presence of the ligand, suggesting that the ligand is capable of binding across two EthR dimers. The binding of one molecule of **193** per EthR dimer could occur through two possible binding modes. The first is where the ligand occupies both binding sites of the dimer (Figure 46A), while the second is where the ligand binds to one monomer, leaving the other site unoccupied, with one end of the ligand free (Figure 46B). Reduction in the signal of the EthR-DNA complex was seen in the presence of promoter DNA and the compound, indicating that the DNA binding is reduced in the presence of the ligand.
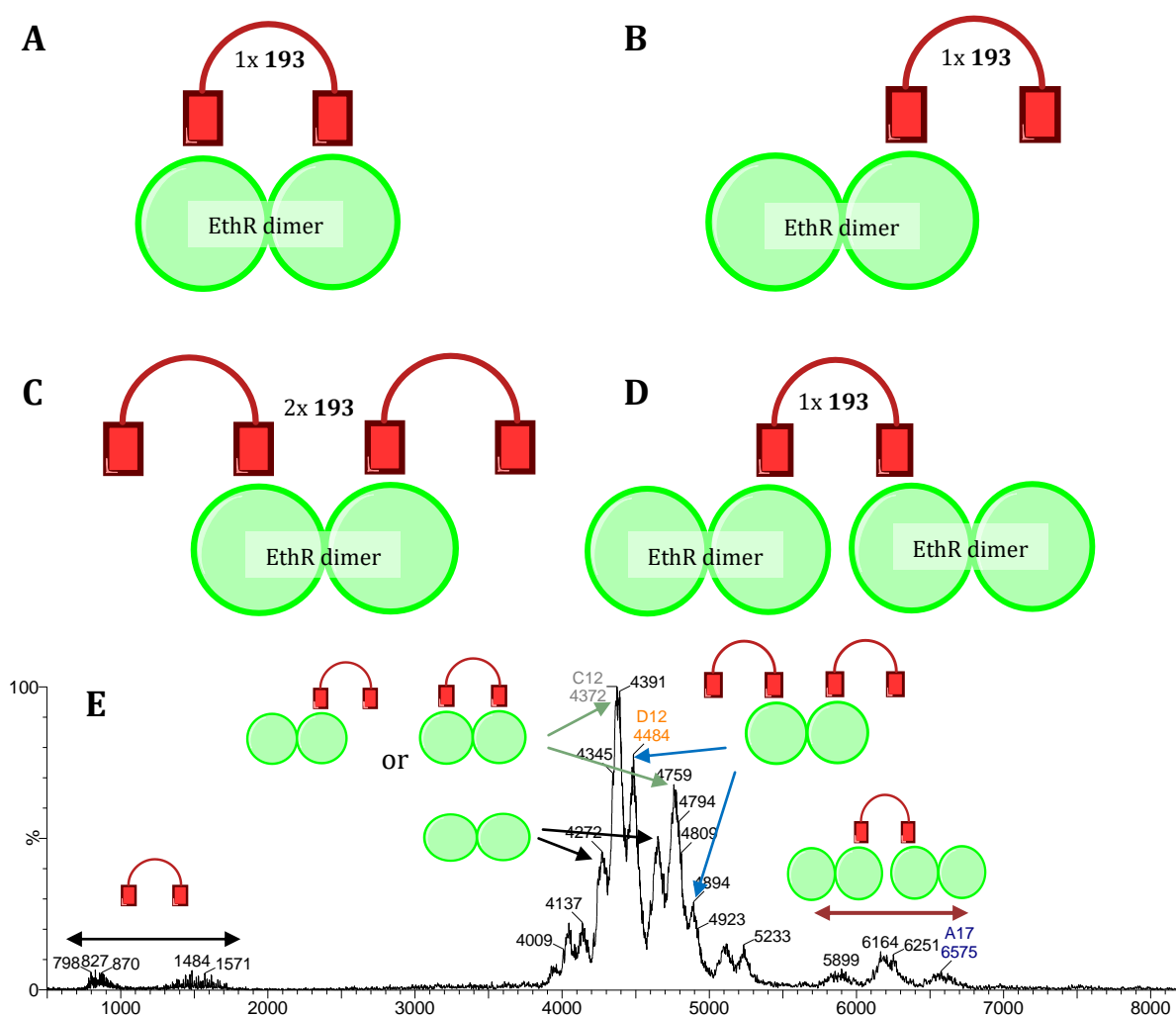
Figure 46: Potential binding modes of compound **193** to EthR. (A) – 1 molecule of compound **193** per EthR dimer; (B) – 1 molecule of **193** per dimer of EthR; (C) – 2 molecules of **193** binding to one EthR dimer; (D) – 1 molecule of compound **193** binding two dimers of EthR; (E) – Mass spectrometry data (Daniel Chan) showing the various states of the EthR-**193** complex in the absence of promotor DNA.

Compound **193** was developed and shown to be able to bind to the dimer state of EthR and inhibit the EthR-DNA interaction. This has demonstrated a plausible strategy for targeting EthR. Although in the early stages, this approach could lead to highly potent compounds for use as ethionamide boosters and future work would be needed to develop this strategy further.

4.4   Conclusions

The CF_3 group of compound **155** which binds to the solvent exposed end of the EthR ligand binding pocket has been shown to be a potential vector for extending molecules outside the EthR binding pocket. Compound **183** was synthesised to examine whether a hexyl chain would be tolerated as the molecule approached the solvent exposed end of the binding pocket and it was observed that this bound with a K_D of 4.8 µM. X-ray crystallography confirmed that **183** maintained the expected binding mode with the alkyl chain positioned facing out of the pocket.

The use of an amide in place of the amine was explored and compounds **187**-**189** were developed to determine the influence of these functional groups at the 5-position of the pyridine ring. Biophysical assays showed that the acid (**188**) was less tolerated than ester (**187**) or amide (**189**) functional groups, and both the ester and amide substituted compounds gave similar affinities by ITC (K_D 4.8 µM and 3.9 µM) and SPR (IC_{50} 0.5 µM and 0.6 µM). A further strategy was employed to see whether the Arg159, which is found at the end of the binding cavity could be targeted, and compounds **191** and **190** were designed to include a phenyl group at the end of a chain. Compounds **190** and **191** yielded sub-micromolar IC_{50}s by SPR (0.6 µM and 0.3 µM respectively), showing that this strategy was successful and that compounds which occupy the top of the binding pocket can pick up further interactions.

The bivalent compound **193** was developed and when screened by SPR gave an IC_{50} of 11 µM. This compound was also examined using mass spectrometry, which demonstrated that this bifunctional compound can successfully bind to and inhibit EthR. However, further work is needed to determine the optimal linker length for these compounds.

5.0   Experimental

5.0.1   Solvents and Reagents
Reagents and anhydrous solvents purchased from commercial sources were used as received. Solvents were used as received from commercial sources, with the exception DCM, toluene, and methanol, which were distilled over calcium hydride, and THF, which was distilled over calcium hydride with $LiAlH_4$ and triphenylphosphine.

5.0.2   Nuclear Magnetic Resonance Spectroscopy
NMR were recorded on a Bruker DPX-400 MHz or Bruker Avance 500 MHz Cryo Ultrashield and processed with NMR Kiosk (Bruker), Topspin (Bruker), or NMR processor (academic edition; Advanced Chemistry Development Labs).

5.0.3   Liquid-Chromatography Mass-Spectrometry
LCMS were recorded on a Waters Alliance HT machine using a 2795 separation module and 2996 photodiode detector array connected to a Waters micromass ZQ quadrupole mass spectrometer, or a Waters Acquity HClass UPLC fitted with TUV and SQ detectors. Both systems operate on MassLynx software (Waters Ltd.). Samples were run using a gradient of water (1–5%) (+0.1% formic acid) in acetonitrile over a period of 8 min. (Alliance) or 4 min. (Acquity)

5.0.4   High Resolution Mass Spectrometry
High resolution MS were recorded with a Waters LCT Premier Micromass machine with an Agilent 1100 series LC system. Samples were run using a gradient of water (1–5%) (+0.1% formic acid) in acetonitrile over a period of 8 min.

5.0.5   Infrared Spectroscopy
IR spectra were obtained on a PerkinElmer Spectrum One Fourier transform IR spectrophotometer with ATR using Spectrum version 5.0.1 (PerkinElmer Inc.) and processed within the operating software, or using KnowItAll Informatics System 2013 (academic edition; Bio-Rad Laboratories, Inc.). Scanning range was 4000-650 cm^{-1}, with 4 transients per spectrum.

5.0.6   Flash Column Chromatography
Chromatographic purification was carried out on either an Isolera One or Isolera Four chromatography system (Biotage) using pre-packed KP-SIL columns (4, 10, 12, 24, 25, 40 or 50 g) and solvent systems as per the synthetic procedures.

5.0.7   Microwave Reactions
Microwave reactions were performed with a Biotage Initiator.

5.0.8 Thin Layer Chromatography

TLC was carried out on pre-prepared glass-backed silica plates from Merck, and visualised with ultraviolet light (λ = 256 nm), or with ninhydrin, iodine or potassium permanganate stains as necessary.

5.0.9 Melting Point Analysis

Melting point analyses was performed with a Griffin Melting Point Apparatus (MPA350.BM2.5) from Gallenkamp and are uncorrected.

5.0.10 Computational Docking

Docking was performed using GOLD Suite version 5.3 (CCDC Software Limited) on EthR (PDB: 1T56) with a 10 Å binding site centred around CE2 of Phe110. Docking used the chemscore_kinase configuration template in conjunction with the CHEMPLP scoring function. Ligands were generated in ChemDraw (CambridgeSoft) and prepared for docking using Discovery Studio 4 (Accelrys Software Inc.) or VegaZZ version 3.1.0.21 (A. Pedretti and G. Viscoli).

5.0.11 Protein Preparation

EthR was expressed in *Escherichia Coli* BL21 (DE3) (Novagen) with the EthR gene cloned into a pHAT5 vector (BamHI/EcoRI). Overnight culture was added to LB media (25 mL/L) and the bacteria grown into exponential phase (37 °C, 230 rpm) before being induction with IPTG (0.5-1 mM) for 3 hours. The culture was centrifuged (4,200 g, 15 minutes, 4 °C) and the resulting cell pellets suspended in lysis buffer (50 mM HEPES pH 7.5, 150 mM NaCl, EDTA-free complete protease inhibitor cocktail (Roche); 30 mL/1L culture pellet) and lysed by sonication (10x 30 seconds). After centrifugation (35,000 g, 1 hour, 4 °C), the HIS-tagged EthR was captured with a Ni^{2+} charged HiTrap IMAC Fast Flow Column (5 mL, GE Healthcare), washed with wash buffer (50 mM HEPES pH 7.5, 150 mM NaCl, 20 mM imidazole; 50 mL) and eluted with elution buffer (50 mM HEPES pH 7.5, 150 mM NaCl, 250 mM imidazole. Final purification was performed by gel filtration (Superdex 200) and the purified protein concentrated by centrifugation (4,500 g, 4 °C; 10 kDa Amicon Ultra concentrator). Protein concentration was determined by amino acid analysis, confirmed by UV A_{280} (Nanodrop 2000c; Thermo Scientific Inc.).

Protein preparation was carried out in the Department of Biochemistry by Dr Sachin Surade, Dr Michal Blaszczyk and Dr Vitor Mendes. Amino acid analysis was carried out by the Amino Acid Analysis Service in the Department of Biochemistry.

5.0.12 Thermal Shift Assay (Differential Scanning Fluorimetry)

Thermal shift were obtained using an iQ5 (Bio-Rad Laboratories, Inc.), CFX Connect (Bio-Rad Laboratories, Inc.), or Thermal Cycler LC480 (Roche). Testing was performed in a 96 well format with all samples run in duplicate. Fragments were typically prepared as 100 mM stocks in DMSO. Sample wells contained the fragment of interest (1 mM), NaCl (150 mM), Tris-HCl (20 mM, pH 8.0), SYPRO® Orange (2.5x) and EthR (20 μM). The samples were heated at 0.5 °C increments from 25 °C (Bio-Rad) or 37 °C (Roche) to 95 °C, and fluorescence read after each increment (λ_{ex} 490 nm, λ_{em} 575 nm). The first derivative of the fluorescence reading was calculated, wherein the minima corresponded to the melting temperature. These were compared with the controls to determine the change in melting temperature in the presence of the test compounds.

5.0.13 Isothermal Titration Calorimetry

ITC were produced on a MicroCal ITC200 operating with Origin 7 software (OriginLab). Fragments were typically prepared as 100 mM stock solutions in DMSO. The ITC syringe solution contained the fragment of interest at a concentration of 0.5-1.0 mM in NaCl (300 mM), Tris-HCl (20 mM, pH 8.0), glycerol (to match the concentration in the EthR stock) and a final concentration of 10% DMSO (in some cases, 15% was used to increase solubility of the fragments). The cell solution contained EthR (75-100 μM), NaCl (300 mM) Tris-HCl (20 mM, pH 8.0) and 10% DMSO (or 15% as noted above). The fragment was titrated into the protein solution in 1.0-2.0 μL aliquots over 25-36 injections (the first injection 0.4 μL) with a 120 second interval between injections. The raw data was processed in Origin 7 (OriginLab) and fitted using a single site model to give the K_D and thermodynamic values.

5.0.14 Surface Plasmon Resonance

SPR was carried out on a BIAcore T100 using the EthA promotor DNA immobilised on a CM5 chip (BIAcore) with a biotin/streptavidin linkage. Biotinylated DNA (with pUC19 DNA as a control) was flowed over the streptavidin-coated chip to produce a stable resonance reading. EthR (2 μM) and the test fragment (at varying concentration) were flowed at 20 μL/min in running buffer (2mM $MgCl_2$, 10 mM Tris-HCl pH 7.5, 0.1 mM EDTA, 200 mM NaCl, 2% DMSO) for 120 seconds, followed by a dissociation time of 150 seconds. The difference in resonance compared to the stable reading to give the binding level. Between samples, the chip was regenerated for 60 seconds with 20 μL/min 0.03% SDS in running buffer. IC_{50} values were calculated as the concentration which gave a binding level of 50% compared to the maximum binding level.

SPR was carried out in the Department of Biochemistry by Dr Sachin Surade, Dr Michal Blaszczyk, Dr Vitor Mendes and Ms Sherine Thomas.

5.0.15   X-Ray Crystallography

EthR crystals were grown using the hanging-drop vapour-diffusion method using previously described conditions (*35*) using 2 μL protein solution (>20 mg/mL EthR, 500 mM NaCl, 20 mM Tris-HCl pH 8.0, 10% v/v glycerol) and 4 μL reservoir (1.8-2.2 M ammonium sulfate, 100 mM MES-Na pH 6-7, 5-10% v/v glycerol, 7-10% 1,4-dioxane) at 16 °C. Crystals were washed in 1,4-dioxane-free mother liquor for a few hours, then soaked for 1-16 hours in fragment solutions (1-10 mM fragment, 1.8 M ammonium sulfate, 100 mM MES-Na pH 6.75, 12.5% v/v glycerol) prepared from 100 mM DMSO stock solutions. Soaked crystals were cryoprotected with mother liquor supplemented with 20% v/v ethylene glycol, then frozen in liquid nitrogen.

Data collection was performed at the European Synchrotron Radiation Facility (Grenoble, France), Diamond Light Source (Harwell, UK) or the Department of Biochemistry, University of Cambridge (X8 Proteum, Bruker). X-ray diffraction data was processed with CCP4 suite, indexed and integrated with Mosflm and scaled with Scala. Molecular replacement using PDB: 1T56 was performed with Phaser, and refined using Refmac5. Fitting was performed manually with Coot.

X-ray crystallography was carried out by Dr Sachin Surade, Dr Michal Blaszczyk and Dr Vitor Mendes, Department of Biochemistry, University of Cambridge.

5.0.16   Resazurin Microtiter Assay (REMAssay)

Determination of ethionamide MIC boosting activity was performed in duplicate using the REMAssay (resazurin microtiter assay) as described by Palomino *et al.*[113] Liquid culture of *M.tb.* H37Rv was prepared at an OD of 0.0001 in 7H9 broth (Difco) supplemented with 10% albumin-dextrose-catalase (ADC), 0.2% glycerol and 0.05% Tween-80. 2-fold serial dilutions of ethionamide were prepared in 96-well plates alone or supplemented with a fixed concentration of EthR inhibitors (1 μM). As control, EthR inhibitors were also tested alone in 2-fold serial dilutions. Plates were incubated for 6 days at 37 °C before the addition of 0.025% resazurin. After overnight incubation the fluorescence of the resazurin metabolite resorufin was measured (λ_{ex} 560 nm; λ_{em} 590 nm) (Tecan Infinite M200 microplate reader). IC_{50} and MIC were calculated using GraphPad Prism software.

REMAssay was carried out by Anthony Vocat of Prof. Stewart Cole's laboratory, Ecole Polytechnique Fédérale de Lausanne, Switzerland.
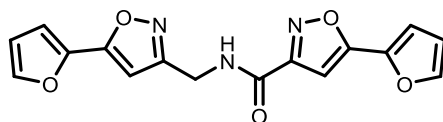
5.0.17   Other

Protein properties were estimated from the amino acid sequence (Rv3855, genome.tbdb.org) using Proteins version 2.5 (Programme Collection for Structural Biology and Biophysical Chemistry; A. Hofmann and N. Hu.).

5.1   Synthesis

*5-(Furan-2-yl)-N-{[5-(furan-2-yl)-1,2-oxazol-3-yl]methyl}-1,2-oxazole-3-carboxamide (**79**)*

Acid **78** (53 mg, 0.3 mmol) and amine **77** (48 mg, 0.3 mmol) were dissolved in anhydrous DCM (2.5 mL) under argon, and DIPEA (0.25 mL, 1.4 mmol) added. The reaction was allowed to stir for 5 minutes, and then COMU (0.128 g, 0.3 mmol) added. The reaction was allowed to stir at room temperature for 16 hours, and then the solvent was evaporated. The residue was redissolved in EtOAc (10 mL), washed with water (2 x 10 mL) and dried over Na_2SO_4, and the EtOAc evaporated *in vacuo*. The resulting powder was purified by flash column chromatography (2-8% MeOH/DCM), and residual impurities removed by washing with water (15 mL), yielding the product **79** as a yellow solid (65 mg, 0.2 mmol, 69%).

^{1}H NMR (400 MHz, $CDCl_3$) δ ppm 4.75 (d, *J* = 6.1 Hz, 2H), 6.49 (s, 1H), 6.52 (dd, *J* = 3.5, 1.8 Hz, 1H), 6.56 (dd, *J* = 3.5, 1.8 Hz, 1H), 6.88 (s, 1H), 6.90 (d, *J* = 3.5 Hz, 1H), 6.96 (d, *J* = 3.5 Hz, 1H), 7.32 (br. s, 1H), 7.52 (dd, *J* = 1.8, 0.7 Hz, 1H), 7.58 (dd, *J* = 1.8, 0.7 Hz, 1H); ^{13}C NMR (100 MHz, $CDCl_3$) δ ppm 35.3, 98.4, 98.6, 110.8, 111.4, 111.9, 112.1, 142.4, 143.0, 144.3, 144.8, 158.3, 158.9, 160.7, 162.4, 163.3; LCMS r.t. 2.01 min, found 326.2 [M+H]$^+$; HRMS calc $C_{16}H_{12}N_3O_5$ 326.0777, found [M+H]$^+$ 326.0783; TLC r.t. 0.88 (10% MeOH/DCM); IR (cm^{-1}) 3338 (m), 3111 (m), 1675 (s), 1562 (s), 1447 (s), 1261 (s); MP 144-145 °C; Purity 97% (LCMS).

*Bis((5-(furan-2-yl)isoxazol-3-yl)methyl)amine (**81**)*
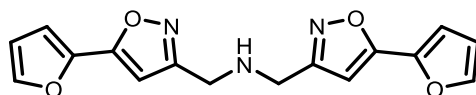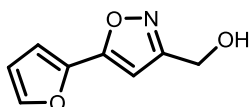

Alcohol **80** (30 mg, 0.2 mmol) was dissolved in anhydrous DCM (2 mL) under nitrogen and DMF (5 drops) added. The reaction was cooled on ice before oxalyl chloride (0.15 mL, 1.8 mmol) added slowly. The mixture was stirred at 0 °C for 5 minutes, the allowed to warm to room temperature over 1 hour before the solvent was evaporated *in vacuo*, and used without further purification.

The alkyl chloride was dissolved in anhydrous DMF (2.5 mL) was added dropwise to a solution of amine **77** (47 mg, 0.3 mmol) in anhydrous DMF (2.5 mL), and heated at 80 °C for 4 hours. The resulting mixture was diluted with DCM (10 mL), washed with water (15 mL) and back extracted with DCM (15 mL). The combined organic phases were washed with NaHCO$_3$ (2x, 30 mL) and brine (30 mL), then dried over MgSO$_4$ and evaporated. The crude material was then purified by flash column chromatography (0-5% MeOH/DCM), yielding a white solid of **81** (3 mg, 0.01 mmol, 3%).

^{1}H NMR (400 MHz, CDCl$_3$) δ ppm 2.17 (s, 1H), 4.62 (s, 4H), 6.53-6.57 (m, 4H), 6.93 (dd, *J* = 3.5, 0.6 Hz, 2H), 7.55 (dd, *J* = 1.8, 0.6 Hz, 2H); ^{13}C NMR (100 MHz, CDCl$_3$) δ ppm 34.3, 35.5, 98.6, 110.9, 112.0, 136.2, 144.4, 161.2; HRMS calc 312.0984 C$_{16}$H$_{14}$N$_3$O$_4$, found 312.0979 [M+H][+]; TLC r.f. 0.55 (10% MeOH/DCM); Purity >95% (NMR).

It was found that this compound was found to be unstable under LCMS conditions.

[5-(Furan-2-yl)-1,2-oxazol-3-yl]methanol (**80**)[114]

Acid **78** (27 mg, 0.2 mmol) was dissolved in anhydrous THF (2 mL) under nitrogen and LiAlH$_4$ (0.40 mL, 2.5 M in THF, 1.0 mmol) added dropwise. The reaction was stirred a room temperature for 3 hours, then quenched with MeOH (1 mL) and NaOH (0.1 mL, 10% aq), and the solvent evaporated *in vacuo*, yielding the alcohol **80** (23 mg, 0.1 mmol, 87%).

^{1}H NMR (400 MHz, CDCl$_3$) δ ppm 4.81 (s, 2H), 6.51 (s, 1H), 6.55 (dd, *J* = 3.5, 1.8 Hz, 1H), 6.91 (d, *J* = 3.5 Hz, 1H), 7.55 (d, *J* = 1.8 Hz, 1H); ^{13}C NMR (100 MHz, CDCl$_3$) δ ppm 57.0, 97.8, 110.6, 111.9, 143.1, 144.2, 162.0, 167.8; LCMS r.t. 1.52 min, found 166.1 [M+H][+]; TLC r.f. 0.60 (10% MeOH/DCM); IR (cm^{-1}) 3354 (br. w), 1616 (s), 1435 (m), 1345 (s).

## Benzamidoxime (**83**)[23,101,115]
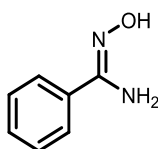
Hydroxylamine hydrochloride (1.01 g, 14.5 mmol) was dissolved in ethanol (15 mL) with benzonitrile (1.00 mL, 9.7 mmol). DIPEA (2.7 mL, 15.5 mmol) was added and the mixture heated at reflux for 1 hour. The solvent was evaporated *in vacuo* and the clear oil remaining was

dissolved in ethyl acetate (25 mL) and washed with water (2 x 25 mL) then brine (25 mL). The organic phase was dried over MgSO$_4$, filtered and concentrated to dryness *in vacuo* yielding a clear, colourless oil which solidified on standing to produce the product (**83**) as a white solid (0.941 g, 7.4 mmol, 76%). This was used without further purification.

^{1}H NMR (400 MHz, DMSO-d_6) δ ppm 5.80 (s, 2H), 7.29-7.42 (m, 3H), 7.62-7.74 (m, 2H), 9.63 (s, 1H); ^{13}C NMR (100 MHz, DMSO-d_6) δ ppm 125.7, 128.4, 129.2, 133.7, 151.2; LCMS r.t. 1.81 min, found 137.1 [M+H]$^+$; TLC r.f. 0.51 (10% MeOH/DCM); IR (cm^{-1}) 3452 (m), 3359 (s), 3210 (m), 1646 (s), 1578 (m), 1386 (m).

*tert-Butyl ((3-phenyl-1,2,4-oxadiazol-5-yl)methyl)carbamate (*85a*)*
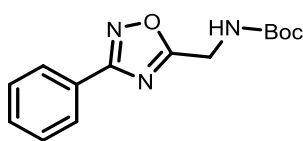
 N-Boc-glycine hydrochloride (0.385 g, 2.2 mmol) and HBTU (0.918 g, 2.4 mmol) were dissolved in anhydrous DMF (5 mL) and DIPEA (1.15 mL, 6.6 mmol) was added. After stirring for 5 minutes, **83** (0.300 g, 2.2 mmol) was added and the reaction stirred at room temperature for 4 hours. The reaction mixture was then poured into water (50 mL) and the resulting white precipitate filtered and dissolved in DMF (10 mL). The solution was heated at 120 °C for 4 hours, then allowed to cool, water (15 mL) added and extracted into ethyl acetate (30 mL). The organic layer was washed with HCl (5% aq, 2 x 15 mL) and brine (15 mL), before being dried over MgSO$_4$, filtered and evaporated to dryness *in vacuo*, yielding **85a** as a white solid (0.303 g, 1.1 mmol, 50%).

^{1}H NMR (400 MHz, CDCl$_3$) δ ppm 1.48 (s, 9H), 4.64 (d, *J* = 5.0 Hz, 2H), 5.26 (br. s, 1H), 7.38-7.52 (m, 3H), 8.07 (d, *J* = 6.5 Hz, 2H); ^{13}C NMR (100 MHz, CDCl$_3$) δ ppm 28.3, 37.2, 80.6, 126.4, 127.4, 128.8, 131.3, 155.4, 168.4, 176.5; LCMS r.t. 2.07 min, found 220.1 [M - *tert*-butyl + 2H]$^+$; HRMS calc C$_{14}$H$_{18}$N$_3$O$_3$ 276.1348, found [M+H]$^+$ 276.1352; TLC r.f. 0.26 (20% EtOAc/hexane); IR (cm^{-1}) 3365 (m), 1679 (s), 1523 (s).

*(3-Phenyl-1,2,4-oxadiazol-5-yl)methanamine (*85*)*
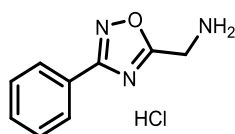
Compound **85a** (0.100 g, 0.4 mmol) in methanol (5 mL) was cooled to 0 °C, before HCl (3.0 mL, 1.25 M in methanol) was added. The reaction was stirred at 0 °C for 0.5 hour, then allowed to warm to room temperature. The solvent was removed *in vacuo* to yield the product **85** as a white solid (53 mg, 0.3 mmol, 83%). The product was used without further purification.

^{1}H NMR (400 MHz, DMSO-d_6) δ ppm 4.58 (s, 2H), 7.43-7.54 (m, 3H), 8.03-8.10 (m, 2H), 8.95 (br. s, 2H); ^{13}C NMR (100 MHz, DMSO-d_6) δ ppm 35.1, 126.0, 127.5, 129.9, 132.4, 168.2, 174.8; LCMS r.t. 2.71 min, found 176.2 [M+H]$^+$; HRMS calc $C_9H_{10}N_3O$ 176.0824, found [M+H]$^+$ 176.0820; TLC r.f. 0.57 (10% MeOH/CHCl$_3$); IR (cm^{-1}) 3350 (w, br.), 2875 (w, br.), 1604 (m), 1446 (s), 1350 (s).

*Ethyl 3-phenyl-1,2,4-oxadiazole-5-carboxylate (*87*)*[101]
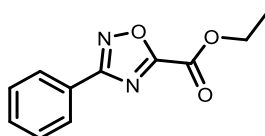
Benzamidoxime **83** (0.100 g, 0.7 mmol) was dissolved in dry DCM (5 mL) and pyridine (0.07 mL, 0.9 mmol) added. The mixture was cooled to 0 °C before monoethyloxalyl chloride (0.10 mL, 0.9 mmol) was added dropwise. The mixture was stirred at 0°C for 2 hours, then concentrated *in vacuo*. The residue was redissolved in DCM (10 mL) and washed with saturated sodium bicarbonate solution (2 x 10 mL). The organic phase was dried over Na$_2$SO$_4$, filtered and dried *in vacuo* yielding the product **87** as a yellow solid (40 mg, 0.2 mmol, 25%).

^{1}H NMR (400 MHz, CDCl$_3$) δ ppm 1.50 (t, *J* = 7.2 Hz, 3H), 4.58 (q, *J* = 7.2 Hz, 2H), 7.60-7.70 (m, 3H), 8.05-8.16 (m, 2H); ^{13}C NMR (100 MHz, CDCl$_3$) δ ppm 14.0, 63.9, 125.6, 127.6, 128.9, 131.8, 154.1, 166.6, 169.4; LCMS r.t. 2.07 min, found 219.1 [M+H]$^+$; TLC r.f. 0.70 (33% EtOAc/40-60 petrol ether); IR (cm^{-1}) 1741 (s), 1560 (m), 1445 (s), 1319 (s).

*Isobutyl ((3-phenyl-1,2,4-oxadiazol-5-yl)methyl) carbonate (*91*)*
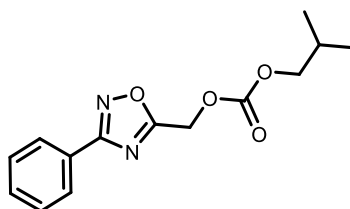

Glycolic acid (0.100 g, 1.3 mmol) in toluene (35 mL) was cooled to 0 °C, and triethylamine (0.37 ml, 2.6 mmol) and isobutyl chloroformate (0.34 mL, 2.6 mmol) added. The reaction was stirred at 0 °C for 10 minutes, before benzamidoxime (**83**) (0.178 g, 1.3 mmol) and powdered

activated 4 Å molecular sieves (0.5 g) were added. The reaction was heated under reflux overnight, after which the reaction was allowed to cool, filtered and concentrated to dryness *in vacuo*. The residue was purified by flash column chromatography (30-70% EtOAc/40-60 petrol ether) to yield the product **91** (0.309 g, 1.1 mmol, 86%).

^{1}H NMR (400 MHz, CDCl$_3$) δ ppm 0.99 (d, *J* = 6.9 Hz, 6H), 1.93-2.11 (m, 1H), 4.04 (d, *J* = 6.7 Hz, 2H), 5.42 (s, 2H), 7.44-7.57 (m, 3H), 8.05-8.14 (m, 2H); ^{13}C NMR (100 MHz, CDCl$_3$) δ ppm 18.7, 27.7, 59.3, 75.1, 126.2, 127.5, 128.8, 131.4, 154.5, 168.4, 173.5; LCMS r.t. 2.30 min found 277.2 [M+H]$^+$; HRMS calc C$_{14}$H$_{17}$N$_2$O$_4$ 277.1188, found [M+H]$^+$ 277.1177; TLC r.f. 0.78 (25% EtOAc/40-60 petrol ether); IR (cm^{-1}) 2960 (w), 1753 (s), 1248 (s, br.).

(3-Phenyl-1,2,4-oxadiazol-5-yl)methanol (**92**)[116]
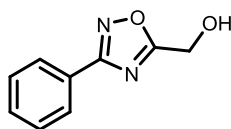
Carbonate **91** (75 mg, 0.3 mmol) was dissolved in MeOH (4 mL) and NaOH (0.15 mL, 2.0 M) was added. The reaction was stirred at ambient temperature for 1.5 hours, then acidified to pH 4 with HCl, (0.1 mL, 1.0 M in MeOH). The product was extracted with EtOAc (10 mL) and dried *in vacuo* to yield the product **92** as a white powder (40 mg, 0.2 mmol, 85%).

^{1}H NMR (400 MHz, CDCl$_3$) δ ppm 3.38 (br. s, 1H), 4.97 (s, 2H), 7.45-7.56 (m, 3H), 8.02-8.10 (m, 2H); ^{13}C NMR (100 MHz, CDCl$_3$) δ ppm 56.5, 126.2, 127.4, 128.9, 131.5, 168.1, 178.3; LCMS r.t. 1.61 min, found 177.1 [M+H]$^+$; HRMS calc C$_9$H$_9$N$_2$O$_2$ 177.0664, found [M+H]$^+$ 177.0661; TLC r.f. 0.60 (10% MeOH/DCM); IR (cm^{-1}) 3275 (m, br.), 1456 (m), 1366 (s).

Bis((3-phenyl-1,2,4-oxadiazol-5-yl)methyl)amine (**93**)
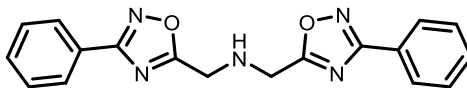
Alcohol **92** (61 mg, 0.3 mmol) was dissolved in anhydrous DCM (15 mL) under nitrogen and cooled to 0 °C. Oxalyl chloride (0.27 mL, 3.3 mmol) was added dropwise and the solution stirred for 5 minutes before being allowed to warm to room temperature where it was stirred for 1 hour, after which the solvent was evaporated *in vacuo*. Amine **85** (91 mg, 0.3 mmol) was dissolved in anhydrous DMF (15 mL) under nitrogen and the alkyl chloride added dropwise. The reaction mixture was heated at 80 °C for two hours. The reaction mixture was cooled, extracted with DCM (15 mL) and washed with water (30 mL), NaHCO$_3$ (30 mL) and brine

(30 mL), before the solvent was evaporated *in vacuo*. The resulting crude compound was purified by flash column chromatography (0-5% MeOH/DCM), yielding the product **93** as a white solid (65 mg, 0.2 mmol, 59%).

^{1}H NMR (400 MHz, CDCl$_3$) δ ppm 4.75 (s, 4H), 7.42-7.57 (m, 6H), 8.01-8.16 (m, 4H); ^{13}C NMR (100 MHz, CDCl$_3$) δ ppm 33.3, 126.1, 127.5, 128.9, 131.5, 168.9, 174.3; HRMS calc 334.1304 C$_{18}$H$_{16}$N$_5$O$_2$, found 334.1299 [M+H]$^+$; TLC r.f. 0.57 (10% EtOAc/40-60 petrol ether); IR (cm^{-1}) 3036 (w), 1598 (m), 1445 (m), 1361 (s); MP 37-38 °C; Purity >95% (NMR).

It was found that this compound was unstable under LCMS and HRMS conditions.

Ethyl 5-phenyl-1,2,4-oxadiazole-3-carboxylate (**96**)[101]
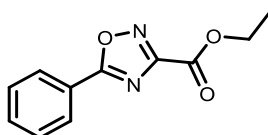
Amidoxime **95** (0.102 g, 0.8 mmol) was dissolved in DCM (7.0 mL) with DMF (3 drops) and cooled to -15 °C, then DIPEA (0.18 mL, 1.1 mmol) was added. Benzoyl chloride (0.08 mL, 0.7 mmol) was added and the reaction stirred for 30 minutes, then warmed up to room temperature where it was stirred overnight. The reaction mixture was poured into cold water (0 °C, 40 mL), extracted with DCM (40 mL) and dried over MgSO$_4$ before being evaporated to dryness *in vacuo*. The resulting material was dissolved in DMF (10 mL) and heated to 120 °C overnight, then diluted with water (25 mL) and extracted with DCM (2 x 30 mL). The organic phases were combined and dried over MgSO$_4$, concentrated *in vacuo*, then purified by flash column chromatography (30-50% EtOAc/40-60 petrol ether) to yield the product **96** as a yellow crystalline solid (0.134 g, 0.6 mmol, 80%).

^{1}H NMR (400 MHz, CDCl$_3$) δ ppm 1.46 (t, *J* = 7.2 Hz, 3H), 4.54 (q, *J* = 7.2 Hz, 2H), 7.52-7.59 (m, 2H), 7.61-7.68 (m, 1H), 8.19-8.26 (m, 2H); ^{13}C NMR (100 MHz, CDCl$_3$) δ ppm 14.1, 63.0, 123.2, 128.3, 129.2, 133.5, 157.8, 162.4, 177.2; LCMS r.t. 2.11 min, found 219.2 [M+H]$^+$; HRMS calc C$_{11}$H$_{11}$N$_3$O$_3$ 219.0770, found [M+H]$^+$ 219.0779; TLC r.f. 0.76 (5% MeOH/DCM); IR (cm^{-1}) 2992 (w, br.), 1734 (m), 1607 (m), 1557 (m), 1475 (m), 1450 (m), 1377 (m), 1353 (m), 1215 (s); MP 48-49 °C.

5-Phenyl-1,2,4-oxadiazole-3-carboxylic acid (**97**)[101]
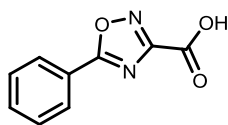
Ester **96** (28 mg, 0.1 mmol) was dissolved in a mixture of THF (10 mL), water (2.5 mL) and EtOH (2.5 mL) before LiOH monohydrate (32 mg, 0.8 mmol) was added and the reaction was stirred for 1.5 hours, until TLC indicated complete reaction of the starting material. The reaction was acidified with HCl (0.5 mL, 3.0 M), diluted with water (10 mL) and then extracted with DCM (2 x 30 mL). The combined organic phase was dried *in vacuo*, yielding the product **97** as a yellow solid (15 mg, 0.1 mmol, 62%).

^{1}H NMR (400 MHz, DMSO-d_6) δ ppm 7.66-7.74 (m, 2H), 7.76-7.83 (m, 1H), 8.16-8.25 (m, 2H); ^{13}C NMR (100 MHz, DMSO-d_6) δ ppm 128.0, 128.2, 128.7, 129.6, 133.1, 133.7, 158.6; LCMS r.t. 1.87 min, found 191.1 [M+H]$^+$; TLC r.f. 0.00 (33% EtOAc/40-60 petrol ether); IR (cm^{-1}) 3500 (w, br.), 2937 (w, br.), 1728 (m), 1604 (m), 1556 (s), 1449 (m), 1248 (s), 1200 (s).

2-((4-Bromophenyl)thio)acetamide (**99**)
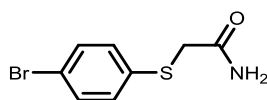
4-Bromothiophenol (0.511 g, 2.6 mmol), 2-bromoacetamide (0.714 g, 5.2 mmol), K$_2$CO$_3$ (0.375 g, 2.6 mmol) and 3 Å molecular sieves (1.00 g) were suspended in acetone (15 mL) and the reaction heated to 50 °C overnight. The reaction was mixture allowed to cool, filtered and washed with acetone (30 mL) and the solvent evaporated under reduced pressure. The white solid was re-suspended in DCM (60 mL), washed with sodium bicarbonate (2 x 30 mL), water (2 x 30 mL) and brine (30 mL). The organic phase was dried over MgSO$_4$, filtered and evaporated *in vacuo*, yielding the product **99** as white crystalline solid (0.551 g, 2.2 mmol, 83%).

^{1}H NMR (400 MHz, acetone-d_6) δ ppm 3.67 (s, 2H), 6.52 (br. s, 1H), 7.05 (br. s, 1H), 7.31-7.38 (m, 2H), 7.44-7.52 (m, 2H); ^{13}C NMR (100 MHz, acetone-d_6) δ ppm 37.5, 120.2, 131.0, 132.8, 137.1, 170.5; LCMS r.t. 1.65 min, found 265.9; HRMS calc C$_8$H$_9$NOSBr 245.9588, found [M+H]$^+$ 245.9599; TLC r.f. 0.36 (5% MeOH/DCM); IR 3401 (m), 3172 (m, br), 1642 (s), 1473 (m), 1384 (s); MP 138-139 °C; Purity >98% (LCMS).

2-((4-Bromophenyl)sulfinyl)acetamide (**100**)
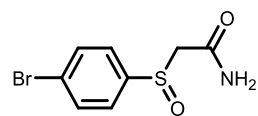
Compound **99** (0.1004 mg, 0.4 mmol) was dissolved in MeOH (2.0 mL) and THF (2.0 mL) with stirring. Oxone™ (0.182 g, 0.6 mmol) in water (3.0 mL) was added dropwise, and the mixture stirred at room temperature for 21 hours. The reaction mixture was filtered and evaporated under reduced pressure. The solid formed was re-suspended in DCM (20 mL), washed with water (10 mL) and brine (2 x 10 mL) and the organic solvent was evaporated in vacuo. The material was purified by flash column chromatography (3-7% MeOH/DCM), yielding the product **100** as a white solid (52 mg, 0.2 mmol, 48%).

^{1}H NMR (400 MHz, DMSO-d_6) δ ppm 3.64-3.73 (m, 1H), 3.76-3.86 (m, 1H), 7.32 (br. s., 1H), 7.58 (br. s. 1H), 7.63 (d, J = 8.5 Hz, 2H), 7.80 (d, J = 8.5 Hz, 2H); ^{13}C NMR (125 MHz, DMSO-d_6) δ ppm 62.4, 124.5, 126.3, 1322.1, 143.6, 165.6; LCMS r.t. 1.32 min, found 262.0 (Br[79]) + 264.0 (Br[81]) [M+H][+]; HRMS calc $C_8H_9NO_2SBr^{79}$ 261.9537, found [M+H][+] 261.9537; TLC r.f. 0.13 (5% MeOH/DCM); IR (cm^{-1}) 3770 (w, br.),1668 (s); Purity 95% (LCMS).

2-((4-Bromophenyl)sulfonyl)acetamide (**101**)[117]
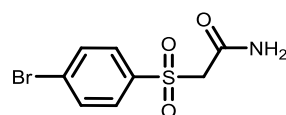
Compound **99** (99 mg, 0.4 mmol) was dissolved in MeOH (2.0 mL) and THF (2.0 mL) and stirred for 5 minutes at ambient temperature. Oxone™ (0.49 g, 1.6 mmol) was dissolved in water (3.0 mL), and added dropwise to the solution. The mixture was stirred at room temperature overnight. The reaction was filtered and was then evaporated *in vacuo*. The solid material which was obtained was dissolved in DCM (40 mL), washed with water (2 x 20 mL) and brine (20 mL), then the organic phase was evaporated under reduced pressure, yielding the product **101** as a white solid (79 mg, 0.3 mmol, 71%).

^{1}H NMR (400 MHz, DMSO-d_6) δ ppm 4.27 (s, 2H), 7.35 (br. s, 1H), 7.60 (br. s, 1H), 7.77-7.82 (m, *2*H), 7.85-7.90 (m, *2*H); ^{13}C NMR (100 MHz, DMSO-d_6) δ ppm 61.2, 128.4, 130.6, 132.6, 139.2, 163.1; LCMS r.t. 1.43 min, found 277.94 [M+H][+]; HRMS calc $C_8H_9NO_3SBr$ 277.9487, found [M+H][+] 277.9488; TLC r.f. 0.25 (5% MeOH/DCM); IR (cm^{-1}) 3395 (w), 3170 (w), 1691 (s), 1306 (s); MP 152-154 °C; Purity 96% (LCMS).

## 2-((4-Bromophenyl)sulfonyl)ethanethioamide (**102**)
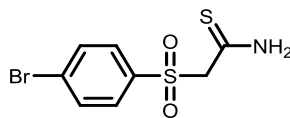
Compound **99** (0.100 g, 0.4 mmol) was suspended in dry THF (20 mL) and Lawesson's reagent (0.170 g, 0.4 mmol) added with dry THF (10 mL). The mixture was then heated to reflux for 3 hours before the solvent was evaporated *in vacuo*. The resulting solid was dissolved in DCM (40 mL), washed with water (2 x 40 mL) and brine (40 mL) and the organic layer was evaporated *in vacuo*. The crude product was purified by flash column chromatography (0-10% MeOH/DCM), yielding the product **102** as a yellow solid (42 mg, 0.1 mmol, 39%).

^{1}H NMR (400 MHz, DMSO-d_6) δ ppm 4.61 (s, 2H), 7.76-7.83 (m, 2H), 7.84-7.90 (m, 2H), 9.41 (br. s, 1H), 9.85 (br. s, 1H); ^{13}C NMR (100 MHz, DMSO-d_6) δ ppm 68.5, 128.2, 130.5, 132.0, 137.6, 191.4; LCMS r.t. 1.69 min found 294.0 [M+H]$^+$; HRMS calc $C_8H_9NO_2{}^{32}S_2{}^{79}Br$ 293.9253, found [M+H]$^+$ 293.9243; TLC r.f. 0.43 (5% MeOH/DCM); IR (cm^{-1}) 3422 (m), 3329 (m), 3230 (w), 2928 (w, br), 1626 (m), 1596 (m), 1576 (m), 1422 (s), 1299 (s), 1257 (s); MP 179-180 °C; Purity >98% (LCMS).

Caution: Stench, both Lawesson's reagent and the product should be kept in a fumehood at all times.

2-(Biphenyl-4-ylsulfonyl)acetamide (**106**)[118]
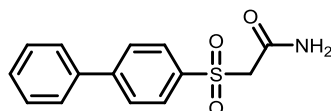
Phenylboronic acid (33 mg, 0.3 mmol), sodium carbonate (32 mg, 0.3 mmol) and Pd(PPh$_3$)$_4$ (35 mg, 10 mol%) were dissolved in toluene/EtOH (5.0 mL, 1:1) with compound **101** (75 mg, 0.3 mmol) and heated under microwave conditions at 100 °C for 60 minutes. This was filtered through Celite™ and evaporated *in vacuo*. The crude product was purified by flash column chromatography (5-10% MeOH/DCM), yielding the product **106** as a yellow solid (45 mg, 0.2 mmol, 61%).

^{1}H NMR (400 MHz, MeCN-d_3) δ ppm 4.08 (s, 2H), 6.03 (br. s, 1H), 6.49 (br. s, 1H), 7.42-7.57 (m, 3H), 7.69-7.75 (m, 2H), 7.85-7.90 (m, 2H), 7.95-8.01 (m, 2H); ^{13}C NMR (100 MHz, DMSO-d_6) δ ppm 47.7, 127.3, 127.4, 128.8, 128.9, 129.3, 131.6, 138.6, 145.5; LCMS r.t. 1.71 min,

found 276.2 [M+H]+; HRMS calc $C_{14}H_{13}NO_3SNa$ 298.0514, found [M+Na]+ 298.0528; TLC r.f. 0.42 (10% MeOH/DCM); IR (cm-1) 3394 (m), 3194 (w), 1664 (s), 1317 (s); Purity 98% (LCMS).

2-(Biphenyl-4-ylsulfonyl)ethanethioamide (**104**)
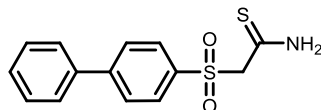
Compound **106** (55 mg, 0.2 mmol) was dissolved in anhydrous THF (7.5 mL) and Lawesson's reagent (85 mg, 0.2 mmol) in dry THF (7.5 mL) was added and the reaction mixture heated to reflux for 3 hours. The solvent was evaporated under reduced pressure. The solid was dissolved in DCM (20 mL), washed with water (2 x 20 mL) and brine (20 mL) then evaporated in vacuo. The remaining solid was extracted with DCM (20 mL), filtered and evaporated in vacuo. The resulting material was purified by flash column chromatography (0-10% MeOH/DCM) and the product dried under reduced pressure to yield the product **104** as a white solid (32 mg, 0.1 mmol, 53%).

1H NMR (400 MHz, DMSO-d_6) δ ppm 4.62 (s, 2H), 7.42-7.57 (m, 3H), 7.72-7.85 (m, 2H), 7.90-8.02 (m, 4H), 9.40 (br. s, 1H), 9.85 (br. s, 1H); 13C NMR (100 MHz, DMSO-d_6) δ ppm 68.7, 127.1, 127.2, 128.7, 129.1, 129.2, 137.2, 138.2, 145.3, 191.6; LCMS r.t. 1.92 min; found 292.1 [M+H]+; HRMS calc $C_{14}H_{14}NO_2S_2$ 292.0466, found [M+H]+ 292.0489; TLC r.f. 0.70 (10% MeOH/DCM); IR (cm-1) 3397 (br. w), 3310 (br. w), 3211 (br. w), 2924 (w), 1630 (m), 1594 (m), 1448 (m), 1399 (m), 1291 (m), 1258 (m); Purity 97% (LCMS).

Caution: Stench, both Lawesson's reagent and the product should be kept in a fumehood at all times.
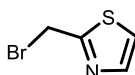
2-Bromomethyl-1,3-thiazole (**109**)[119]

1,3-Thiazol-2-ylmethanol (0.106 g, 0.9 mmol) was dissolved in chloroform (1.00 mL) and PBr₃ (0.03 mL, 0.3 mmol) added slowly. The reaction mixture was heated at reflux for 1 hour, then diluted with Na₂CO₃ (satd., 10 mL) and extracted with chloroform (2 x 10 mL). The organic phases were dried over MgSO₄ and evaporated *in vacuo* to yield the product **109** as a yellow oil, which was used without further purification.

^{1}H NMR (400 MHz, CDCl$_3$) δ ppm 4.75 (s, 2H), 7.37 (d, *J* = 3.3 Hz, 1H), 7.74 (d, *J* = 3.3 Hz, 1H); ^{13}C NMR (100 MHz, CDCl$_3$) δ ppm 26.4, 121.2, 142.9, 165.5; TLC r.f. 0.69 (neat EtOAc).

2-(Bromomethyl)thiophene (**109a**)[120]
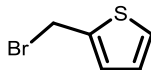
Synthesised using the same procedure as compound **109** using 2-thiophenemethanol (0.08 mL, 0.9 mmol).

Yellow oil; ^{1}H NMR (400 MHz, CDCl$_3$) δ ppm 4.77 (s, 2H), 6.97 (dd, *J* = 5.0, 3.5 Hz, 1H) 7.14 (d, *J* = 3.5 Hz, 1H), 7.34 (dd, *J* = 5.0, 0.9 Hz, 1H).

2-(((1,1'-Biphenyl)-4-ylsulfonyl)methyl)thiazole (**110**)
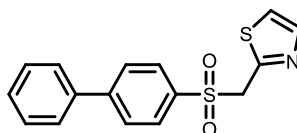
Biphenyl-4-sulfonic acid (75 mg, 0.3 mmol) was suspended in DMF (2.0 mL) with pyridine (0.03 mL, 0.4 mmol) and compound **109** (0.15 g, 0.8 mmol) was added in DMF (2.0 mL). The reaction was stirred at room temperature overnight, before being diluted with DCM (15 mL), washed with HCl (3.0 M, 15 mL), saturated sodium bicarbonate (15 mL), and brine (15 mL). The organic phase was evaporated and the residue purified by flash column chromatography (neat DCM) to yield the product **110** as a white crystalline solid (18 mg, 0.1 mmol, 7%).

^{1}H NMR (400 MHz, CDCl$_3$) δ ppm 4.83 (s, 2H), 7.39-7.52 (m, 4H), 7.56-7.65 (m, 2H), 7.66-7.75 (m, 3H), 7.76-7.82 (m, 2H); ^{13}C NMR (100 MHz, CDCl$_3$) δ ppm 59.7, 122.1, 127.4, 127.8, 128.7, 129.1, 136.0, 138.9, 143.1, 147.1, 155.9; LCMS r.t.2.12 min, found 315.9[M+H]$^+$; HRMS calc C$_{16}$H$_{14}$NO$_2$S$_2$ 316.0466, found [M+H]$^+$ 316.0483; TLC r.f. 0.76 (5% MeOH/DCM); IR (cm^{-1}) 2989 (w), 2923 (w), 1733 (w), 1594 (m), 1492 (m), 1478 (m), 1394 (m), 1314 (s), 1206 (m); MP 143-146 °C (decomposes); Purity 87% (LCMS).

2-[(Biphenyl-4-ylsulfonyl)methyl]thiophene (**111**)

Biphenyl-4-sulfinic acid (75 mg, 0.3 mmol) was suspended in DMF (2.0 mL) with pyridine (0.03 mL, 0.4 mmol) before compound **109a** (0.15 g, 0.8 mmol) was added in DMF (2.0 mL). The reaction mixture was stirred at ambient temperat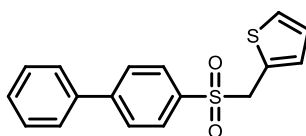ure for 6 hours. The mixture was diluted with DCM (15 mL), washed with HCl (3.0 M, 15 mL), sodium bicarbonate (15 mL) and brine (15 mL), dried over Na_2SO_4 and dried under reduced pressure. The residue was purified by flash column chromatography (10-50% EtOAc/petrol ether) to yield the product **111** as a yellow solid (9 mg, 0.03 mmol, 9% over 2 steps).

^{1}H NMR (400 MHz, CDCl$_3$) δ ppm 4.57 (s, 2H), 6.91 (d, *J* = 3.5 Hz, 1H), 6.96 (dd, *J* = 5.1, 3.5 Hz, 1H), 7.30 (d, *J* = 5.1 Hz, 1H), 7.40-7.53 (m, 3H), 7.59-7.64 (m, 2H), 7.70 (d, *J* = 8.4 Hz, 2H), 7.77 (d, *J* = 8.4 Hz, 2H); ^{13}C NMR (100 MHz, CDCl$_3$) δ ppm 57.4, 127.2, 127.4, 127.5, 127.6, 128.6, 128.7, 129.1, 129.2, 130.3, 136.0, 139.0, 146.8; LCMS r.t. 2.33 min, found 336.6 [M+Na]$^+$; HRMS calc $C_{17}H_{14}O_2S_2Na$ 337.0327, found [M+Na]$^+$ 337.0323; TLC r.f. 0.60 (33% EtOAc/petrol ether); IR (cm^{-1}) 2986 (br. w), 2913 (w), 1595 (m), 1479 (w), 1400 (w), 1305 (s), 1258 (m); MP 127-129 °C; Purity 90% (LCMS).

*2-(((4-Bromophenyl)sulfonyl)methyl)thiophene (**112**)*
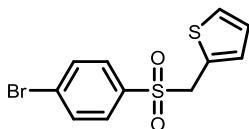
2-(Bromomethyl)thiophene (**109a**) (0.34 g, 2.0 mmol) was suspended in DCM (6.0 mL) under nitrogen, and sodium 4-bromobenzenesulfinate (0.30 g, 1.2 mmol) was added, followed by DMF (1.00 mL) and pyridine (0.30 mL, 3.6 mmol). The reaction mixture was heated to reflux for 4 hours, then evaporated to dryness. The residue was suspended in brine (20 mL) and extracted with DCM (20 mL). The organic phase was purified by flash column chromatography (10-30% EtOAc/40-60 petrol ether) yielding the product **112** as a colourless crystalline solid (94 mg, 0.3 mmol, 15%).

^{1}H NMR (400 MHz, CDCl$_3$) δ ppm 4.53 (s, 2H), 6.88 (d, *J* = 3.5 Hz, 1H), 6.96 (dd, *J* = 5.1, 3.5 Hz, 1H), 7.30 (dd, *J* = 5.1, 1.2 Hz, 1H), 7.55 (d, *J* = 8.7 Hz, 2H), 7.63 (d, *J* = 8.7 Hz, 2H); LCMS r.t. 2.15 min, found 338.7 (Br^{79}) + 340.8 (Br^{81}) [M+Na]$^+$; HRMS calc $C_{11}H_9S_2O_2Br^{79}Na$ 338.9120, found [M+Na]$^+$ 338.9114; TLC r.f. 0.58 (33% EtOAc/40-60 petrol ether); IR (cm^{-1}) 2970 (w), 2915 (w), 1575 (m), 1468 (w), 1389 (m), 1310 (s), 1250 (s); MP 114-116 °C; Purity 95% (LCMS).

3-(4-((Thiophen-2-ylmethyl)sulfonyl)phenyl)pyridine (114)
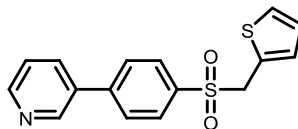
Compound **112** (66 mg, 0.2 mmol) was dissolved in DMF (2.6 mL). While degassing with nitrogen, pyridine-3-boronic acid (29 mg, 0.2 mmol), K_2CO_3 (89 mg, 0.6 mmol) in water (1.3 mL), and $Pd(PPh_3)_4$ (23 mg, 10 mol%) were added. The reaction mixture was heated to 90 °C for 2 hours, then filtered through Celite™ and evaporated, then purified by flash column chromatography (0-5% MeOH/DCM) to yield the product **114** as a yellow solid (14 mg, 0.04 mmol, 22%).

^{1}H NMR (400 MHz, CDCl$_3$) δ ppm 4.58 (s, 2H), 6.92 (d, J = 3.5 Hz, 1H), 6.97 (dd, J = 5.1, 3.5 Hz, 1H), 7.31 (dd, J = 5.1, 1.3 Hz, 1H), 7.44 (dd, J = 7.8, 4.8 Hz, 1H), 7.70 (d, J = 8.6 Hz, 2H), 7.82 (d, J = 8.6 Hz, 2H), 7.91 (dt, J = 7.8, 2.0 Hz, 1H), 8.69 (dd, J = 4.8, 1.8 Hz, 1H), 8.88 (d, J = 1.8 Hz, 1H); ^{13}C NMR (100 MHz, CDCl$_3$) δ ppm 57.4, 77.2, 123.8, 127.3, 127.6, 127.7, 128.4, 129.5, 130.3, 134.7, 137.0, 143.4, 148.4, 149.8; LCMS r.t. 1.75 min, found 316.0 [M+H]$^+$; HRMS calc $C_{16}H_{14}NO_2S_2$ 316.0466, found [M+H]$^+$ 316.0487; TLC r.f. 0.60 (5% MeOH/DCM); IR (cm^{-1}) 2915 (w), 1307 (m); MP 122-126 °C; Purity >98% (LCMS).

Ethyl 2-((4-bromophenyl)thio)acetate (115)[121]
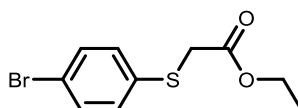
A mixture of 4-bromothiophenol (0.5 g, 2.6 mmol), K_2CO_3 (1.01 g, 7.3 mmol) and ethyl bromoacetate (0.35 mL, 3.2 mmol) in acetone (10.0 mL) was heated to reflux for 5 hours. The reaction was then cooled and filtered, and the solvent evaporated under reduced pressure. The residue was dissolved in DCM (20 mL), washed with water (2 x 15 mL) and brine (15 mL), and again evaporated under reduced pressure. The resulting material was purified by flash column chromatography (0-5% MeOH/DCM) to yield the product **115** as a clear, colourless oil (0.269 g, 1.0 mmol, 38%).

^{1}H NMR (400 MHz, CDCl$_3$) δ ppm 1.24 (t, J = 7.2 Hz, 3H), 3.62 (s, 2H), 4.18 (q, J = 7.2 Hz, 2H), 7.29 (d, J = 8.6 Hz, 2H), 7.43 (d, J = 8.6 Hz, 2H); ^{13}C NMR (100 MHz, CDCl$_3$) δ ppm 14.1, 36.6, 61.6, 121.0, 131.5, 132.0, 134.2, 169.3; LCMS r.t. 4.68 min, found 277.4 [M+H]$^+$; TLC r.f. 0.78 (33% EtOAc/40-60 petrol ether).

Ethyl 2-((4-bromophenyl)sulfonyl)acetate (116)[121]
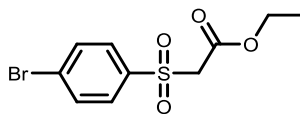
Compound **115** (0.269 g, 1.0 mmol) was dissolved in a 1:1 mixture of MeOH/THF (10.8 mL). Oxone™ (1.12 g, 1.8 mmol) was dissolved in water (7.2 mL) and added dropwise to the MeOH/THF solution. The reaction as stirred at room temperature for 3 days, then filtered and evaporated *in vacuo*. The residue was taken up in DCM (30 mL), washed with H_2O (2 x 30 mL) brine (30 mL) and evaporated under reduced pressure to yield the product **116** as colourless crystals (0.184 g, 0.6 mmol, 61%).

^{1}H NMR (400 MHz, CDCl$_3$) δ ppm 1.18 (t, *J* = 7.1 Hz, 3H), 4.08-4.16 (m, 4H), 7.70 (d, *J* = 8.6 Hz, 2H), 7.79 (d, *J* = 8.6 Hz, 2H); ^{13}C NMR (100 MHz, CDCl$_3$) δ ppm 13.7, 60.7, 62.3, 129.6, 130.0, 132.4, 137.5, 162.1; LCMS r.t 4.10 min, found 307.7 [M-H]$^-$; TLC r.f. 0.17 (10% EtOAc/40-60 petrol ether); IR (cm^{-1}) 3094 (w), 3012 (w), 2951 (w), 1731 (s), 1572 (m), 1463 (m), 1408 (m), 1388 (m), 1318 (m), 1270 (s), 1223 (m); MP 49-51 °C.

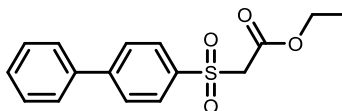## Ethyl 2-([1,1'-biphenyl]-4-ylsulfonyl)acetate (117)[121]

Compound **116** (51 mg, 0.2 mmol) and phenylboronic acid (48 mg, 0.4 mmol) were placed in a flask with Pd(OAc)$_2$ (4 mg, 10 mol%), triphenylphosphine (13 mg, 0.04 mmol) and K_2CO_3 (71 mg, 0.5 mmol). The flask was charged with nitrogen before the material was dissolved in anhydrous DMF (1.5 mL). The reaction mixture was heated to 90 °C for 20 hours, then poured into cold HCl (3 mL, 1.0 M). This solution was extracted with EtOAc (10 mL) and the organic phase washed with brine (10 mL), dried over Na_2SO_4 and evaporated to dryness *in vacuo*. The residue was purified by flash column chromatography (10-20% EtOAc/40-60 petrol ether) to yield the product **117** as colourless crystals (23 mg, 0.1 mmol, 45%).

^{1}H NMR (400 MHz, CDCl$_3$) δ ppm 1.23 (t, *J* = 7.1 Hz, 3H), 4.14-4.22 (m, 4H), 7.41-7.54 (m, 3H), 7.59-7.66 (m, 2H), 7.76-7.83 (m, 2H), 7.99-8.06 (m, 2H); ^{13}C NMR (100 MHz, CDCl$_3$) δ ppm 13.9, 61.1, 62.4, 127.4, 127.8, 128.8, 129.1, 137.2, 139.0, 147.3, 162.4; TLC r.f. 0.48 (33% EtOAc/40-60 petrol ether); IR (cm^{-1}) 3010 (w), 2944 (w), 1723 (s), 1593 (m), 1480 (w), 1397 (m), 1368 (m), 1324 (s), 1284 (s); MP 106-108 °C; Purity >95% (NMR).

2-([1,1'-Biphenyl]-4-ylsulfonyl)acetic acid (118)[122]
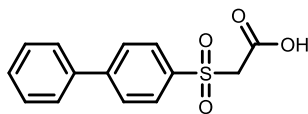
Compound **117** (0.101 g, 0.4 mmol) was dissolved in MeOH/THF (5:1, 6.0 mL) and NaOH (2.5 M, 1.4 mL, 3.5 mmol) added. The reaction was heated to 50 °C for 4 hours, then the mixture was washed with DCM (3 x 15 mL), acidified (3.0 M HCl, 0.2 mL) and extracted with DCM (3 x 50 mL). The DCM extracts were combined, dried over Na_2SO_4 and evaporated under reduced pressure to yield the product **118** as a white powder (81 mg, 0.3 mmol, 88%).

^{1}H NMR (400 MHz, CDCl$_3$) δ ppm 4.21 (s, 2H), 7.41-7.54 (m, 3H), 7.59-7.66 (m, 2H), 7.79 (d, J = 8.5 Hz, 2H), 8.03 (d, J = 8.5 Hz, 2H); Purity >95% (NMR).

2-([1,1'-Biphenyl]-4-ylsulfonyl)-N-hexylacetamide (119)
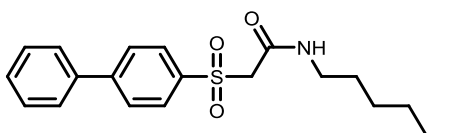
Compound **118** (81 mg, 0.3 mmol) was dissolved in dry DCM (8.0 mL). COMU (0.137 g, 0.3 mmol) was added, followed by DMF (8 drops), DIPEA (0.24 mL, 1.3 mmol) and hexylamine (0.05 mL, 0.6 mmol). The reaction was stirred at ambient temperature for 20 hours, then evaporated *in vacuo* and the resulting powder purified by flash column chromatography (30-60% EtOAc/40-60 petrol ether) to yield the product **119** as a white powder (57 mg, 0.2 mmol, 54%).

^{1}H NMR (400 MHz, CDCl$_3$) δ ppm 0.89 (t, J = 6.6 Hz, 3H), 1.23-1.40 (m, 6H), 1.53 (quin, J = 7.2 Hz, 2H), 3.28 (q, J = 6.8 Hz, 2H), 4.08 (s, 2H), 6.83 (br. t, J = 5.7 Hz, 1H), 7.40-7.52 (m, 3H), 7.57-7.65 (m, 2H), 7.77 (d, J = 8.5 Hz, 2H), 7.97 (d, J = 8.5 Hz, 2H); ^{13}C NMR (100 MHz, CDCl$_3$) δ ppm 14.0, 22.5, 26.5, 29.2, 31.4, 40.2, 62.0, 127.4, 127.9, 128.6, 128.8, 129.0, 136.6, 138.9, 147.3, 160.4; LCMS r.t. 2.30 min, found 360.3 [M+H]$^+$; HRMS calc $C_{20}H_{26}NO_3S$ 360.1633, found [M+H]$^+$ 360.1614; TLC r.f. 0.52 (33% EtOAc/40-60 petrol ether); IR (cm^{-1}) 3307 (br, w), 2928 (br, w), 2853 (w), 1659 (s), 1538 (m), 1290 (s); MP 114-115 °C.

2-([1,1'-Biphenyl]-4-ylsulfonyl)-N-hexylethanethioamide (**120**)
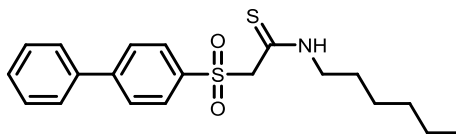
Compound **119** (30 mg, 0.1 mmol) and Lawesson's reagent (59 mg, 0.1 mmol) were dissolved in dry THF (5.0 mL) under inert atmosphere. The reaction was heated at reflux for 2 hours, then solvent was evaporated *in vacuo* and the residue purified by passing it through a pad of silica with DCM to yield the product **120** as a yellow powder (14 mg, 0.04 mmol, 42%).

^{1}H NMR (400 MHz, CDCl$_3$) δ ppm 0.85-0.96 (m, 3H), 1.25-1.46 (m, 6H), 1.69 (quin, J = 7.3 Hz, 2H), 3.58-3.67 (m, 2H), 4.57 (s, 2H), 7.39-7.53 (m, 3H), 7.61 (d, J = 7.2 Hz, 2H), 7.76 (d, J = 8.3 Hz, 2H), 7.87-7.96 (m, 2H), 8.53 (br. s, 1H); ^{13}C NMR (100 MHz, CDCl$_3$) δ ppm 14.0, 22.5, 26.6, 27.5, 31.3, 46.9, 69.1, 127.4, 127.8, 128.8, 128.9, 129.0, 135.5, 138.8, 147.4, 187.1; LCMS r.t. 2.51 min, found 376.3 [M+H]$^+$; HRMS calc C$_{20}$H$_{26}$NO$_2$S$_2$ 376.1405, found [M+H]$^+$ 376.1386; TLC r.f. 0.62 (neat DCM); IR (cm^{-1}) 3302 (br, w), 2934 (br, w), 2839 (br, w), 1595 (s)1502 (m), 1439 (m), 1299 (m), 1258 (s); MP 160-165 °C; Purity 98% (LCMS).

1,4-Bis(5-(trifluoromethyl)pyridine-2-yl)piperazine (**130**)
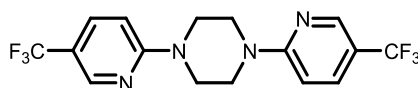
A solution of fragment **66** (0.15 g, 0.7 mmol), 2-bromo-5-trifluoromethylpyridine (0.15 g, 0.7 mmol) and K$_2$CO$_3$ (0.10 g, 0.7 mmol) in acetonitrile (7.5 mL) and DMF (0.50 mL) was heated at reflux under nitrogen for 20 hours. The reaction mixture was then evaporated under reduced pressure, diluted with water (10 mL) and extracted with DCM (3 x 10 mL). The combined organic phases were purified by flash column chromatography (15-30% EtOAc/40-60 petrol ether) to yield the product **130** as a white crystalline solid (0.120 g, 0.3 mmol, 49%).

^{1}H NMR (400 MHz, CDCl$_3$) δ ppm 3.83 (s, 8H), 6.67 (d, J = 9.0 Hz, 2H), 7.68 (dd, J = 9.0, 2.2 Hz, 2H), 8.44 (s, 2H); ^{13}C NMR (100 MHz, CDCl$_3$) δ ppm 44.0, 105.5, 115.6 (q, J = 33.1 Hz), 124.5 (q, J = 270.5 Hz), 134.6 (d, J = 3.5 Hz), 145.8 (d, J = 4.3 Hz), 160.1; LCMS r.t. 2.64 min, found 377.2 [M+H]$^+$; HRMS calc C$_{16}$H$_{15}$N$_4$F$_6$ 377.1195, found [M+H]$^+$ 377.1183; TLC r.f. 0.74 (33% EtOAc/40-60 petrol ether); IR (cm^{-1}) 1609 (m), 1508 (m), 1319 (m), 1231 (m); MP 210-212 °C; Purity >98% (NMR).

1-[4-(Trifluoromethyl)benzyl]-4-[5-(trifluoromethyl)pyridine-2-yl] piperazine (132)
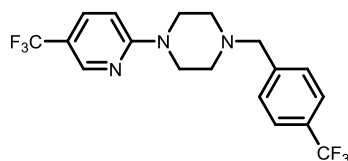
Fragment **66** (0.110 g, 0.5 mmol) and triethylamine (0.07 mL, 0.5 mmol) were dissolved in absolute ethanol and heated to 55 °C. To this solution was added 4-trifluoromethylbenzylbromide (0.113 g, 0.5 mmol), and the reaction stirred at 55 °C for 18 hours. The reaction mixture was evaporated under reduced pressure, then the residue was dissolved in H_2O (5 mL) and extracted with DCM (4 x 5 mL). The combined organic phases were dried *in vacuo* and purified by flash column chromatography (30-50% EtOAc/40-60 petrol ether) yielding the product **132** as a white powder (0.157 mg, 0.4 mmol, 85%).

^{1}H NMR (400 MHz, CDCl$_3$) δ ppm 2.56 (t, J = 5.1 Hz, 4H), 3.61 (s, 2H), 3.67 (t, J = 5.1 Hz, 4H), 6.63 (d, J = 9.0 Hz, 1H), 7.49 (d, J = 8.0 Hz, 2H), 7.58-7.66 (m, 3H), 8.40 (s, 1H); ^{13}C NMR (100 MHz, CDCl$_3$) δ ppm 44.7, 52.8, 62.4, 105.5, 125.3 (d, J = 3.5 Hz), 129.2, 134.4 (d, J = 3.5 Hz), 142.1, 145.7 (d, J = 4.3 Hz), 160.4; LCMS r.t. 1.73 min, found 390.2 [M+H]$^+$; HRMS calc C$_{18}$H$_{18}$N$_3$F$_6$ 390.1399, found [M+H]$^+$ 390.1386; TLC r.f. 0.77 (50% EtOAc/40-60 petrol ether); IR (cm^{-1}) 2822 (w, br.), 1610 (m), 1507 (w), 1419 (w), 1311 (s), 1248 (m); MP 75-78 °C; Purity 96% (LCMS).

1-(Pyridin-4-ylmethyl)-4-[5-(trifluoromethyl)pyridin-2-yl]piperazine (133)
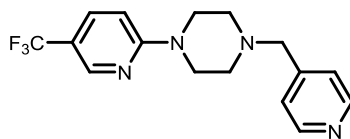
Synthesised using the same procedure as compound **132**, using 4-(bromomethyl)pyridine hydrobromide (0.111 g, 0.4 mmol).

Orange solid (0.112 g, 0.4 mmol, 81%); ^{1}H NMR (400 MHz, CDCl$_3$) δ ppm 2.55 (t, J = 5.1 Hz, 4H), 3.56 (s, 2H), 3.67 (t, J = 5.1 Hz, 4H), 6.63 (d, J = 9.0 Hz, 1H), 7.31 (d, J = 5.4 Hz, 2H), 7.62 (dd, J = 9.0, 2.4 Hz, 1H), 8.40 (s, 1H), 8.57 (d, J = 5.4 Hz, 2H); ^{13}C NMR (100 MHz, CDCl$_3$) δ ppm 44.7, 52.8, 61.7, 105.5, 115.2 (q, J = 32.9 Hz) 123.8, 124.5 (q, J = 271.4 Hz), 134.5 (d, J = 2.6), 145.7 (q, J = 4.3 Hz), 147.2, 149.9, 160.3; LCMS r.t. 1.25 min, found 323.3 [M+H]$^+$; HRMS calc C$_{16}$H$_{18}$N$_4$F$_3$

323.1484, found [M+H]⁺ 323.1477; TLC r.f. 0.55 (10% MeOH/DCM); IR (cm⁻¹) 2933 (w, br.), 2819 (w, br.), 1613 (m), 1316 (s), 1284 (m), 1254 (m); MP 100-101 °C ; Purity >98% (LCMS).

4-({4-[5-(Trifluoromethyl)pyridin-2-yl]piperazin-1-yl}methyl) benzonitrile (134)
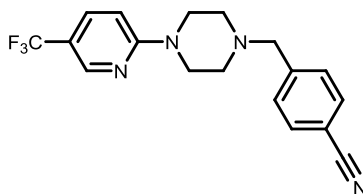
Synthesised using the same procedure as compound **132**, using 4-(bromomethyl)benzonitrile (85 mg, 0.5 mmol).

Colourless crystalline solid (0.139 g, 0.4 mmol, 89%); ¹H NMR (400 MHz, CDCl₃) δ ppm 2.54 (t, J = 5.1 Hz, 4H), 3.60 (s, 2H), 3.66 (t, J = 5.1 Hz, 4H), 6.60-6.67 (m, 1H), 7.49 (d, J = 8.3 Hz, 2H), 7.59-7.67 (m, 3H), 8.39 (s, 1H); ¹³C NMR (100 MHz, CDCl₃) δ ppm 44.6, 52.7, 62.3, 105.5, 111.0, 115.2 (q, J = 32.1 Hz), 118.8, 124.5 (q, J = 269.6 Hz), 129.4, 132.2, 134.4 (d, J = 3.5 Hz), 143.8, 145.7 (q, J = 4.3 Hz), 160.3; LCMS r.t. 1.51 min, found 347.2 [M+H]⁺; HRMS calc $C_{18}H_{18}N_4F_3$ 347.1484, found [M+H]⁺ 347.1482; TLC r.f. 0.48 (50% EtOAc/40-60 petrol ether); IR (cm⁻¹) 2819 (w, br.), 2225 (w), 1608 (s), 1507 (s), 1416 (m), 1314 (s), 1249 (s); MP 99-102 °C; Purity 98% (LCMS).

Methyl 4-({4-[5-(trifluoromethyl)pyridin-2-yl]piperazin-1-yl}methyl) benzoate (135)
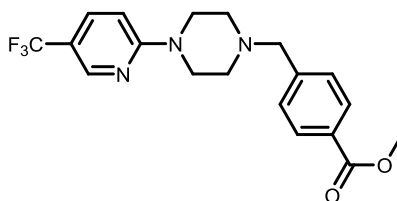
Synthesised using the same procedure as compound **132**, using methyl 4-(bromomethyl)benzoate (0.103 g, 0.5 mmol).

Colourless crystalline solid (0.144 g, 0.4 mmol, 84%); ¹H NMR (400 MHz, CDCl₃) δ ppm 2.55 (t, J = 5.1 Hz, 4H), 3.61 (s, 2H), 3.66 (t, J = 5.1 Hz, 4H), 3.92 (s, 3H), 6.62 (d, J = 9.0 Hz, 1H), 7.44 (d, J = 8.2 Hz, 2H), 7.62 (dd, J = 9.0, 2.5 Hz, 1H), 8.02 (d, J = 8.2 Hz, 2H), 8.39 (s, 1H); ¹³C NMR (100 MHz, CDCl₃) δ ppm 44.7, 52.1, 52.8, 62.6, 105.5, 115.1 (q, J = 32.1 Hz), 124.6

(q, J = 269.6 Hz), 128.9, 129.2, 129.6, 134.4 (d, J = 2.6 Hz), 143.3, 145.7 (q, J = 4.3 Hz), 160.4, 167.0; LCMS r.t. 1.53 min, found 380.2 [M+H]+; HRMS calc $C_{19}H_{21}O_2N_3F_3$ 380.1580, found [M+H]+ 380.1567; TLC r.f. 0.62 (50% EtOAc/40-60 petrol ether); IR (cm-1) 2830 (w, br.), 1713 (s), 1609 (s), 1506 (m), 1415 (m), 1315 (s), 1257 (s); MP 99-100 °C; Purity >98% (LCMS).

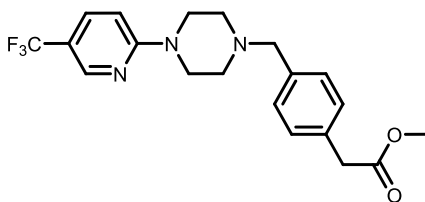## Methyl [4-({4-[5-(trifluoromethyl)pyridin-2-yl]piperazin-1-yl}methyl) phenyl]acetate (**136**)

Synthesised using the same procedure as compound **132**, using methyl 4-(bromomethyl)phenylacetate (0.109 g, 0.4 mmol).

White solid (84 mg, 0.2 mmol, 49%); ¹H NMR (400 MHz, CDCl₃) δ ppm 2.57 (t, J = 5.0 Hz, 4H), 3.57 (s, 2H), 3.62-3.71 (m, 6H), 3.73 (s, 3H), 6.64 (d, J = 9.1 Hz, 1H), 7.29 (s, 2H), 7.31-7.38 (m, 2H), 7.63 (dd, J = 9.1, 2.5 Hz, 1H), 8.37-7.46 (m, 1H); ¹³C NMR (100 MHz, CDCl₃) δ ppm 40.8, 44.7, 52.1, 52.7, 62.7, 105.5, 115.0 (q, J = 32.1 Hz), 124.6 (q, J = 268.8 Hz), 129.2, 129.4, 132.9, 134.4 (d, J = 2.6 Hz), 136.6, 145.7 (q, J = 4.3 Hz), 145.8, 160.4, 172.1; LCMS r.t. 1.50 min, found 394.3 [M+H]+; HRMS calc $C_{20}H_{23}O_2N_3F_3$ 394.1737, found [M+H]+ 394.1724; TLC r.f. 0.42 (50% EtOAc/40-60 petrol ether); IR (cm-1) 2828 (w, br.), 1735 (m), 1611 (m), 1507 (m), 1321 (s), 1255 (s); MP 67-69 °C; Purity >98% (LCMS).

1-[3-Fluoro-5-(trifluoromethyl)benzyl]-4-[5-(trifluoromethyl)pyridin-2-yl]piperazine (**137**)
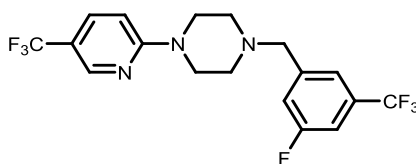
Synthesised using the same procedure as compound **132**, using 3-fluoro-5-(trifluoromethyl)benzyl bromide (0.08 mL, 0.5 mmol).

Yellow solid (0.183 g, 0.5 mmol, 87%); ¹H NMR (400 MHz, CDCl₃) δ ppm 2.58 (t, J = 5.0 Hz, 4H), 3.62 (s, 2H), 3.70 (t, J = 5.0 Hz, 4H), 6.66 (d, J = 9.1 Hz, 1H), 7.36 (s, 1H), 7.40-7.52 (m, 1H), 7.65 (dd, J = 9.1, 1.9 Hz, 1H), 8.42 (s, 1H); ¹³C NMR (100 MHz, CDCl₃) δ ppm 44.6, 52.7, 61.9, 105.5,

111.7 (dd, J = 24.3, 4.3 Hz), 115.2 (q, J = 32.1 Hz), 119.0 (d, J = 21.7 Hz), 121.1 (t, J = 3.5 Hz), 123.3 (q, J = 269.6 Hz), 124.6 (q, J = 270.5 Hz), 132.4 (qd, J = 32.9, 8.7 Hz), 134.5 (d, J = 2.6 Hz), 142.3 (d, J = 6.9 Hz), 145.7 (q, J = 4.3 Hz), 160.3, 162.6 (d, J = 248.8 Hz); ^{19}F NMR (376 MHz, CDCl$_3$) δ ppm -61.2, -62.7, -111.1; LCMS r.t. 1.92 min, found 408.3 [M+H]$^+$; HRMS calc C$_{18}$H$_{17}$F$_7$N$_3$ 408.1311, found [M+H]$^+$ 408.1288; TLC r.f. 0.75 (33% EtOAc/40-60 petrol ether); IR (cm^{-1}) 2832 (br. w), 1614 (m), 1326 (m), 1225 (m); MP 40-44 °C; Purity 95% (LCMS).

1-(3-Fluorobenzyl)-4-[5-(trifluoromethyl)pyridin-2-yl]piperazine (**138**)
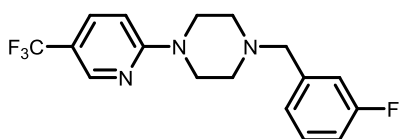
Synthesised using the same procedure as compound **132**, using 3-fluorobenzyl bromide (0.06 mL, 0.5 mmol).

White solid (0.149 g, 0.4 mmol, 85%) ^{1}H NMR (400 MHz, CDCl$_3$) δ ppm 2.58 (t, J = 5.0 Hz, 4H), 3.58 (s, 2H), 3.68 (t, J = 5.0 Hz, 4H), 6.63 (d, J = 9.1 Hz, 1H), 6.93-7.01 (m, 1H), 7.07-7.17 (m, 1H), 7.62 (dd, J = 9.1, 2.5 Hz, 1H), 8.39 (s, 1H); ^{13}C NMR (100 MHz, CDCl$_3$) δ ppm 44.5, 52.6, 62.3, 105.5, 114.2 (d, J = 20.8 Hz), 115.1 (q, J = 33.1 Hz), 115.8 (d, J = 20.8 Hz), 124.6 (q, J = 270.0 Hz; d, J = 2.6 Hz), 129.8 (d, J = 7.8 Hz), 134.4 (d, J = 2.6 Hz), 140.1, 145.7 (q, J = 4.3 Hz), 160.3, 162.9 (d, J = 245.4 Hz); LCMS r.t. 1.52 min, found 340.2 [M+H]$^+$; HRMS calc C$_{17}$H$_{18}$N$_3$F$_4$ 340.1437, found [M+H]$^+$ 340.1436; TLC r.f. 0.62 (33% EtOAc/40-60 petrol ether); IR (cm^{-1}) 2817 (w), 1609 (s), 1508 (m), 1416 (m), 1319 (s), 1244 (s); MP 50-53 °C; Purity 92% (LCMS).

1-{2-[4-(Trifluoromethyl)phenyl]ethyl}-4-[5-(trifluoromethyl)pyridin-2-yl]piperazine (**140**)

Synthesised using the same procedure as compound **132**, using 4-(trifluoromethyl)phenethylbromide (0.07 mL, 0.4 mmol).

Off-white crystalline solid (81 mg, 0.2 mmol, 47%); ^{1}H NMR (400 MHz, CDCl$_3$) δ ppm 2.58-2.76 (m, 6H), 2.86-2.97 (m, 2H), 3.62-3.75 (m, 4H), 6.65 (d, J = 9.1 Hz, 1H), 7.34 (d, J = 8.0 Hz, 2H), 7.56 (d, J = 8.0 Hz, 2H), 7.63 (dd, J = 9.1, 2.5 Hz, 1H), 8.41 (d, J = 0.7 Hz, 1H); ^{13}C NMR (100 MHz,

CDCl$_3$) δ ppm 33.3, 44.7, 52.8, 59.8, 105.6, 115.2 (q, *J* = 32.9 Hz), 124.3 (q, *J* = 271.4 Hz), 124.6 (q, *J* = 269.6 Hz), 125.3 (q, *J* = 3.5 Hz), 129.0, 134.5 (d, *J* = 2.6 Hz), 144.2, 145.7 (q, *J* = 4.3 Hz), 160.3; LCMS r.t. 1.68 min, found 404.3 [M+H]$^+$; HRMS calc C$_{19}$H$_{20}$N$_3$F$_6$ 404.1561, found [M+H]$^+$ 404.1556; TLC r.f. 0.53 (50% EtOAc/40-60 petrol ether); IR (cm^{-1}) 2815 (w, br.), 1610 (m), 1508 (m), 1414(m), 1314 (s), 1254 (m); MP 95-99 °C; Purity 96% (LCMS).

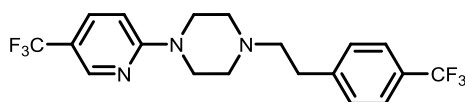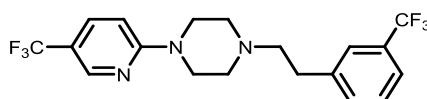## 1-{2-[3-(Trifluoromethyl)phenyl]ethyl}-4-[5-(trifluoromethyl) pyridin-2-yl]piperazine (**141**)

Synthesised using the same procedure as compound **132**, using 3-(trifluoromethyl)phenethylbromide (0.07 mL, 0.4 mmol).

White crystalline solid (56 mg, 0.1 mmol, 32%); ^{1}H NMR (400 MHz, CDCl$_3$) δ ppm 2.57-2.72 (m, 6H), 2.85-2.96 (m, 2H), 3.62-3.75 (m, 4H), 6.65 (dd, *J* = 9.1 Hz, 1H), 7.37-7.54 (m, 4H), 7.63 (dd, *J* = 9.1, 2.4 Hz, 1H), 8.41 (d, *J* = 0.7 Hz, 1H); ^{13}C NMR (100 MHz, CDCl$_3$) δ ppm 33.3, 44.7, 52.8, 59.9, 105.6, 115.2 (q, *J* = 32.1 Hz), 123.0 (d, *J* = 4.3 Hz), 124.2 (q, *J* = 271.4 Hz), 124.5 (q, *J* = 270.5 Hz), 125.4 (q, *J* = 3.5 Hz), 128.8, 130.7 (q, *J* = 31.2 Hz), 132.1, 134.4 (d, *J* = 3.5 Hz), 141.0, 145.7 (q, *J* = 4.3 Hz), 160.4; LCMS r.t. 1.66 min, found 404.3 [M+H]$^+$; HRMS calc C$_{19}$H$_{20}$N$_3$F$_6$ 404.1561, found [M+H]$^+$ 404.1559; TLC r.f. 0.61 (50% EtOAc/40-60 petrol ether); IR (cm^{-1}) 2819 (w, br), 1613 (m), 1314 (m), 1249 (m); MP 50-52 °C; Purity >98% (LCMS).

1-Phenethyl-4-(5-(trifluoromethyl)pyridine-2-yl)piperazine (**142**)
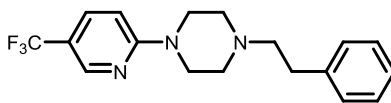
Synthesised using the same procedure as compound **132**, using 2-bromoethyl)benzene (0.07 mL, 0.5 mmol).

Colourless crystalline solid (60 mg, 0.2 mmol, 41%); ^{1}H NMR (400 MHz, MeOD) δ ppm 2.59-2.71 (m, 6H), 2.81-2.91 (m, 2H), 3.70 (t, *J* = 5.2 Hz, 4H), 6.88 (d, *J* = 9.1 Hz, 1H), 7.14-7.33 (m, 5H), 7.72 (dd, *J* = 9.1, 2.5 Hz, 1H), 8.34 (s, 1H); ^{13}C NMR (100 MHz, MeOD) δ ppm 34.3, 45.6, 54.0, 61.7, 107.6, 127.3, 129.6, 129.9, 135.8, 141.4, 146.5 (d, *J* = 4.3 Hz), 162.1; LCMS r.t. 1.52 min, found 336.3 [M+H]$^+$; HRMS calc C$_{18}$H$_{21}$F$_3$N$_3$ 336.1688, found [M+H]$^+$ 336.1708; TLC r.f. 0.30

(33% EtOAc/40-60 petrol ether); IR (cm^{-1}) 2820 (br. w), 2159 (br. w), 1608 (m), 1507 (m), 1422 (m), 1314 (s), 1249 (s); MP 79-81 °C; Purity >98% (LCMS).

1-(3-Methylphenethyl)-4-(5-(trifluoromethyl)pyridin-2-yl)piperazine (143)
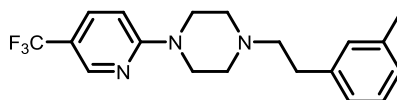
Synthesised using the same procedure as compound **132**, using 3-methylphenethyl bromide (0.08 mL, 0.5 mmol) and fragment **66** (0.100g, 0.4 mmol).

Off-white solid (38 mg, 0.1 mmol, 25%); ^{1}H NMR (400 MHz, MeOD) δ ppm 2.31 (s, 3H), 2.59-2.69 (m, 6H), 2.77-2.87 (m, 2H) 3.70 (t, J = 5.2 Hz, 4H), 6.88 (d, J = 9.1 Hz, 1H), 6.96-7.08 (m, 3H), 7.15 (t, J = 7.5 Hz, 1H), 7.72 (dd, J = 9.1, 2.4 Hz, 1H), 8.34 (br. s, 1H); ^{13}C NMR (100 MHz, MeOD) δ ppm 21.6, 34.2, 54.0, 61.7, 107.6, 126.9, 128.0, 129.5, 130.5, 135.8, 139.3, 141.2, 146.5, 162.1; LCMS r.t. 3.80 min, found 350.1 [M+H]$^+$; HRMS calc C$_{19}$H$_{23}$N$_3$F$_3$ 350.1844, found [M+H]$^+$ 350.1835; TLC r.f. 0.53 (50% EtOAc/40-60 petrol ether); IR (cm^{-1}) 2821 (br. w), 1613 (m), 1506 (w), 1317 (s), 1252 (s); MP 62-65 °C; Purity 98% (LCMS).

2-(3-Fluorophenyl)-1-{4-[5-(trifluoromethyl)pyridin-2-yl]piperazin-1-yl}ethanone (145)
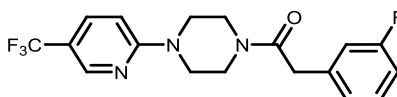
3-fluorophenylacetic acid (0.23 g, 1.4 mmol) was dissolved in DCM (15.0 mL), and EDC (0.42 g, 2.2 mmol), DIPEA (0.33 mL, 1.9 mmol) and DMAP (17 mg, 10 mol%) added. To this stirring solution was added fragment **66** (0.30 g, 1.3 mmol) and the solution stirred at room temperature for 3 hours. The reaction mixture was diluted with DCM (15 mL) and washed with saturated sodium bicarbonate (2 x 30 mL) and brine (2 x 30 mL). The organic phase was concentrated to dryness and purified by flash column chromatography (20-50% EtOAc/40-60 petrol ether) to yield the product **145** as a colourless crystalline solid (0.180 g, 0.5 mmol, 38%).

^{1}H NMR (400 MHz, MeOD) δ ppm 3.56-3.78 (m, 8H), 3.86 (s, 2H), 6.87 (d, J = 9.1 Hz, 1H), 6.94-7.13 (m, 3H), 7.27-7.38 (m, 1H), 7.73 (dd, J = 9.1, 2.2 Hz, 1H), 8.35 (s, 1H); ^{13}C NMR (100 MHz, MeOD) δ ppm 40.9, 42.8, 45.5, 45.7, 46.8, 107.7, 114.8 (d, J = 21.7 Hz), 116.7 (q, J = 32.9 Hz), 117.0 (d, J = 21.7 Hz), 126.0 (d, J = 2.6 Hz), 126.2 (q, J = 268.8 Hz), 131.6

(d, J = 8.7 Hz), 135.9 (d, J = 2.6 Hz), 139.2 (d, J = 7.8 Hz), 145.6 (q, J = 4.3 Hz), 161.8, 164.6 (d, J = 244.5 Hz), 172.0; LCMS r.t. 1.92 min, found 368.2 [M+H]⁺; HRMS calc $C_{18}H_{18}F_4N_3O$ 368.1386, found [M+H]⁺ 368.1342; TLC r.f. 0.53 (50% EtOAc/40-60 petrol ether); IR (cm⁻¹) 2924 (br. w), 1643 (s), 1612 (s), 1512 (m), 1444 (m), 1417 (m), 1315 (m), 1251 (m), 1231 (m); MP 125-126 °C; Purity >98% (LCMS).

1-[2-(3-Fluorophenyl)ethyl]-4-[5-(trifluoromethyl)pyridin-2-yl] piperazine (**146**)
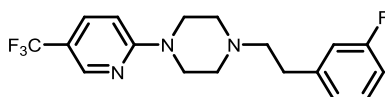
Compound **145** (79.8 mg, 0.2 mmol) was dissolved in anhydrous THF (6.0 mL) under argon. Borane dimethylsulfide (0.04 mL, 0.4 mmol) was added and the reaction stirred for 5 hours at room temperature. The reaction was quenched with HCl (3.0 M, 2.0 mL), diluted with H_2O (20 mL) and extracted with DCM (2 x 40 mL). The organic phases were combined and evaporated to dryness. The resulting solid was purified by flash column chromatography (30-60% EtOAc/40-60 petrol ether) and the product **146** was isolated as a colourless crystalline solid (50 mg, 0.1 mmol, 66%),

¹H NMR (400 MHz, CDCl₃) δ ppm 2.78-2.89 (m, 2H), 2.99-3.07 (m, 2H), 3.17-3.30 (m, 4H), 3.88-4.02 (m, 4H), 6.67 (d, J = 9.0 Hz, 1H), 6.90-6.99 (m, 2H), 7.02 (d, J = 7.8 Hz, 1H), 7.28-7.34 (m, 1H), 7.70 (dd, J = 9.0, 2.3 Hz, 1H), 8.44 (s, 1H); ¹³C NMR 25.9, 39.9, 57.5, 85.9, 105.7, 113.8 (d, J = 20.7 Hz), 115.8 (d, J = 20.7 Hz), 116.3 (q, J = 33.2 Hz), 124.3 (q, J = 270.3 Hz), 124.5 (d, J = 2.5 Hz), 130.3 (d, J = 8.3 Hz), 134.8 (d, J = 3.3 Hz), 140.5 (d, J = 6.6 Hz), 145.8 (q, J = 4.1 Hz), 159.8, 163.0 (d, J = 247.1 Hz); LCMS r.t. 2.13 min, found 354.2 [M+H]⁺; HRMS calc $C_{18}H_{20}F_4N_3$ 354.1593, found [M+H]⁺ 354.1617; TLC r.f. 0.89 (50% EtOAc/40-60 petrol ether); IR (cm⁻¹) 2925 (br., w), 2356 (br., w), 1610 (s), 1521 (m), 1509 (m), 1431 (m), 1321 (s), 1254 (s); MP 111-113 °C; Purity 97% (LCMS).

1-(4-(5-(Trifluoromethyl)pyridine-2-yl)piperazin-1-yl)ethan-1-one (**147**)
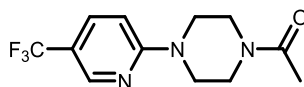
Compound **66** (0.100 g, 0.4 mmol) was dissolved in dry DCM (1.00 mL) under argon and acetyl chloride (0.06 mL, 0.9 mmol) was added. The mixture was stirred for 2 hours at ambient

temperature, then diluted with DCM (10 mL), washed with saturated sodium bicarbonate (10 mL), HCl (3.0 M, 10 mL) and brine (10 mL). The combined aqueous phases were neutralised with NaOH (2.5 M) and extracted with DCM (20 mL). The final DCM phase was dried *in vacuo*, yielding the product **147** as white crystals (0.118 g, 0.4 mmol, >98%).

^{1}H NMR (400 MHz, CDCl$_3$) δ ppm 2.13 (s, 3H), 3.52-3.62 (m, 4H), 3.69-3.78 (m, 4H), 6.64 (d, J = 8.9 Hz, 1H), 7.64 (dd, J = 8.9, 2.4 Hz, 1H), 8.39 (s, 1H); ^{13}C NMR (100 MHz, CDCl$_3$) δ ppm 21.3, 40.7, 44.2, 44.5, 45.7, 105.6, 115.7 (q, J = 32.9 Hz), 124.4 (q, J = 271.4 Hz), 134.7, 145.7, 160.0, 169.2; LCMS r.t. 1.77 min, found 274.2 [M+H]+; HRMS calc C$_{12}$H$_{15}$N$_3$OF$_3$ 274.1162, found [M+H]+ 274.1155; TLC r.f. 0.40 (5% MeOH/DCM); IR (cm^{-1}) 1635 (m), 1611 (m), 1558 (w), 1514 (m), 1422 (m), 1343 (w), 1316 (m), 1285 (m), 1239 (m); MP 128-130 °C; Purity > 98% (LCMS).

*2-Phenyl-1-(4-(5-(trifluoromethyl)pyridine-2-yl)piperazin-1-yl)ethan-1-one (***148***)*
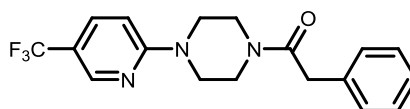
Compound **66** (0.100 g, 0.4 mmol) was dissolved in DCM (3.0 mL) before triethylamine (0.07 mL, 0.5 mmol) and phenylacetyl chloride (0.05 mL, 0.4 mmol) were added. The reaction was stirred at room temperature for 1 hour, then the solvent was evaporated under reduced pressure. The remaining solid was dissolved in DCM (10 mL), washed with HCl (3.0 M, 10 mL), saturated sodium bicarbonate solution (10 mL) and brine (10 mL). The organic phase was dried *in vacuo* and purified by flash column chromatography (EtOAc/40-60 petrol ether) to yield the product **148** as a white, crystalline solid (65 mg, 0.2 mmol, 49%).

^{1}H NMR (400 MHz, acetone-d_6) δ ppm 3.57-3.73 (m, 8H), 3.82 (s, 2H), 6.91 (d, J = 9.1 Hz, 1H), 7.18-7.27 (m, 1H), 7.28-7.35 (m, 4H), 7.76 (dd, J = 9.1, 2.5 Hz, 1H), 8.39 (dd, J = 1.5, 0.8 Hz, 1H); ^{13}C NMR (100 MHz, acetone-d_6) δ ppm 41.6, 42.4, 45.7, 45.8, 46.7, 107.6, 115.9 (q, J = 32.1 Hz), 126.4 (q, J = 268.8 Hz), 127.9, 129.8, 130.3, 135.8 (d, J = 3.5 Hz), 137.4, 146.8 (q, J = 4.3 Hz), 161.9, 170.4; LCMS r.t. 2.15 min, found 350.2 [M+H]+; HRMS calc C$_{18}$H$_{19}$ON$_3$F$_3$ 350.1475, found [M+H]+ 350.1460; TLC r.f. 0.33 (50% EtOAc/40-60 petrol ether); IR (cm^{-1}) 2863 (w), 2163 (br. w), 2026 (br. w), 1633 (m), 1613 (m), 1421 (m), 1324 (s), 1247 (m); MP 121-123 °C; Purity 94% (LCMS).

2-(3-(Trifluoromethyl)phenyl)-1-(4-(5-(trifluoromethyl)pyridine-2-yl)piperazin-1-yl)ethan-1-one (149)
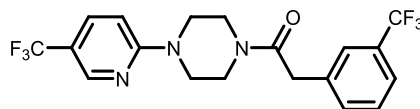
Synthesised using the same procedure as compound **145**, using 3-(trifluoromethyl)phenyl acetic acid (0.103 g, 0.5 mmol).

White, crystalline solid (86 mg, 0.2 mmol, 45%); ^{1}H NMR (400 MHz, MeCN-d_3) δ ppm 3.64 (br. s, 8H), 3.83 (s, 2H), 6.79 (d, J = 9.1 Hz, 1H), 7.45-7.62 (m, 4H), 7.74 (dd, J = 9.1, 2.2 Hz, 1H), 8.41 (s, 1H); ^{13}C NMR (100 MHz, MeCN-d3) δ ppm 40.3, 42.0, 45.2, 45.3, 46.0, 107.2, 115.5 (q, J = 32.9 Hz), 124.3 (d, J = 4.3 Hz), 125.5 (q, J = 271.4 Hz), 126.1 (q, J = 270.5 Hz), 127.1 (d, J = 4.3 Hz), 130.2, 130.9 (q, J = 32.1 Hz), 134.5, 135.5 (d, J = 2.6 Hz), 138.5, 146.5 (q, J = 4.3 Hz), 161.5, 169.9; LCMS r.t. 2.32 min, found 418.2 [M+H]$^+$; HRMS calc $C_{19}H_{18}F_6N_3O$ 418.1354, found [M+H]$^+$ 418.1375; TLC r.f. 0.57 (50% EtOAc/40-60 petrol ether); IR (cm^{-1}) 1649 (m), 1610 (m), 1514 (w), 1418 (br. m), 1327 (s), 1315 (s), 1232 (m); MP 96-99 °C; Purity 98% (LCMS).

2-(Thiophen-2-yl)-1-(4-(5-(trifluoromethyl)pyridine-2-yl)piperazone-1-yl)ethan-1-one (150)
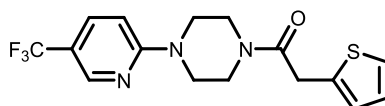
Synthesised using the same procedure as compound **145**, using 2-thiopheneacetic acid (72 mg, 0.5 mmol).

Yellow crystalline solid (0.113 g, 0.3 mmol, 74%); ^{1}H NMR (400 MHz, CDCl$_3$) δ ppm 3.57-3.69 (m, 6H), 3.73-3.83 (m, 2H), 3.97 (s, 2H), 6.63 (d, J = 9.0 Hz, 1H), 6.91-6.94 (m, 1H), 6.95-6.99 (m, 1H), 7.22 (dd, J = 5.1, 1.3 Hz, 1H), 7.66 (dd, J = 9.0, 2.5 Hz, 1H), 8.40 (s, 1H); ^{13}C NMR (100 MHz, CDCl$_3$) δ ppm 35.2, 41.4, 44.2, 44.5, 45.7, 105.7, 115.9 (q, J = 32.9 Hz), 124.4 (q, J = 268.8 Hz), 124.9, 126.1, 126.9, 134.7, 136.1, 145.7, 160.0, 168.7; LCMS r.t. 2.21 min, found 356.2 [M+H]$^+$; HRMS calc $C_{16}H_{16}ON_3F_3SN$ 378.0858, found [M+Na]$^+$ 378.0849; TLC r.f. 0.33 (50% EtOAc/40-60 petrol ether); IR (cm^{-1}) 1638 (m), 1611 (s), 1513 (m), 1422 (m), 1323 (s), 1242 (m); MP 102-103 °C; Purity >95% (NMR).

Phenyl 4-(5-(trifluoromethyl)pyridine-2-yl)piperazine-1-carboxylate (151)
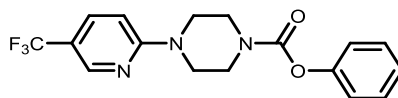
Synthesised using the same procedure as compound **132**, using phenylchloroformate (0.07 mL, 0.5 mmol).

White solid (60 mg, 0.2 mmol, 40%); ^{1}H NMR (400 MHz, acetone-d_6) δ ppm 3.66 (br. s, 2H), 3.83 (br. s, 6H), 6.97 (d, J = 9.0 Hz, 1H), 7.12-7.25 (m, 3H), 7.39 (t, J = 7.9 Hz, 2H), 7.80 (d, J = 9.0 Hz, 1H), 8.44 (s, 1H); ^{13}C NMR (100 MHz, acetone-d_6) δ ppm 45.1, 107.2, 122.8, 126.0, 130.0, 135.4 (d, J = 3.5 Hz), 146.3 (q, J = 4.3 Hz), 152.7, 154.2, 161.4; LCMS r.t. 2.31 min, found 352.2 [M+H]$^+$; HRMS calc $C_{17}H_{17}N_3O_2F_3$ 352.1273, found [M+H]$^+$ 352.1317; TLC r.f. 0.55 (33% EtOAc/40-60 petrol ether); IR (cm^{-1}) 2858 (w), 2159 (br. w), 1735 (m), 1712 (m), 1608 (m), 1507 (m), 1419 (m), 1339 (m), 1323 (m), 1235 (m); MP 120-125 °C; Purity 95% (LCMS).

Benzyl 4-[5-(trifluoromethyl)pyridin-2-yl]piperazine-1-carboxylate (152)
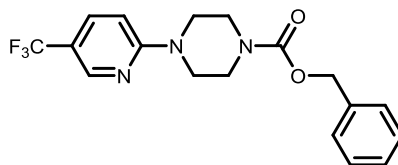
Synthesised using the same procedure as compound **132**, using benzyl chloroformate (0.07 mL, 0.5 mmol).

White crystalline solid (0.190 g, 0.5 mmol, >98%); ^{1}H NMR (400 MHz, CDCl$_3$) δ ppm 3.58-3.74 (m, 8H), 5.19 (s, 2H), 6.64 (d, J = 9.0 Hz, 1H), 7.30-7.46 (m, 5H), 7.66 (dd, J = 9.0, 2.5 Hz, 1H), 8.41 (d, J = 0.8 Hz, 1H); ^{13}C NMR (100 MHz, CDCl$_3$) δ ppm 43.2, 44.4, 67.4, 105.7, 115.7 (q, J = 33.8 Hz), 124.4 (q, J = 270.5 Hz), 126.9, 128.0, 128.5, 134.6 (d, J = 2.6 Hz), 136.4, 145.7 (q, J = 4.3 Hz), 155.2, 160.1; LCMS r.t. 2.39 min, found 366.2 [M+H]$^+$; HRMS calc $C_{18}H_{19}N_3O_2F_3$ 366.1429, found [M+H]$^+$ 366.1461; TLC r.f. 0.61 (33% EtOAc/40-60 petrol ether); IR (cm^{-1}) 2838 (w), 1679 (s), 1609 (m), 1504 (m), 1440 (m), 1329 (m), 1241 (m); MP 87-88 °C; Purity > 98% (LCMS).

## 3-Phenyl-1-(4-(5-(trifluoromethyl)pyridin-2-yl)piperazin-1-yl)propan-1-one (153)
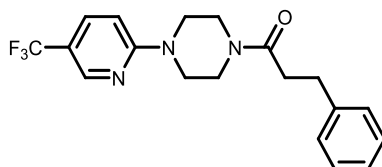
Synthesised using the same procedure as compound **132**, using 3-phenylpropionyl chloride (0.16 mL, 1.0 mmol).

White crystalline solid (0.1175 g, 0.3 mmol, 73%); ^{1}H NMR (400 MHz, MeOD) δ ppm 2.70-2.79 (m, 2H), 2.90-2.95 (m, 2H), 3.53 (br. s, 4H), 3.58-3.74 (m, 4H), 6.84 (d, J = 9.0 Hz, 1H), 7.12-7.31 (m, 5H), 7.73 (dd, J = 9.0, 1.9 Hz, 1H), 8.34 (s, 1H); ^{13}C NMR (100 MHz, MeOD) δ ppm 32.9, 35.8, 42.5, 45.5, 45.6, 46.5, 107.6, 116.6 (q, J = 32.1 Hz), 126.2 (q, J = 270.5 Hz) 127.5, 129.7 (d, J = 6.1 Hz), 135.9 (d, J = 3.5 Hz), 142.3, 146.5 (q, J = 4.3 Hz), 161.8, 173.8; LCMS r.t. 2.24 min, found 364.3 [M+H]$^+$; HRMS calc $C_{19}H_{21}N_3OF_3$ 364.1637, found [M+H]$^+$ 364.1661; TLC r.f. 0.26 (33% EtOAc/40-60 petrol ether); IR (cm^{-1}) 2864 (br. w), 2158 (br. w), 1611 (s), 1416 (m), 1326 (m), 1239 (s); MP 91-93 °C; Purity >98% (LCMS).

3-(Pyridine-3-yl)-1-(4-(5-(trifluoromethyl)pyridin-2-yl)piperazin-1-yl)propan-1-one (154)
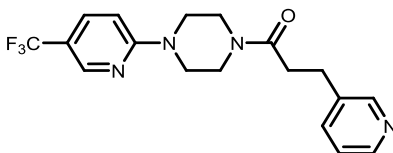
Synthesised using the same procedure as compound **145**, using 3-pyridnepropionic acid (75 mg, 0.5 mmol).

White crystalline solid (0.101 g, 0.3 mmol, 65%); ^{1}H NMR (400 MHz, CDCl$_3$) δ ppm 2.69 (t, J = 7.6 Hz, 2H), 3.03 (t, J = 7.6 Hz, 2H), 3.47-3.56 (m, 2H), 3.56-3.62 (m, 2H), 3.63-3.71 (m, 2H), 3.71-3.82 (m, 2H), 6.63 (d, J = 9.0 Hz, 1H), 7.22 (dd, J = 7.7, 4.8 Hz, 1H), 7.58 (dt, J = 7.7, 1.9 Hz, 1H), 7.66 (dd, J = 9.0, 2.4 Hz, 1H), 8.40 (s, 1H), 8.46 (dd, J = 4.8, 1.6 Hz, 1H), 8.51 (d, J = 1.9 Hz, 1H); ^{13}C NMR (100 MHz, CDCl$_3$) δ ppm 28.3, 34.5, 41.0, 44.2, 44.6, 44.9, 105.6, 115.9 (q, J = 33.8 Hz), 123.4, 124.4 (q, J = 270.5 Hz), 134.7, 136.1, 136.4, 145.7, 147.8, 149.9, 159.9, 170.2; LCMS r.t. 1.75 min, found 365.2 [M+H]$^+$; HRMS calc $C_{18}H_{20}ONF_3$ 365.1584, found [M+H]$^+$ 365.1576;

TLC r.f. 0.22 (5% MeOH/DCM); IR (cm^{-1}) 1613 (m), 1425 (m), 1319 (m), 1229 (s); MP 119-120 °C; Purity >95% (NMR).

## *3-(Thiophen-2-yl)-1-(4-(5-(trifluoromethyl)pyridine-2-yl)piperazin-1-yl)propan-1-one (155)*
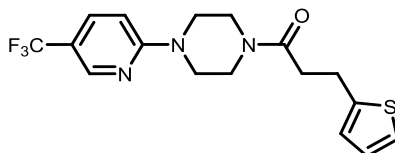
Synthesised using the same procedure as compound **145**, using 2-thiophenepropionic acid (81 mg, 0.5 mmol).

White crystalline solid (0.141 g, 0.4 mmol, 73%); ^{1}H NMR (400 MHz, CDCl$_3$) δ ppm 2.74 (t, *J* = 7.6 Hz, 2H), 3.25 (t, *J* = 7.6 Hz, 2H), 3.49-3.70 (m, 6H), 3.63 (t, *J* = 4.9 Hz, 2H), 6.64 (d, *J* = 9.0 Hz, 1H), 6.82-6.88 (m, 1H), 6.93 (dd, *J* = 5.1, 3.4 Hz, 1H), 7.13 (dd, *J* = 5.1, 1.2 Hz, 1H), 7.67 (dd, *J* = 9.0, 2.5 Hz, 1H), 8.41 (s, 1H); ^{13}C NMR (100 MHz, CDCl$_3$) δ ppm 25.6, 35.3, 41.1, 44.3, 44.7, 45.1, 105.7, 123.6, 124.9, 127.0, 134.8, 143.7, 145.8, 160.1, 170.5; LCMS r.t. 2.31 min, found 370.2 [M+H]$^+$; HRMS calc C$_{17}$H$_{18}$ON$_3$F$_3$SNa 392.1015, found [M+Na]$^+$ 392.1003; TLC r.f. 0.36 (50% EtOAc/40-60 petrol ether); IR (cm^{-1}) 1637 (m), 1610 (m), 15108 (m), 1421 (m), 1328 (m), 1316 (m), 1231 (m);
MP 82-84 °C; Purity >95% (NMR).

tert-Butyl   4-(3-(thiophen-2-yl)propanoyl)piperazine-1-carboxylate (158)

Synthesised using the same procedure as compound **145**, using 2-thiophenepropionic acid (0.10 g, 0.6 mmol) and *N*-Boc-piperazine (0.10 g, 0.5 mmol).

White crystalline solid (0.154 g, 0.5 mmol, 89%); ^{1}H NMR (400 MHz, CDCl$_3$) δ ppm 1.45 (s, 9H), 2.67 (t, *J* = 7.5 Hz, 2H), 3.19 (t, *J* = 7.5 Hz, 2H), 3.29-3.50 (m, 6H), 3.53-3.68 (m, 2H), 6.80-6.85 (m, 1H), 6.90 (dd, *J* = 5.1, 3.4 Hz, 1H), 7.11 (dd, *J* = 5.1, 1.1 Hz, 1H); ^{13}C NMR (100 MHz, CDCl$_3$) δ ppm 25.4, 28.3, 35.1, 41.4, 45.2, 80.2, 123.4, 124.7, 126.8, 143.5, 154.4, 170.2; LCMS r.t. 2.06 min, found 269.2 [M-^{t}bu+2H]$^+$; HRMS calc C$_{16}$H$_{24}$N$_2$O$_3$SNa 347.1400, found [M+Na]$^+$ 347.1396;

TLC r.f. 0.40 (33% EtOAc/40-60 petrol ether); IR (cm⁻¹) 2977 (w), 2364(w), 16779 (s), 1641 (s), 1426 (m), 1359 (m), 1284 (m), 1268 (m), 1239 (m), 1221 (m); MP 82-83 °C; Purity >95% (NMR).

*1-(Piperazin-1-yl)-3-(thiophen-2-yl)propan-1-one TFA salt (**159**)*
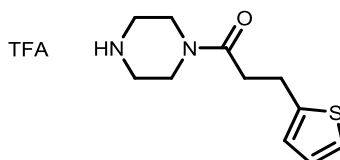
Compound **158** (0.151 g, 0.5 mmol) was dissolved in DCM (2.5 mL) under N₂, and TFA (0.05 mL, 0.7 mmol) was added. The reaction was stirred at room temperature for 3 hours, then evaporated under reduced pressure yielding a light yellow oil, which was carried forward without further purification.

*1-(4-(Pyridin-2-yl)piperazin-1-yl)-3-(thiophen-2-yl)propan-1-one (**161**)*
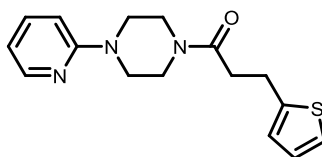
Potassium carbonate (0.13 g, 0.9 mmol) was added to toluene (7.0 mL) under N₂ before compound **159** (0.10 g, 0.3 mmol) and 2-fluoropyridine (0.03 mL, 0.3 mmol) were added. The solution was heated to reflux for 24 hours, at which time additional 2-fluoropyridine (0.30 mL, 0.3 mmol) was added. The reaction was refluxed for a further 24 hours, then cooled and evaporated under reduced pressure. The residue was purified by flash column chromatography (20-50% EtOAc/40-60 petrol ether), and the relevant fractions combined and dried *in vacuo*, yielding the product **161** as a white crystalline solid (0.242 g, 0.8 mmol, 80%).

¹H NMR (400 MHz, CDCl₃) δ ppm 2.73 (t, *J* = 7.6 Hz, 2H), 3.23 (t, *J* = 7.6 Hz, 2H), 3.49 (t, *J* = 5.2 Hz, 2H), 3.54 (s, 4H), 3.76 (t, *J* = 5.2 Hz, 2H), 6.60-6.70 (m, 2H), 6.85 (d, *J* = 3.4 Hz, 1H), 6.92 (dd, *J* = 5.1, 3.4 Hz, 1H), 7.12 (dd, *J* = 5.1, 1.1 Hz, 1H), 7.50 (ddd, *J* = 8.6, 7.1, 1.9 Hz, 1H), 8.19 (dd, *J* = 5.0, 1.1 Hz, 1H); ¹³C NMR (100 MHz, CDCl₃) δ ppm 25.5, 35.2, 41.2, 45.0, 45.1, 45.2, 107.1, 113.8, 123.4, 124.7, 126.8, 137.6, 143.7, 147.9, 158.9, 170.2; LCMS r.t. 1.36 min, found 302.2 [M+H]⁺; HRMS calc C₁₆H₂₀N₃OS 302.1327, found [M+H]⁺ 302.1303; TLC r.f. 0.17 (50% EtOAc/40-

60 petrol ether); IR (cm^{-1}) 1641 (s), 1596 (m), 1477 (m), 1434 (s)1250 (m), 1230 (m), 1217 (m); MP 58-59 °C; Purity >95% (NMR).

*3-(Thiophen-2-yl)-1-(4-(4-(trifluoromethyl)phenyl)piperazin-1-yl)propan-1-one (**163**)[123]*
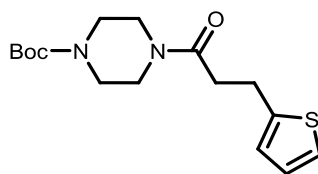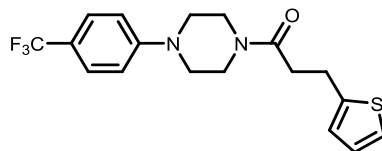

Synthesised using the same procedure as compound **145** using 2-thiophenepropionic acid (0.17 g, 1.1 mmol) and 1-(4-(trifluoromethyl)phenyl)piperazine (0.23 g, 1.0 mmol).

White crystalline solid (0.318 g, 0.9 mmol, 86%); ^{1}H NMR (400 MHz, CDCl$_3$) δ ppm 2.74 (t, J = 7.9 Hz, 2H), 3.15-3.31 (m, 6H), 3.60 (t, J = 5.3 Hz, 2H), 3.81 (t, J = 5.3 Hz, 2H), 6.83-6.88 (m, 1H), 6.88-6.96 (m, 3H), 7.14 (dd, J = 5.1, 0.9 Hz, 1H), 7.51 (d, J = 8.7 Hz, 2H); ^{13}C NMR (100 MHz, CDCl$_3$) δ ppm 25.5, 35.1, 41.2, 45.0, 48.1, 48.2, 115.0, 123.5, 124.8, 126.5 (q, J = 3.5 Hz), 126.9, 143.6, 152.8, 170.2; LCMS r.t. 2.35 min, found 369.2 [M+H]$^+$; HRMS calc C$_{18}$H$_{20}$N$_2$F$_3$OS 369.1248, found [M+H]$^+$ 369.1212; TLC r.f. 0.45 (50% EtOAc/40-60 petrol ether); IR (cm^{-1}) 1630 (s), 1614 (s), 1439 (m), 1335 (s), 1227 (s), 1204 (s); MP 64-66 °C; Purity >95% (NMR).

*1-(4-Phenylpiperazin-1-yl)-3-(thiophen-2-yl)propan-1-one (**164**)*
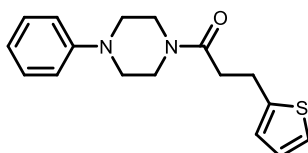

Synthesised using the same procedure as compound **145** using 2-thiophenepropionic acid (0.17 g, 1.1 mmol) and 1-phenylpiperazine (0.15 mL, 1.0 mmol).

Orange crystalline solid (0.240g, 0.8 mmol, 80%); ^{1}H NMR (400 MHz, CDCl$_3$) δ ppm 2.70-2.78 (m, 2H), 3.10 (t, J = 5.2 Hz, 2H), 3.15 (t, J = 5.2 Hz, 2H), 3.26 (t, J = 7.6 Hz, 2H), 3.58 (t, J = 5.1 Hz, 2H), 3.81 (t, J = 5.1 Hz, 2H), 6.87 (dd, J = 3.3, 1.0 Hz, 1H), 6.90-6.98 (m, 4H), 7.14 (dd, J = 5.1, 1.0 Hz, 1H), 7.30 (t, J = 7.8 Hz, 2H); ^{13}C NMR (100 MHz, CDCl$_3$) δ ppm 25.4, 35.0, 41.4, 45.2, 49.2, 49.4, 116.4, 120.3, 123.3, 124.6, 126.7, 129.1, 143.6, 150.7, 169.9; LCMS r.t. 2.12 min, found 301.3 [M+H]$^+$; HRMS calc C$_{17}$H$_{21}$N$_2$OS 301.1375, found [M+H]$^+$ 301.1338; TLC r.f. 0.40 (50% EtOAc/40-60 petrol ether); IR (cm^{-1}) 1843 (br. w), 1635 (s), 1600 (m), 1435 (m), 1386 (m), 1333 (m), 12.79 (m), 1237 (m), ; MP 66-67 °C; Purity >95% (NMR).

1-(4-(Pyrimidin-2-yl)piperazin-1-yl)-3-(thiophen-2-yl)propan-1-one (165)
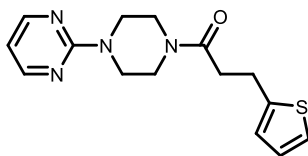
Synthesised using the same procedure as compound **145**, using 2-thiophenepropionic acid (0.17 g, 1.1 mmol) and 1-(2-pyrimidyl)piperazine (0.14 mL, 1.0 mmol).

White crystalline solid (0.221g, 0.7 mmol, 73%); ^{1}H NMR (400 MHz, CDCl$_3$) δ ppm 2.74 (t, J = 7.7 Hz, 2H), 3.24 (t, J = 7.7 Hz, 2H), 3.46-3.54 (m, 2H), 3.68-3.86 (m, 6H), 6.54 (t, J = 4.8 Hz, 1H), 6.83-6.88 (m, 1H), 6.92 (dd, J = 5.1, 3.4 Hz, 1H), 7.13 (dd, J = 5.1, 1.1 Hz, 1H), 8.33 (d, J = 4.8 Hz, 2H); ^{13}C NMR (100 MHz, CDCl$_3$) δ ppm 25.5, 35.3, 41.5, 43.5, 43.6, 45.3, 110.4, 123.5, 124.8, 126.9, 143.7, 157.7, 161.4, 170.3; LCMS r.t. 1.83 min, found 303.2 [M+H]$^+$; HRMS calc C$_{15}$H$_{19}$N$_4$OS 303.1280, found [M+H]$^+$ 303.1259; TLC r.f. 0.19 (50% EtOAc/40-60 petrol ether); IR (cm^{-1}) 1632 (s), 1584 (s), 1546 (m), 1507 (s), 1435 (s), 1358 (s), 1266 (m), 1216 (m); MP 98-100 °C; Purity >95% (NMR).

tert-Butyl 4-(1H-pyrrolo[2,3-b]pyridin-5-yl)piperazine-1-carboxylate (167)
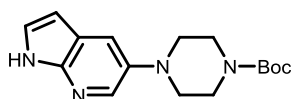
RuPhos (19 mg, 10 mol%), *N*-Boc-piperazine (85 mg, 0.5 mmol), Pd(OAc)$_2$ (9 mg, 10 mol%) and 5-bromo-7-azaindole (76 mg, 0.4 mmol) were sealed in a vial under a nitrogen atmosphere, and LiHMDS (0.91 mL, 1.0 M in THF, 0.9 mol) was added. The reaction was heated to 62 °C for 2 hours, then evaporated under reduced pressure and purified by flash column chromatography (0-5% MeOH/DCM) to yield the product **167** as yellow crystals (92 mg, 0.3 mmol, 79%).

^{1}H NMR (400 MHz, CDCl$_3$) δ ppm 1.50 (s, 9H), 1.75-1.81 (m, 1H), 3.06-3.13 (m, 4H), 3.61-3.68 (m, 4H), 6.43 (dd, J = 3.4, 2.0 Hz, 1H), 7.29-7.33 (m, 1H), 7.54 (d, J = 2.5 Hz, 1H), 8.17 (d, J = 2.5 Hz, 1H); ^{13}C NMR (100 MHz, CDCl$_3$) δ ppm 28.4, 52.0, 79.8, 100.0, 117.8, 120.3, 126.0, 136.9, 142.6, 145.0, 154.6; LCMS r.t. 1.80 min, found 303.3 [M+H]$^+$; HRMS calc C$_{16}$H$_{23}$N$_4$O$_2$ 303.1821, found [M+H]$^+$ 303.1793; TLC r.f. 0.19 (5% MeOH/DCM).

5-(Piperazin-1-yl)-1H-pyrrolo[2,3-b]pyridine hydrochloride (168)
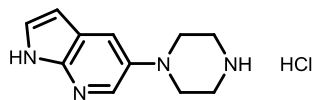
Compound **167** (0.177 g, 0.6 mmol) was dissolved in dioxane (2.4 mL) under inert atmosphere, before HCl (0.90 mL, 4.0 M in 1,4-dioxane) was added. The reaction was stirred for 4 hours at ambient temperature, then evaporated under reduced pressure to yield a white solid which was carried forward without further purification.

## 1-(4-(1H-Pyrrolo[2,3-b]pyridin-5-yl)piperazin-1-yl)-3-(thiophen-2-yl)propan-1-one (169)
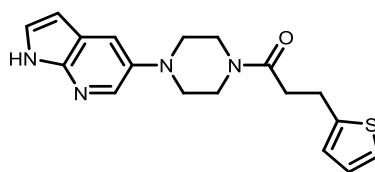
Synthesised using the same procedure as compound **145** using compound **157** (0.11 g, 0.7 mmol) and compound **168** (0.15 g, 0.6 mmol).

Off-white solid (77 mg, 0.2 mmol, 37%); ^{1}H NMR (400 MHz, CDCl$_3$) δ ppm 2.76 (t, J = 7.6 Hz, 2H), 3.05 (t, J = 5.0 Hz, 2H), 3.10 (t, J = 5.0 Hz, 2H), 3.26 (t, J = 7.6 Hz, 2H), 3.64 (t, J = 4.9 Hz, 2H), 3.85 (t, J = 4.9 Hz, 2H), 6.44 (dd, J = 3.4, 2.0 Hz, 1H), 6.87 (dd, 3.4, 0.8 Hz, 1H), 6.94 (dd, J = 5.1, 3.4 Hz, 1H), 7.14 (dd, J = 5.1, 1.1 Hz, 1H), 7.32 (t, J = 3.0 Hz, 1H), 7.52 (d, J = 2.5 Hz, 1H), 8.16 (d, J = 2.5 Hz, 1H), 9.66 (br. s, 1H); ^{13}C NMR (100 MHz, CDCl$_3$) δ ppm 25.6, 35.2, 41.9, 45.7, 52.0, 52.3, 100.6, 117.8, 120.1, 123.4, 124.8, 125.6, 126.9, 137.5, 142.5, 143.7, 144.8, 170.1; LCMS r.t. 1.67 min, found 341.2 [M+H]$^+$; HRMS calc C$_{18}$H$_{21}$N$_4$OS 341.1436, found [M+H]$^+$ 341.1418; TLC r.f. 0.18 (5% MeOH/DCM); IR (cm^{-1}) 3131 (br. w), 2859 (br. w), 2797 (br. w), 1640 (s), 1437 (s), 1344 (m), 1272 (m), 1217 (s); MP 139-140 °C; Purity >98% (LCMS).

tert-Butyl 4-(1H-indol-5-yl)piperazine-1-carboxylate (167a)
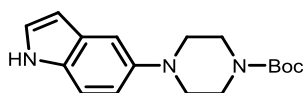
Synthesised using the same procedure as compound **167**, using 5-Bromoindole (0.10 g, 0.5 mmol).

Clear, purple oil (31 mg, 0.1 mmol, 20%); ^{1}H NMR (400 MHz, CDCl$_3$) δ ppm 1.51 (s, 9H), 3.09 (t, J = 5.1 Hz, 4H), 3.64 (t, J = 5.1 Hz, 4H), 6.48 (td, J = 2.0, 1.0 Hz, 1H), 6.98 (dd, J = 8.8, 2.3 Hz, 1H), 7.14-7.22 (m, 2H), 7.31 (d, J = 8.8 Hz, 1H), 8.26 (br. s, 1H); ^{13}C NMR (100 MHz, CDCl$_3$) δ ppm 28.4, 52.0, 79.7, 102.3, 108.3, 111.5, 116.1, 124.7, 128.3, 131.6, 145.8, 154.8; LCMS r.t. 1.64 min, found 302.3 [M+H]$^+$; HRMS calc C$_{17}$H$_{24}$N$_3$O$_2$ 302.1869, found [M+H]$^+$ 302.1858; TLC r.f. 0.66 (50% EtOAc/40-60 petrol ether).

5-(Piperazin-1-yl)-1H-indole hydrochloride (168a)
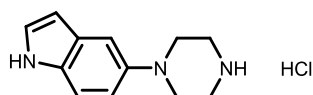
Synthesised using the same procedure as compound **168** using **167a** (30 mg, 0.1 mmol), and carried forward without further purification.

1-(4-(1H-Indol-5-yl)piperazin-1-yl)-3-(thiophen-2-yl)propan-1-one (170)

Synthesised using the same procedure as compound **145** using 2-thiophenepropionic acid (75 mg, 0.5 mmol) and compound **168a** (0.12 g, 0.4 mmol).

Brown oil (70 mg, 0.21 mmol, 49% over 2 steps); ^{1}H NMR (400 MHz, CDCl$_3$) δ ppm 2.76 (t, J = 7.6 Hz, 2H), 3.05 (t, J = 5.1 Hz, 2H), 3.09 (t, J = 5.1 Hz, 2H), 3.26 (t, J = 7.6 Hz, 2H), 3.57-3.67 (m, 2H), 3.84 (t, J = 5.2 Hz, 2H), 6.49 (ddd, J = 3.0, 2.1, 1.0 Hz, 1H), 6.87 (dd, J = 3.3, 1.0 Hz, 1H), 6.85-6.98 (m, 2H), 7.12-7.21 (m, 3H), 7.31 (d, J = 8.8 Hz, 1H), 8.39 (br. s, 1H); ^{13}C NMR (100 MHz, CDCl$_3$) δ ppm 25.5, 35.1, 41.9, 45.7, 51.9, 52.1, 102.2, 108.3, 111.6, 115.9, 123.4, 124.7, 124.8, 126.8, 128.2, 131.7, 143.7, 145.3, 170.1; LCMS r.t. 1.66 min, found 340.2 [M+H]$^+$; HRMS calc C$_{19}$H$_{22}$N$_3$OS 340.1484, found [M+H]$^+$ 340.1492; TLC r.f. 0.39 (5% MeOH/DCM); IR (cm^{-1}) 3256 (br. m), 1627 (s), 1434 (s), 1230 (m); MP 112-114 °C; Purity 95% (LCMS).

tert-Butyl 4-(1H-indol-6-yl)piperazine-1-carboxylate (167b)

Synthesised using the same procedure as compound **167**, using 6-Bromoindole (0.10 g, 0.5 mmol).

Yellow solid (29 mg, 0.1 mmol, 19%); ^{1}H NMR (400 MHz, CDCl$_3$) δ ppm 1.52 (s, 9H), 3.11 (t, J = 5.1 Hz, 4H), 3.63 (t, J = 5.1 Hz, 4H), 6.47 (t, J = 2.3 Hz, 1H), 6.86-6.92 (m, 2H), 7.11 (dd, J = 3.1, 2.3 Hz, 1H), 7.54 (d, J = 8.3 Hz, 1H), 8.26 (br. s, 1H); ^{13}C NMR (100 MHz, CDCl$_3$) δ ppm 28.5, 51.3, 79.8, 98.9, 102.2, 113.3, 121.0, 122.5, 123.2, 136.6, 147.8, 154.8; LCMS r.t. 1.86 min, found 302.3 [M+H]$^+$; HRMS calc C$_{17}$H$_{24}$N$_3$O$_2$ 302.1869, found [M+H]$^+$ 302.1865; TLC r.f. 0.64 (50% EtOAc/40-60 petrol ether).

6-(Piperazin-1-yl)-1H-indole hydrochloride (**168b**)
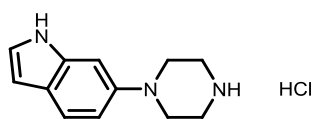
Synthesised using the same procedure as compound **168** using **167b** (0.135 g, 0.4 mmol), and carried forward as a crude pink solid without further purification.

## 1-(4-(1H-Indol-6-yl)piperazin-1-yl)-3-(thiophen-2-yl)propan-1-one (**171**)
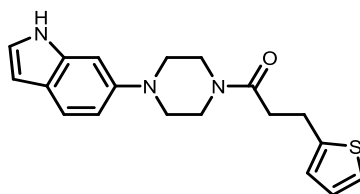
Synthesised using the same procedure as compound **145** using 2-thiophenepropionic acid (62 mg, 0.4 mmol) and compound **168b** (81 mg, 0.3 mmol).

Yellow crystalline solid (41 mg, 0.1 mmol, 52%); ^{1}H NMR (400 MHz, CDCl$_3$) δ ppm 2.76 (t, J = 7.7 Hz, 2H), 3.07 (t, J = 5.0 Hz, 2H), 3.11 (t, J = 5.0 Hz, 2H), 3.27 (t, J = 7.7 Hz, 2H), 3.60 (t, J = 5.0 Hz, 2H), 3.85 (t, J = 5.0 Hz, 2H), 6.48 (t, J = 2.3 Hz, 1H), 6.82-6.91 (m, 3H), 6.94 (dd, J = 5.1, 3.5 Hz, 1H), 7.12 (t, J = 2.8 Hz, 1H), 7.15 (dd, J = 5.1, 1.0 Hz, 1H), 7.55 (d, J = 8.3 Hz, 1H), 8.46 (br. s, 1H); ^{13}C NMR (100 MHz, CDCl$_3$) δ ppm 25.5, 35.1, 41.8, 45.6, 51.0, 51.7, 99.0, 102.1, 113.1, 121.1, 122.7, 123.3, 123.4, 124.7, 126.8, 136.6, 143.7, 147.3, 170.1; LCMS r.t. 1.87 min, found 340.2 [M+H]$^+$; HRMS calc C$_{19}$H$_{22}$N$_3$OS 340.1484, found [M+H]$^+$ 340.1477; TLC r.f. 0.28 (75% EtOAc/40-60 petrol ether); IR (cm^{-1}) 3257 (br. w), 1627 (s), 1434 (s), 1230 (s); MP 55-57 °C; Purity >98% (LCMS).

1-(3,5-Dichlorophenyl)piperazine hydrochloride (**168c**)

Synthesised using the same procedure as compound **167** using 3,5-dichloroiodobenzene (0.50 g, 1.8 mmol) to produce the Boc-protected amine. This was used with the same procedure as compound **168** to synthesise the product **168c** as a brown solid which was used without further purification.

1-(4-(3,5-Dichlorophenyl)piperazin-1-yl)-3-(thiophen-2-yl)propan-1-one (**172**)
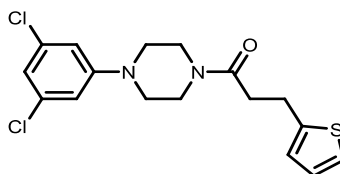
Synthesised using the same procedure as compound **145** using 2-thiophenepropionic acid (64 mg, 0.4 mmol) and compound **168c** (94 mg, 0.4 mmol).

Yellow oil (6 mg, 0.02 mmol, 4%); ^{1}H NMR (400 MHz, CDCl$_3$) δ ppm 2.73 (t, J = 7.5 Hz, 2H), 3.11 (t, J = 5.0 Hz, 2H), 3.17 (t, J = 5.1 Hz, 2H), 3.24 (t, J = 7.5 Hz, 2H), 3.57 (t, J = 5.0 Hz, 2H), 3.78 (t, J = 5.1 Hz, 2H), 6.73 (d, J = 1.6 Hz, 2H), 6.82-6.88 (m, 2H), 6.93 (dd, J = 5.1, 3.5 Hz, 1H), 7.14 (dd, J = 5.1, 0.9 Hz, 1H); ^{13}C NMR (100 MHz, CDCl$_3$) δ ppm 25.5, 35.1, 41.2, 45.0, 48.5, 70.6, 114.3, 119.7, 123.6, 124.9, 126.9, 135.6, 143.6, 152.2, 170.2; LCMS r.t. 2.45 min, found 369.0 [M+H]$^+$; HRMS calc C$_{17}$H$_{19}$N$_2$OSCl$_2$ 369.0595, found [M+H]$^+$ 369.0585; TLC r.f. 0.53 (50% EtOAc/40-60 petrol ether); IR (cm^{-1}) 3096 (w), 2833 (w), 1641 (s), 1581 (m), 1553 (m), 1467 (m), 1438 (s), 1233 (s); MP 95-97 °C; Purity >98% (LCMS).

tert-Butyl 4-(4-cyano-3-hydroxyphenyl)piperazine-1-carboxylate (**167d**)
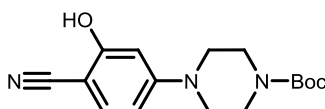
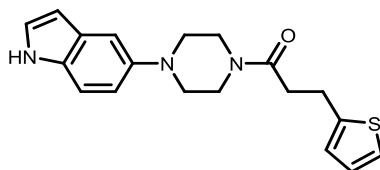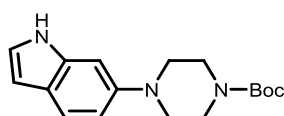Synthesised using the same procedure as compound **167** using 5-bromo-1,2-isoxazole (0.15 g, 0.8 mmol).

White powder (98 mg, 0.4 mmol, 49%); ^{1}H NMR (500 MHz, CDCl$_3$) δ ppm 1.49 (s, 9H), 2.96-3.05 (m, 4H), 3.58 (t, *J* = 5.1 Hz, 4H), 6.93 (d, *J* = 9.1 Hz, 1H), 6.98 (d, *J* = 2.9 Hz, 1H), 7.10 (dd, *J* = 9.1, 2.9 Hz, 1H); ^{13}C NMR (125 MHz, CDCl$_3$) δ ppm 28.4, 50.3, 80.4, 99.8, 116.6, 117.5, 120.1, 125.0, 145.3, 153.1, 154.8; LCMS r.t. 1.95 min, found 302.2 [M-H]$^-$; TLC r.f. 0.30 (50% EtOAc/40-60 petrol ether).

2-Hydroxy-4-(piperazin-1-yl)benzonitrile hydrochloride (**168d**)
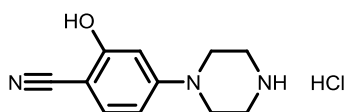
Synthesised using the same procedure as compound **168** using **167d** (98 mg, 0.3 mmol), and the resulting white powder of **168d** was carried forward without further purification.

2-Hydroxy-4-(4-(3-(thiophen-2-yl)propanoyl)piperazin-1-yl)benzonitrile (**173**)
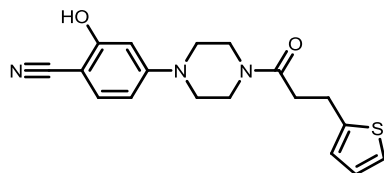
Synthesised using the same procedure as compound **145** using 2-thiophenepropionic acid (32 mg, 0.2 mmol) and compound **168d** (64 mg, 0.2 mmol).

Off-white solid (26.0 mg, 0.1 mmol, 47%); ^{1}H NMR (400 MHz, DMSO-*d$_6$*) δ ppm 2.71 (t, *J* = 7.4 Hz, 2H), 2.90-3.00 (m, 4H), 3.04 (t, *J* = 7.4 Hz, 2H), 3.49-3.63 (m, 4H), 6.85-6.95 (m, 3H), 7.09 (d, *J* = 3.0 Hz, 1H), 7.19 (dd, *J* = 9.1, 3.0 Hz, 1H), 7.29 (dd, *J* = 5.0, 1.2 Hz, 1H); ^{13}C NMR (100 MHz, DMSO-*d$_6$*) δ ppm 24.8, 34.0, 40.9, 44.6, 29.3, 49.7, 98.6, 116.9, 117.3, 119.5, 123.6, 124.4, 124.7, 126.8, 143.8, 143.9, 154.0, 169.4; LCMS r.t. 1.82 min, found 342.1 [M+H]$^+$; HRMS calc C$_{18}$H$_{20}$N$_3$O$_2$S 342.1276, found [M+H]$^+$ 342.1289; TLC r.f. 0.10 (66% EtOAc/40-60 petrol ether); IR (cm^{-1}) 3116 (br. m), 2920 (m), 2821 (w), 2223 (m), 1607 (m), 1509 (m), 1421 (m), 1272 (m), 1228 (m), 1208 (s); MP 189-190 °C; Purity >98% (LCMS).

tert-Butyl 4-(benzofuran-5-yl)piperazine-1-carboxylate (**167e**)
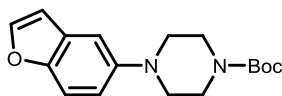
Synthesised using the same procedure as compound **167** using 5-bromo-1-benzofuran (0.30 mL, 2.8 mmol).

Yellow oil (77 mg, 0.3 mmol, 9%); ^{1}H NMR (400 MHz, CDCl$_3$) δ ppm 1.50 (s, 9H), 3.08 (t, J = 5.0 Hz, 4H), 3.61 (t, J = 5.0 Hz, 4H), 6.69 (dd, J = 2.1, 0.8 Hz), 1H), 6.99 (dd, J = 8.9, 2.4 Hz, 1H), 7.11 (d, J = 2.4 Hz, 1H), 7.41 (d, J = 8.9 Hz, 1H), 7.58 (d, J = 2.1 Hz, 1H); ^{13}C NMR (100 MHz, CDCl$_3$) δ ppm 28.3, 28.4, 51.5, 79.8, 106.6, 108.8, 111.6, 116.7, 127.9, 145.5, 148.0, 150.4, 154.7; LCMS r.t. 2.30 min, found 247 [M-^{t}Bu+2H]$^+$; TLC r.f. 0.89 (33% EtOAc/40-60 petrol ether).

1-(Benzofuran-5-yl)piperazine hydrochloride (**168e**)
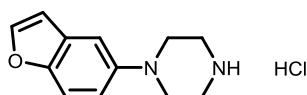
Synthesised using the same procedure as compound **168** using **167e** (77 mg, 0.3 mmol), with the resulting off-white powder of **168e** used without further purification or analysis.
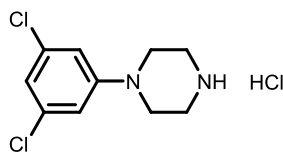
1-(4-(Benzofuran-5-yl)piperazin-1-yl)-3-(thiophen-2-yl)propan-1-one (**174**)
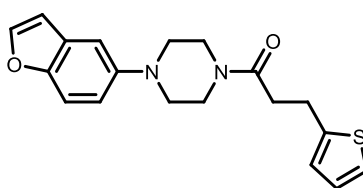
Synthesised using the same procedure as compound **145** using 2-thiophenepropionic acid (52 mg, 0.3 mmol) and compound **168e** (66 mg, 0.3 mmol).

Yellow oil (48 mg, 0.1 mmol, 50%); ^{1}H NMR (400 MHz, CDCl$_3$) δ ppm 2.75 (t, J = 7.6 Hz, 2H), 3.05 (t, J = 5.0 Hz, 2H), 3.10 (t, J = 5.0 Hz, 2H), 3.25 (t, J = 7.6 Hz, 2H), 3.60 (t, J = 5.0 Hz, 2H), 3.83 (t, J = 5.0 Hz, 2H), 6.71 (d, J = 1.4 Hz, 1H), 6.87 (d, J = 2.8 Hz, 1H), 6.90-7.02 (m, 2H), 7.10 (d, J = 2.2 Hz, 1H), 7.14 (d, J = 5.0 Hz, 1H), 7.42 (d, J = 8.9 Hz, 1H), 7.59 (d, J = 2.2 Hz, 1H); ^{13}C NMR (100 MHz, CDCl$_3$) δ ppm 25.5, 35.1, 41.8, , 45.6, , 51.3, 51.6, 106.5, 108.8, 111.6, 116.6, 123.4, 124.7, 126.8, 127.9, 143.7, 145.5, 147.6, 150.5, 170.0; LCMS r.t. 2.12 min, found 341.0

[M+H]+; HRMS calc $C_{19}H_{21}N_2O_2S$ 341.1324, found [M+H]+ 341.1328; TLC r.f. 0.15 (33% EtOAc/40-60 petrol ether); IR (cm-1) 2808 (br. w), 1632 (m), 1439 (s), 1279 (m), 1209 (m); MP 72-73 °C; Purity >95% (NMR).

1-(4-(5-Bromopyridin-2-yl)piperazin-1-yl)-3-(thiophen-2-yl)propan-1-one (**182**)
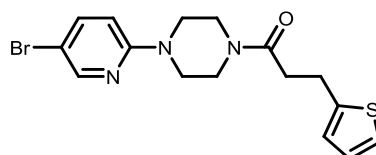
Compound **159** (0.596 g, 1.8 mmol) was dissolved in NMP (2.0 mL), then K_2CO_3 (0.19 g, 1.4 mmol) and 5-bromo-2-fluoropyridine (0.08 mL, 0.5 mmol) were added. The mixture was heated to 120 °C for 4 hours before being diluted with water (10 mL). The product was extracted with DCM (4 x 30 mL) and the combined organic phases dried over Na_2SO_4, then purified by flash column chromatography (30-50% EtOAc/40-60 petrol ether) to yield the product **182** as a clear, colourless oil (0.325 g, 0.9 mmol, 50%).

1H NMR (400 MHz, CDCl3) δ ppm 2.59-2.68 (m, 2H), 3.13 (t, *J* = 7.5 Hz, 2H), 3.35-3.51 (m, 6H), 3.65 (t, *J* = 5.0 Hz, 2H), 6.47 (d, *J* = 9.0 Hz, 1H), 6.75 (dd, *J* = 3.4, 0.9 Hz, 1H), 6.82 (dd, *J* = 5.1, 3.4 Hz, 1H), 7.03 (dd, *J* = 5.1, 0.9 Hz, 1H), 7.47 (dd, *J* = 9.0, 2.5 Hz, 1H), 8.09 (d, *J* = 2.5 Hz, 1H); 13C NMR (100 MHz, CDCl3) δ ppm 25.2, 34.9, 40.8, 44.6, 44.7, 44.9, 107.9, 108.3, 123.2, 124.5, 125.6, 139.6, 143.4, 148.2, 157.2, 170.0; LCMS r.t. 2.69 min, found 382.2 [M+H]+; TLC r.f. 0.27 (33% EtOAc/40-60 petrol ether).

1-(4-(5-(Hexylamino)pyridine-2-yl)piperazin-1-yl)-3-(thiophen-2-yl)propan-1-one (**183**)
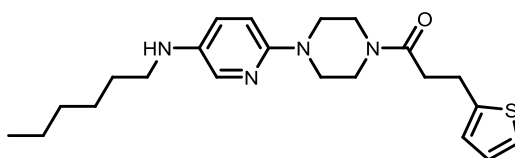
To a mixture of compound **182** (0.108 g, 0.3 mmol) in dry toluene (1.5 mL) under nitrogen was added tri-*tert*-butylphosphine (0.12 mL, 0.5 mmol), sodium *tert*-butoxide (56 mg, 0.6 mmol), hexylamine (0.06 mL, 0.5 mmol) and $Pd_2(dba)_3$ (27 mg, 10 mol%). The reaction mixture was heated under microwave conditions at 120 °C for 6 hours, then filtered through Celite® and evaporated *in vacuo*. The residue was purified by flash column chromatography (RP-C18,

50-60% MeCN/0.1% aqueous formic acid) to yield the product **183** as a purple oil (8 mg, 0.02 mmol, 7%).

^{1}H NMR (400 MHz, acetone-d_6) δ ppm 0.80-0.94 (m, 3H), 1.14-1.36 (m, 5H), 1.38-1.47 (m, 2H), 1.60 (quin, J = 7.2 Hz, 2H), 2.75 (t, J = 7.4 Hz, 2H), 3.06 (t, J = 7.2 Hz, 2H), 3.14 (t, J = 7.4 Hz, 2H), 3.29 (br. s, 2H), 3.34 (br. s, 2H), 3.61 (t, J = 5.0 Hz, 2H), 6.65 (t, J = 2.1 Hz, 2H), 6.73 (d, J = 8.9 Hz, 1H), 6.85-6.95 (m, 2H), 7.03 (dd, J = 8.9, 2.9 Hz, 1H), 7.20 (dd, J = 5.0, 1.4 Hz, 1H), 7.67 (d, J = 2.9 Hz, 1H); ^{13}C NMR (125 MHz, acetone-d_6) δ ppm 14.4, 23.4, 26.1, 27.7, 32.5, 35.5, 42.1, 45.1, 45.9, 47.7, 48.0, 109.9, 124.2, 124.3, 125.6, 127.6, 132.8, 139.7, 145.2, 153.4, 170.3; LCMS r.t. 2.88 min, found 401.4 [M+H]$^+$; HRMS calc $C_{22}H_{33}N_4OS$ 401.2375, found [M+H]$^+$ 401.2350; TLC r.f. 0.22 (RP-C_{18}, 40% water (0.1% ammonia)/MeCN); Purity >98% (LCMS).

*tert-Butyl 4-(5-(methoxycarbonyl)pyridine-2-yl)piperazine-1-carboxylate (*185*)[124]*
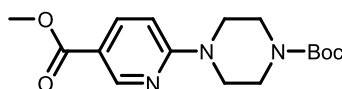
Methyl-6-bromonicotinate (0.50 g, 2.3 mmol) and *N*-Boc-piperazine (0.43 g, 2.3 mmol) were suspended in acetonitrile (18.0 mL) and heated to reflux under nitrogen atmosphere for 3 hours. Additional N-Boc-piperazine (0.22 g, 1.2 mmol) was added with K_2CO_3 (0.69 g, 5.0 mmol) and DMF (3.0 mL). The mixture was refluxed for a further 2 hours, then evaporated under reduced pressure. The residue was diluted with DCM (25 mL) and washed with water (3 x 25 mL), dried over MgSO$_4$ and evaporated *in vacuo*. The resulting material was purified by flash column chromatography (20-40% EtOAc/40-60 petrol ether) to yield the product **185** as a white solid (0.338 g, 1.1 mmol, 45%).

^{1}H NMR (400 MHz, CDCl$_3$) δ ppm 1.49 (s, 9H), 3.50-3.60 (m, 4H), 3.64-3.74 (m, 4H), 3.88 (s, 3H), 6.59 (d, *J* = 9.0 Hz, 1H), 8.04 (dd, *J* = 9.0, 2.4 Hz, 1H), 8.80 (d, *J* = 2.4 Hz, 1H); ^{13}C NMR (125 MHz, CDCl$_3$) δ ppm 28.4, 44.4, 51.7, 80.1, 105.2, 115.0, 138.6, 151.0, 154.7, 160.5, 168.3; LCMS r.t. 2.13 min, found 222.0 [M-^{t}Bu+2H]$^+$.

*Methyl 6-(piperazin-1-yl)nicotinate hydrochloride (*186*)*
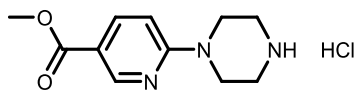
Compound **185** (1.146 g, 3.6 mmol) was dissolved in 1,4-dioxane (20 mL) and HCl (9.0 mL, 4.0 M in 1,4-dioxane, 36.0 mmol) was added. The reaction mixture was allowed to stir at

ambient temperature under nitrogen atmosphere overnight, before the solvent was evaporated to yield the product **186** as a white solid which was carried forward without further purification.

Methyl 6-(4-(3-(thiophen-2-yl)propanoyl)piperazin-1-yl)nicotinate (187)
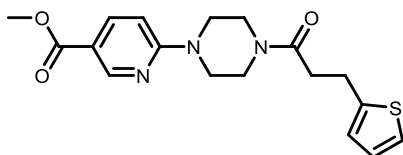
Synthesised using the same procedure as compound **145** using acid **157** (0.19 g, 1.2 mmol) and compound **186** (0.29 g, 1.1 mmol).

White solid (0.320 g, 0.89 mmol, 79%); ^{1}H NMR (400 MHz, CDCl$_3$) δ ppm 2.69-2.78 (m, 2H), 3.24 (t, *J* = 7.5 Hz, 2H), 3.51-3.59 (m, 2H), 3.60-3.67 (m, 2H), 3.67-3.73 (m, 2H), 3.74-3.82 (m, 2H), 3.88 (s, 3H), 6.58 (d, *J* = 9.0 Hz, 1H), 6.83-6.88 (m, 1H), 6.92 (d, *J* = 5.1, 3.4 Hz, 1H), 7.13 (dd, *J* = 5.1, 1.2 Hz, 1H), 8.05 (dd, *J* = 9.0, 2.4 Hz, 1H), 8.80 (d, *J* = 2.4 Hz, 1H); ^{13}C NMR (100 MHz, CDCl$_3$) δ ppm 25.5, 35.2, 41.1, 44.2, 44.6, 45.0, 51.8, 105.2, 115.4, 123.5, 124.8, 126.9, 138.7, 143.6, 151.0, 160.3, 166.3, 170.4; LCMS r.t. 1.95 min, found 359.9 [M+H]+; HRMS calc C$_{18}$H$_{22}$N$_3$O$_3$SNa 382.1196, found [M+Na]+ 382.1202; TLC r.f. 0.58 (neat EtOAc); IR (cm^{-1}) 3102 (w), 2847 (br. w), 1696 (m), 1638 (m), 1599 (s), 1498 (m), 1410 (s), 1280 (m), 1229 (s); MP 121-122 °C; Purity >95% (NMR).

6-(4-(3-(Thiophen-2-yl)propanoyl)piperazin-1-yl)nicotinic acid (188)
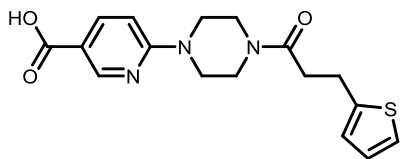
Compound **187** (0.22 g, 0.6 mmol) and lithium hydroxide monohydrate (76 mg, 3.5 mmol) were suspended in MeOH (5 mL) and water (1.5 mL), and stirred for 3 hours, after which additional LiOH.H$_2$O (76 mg, 3.5 mmol) was added and the reaction stirred at ambient temperature overnight. The resulting solution was evaporated *in vacuo*, dissolved in water (15 mL) and acidified with HCl (2.5 mL, 3.0 M). The precipitate was collected by filtration and dried *in vacuo* yielding the product **188** as a white solid (0.108 g, 0.3 mmol, 51%).

^{1}H NMR (400 MHz, MeOD) δ ppm 2.80 (t, J = 7.3 Hz, 2H), 3.18 (t, J = 7.3 Hz, 2H), 3.63-3.80 (m, 8H), 6.85-6.93 (m, 2H), 7.00 (d, J = 9.3 Hz, 1H), 7.18 (dd, J = 5.0, 1.1 Hz, 1H), 8.17 (dd, J = 9.3, 2.1 Hz, 1H), 8.63 (d, J = 2.1 Hz, 1H); ^{13}C NMR (100 MHz, MeOD) δ ppm 26.5, 35.8, 42.1, 45.7, 45.9, 46.0, 109.3, 117.1, 124.5, 126.0, 127.9, 141.3, 144.5, 148.2, 159.4, 167.8, 173.2; LCMS r.t. 1.64 min, found 345.9 [M+H]$^+$; HRMS calc $C_{17}H_{20}N_3O_3S$ 346.1225, found [M+H]$^+$ 346.1249; IR (cm^{-1}) 3382 (br. w), 2868 (br. w), 2554 (br. w), 1625 (s), 1604 (s), 1513 (m), 1427 (s)1280 (m), 1229 (m); MP 171-175 °C; Purity 95% (LCMS).

6-(4-(3-(Thiophen-2-yl)propanoyl)piperazin-1-yl)nicotinamide (**189**)
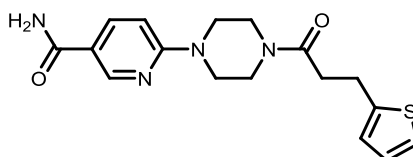
Compound **188** (50 mg, 0.1 mmol), DMAP (1 mg, 10 mol%), and EDC (42 mg, 0.2 mmol) were dissolved in DCM (2.0 mL) with DIPEA (0.12 mL, 0.7 mmol) before ammonia (0.35 mL, 2 M in MeOH, 0.7 mmol) was added. The reaction was stirred at room temperature overnight. To this solution was added HOBt (23 mg, 0.2 mmol) and additional EDC and ammonia, and stirred for a further 18 hours. The solution was evaporated under reduced pressure and purified by flash column chromatography (10-15% MeOH/DCM) to yield the product **189** as a white solid (13 mg, 0.04 mmol, 29%).

^{1}H NMR (400 MHz, CDCl$_3$) δ ppm 3.06 (t, J = 7.4 Hz, 2H), 3.50 (t, J = 7.4 Hz, 2H), 3.61-3.66 (m, 2H), 3.84-3.98 (m, 6H), 3.99-4.08 (m, 2H), 7.00 (d, J = 9.0 Hz, 1H), 7.15 (dd, J = 2.4, 1.0 Hz, 1H), 7.20 (dd, J = 5.1, 3.5 Hz, 1H), 7.43 (dd, J = 5.1, 1.0 Hz, 1H), 8.29 (dd, J = 9.0, 2.4 Hz, 1H), 8.94 (d, J = 1.9 Hz, 1H); ^{13}C NMR (100 MHz, CDCl$_3$) δ ppm 26.1, 35.6, 42.0, 45.0, 45.1, 45.8, 106.6, 118.9, 124.2, 125.6, 127.5, 135.0, 138.0, 143.7, 149.1, 160.7, 172.1; LCMS r.t. 1.48 min, found 344.8 [M+H]$^+$; HRMS calc $C_{17}H_{20}N_4O_2S$ 367.1199, found 367.1200 [M+Na]$^+$; IR (cm^{-1}) 3363 (w), 3167 (br. w), 2919 (w), 2822 (w), 1669 (m), 1627 (s), 1600 (s), 1549 (m), 1503 (m), 1402 (s), 1357 (s), 1227 (s); MP 199-200 °C; Purity >98% (LCMS).

2-(2-(Benzyloxy)ethoxy)ethyl 6-(4-(3-(thiophen-2-yl)propanoyl) piperazin-1-yl)nicotinate (190)
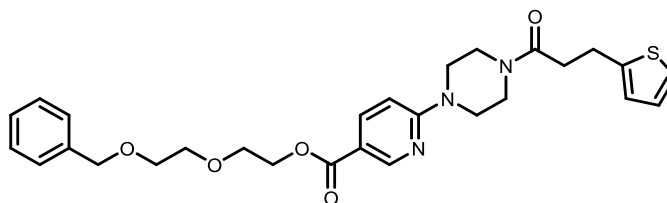
A suspension of compound **188** (0.20 g, 0.6 mmol) in anhydrous DCM (2.0 mL) under nitrogen atmosphere was cooled to 0 °C. To this was added Et₃N (0.12 mL, 0.9 mmol) and 2,4,6-trichlorobenzyl chloride (0.14 mL, 0.9 mmol) and the solution stirred on ice for 2 hours, after which toluene (2.0 mL) was added and the DCM evaporated under reduced pressure, and backfilled with nitrogen. DMAP (7 mg, 10 mol%) was added, followed by di(ethylene glycol)benzyl ether (0.05 mL, 0.3 mmol) and the reaction stirred at ambient temperature for 2 hours. The precipitate was removed by filtration and the toluene evaporated under reduced pressure to leave a yellow oil. The oil was purified by flash column chromatography (35-50% EtOAc/40-60 petrol ether, then 10% MeOH/DCM). The residue was dried under reduced pressure, diluted with DCM (15 mL), washed with saturated sodium bicarbonate (15 mL) and evaporated under reduced pressure to yield the product **190** as a yellow oil (22 mg, 0.04 mmol, 14%).

^{1}H NMR (400 MHz, CDCl₃) δ ppm 2.74 (dd, *J* = 8.2, 6.9 Hz, 2H), 3.25 (t, *J* = 7.4 Hz, 2H), 3.51-3.58 (m, 2H), 3.60-3.67 (m, 4H), 3.68-3.75 (m, 4H), 3.75-3.80 (m, 2H), 3.81-3.86 (m, 2H), 4.43-4.49 (m, 2H), 4.58 (s, 2H), 6.55 (dd, *J* = 9.0, 0.5 Hz, 1H), 6.84-6.87 (m, 1H), 6.92 (dd, *J* = 5.1, 3.4 Hz, 1H), 7.13 (dd, *J* = 5.1, 1.2 Hz, 1H), 7.28-7.37 (m, 5H), 8.06 (dd, *J* = 9.0, 2.4 Hz, 1H), 8.83 (dd, *J* = 2.4, 0.5 Hz, 1H); ^{13}C NMR (100 MHz, CDCl₃) δ ppm 25.5, 35.2, 41.1, 44.1, 44.6, 45.0, 63.8, 69.3, 69.4, 70.8, 73.3, 105.1, 115.3, 123.5, 124.8, 126.9, 127.6, 127.7, 128.3, 138.2, 138.8, 143.6, 151.1, 160.3, 165.7, 170.4; LCMS r.t. 2.42 min, found 524.4 [M+H]⁺; IR (cm⁻¹) 2855 (br. w), 1704 (m), 1598 (s), 1503 (m), 1418 (m), 1228 (s); Purity 92% (LCMS).

*N-(4-Phenylbutyl)-6-(4-(3-(thiophen-2-yl)propanoyl)piperazin-1-yl)nicotinamide (**191**)*
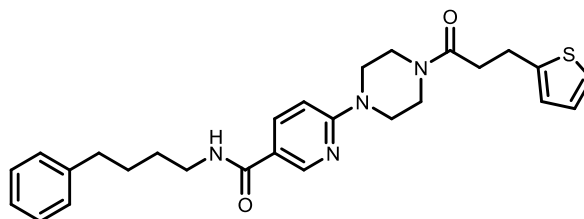
A solution of compound **188** (0.10 g, 0.3 mmol), DMAP (4 mg, 10 mol%), EDC hydrochloride (86 mg, 0.4 mmol) and 4-phenylbutylamine (0.06 mL, 0.4 mmol) in DMF (1.00 mL) was stirred under nitrogen overnight. The reaction mixture was evaporated *in vacuo*, then diluted with DCM and water. The organic phase was purified by flash column chromatography (70-100% EtOAc/40-60 petrol ether) to yield the product **191** as a white solid (21 mg, 0.04 mmol, 14%).

^{1}H NMR (400 MHz, CDCl$_3$) δ ppm 1.60-1.82 (m, 6H), 2.66 (t, *J* = 6.9 Hz, 2H), 2.73 (t, *J* = 7.6 Hz, 2H), 3.24 (t, *J* = 7.6 Hz, 2H), 3.41-3.49 (m 2H), 3.50-3.56 (m, 2H), 3.62-3.68 (m, 2H), 3.72-3.80 (m, 2H), 6.05 (t, *J* = 5.7 Hz, 1H), 6.60 (d, *J* = 8.9 Hz, 1H), 6.85 (dd, *J* = 3.4, 0.8 Hz, 1H), 6.92 (dd, *J* = 5.1, 3.4 Hz, 1H), 7.13 (dd, *J* = 5.1, 1.2 Hz, 1H), 7.15-7.22 (m, 4H), 7.28-7.32 (m, 1H), 7.92 (dd, *J* = 8.9, 2.5 Hz, 1H), 8.55 (d, *J* = 2.5 Hz, 1H); ^{13}C NMR (100 MHz, CDCl$_3$) δ ppm 25.5, 28.7, 29.3, 25.2, 35.5, 39.7, 41.1, 44.3, 44.7, 45.0, 105.7, 119.7, 123.5, 124.8, 125.8, 126.9, 128.3, 128.4, 136.9, 142.0, 143.6, 147.1, 159.8, 165.8, 170.3; LCMS r.t. 2.36 min, found 477.4 [M+H]$^+$; HRMS calc C$_{27}$H$_{33}$N$_4$O$_2$S 477.2319, found [M+H]$^+$ 477.2311; TLC r.f. 0.51 (neat EtOAc); IR (cm^{-1}) 3320 (w), 2929 (w), 2856 (w), 1620 (s), 1595 (s), 1539 (m), 1491 (m), 1435 (s), 1329 (m), 1296 (m), 1248 (s), 1229 (s); Purity >98% (LCMS).

Jeffamine ED-900 linked molecule (**193**)

$$x + z \cong 6$$
$$y \cong 12.5$$
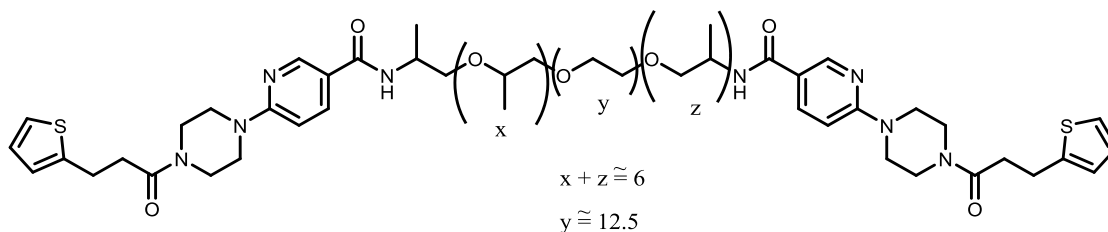
Compound **188** (0.50 g, 1.5 mmol) and COMU (0.62 g, 1.5 mmol) were dissolved in DMF (10 mL) with DIPEA (0.51 mL, 2.9 mmol) under inert atmosphere, before Jeffamine ED-900 (0.41 mL, 0.5 mmol) was added. The reaction was stirred overnight before the solvent was evaporated and the residue purified by flash column chromatography (10-30% EtOAc/40-60 petrol ether, then 10% MeOH/DCM) to yield the product **193** as an orange oil (0.631 g, 0.4 mmol, 83%).

^{1}H NMR (400 MHz, CDCl$_3$) δ ppm 1.03-1.15 (m, 5H), 1.20-1.34 (m, 12H), 1.99-2.06 (m, 5H), 2.67-2.75 (m, 4H), 2.79-2.85 (s, 2H), 3.17-3.26 (m, 6H), 3.30-3.83 (m, 98H), 4.10 (q, *J* = 7.2 Hz, 3H), 4.22-4.40 (m, 2H), 6.60 (d, *J* = 9.1 Hz, 2H), 6.83 (dd, *J* = 3.4, 0.9 Hz, 2H), 6.90 (dd, *J* = 5.1, 3.4 Hz, 2H), 7.11 (dd, *J* = 5.1, 1.1 Hz, 2H), 7.91-8.00 (m, 2H), 8.61 (d, *J* = 2.4 Hz, 2H); ^{13}C NMR (125 MHz, CDCl$_3$) δ ppm 16.1, 18.8, 19.5, 19.6, 19.7, 23.0, 27.4, 37.1, 40.3, 43.1, 46.4, 46.6, 47.0, 47.2, 47.6, 47.7, 49.2, 62.3, 68.6, 72.1, 72.3, 72.4, 72.5, 74.1, 74.2, 76.3, 76.9, 77.1, 77.4, 77.9, 107.5, 107.6, 121.6, 121.7, 125.4, 126.8, 128.8, 138.8, 138.9, 145.5, 149.6, 149.8, 161.7, 167.5, 172.3, 173.1; LCMS r.t. 3.55 min, found mass distribution at m/z 1595 (ESMS$^-$); IR (cm^{-1}) 2869 (m), 1636 (m), 1600 (s), 1494 (m), 1444 (m), 1234 (m).

There was significant overlap in the ^{13}C NMR where not all peaks for the Jeffamine could be distinguished.

6.0 Bibliography

1. World Health Organisation. *Global Tuberculosis Report 2016;* World Health Organisation: Geneva, 2016.

2. Godreuil, S.; Tazi, L.; Banuls, A.-L. Pulmonary tuberculosis and mycobacterium tuberculosis: modern molecular epidemiology and perspectives. In *Encyclopedia of infectious diseases: modern methodologies;* Tibayrenc, M., Ed.; John Wiley: Hoboken, NJ, 2007; Chapter 1, pp 1-27.

3. Vale, N.; Gomes, P.; Santos, H. A. Metabolism of the antituberculosis drug ethionamide. *Curr. Drug Metab.* **2013,** *14* (1), 151-158.

4. Grange, J. M.; Zumla, A. I. Tuberculosis. In *Manson's tropical diseases,* 22nd ed.; Cook, G. C., Zumla, A. I., Eds.; Saunders Elsevier: China, 2009; Chapter 56, pp 983-1038.

5. Sidders, B.; Stoker, N. G. Mycobacteria: biology. In *Encyclopedia of life sciences;* John Wiley: Chinchester, U.K., 2002.

6. Leão, S. C.; Portaels, F. History. In *Tuberculosis 2007: from basic science to patient care,* 1st ed.; Palomino, J. C., Leão, S. C., Ritaero, V., Eds.; TuberculosisTextbook.com, 2007; Chapter 1, pp 25-52.

7. Wilks, D.; Farrington, M.; Rubenstein, D. Mycobacteria and mycobacterial infections. In *The infectious diseases manual,* 2nd ed.; Blackwell Science: Oxford, U.K., 2003; Chapter 4, pp 37-48.

8. Gillespie, S. H.; Murphy, M. E. Antimycobacterial drugs. In *eLS;* John Wiley: Chinchester, U.K., 2011.

9. Dartois, V.; Leong, F. J.; Dick, T. Tuberculosis drug discovery: issues, gaps and the way forward. In *Antiparasitic and antibacterial drug discovery: from molecular targets to drug candidates;* Selzer, P. M., Ed.; Wiley VCH: Weinheim, Germany, 2009; Chapter 21, pp 415-440.

10. Loraine, J. *Studies into the role of peptidoglycan in mycobacterial dormancy and resuscitation;* Ph.D. thesis; The University of Leicester: Leicester, 2013.

11. Hopewell, P. C.; Jasmer, R. M. Overview of clinical tuberculosis. In *Tuberculosis and the tubercle bacillus;* Cole, S. T., Eisenach, K. D., McMurray, D. N., Jacobs Jr, W. R., Eds.; ASM: Washington, DC, 2005; Chapter 2, pp 15-31.

12. Herrmann, J. L.; Lagrange, P. H. Molecular or immunological tools for efficient control of tuberculosis. In *Tuberculosis and the tubercle bacillus;* Cole, S. T., Eisenach, K. D., McMurray, D. N., Jacobs Jr, W. R., Eds.; ASM: Washington, DC, 2005; Chapter 5, pp 75-86.

13. Schraufnagel, D. E. Tuberculosis. In *Breathing in America: diseases, progress, and hope;* Schraufnagel, D. E., Ed.; The American Thoracic Society: New York, 2010; Chapter 24, pp 249-258.

14. Wilder-Smith, E. P. Mycobacterium tuberculosis. In *International neurology;* Lisak, R. P., Truong, D. D., Carroll, W. M., Bhidayasiri, R., Eds.; Blackwell: Oxford, U.K., 2009; Chapter 71, pp 258-260.

15. Hernández-Pando, R.; Chancón-Salinas, R.; Serafin-López, J.; Estrada, I. Immunology, pathogenesis, virulence. In *Tuberculosis 2007: from basic science to patient care;* Palomino, J. C., Leão, S. C., Ritaero, V., Eds.; TuberculosisTextbook.com, 2007; Chapter 5, pp 157-206.

16. Tatum, N. J.; Villemangne, B.; Willand, N.; Deprez, B.; Liebeschuetz, J. W.; Baulard, A. R.; Pohl, E. Structural and docking stucies of potent ethionamide boosters. *Acta Crystallogr., Sect. C: Cryst. Struct. Commun.* **2013,** *69* (11), 1243-1250.

17. da Silva, P. A.; Ainsa, J. A. Drugs and drug interactions. In *Tuberculosis 2007: from basic science to patient care;* Palomino, J. C., Leão, S. C., Ritaero, V., Eds.; TuberculosisTextbook.com, 2007; Chapter 18, pp 593-634.

18. Sala, C.; Hartkoorn, R. C. Tuberculosis drugs: new candidates and how to find more. *Future Microbiol.* **2011,** *6* (6), 617-633.

19. Espinal, M. A.; Salfinger, M. Global impact of multidrug resistance. In *Tuberculosis and the tubercle bacillus;* Cole, S. T., Eisenach, K. D., McMurray, D. N., Jacobs Jr, W. R., Eds.; ASM: Washington, DC, 2005; Chapter 7, pp 101-114.

20. Zhang, Y.; Vilcheze, C.; Jacobs Jr, W. R. Mechanisms of drug resistance in mycobacterium tuberculosis. In *Tuberculosis and the tubercle bacillus;* Cole, S. T., Eisenach, K. D., McMurray, D. N., Jacobs Jr, W. R., Eds.; ASM: Washington, DC, 2005; Chapter 8, pp 115-140.

21. Leiba, J.; Carrere-Kremer, S.; Blondiaux, N.; Dimala, M. M.; Wohlkönig, A.; Baulard, A.; Kremer, L.; Molle, V. The mycobacterium tuberculosis transcriptional repressor EthR is negatively regulated by serine/threonine phosphorylation. *Biochem. Biophys. Res. Commun.* **2014,** *446* (4), 1132-1138.

22. Tatum, N. J. *Crystallographic studies for structure-based drug design;* M.A. thesis; University of Durham: Durham, 2012.

23. Flipo, M.; Desroses, M.; Lecat-Guillet, N.; Dirie, B.; Carette, X.; Leroux, F.; Piveteau, C.; Demirkaya, F.; Lens, Z.; Rucktooa, P.; Villeret, V.; Christophe, T.; Jeon, J. K.; Locht, C.; Brodin, P.; Deprez, B.; Baulard, A. R.; Willand, N. Ethionamide boosters: synthesis, biological activity, and structure-activity relationships of a series of 1,2,4-oxadiazole EthR inhibitors. *J. Med. Chem.* **2011,** *54* (8), 2994-3010.

24. Draper, P.; Daffe, M. The cell envelope of mycobacterium tuberculosis with special reference to the capsule and outer permeability barrier. In *Tuberculosis and the tubercle bacillus;* Cole, S. T., Eisenach, K. D., McMurray, D. N., Jacobs, J. W. R., Eds.; ASM: Washington, DC, 2005; Chapter 17, pp 261-273.

25. Grange, J. M. Mycobacterium tuberculosis - the organism. In *Clinical tuberculosis,* 5th ed.; Davies, P. D. O., Gordon, S. B., Davies, G., Eds.; CRC: London, 2014; Chapter 3, pp 39-54.

26. Mahapatra, S.; Basu, J.; Brennan, P. J.; Crick, D. C. Structure, biosynthesis, and genetics of the mycolic acid-arabinogalactan-peptidoglycan complex. In *Tuberculosis and the tubercle bacillus;* Cole, S. T., Eisenach, K. D., McMurray, D. N., Jacobs Jr, W. R., Eds.; ASM: Washington, DC, 2005; Chapter 18, pp 275-285.

27. Takayama, K.; Wang, C.; Besra, G. S. Pathway to synthesis and processing of mycolic acids in mycobacterium tuberculosis. *Clin. Microbiol. Rev.* **2005,** *18* (1), 81-101.

28. Bhatt, A.; Molle, V.; Besra, G. S.; Jacobs Jr, W. R.; Kremer, L. The mycobacterium tuberculosis FAS-II condensing enzymes: their role in mycolic acid biosynthesis, acid-fastness, pathogenesis and in future drug development. *Mol. Microbiol.* **2007,** *64* (6), 1442-1454.

29. DeBarber, A. E.; Mdluli, K.; Bosman, M.; Bekker, L.-G.; Barry, C. E. Ethionamide activation and sensitivity in multidrug-resistant mycobacterium tuberculosis. *Proc. Natl. Acad. Sci. U. S. A.* **2000,** *97* (17), 9677-9682.

30. Barrera, L. The basics of clinical bacteriology. In *Tuberculosis 2007: from basic science to patient care;* Palomino, J. C., Leão, S. C., Ritaero, V., Eds.; TuberculosisTextbook.com, 2007; Chapter 3, pp 93-112.

31. Kremer, L.; Besra, G. S. A waxy tale, by mycobacterium tuberculosis. In *Tuberculosis and the tubercle bacillus;* Cole, S. T., Eisenach, K. D., McMurray, D. N., Jacobs, J. W. R., Eds.; ASM: Washington, DC, 2005; Chapter 19, pp 287-305.

32. Frenois, F.; Baulard, A. R.; Villeret, V. Insights into mechanisms of induction and ligands recognition in the transcriptional repressor EthR from mycobacterium tuberculosis. *Tuberculosis (Oxford, U. K.)* **2006,** *86* (2), 110-114.

33. Villemagne, B.; Flipo, M.; Blondiaux, N.; Crauste, C.; Malaquin, S.; Leroux, F.; Piveteau, C.; Villeret, V.; Brodin, P.; Villoutreix, B. O.; Sperandio, O.; Soror, S. H.; Wohlkonig, A.; Wintjens, R.; Deprez, B.; Baulard, A. R.; Willand, N. Ligand efficiency driven design of new inhibitors of mycobacterium tuberculosis transcriptional repressor EthR using fragment growing, merging and linking approaches. *J. Med. Chem.* **2014,** *57* (11), 4876–4888.

34. Cuthbertson, L.; Nodwell, J. R. The TetR family of regulators. *Microbiol. Mol. Biol. Rev.* **2005,** *77* (3), 440-475.

35. Dover, L. G.; Corsino, P. E.; Daniels, I. R.; Cocklin, S. L.; Tatituri, V.; Besra, G. S.; Fütterer, K. Crystal structure of the TetR/CamR family repressor mycobacterium tuberculosis EthR implicated in ethionamide resistance. *J. Mol. Biol.* **2004,** *340* (5), 1095-1105.

36. Ang, M. L. T.; Siti, Z. Z. R.; Shui, G.; Dianiskova, P.; Madacki, J.; Lin, W.; Koh, V. H. Q.; Gomez, J. M. M.; Sudarkodi, S.; Bendt, A.; Wenk, M.; Mikusova, K.; Kordulakova, J.; Pethe, K.; Alonso, S. An ethA-ethR-deficient mycobacterium bovis BCG mutant displays increased adherence to mammalian cells and greater persistence in vivo, which correlate with altered mycolic acid composition. *Infect. Immun.* **2014,** *82* (5), 1850-1859.

37. Ramos, J. L.; Martinez-Bueno, M.; Molina-Henares, A. J.; Teran, W.; Watanabe, K.; Zhang, X.; Gallegos, M. T.; Brennan, R.; Tobes, R. The TetR family of transcriptional repressors. *Microbiol. Mol. Biol. Rev.* **2005,** *69* (2), 326-356.

38. Engohang-Ndong, J.; Baillat, D.; Aumercier, M.; Bellefontaine, F.; Besra, G. S.; Locht, C.; Baulard, A. R. EthR, a repressor of the TetR/CamR family implicated in ethionamide resistance in mycobacteria, octamerizes cooperatively on its operator. *Mol. Microbiol.*

2004, *51* (4), 175-188.

39. Surade, S.; Ty, N.; Hengrung, N.; Lechartier, B.; Cole, S. T.; Abell, C.; Blundell, T. L. A structure-guided fragment-based approach for the discovery of allosteric inhibitors targeting the lipophilic binding site of transcription factor EthR. *Biochem J.* **2014,** *458* (2), 387-394.

40. Chan, D. S.-H.; Seetoh, W.-G.; McConnell, B. N.; Matak-Vinkovic, D.; Thomas, S. E.; Mendes, V.; Blaszczyk, M.; Coyne, A. G.; Blundell, T. L.; Abell, C. Structural insights intothe EthR-DNA interaction using native mass spectrometry. *Chem. Commun.* **2017,** *53* (25), 3527-3530.

41. Baulard, A. R.; Betts, J. C.; Engohang-Ndong, J.; Quan, S.; McAdam, R. A.; Brennan, P. J.; Locht, C.; Besra, G. S. Activation of the pro-drug ethionamide is regulated in mycobacteria. *J. Biol. Chem.* **2000,** *275* (36), 28326-28331.

42. Flipo, M.; Desroses, M.; Lecat-Guillet, N.; Villemagne, B.; Blondiaux, N.; Leroux, F.; Piveteau, C.; Mathys, V.; Flament, M.-P.; Siepmann, J.; Villeret, V.; Wohlkönig, A.; Wintjens, R.; Soror, S. H.; Christope, T.; Jeon, H. K.; Locht, C.; Brodin, P.; Deprez, B.; Baulard, A. R.; Willand, N. Ethionamide boosters. 2. combining bioisosteric replacement and structure-based drug design to solve pharmacokinetic issues in a series of potent 1,2,4-oxadiazole EthR inhibitors. *J. Med. Chem.* **2012,** *55* (1), 68-83.

43. Frenois, F.; Engohang-Ndong, J.; Locht, C.; Baulard, A. R.; Villeret, V. Structure of EthR in a ligand bound conformation reveals therapeutic perspectives against tuberculosis. *Mol. Cell* **2004,** *16* (2), 301-307.

44. Willand, N.; Dirie, B.; Carette, X.; Bifani, P.; Singhal, A.; Desroses, M.; Leroux, F.; Willery, E.; Mathys, V.; Deprez-Poulain, R.; Delcroix, G.; Frenois, F.; Aumercier, M.; Locht, C.; Villeret, V.; Deprez, B.; Baulard, A. R. Synthetic EthR inhibitors boost antituberculous activity of ethionamide. *Nat. Med.* **2009,** *15* (5), 537-544.

45. Schumacher, M. A.; Miller, M. C.; Grkovic, S.; Brown, M. H.; Skurray, R. A.; Brennan, R. G. Structural basis for cooperative DNA binding by two dimers of the multidrug-binding protein QacR. *EMBO J.* **2002,** *21* (5), 1210–1218.

46. Ma, R.; Wang, P.; Wu, J.; Ruan, K. Process of fragment-based lead discovery - a perspective from NMR. *Molecules* **2016,** *21* (7), 854-867.

47. Ghosh, A. K.; Gegmma, S. *Structure-based design of drugs and other bioactive molecules: tools and strategies;* Wiley-VCH: Weinheim, Germany, 2014.

48. Burley, S. K.; Hirst, G.; Sprengeler, P.; Reich, S. Fragment-based structure-guided drug discovery: strategy, process and lessons from human protein kinases. In *Drug design: structure- and ligand-based approaches;* Merz, J. K. M., Ringe, D., Reynolds, C. H., Eds.; Cambridge University: Cambridge, U.K., 2010; Chapter 3, pp 30-40.

49. Scott, D. E.; Coyne, A. G.; Hudson, S. A.; Abell, C. Fragment-based approaches in drug discovery and chemical biology. *Biochemistry* **2012,** *51* (25), 4990-5003.

50. Giannetti, A. M.; Gilbert, H. N.; Huddler, D. P.; Reiter, M.; Strande, C.; Pitts, K. E.; Bravo, B. J. Getting the most value from your screens: advances in hardware, software, and methodologies to enhance surface plasmon resonance based fragment screening and hit-to-lead support. In *Fragment based drug discovery;* Howard, S., Abell, C., Eds.; The Royal Society of Chemistry: Cambridge, U.K., 2015; Chapter 2, pp 19-48.

51. Erlanson, D. A.; Fesik, S. W.; Hubbard, R. E.; Jahnke, W.; Jhoti, H. Twenty years on: the impact of fragments on drug discovery. *Nat. Rev. Drug Discovery* **2016,** *15* (9), 605-619.

52. Davis, B. J.; Erlanson, D. A. Learning from our mistakes: the 'unknown knowns' in fragment screening. *Bioorg. Med. Chem. Lett.* **2013,** *23* (10), 2844-2852.

53. Renaud, J.-P.; Chung, C.-w.; Danielson, U. H.; Egner, U.; Hennig, M.; Hubbard, R. E.; Nar, H. Biophysics in drug discovery: impact, challenges and opportunities. *Nat. Rev. Drug Discovery* **2016,** *15* (10), 679-698.

54. Scott, D. E.; Bayly, A. R.; Abell, C.; Skidmore, J. Small molecules, big targets: drug discovery faces the protein-protein interaction challenge. *Nat. Rev. Drug Discovery* **2016,** *15* (8), 533-550.

55. Abell, C.; Dagostin, C. Different flavours of fragments. In *Fragment-based drug discovery;* Howard, S., Abell, C., Eds.; The Royal Society of Chemistry: Cambridge, U.K., 2015; Chapter 1, pp 1-18.

56. Howard, S.; Abell, C. Foreword. In *Fragment-based drug discovery;* Howard, S., Abell, C., Eds.; The Royal Society of Chemistry: Cambridge, U.K., 2015; pp ix-ix.

57. Erlanson, D. A. Fragment-based lead discovery: a chemical update. *Curr. Opin. Biotechnol.* **2006,** *17* (6), 643-652.

58. Hajduk, P. J.; Greer, J. A decade of fragment-based drug design: strategic advances and lessons learned. *Nat. Rev. Drug Discovery* **2007,** *6* (3), 211-219.

59. Albert, J. S. Fragment-based lead discovery. In *Lead generation approaches in drug discovery;* Rankovic, Z., Morphy, R., Eds.; John Wiley: Hoboken, NJ, 2010; Chapter 4, pp 105-140.

60. Heakal, Y.; Kester, M.; Savage, S. Vemurafenib (PLX4032): an orally available inhibitor of mutated BRAF for the treatment of metastatic melanoma. *Ann. Pharmacother.* **2011,** *45* (11), 1399-1405.

61. de Kloe, G. E.; Bailey, D.; Leurs, R.; de Esch, I. J. P. Transforming fragments into candidates: small becomes big in medicinal chemistry. *Drug Discovery Today* **2009,** *14* (13/14), 630-646.

62. Tsai, J.; Lee, J. T.; Wang, W.; Zhang, J.; Cho, H.; Mamo, S.; Bremer, R.; Gillette, S.; Kong, J.; Haass, N. K.; Sproesser, K.; Li, L.; Smalley, K. S. M.; Fong, D.; Zhu, Y.-L.; Marimuthu, A.; Nguyen, H.; Lam, B.; Liu, J.; Cheung, I.; RIce, J.; Suzuki, Y.; Luu, C.; Settachatgul, C.; Shellooe, R.; Cantwell, J.; Kim, S.-H.; Schlessinger, J.; Zhang, K. Y. J.; West, B. L.; Powell, B.; Habets, G.; Zhang, C.; Prabha, I. N.; Hirth, P.; Artis, D. R.; Herlyn, M.; Bollag, G. Discovery of a selective inhibitor of oncogenic B-Raf kinase with potent antimelanoma activity. *Proc. Natl. Acad. Sci. U. S. A.* **2008,** *105* (8), 3041-3046.

63. Bollag, G.; Hirth, P.; Tsai, J.; Zhang, J.; Ibrahim, P. N.; Cho, H.; Spevak, W.; Zhang, C.; Zhang, Y.; Habets, G.; Burton, E. A.; Wong, B.; Tsang, G.; West, B. L.; Powell, B.; Shellooe, R.; Marimuthu, A.; Nguyen, H.; Zhang, K. Y. J.; Artis, D. R.; Schlessinger, J.; Su, F.; Higgins, B.; Iyver, R.; D'Andrea, K.; Koehler, A.; Stumm, M.; Lin, P. S.; Lee, R. J.; Grippo, J.; Puzanov, I.; Kim, K. B.; Ribas, A.; McArthur, G. A.; Sosman, J. A.; Chapman, P. B.; Flaherty, K. T.; Xu, X.; Nathanson, K. L.; Nolop, K. Clinical efficacy of a RAF inhibitor needs broad target blockade in BRAF-mutant melanoma. *Nature* **2010,** *467* (7315), 596-599.

64. Ibrahim, P.; Zhang, J.; Zhang, C.; Tsai, J.; Habets, G.; Bollag, G. Discovery and development of vemurafenib: first-in-class inhibitor of mutant BRAF for the treatment of cancer. In *Medicinal chemistry approaches to personalized medicine;* Lackey, L., Roth, B. D., Eds.; Wiley-

VCH: Weinheim, Germany, 2013; Chapter 4, pp 91-100.

65. US Food and Drug Administration. US Food and Drug Administration Website. http://www.fda.gov/NewsEvents/Newsroom/PressAnnouncements/ucm495253.htm (accessed January 21, 2018).

66. Lipinski, C. A.; Lombardo, F.; Dominy, B. W.; Feeney, P. J. Experimental and computational approaches to estimate solubility and permeability in drug discovery and development settings. *Adv. Drug Delivery Rev.* **1997,** *23* (1-3), 3-25.

67. US Food and Drug Administration. Highlights of Prescribing Information (Venclexta), 2016. FDA   Website. http://www.accessdata.fda.gov/drugsatfda_docs/label/2016/208573s000lbl.pdf (accessed January 21, 2018).

68. Carmichael, J. Astex Pharmaceuticals celebrates as cancer drug receives marketing approval in Europe, 2017. Astex Pharmaceuticals website. http://astx.com/astex-pharmaceuticals-celebrates-as-cancer-drug-receives-marketing-approval-in-europe/ (accessed January 23, 2018).

69. Lepre, C. A.; Connolly, P. J.; Moore, J. M. NMR in fragment-based drug discovery. In *Drug design: structure- and ligand-based applications;* Merz, J. K. M., Ringe, D., Reynolds, C. H., Eds.; Cambridge University: Cambridge, U.K., 2010; Chapter 4, pp 41-60.

70. Lachance, H.; Wetzel, S.; Waldmann, H. Role of natural products in drug discovery. In *Lead generation approaches in drug discovery;* Rankovic, Z., Morphy, R., Eds.; John Wiley: Hoboken, NJ, 2010; Chapter 7, pp 187-229.

71. Drew, K. L. M.; Baiman, H.; Khwaounjoo, P.; Yu, B.; Reynisson, J. Size estimation of chemical space: how big is it? *J. Pharm. Pharmacol.* **2012,** *64* (4), 490-495.

72. Polishchuk, P. G.; Madzhidov, T. I.; Varnek, A. Estimation of the size of drug-like chemical space based on GDB-17 data. *J. Comput.—Aided Mol. Des.* **2013,** *27* (8), 675-679.

73. Bienstock, R. J. Overview: fragment-based drug design. In *Library design, search methods, and applications of fragment-based drug design;* Bienstock, R. J., Ed.; American Chemical Society: Washington, DC, 2011; Chapter 1, pp 1-26.

74. Chilingaryan, Z.; Yin, Z.; Oakley, A. J. Fragment-based screening by protein crystallography: successes and pitfalls. *Int. J. Mol. Sci.* **2012,** *13* (10), 12857-12879.

75. Joseph-McCarthy, D.; Campbell, A. J.; Kern, G.; Moustakas, D. Fragment-based lead discovery and design. *J. Chem. Inf. Model.* **2014,** *54* (3), 693-704.

76. Hudson, S. A.; Surade, S.; Coyne, A. G.; McLean, K. J.; Leys, D.; Munro, A. W.; Abell, C. Overcoming the limitations of fragment merging: rescuing a strained merged fragment series targeting mycobacterium tuberculosis CYP121. *ChemMedChem* **2013,** *8* (9), 1451-1456.

77. Hudson, S. A.; McLean, K. J.; Surade, S.; Yang, Y.-Q.; Leys, D.; Ciulli, A.; Munro, A. W.; Abell, C. Application of fragment screening and merging to the discovery of inhibitors of the mycobacterium tuberculosis cytochrome P450 CYP121. *Angew. Chem., Int. Ed.* **2012,** *51* (37), 9311-9316.

78. Schultz, J. Practical aspects of using NMR in fragment-based screening. In *Fragment-based drug discovery: a practical approach;* Zartler, E. R., Shapiro, M. J., Eds.; John Wiley: Chinchester, U.K., 2008; Chapter 4, pp 63-98.

79. Kavanagh, M. E.; Coyne, A. G.; McLean, K. J.; James, G. G.; Levy, C. W.; Marino, L. B.; de Carvalho, L. P. S.; Chan, D. S. H.; Hudson, S. A.; Surade, S.; Leys, D.; Munro, A. W.; Abell, C. Fragment-based approaches to the development of mycobacterium tuberculosis CYP121 inhibitors. *J. Med. Chem.* **2016,** *59* (7), 3272-3302.

80. Harner, M. J.; Frank, A. O.; Fesik, S. W. Fragment-based drug discovery using NMR spectroscopy. *J. Biomol. NMR* **2013,** *56* (2), 65-75.

81. Rees, D. C.; Congreve, M.; Murray, C. W.; Carr, R. Fragment-based lead discovery. *Nat. Rev. Drug Discovery* **2004,** *3* (8), 660-672.

82. Murray, C. W.; Verdonk, M. L. Entropic consequences of linking ligands. In *Fragment-based approaches in drug discovery;* Jahnke, W., Erlanson, D. A., Eds.; Wiley-VCH: Weinheim, Germany, 2006; Chapter 3, pp 55-66.

83. Pelz, N. F.; Bian, Z.; Zhao, B.; Shaw, S.; Tarr, J. C.; Belmar, J.; Gregg, C.; Camper, D. V.; Goodwin, C. M.; Arnold, A. L.; Sensintaffar, J. L.; Friberg, A.; Rossanese, O. W.; Lee, T.; Olejniczak, E. T.; Fesik, S. W. Discovery of 2-indole-acylsulfonamide myeloid cell leukemia 1

(Mcl-1) inhibitors using fragment-based methods. *J. Med. Chem.* **2016,** *59* (5), 2054-2066.

84. Wyatt, P. G.; Woodhead, A. J.; Berdini, V.; Boulstridge, J. A.; Carr, M. G.; Cross, D. M.; Davis, D. J.; Devine, L. A.; Early, T. R.; Feltell, R. E.; Lewis, E. J.; McMcnamin, R. L.; Navarro, E. F.; O'Brian, M. A.; O'Reilly, M.; Reule, M.; Saxty, G.; Seavers, L. C. A.; Smith, D.-M.; Squires, M. S.; Trewartha, G.; Walker, M. T.; Woolford, A. J. A. Identification of N-(4-piperidinyl)-4-(2,6-dichlorobenzoylamino)-1H-pyrazole-3-carboxamide (AT7519), a novel cyclin dependant kinase inhibitor using fragment-based X-ray crystallography and structure based drug design. *J. Med. Chem.* **2008,** *51* (16), 4986-4999.

85. Serdyuk, I. N.; Zaccai, N. R.; Zaccai, J. Surface plasmon resonance and interferometry-based biosensors. In *Methods in molecular biophysics: structure, dynamics, function;* Cambridge University: Cambridge, U.K., 2007; Chapter C4, pp 234-246.

86. Sledz, P.; Abell, C.; Ciulli, A. Ligand-observed NMR in fragment-based approaches. In *NMR of biomolecules: towards mechanistic systems biology,* 1st ed.; Bertini, I., McGreevy, K. S., Parigi, G., Eds.; Wiley-VCH: Weinheim, Gerany, 2012; Chapter 15, pp 265-280.

87. Krimm, I. Applications of NMR in fragment-based drug design. In *Fragment-based drug discovery;* Howard, S., Abell, C., Eds.; The Royal Society of Chemistry: Cambridge, U.K., 2015; Chapter 3, pp 49-72.

88. Mashalidis, E. H.; Sledz, P.; Lang, S.; Abell, C. A three-stage biophysical screening cascade for fragment-based drug discovery. *Nat. Protoc.* **2013,** *8* (11), 2309-2324.

89. Petsko, G. A.; Ringe, D. X-ray crystallography in the service of structure-based drug design. In *Drug design: structure- and ligand-based approaches;* Merz, J. K. M., Ringe, D., Reynolds, C. H., Eds.; Cambridge University: Cambridge, U.K., 2010; Chapter 2, pp 17-29.

90. Marcou, G.; Rognan, D. Optimizing fragment and scaffold docking by use of molecular interaction fingerprints. *J. Chem. Inf. Model.* **2007,** *47* (1), 195-207.

91. Meng, X.-Y.; Zhang, H.-X.; Mezei, M.; Cui, M. Molecular docking: a powerful approach for structure-based drug discovery. *Curr. Comput.—Aided Drug Des.* **2011,** *7* (2), 146-157.

92. Serdyuk, I. N.; Zaccai, N. R.; Zaccai, J. Isothermal titration calorimetry. In *Methods in molecular biophysics: structure, dynamics, function;* Cambridge University: Cambridge, U.K., 2007; Chapter C3, pp 221-233.

93. Thomson, J. A.; Ladbury, J. E. Isothermal titration calorimetry: a tutorial. In *Biocalorimetry 2: applications of calorimetry in the biological sciences;* Ladbury, J. E., Doyle, M. L., Eds.; John Wiley: Chinchester, U.K., 2004; Chapter 2, pp 37-58.

94. Holdgate, G.; Fisher, S.; Ward, W. The application of isothermal titration calorimetry to drug discovery. In *Biocalorimetry 2: applications of calorimetry in the biological sciences;* Ladbury, J. E., Doyle, M. L., Eds.; John Wiley: Chinchester, U.K., 2004; Chapter 3, pp 59-79.

95. Pace, A.; Pierro, P. The new era of 1,2,4-oxadiazoles. *Org. Biomol. Chem.* **2009,** *7* (21), 4337-4348.

96. Boström, J.; Hogner, A.; Llinàs, A.; Wellner, E.; Plowright, A. T. Oxadiazoles in medicinal chemistry. *J. Med. Chem.* **2012,** *55* (5), 1817-1830.

97. Pace, A.; Buscemi, S.; Piccionello, A. P.; Pibiri, I. Recent advances in the chemistry of 1,2,4-oxadiazoles. In *Advances in heterocyclic chemistry;* Scriven, E. F. V., Ramsden, C. A., Eds.; Academic: London, 2015; Chapter 3, Vol. 116, pp 85-136.

98. Joule, J. A.; Mills, K. Heterocycles in medicine. In *Heterocyclic chemistry at a glance,* 2nd ed.; John Wiley: Chinchester, U.K., 2012; Chapter 18, pp 167-179.

99. Li, J. J. Introduction. In *Heterocyclic chemistry in drug discovery;* John Wiley: Hoboken, NJ, 2013; Chapter 1.

100. Goswami, R.; Wohlfahrt, G.; Mukherjee, S.; Ghadiyaram, C.; Nagaraj, J.; Satyam, L. K.; Subbarao, K.; Gopinath, S.; Krishnamurthy, N. R.; Subramanya, H. S.; Ramachandra, M. Discovery of O-(3-carbamimidoylphenyl)-L-serine amides as matriptase inhibitors using a fragment-linking approach. *Bioorg. Med. Chem. Lett.* **2015,** *25* (3), 616-620.

101. Huguet, F.; Melet, A.; Alves de Sousa, R.; Lieutaud, A.; Chevalier, J.; Maigre, L.; Deschamps, P.; Tomas, A.; Leulloit, N.; Pages, J.-M.; Artaud, I. Hydroxamic acids as potent inhibitors of Fe(II) and Mn(II) E. coli methionine aminopeptidase: biological activities and X-ray structures of oxazole hydroxamate-EcMetAP-Mn complexes. *ChemMedChem* **2012,** *7* (6), 1020-1030.

102. Curti, C.; Laget, M.; Carle, A. O.; Gellis, A.; Vanelle, P. Rapid synthesis of sulfone derivatives as potential anti-infectious agents. *Eur. J. Med. Chem.* **2007,** *42* (6), 880-884.

103. Dick, G. R.; Knapp, D. M.; Gillis, E. P.; Burke, M. D. General method for synthesis of 2-heterocyclic N-methyliminodiacetic acid boronates. *Org. Lett.* **2010,** *12* (10), 2314-2317.

104. Dick, G. R.; Woerly, E. M.; Burke, M. D. A general solution for the 2-pyridyl problem. *Angew. Chem., Int. Ed.* **2012,** *51* (11), 2667-2672.

105. Knapp, D. M.; Giles, E. P.; Burke, M. D. A general solution for unstable boronic acids: slow-release cross-coupling from air-stable MIDA boronates. *J. Am. Chem. Soc.* **2009,** *131* (20), 6961-6963.

106. Baumann, M.; Baxendale, I. R. An overview of the synthetic routes to the best selling drugs containing 6-membered heterocycles. *Beilstein J. Org. Chem.* **2013,** *9,* 2265-2319.

107. Singh, K.; Siddiqui, H. H.; Shakya, P.; Bagga, P.; Kumar, A.; Khalid, M.; Arif, M.; Alok, S. Piperazine - a biologically active scaffold. *Int. J. Pharm. Sci. Res.* **2015,** *6* (10), 4145-4158.

108. Christopher, J. A.; Brown, J.; Dore, A. S.; Errey, J. C.; Koglin, M.; Marshall, F. H.; Myszka, D. G.; Rich, R. L.; Tate, C. G.; Tehan, B.; Warne, T.; Congreve, M. Biophysical fragment screening of the ß1-adrenergic receptor: identification of high affinity arylpiperazine leads using structure-based drug design. *J. Med. Chem.* **2013,** *56* (9), 3446-3455.

109. Mangione, P. P.; Deroo, S.; Ellmerich, S.; Bellotti, V.; Kolstoe, S.; Wood, S. P.; Robinson, C. V.; Smith, M. D.; Tennent, G. A.; Broadbridge, R. J.; Council, C. E.; Thurston, J. R.; Steadman, V. A.; Vong, A. K.; Swain, C. J.; Pepys, M. B.; Taylor, G. W. Bifunctional crosslinking ligands for transthyretin. *Open Biol.* **2015,** *5* (9), 150105.

110. Tanaka, M.; Roberts, J. M.; Seo, H.-S.; Souza, A.; Paulk, J.; Scott, T. G.; DeAngelo, S. L.; Dhe-Paganon, S.; Bradner, J. E. Design and characterization of bivalent BET inhibitors. *Nat. Chem. Biol.* **2016,** *12* (12), 1089-1096.

111. Kakkar, D.; Tiwari, A. K.; Khanna, A.; Datta, A.; Singh, H.; Mishra, A. K. Design, synthesis, and antimycobacterial property of PEG-bis(INH) conjugates. *Chem. Biol. Drug Des.* **2012,** *80* (2), 245-253.

112. Bissantz, C.; Kuhn, B.; Stahl, M. A medicinal chemist's guide to molecular interactions. *J. Med. Chem.* **2010,** *53* (14), 5061-5084.

113. Palomino, J.-C.; Martin, A.; Camacho, M.; Guerra, H.; Swings, J.; Portaels, F. Resazurin microtiter assay plate: simple and inexpensive method for detection of drug resistance in

mycobacterium tuberculosis. *Antimicrob. Agents Chemother.* **2002,** *46* (8), 2720-2722.

114. Kiyoto, T.; Ando, J. Novel heterocyclic compound or salt therof and intermediate therof. Int. Patent WO 2007/138974, 2007.

115. Fyfe, M.; Gardener, L.; King-Underwood, J.; Proctor, M.; Rasamison, C.; Schofield, K.; Thomas, G. H. Heterocyclic derivatives as GPCR receptor agonists. Int. Patent WO 2005/061489 A1, July 7, 2005.

116. Neves Filho, R. A. W.; da Silva-Alves, D. C. B.; dos Anjos, J. V.; Srivastava, R. M. One-step protection free synthesis of 3-aryl-5-hydroxyalkyl-1,2,4-oxadiaxoles as building blocks. *Synth. Commun.* **2013,** *43* (19), 2596-2602.

117. Polanski, J.; Jarzembek, K. Search for new sulfonyl-containing glucophores. *Pure Appl. Chem.* **2002,** *74* (7), 1227-1233.

118. Faucher, A.-M.; White, P. W.; Brochu, C.; Grand-Maitre, C.; Rancourt, J.; Fazal, G. Discovery of small-molecule inhibitors of the ATPase activity of human papillomavirus E1 helicase. *J. Med. Chem.* **2004,** *47* (1), 18-21.

119. Meier, H.; Nicklas, F.; Petermann, R. Conjugated compounds based on vinylthiazole units. *Z. Naturforsch., B: J. Chem. Sci.* **2007,** *62b,* 1525-1529.

120. Tan, Z.; Imae, I.; Komaguchi, K.; Ooyama, Y.; Ohshita, J.; Harima, Y. Effects of π-conjugated side chains on properties and performances of photovoltaic copolymers. *Synth. Met.* **2014,** *187* (1), 30-36.

121. Peng, H.; Cheng, Y.; Ni, N.; Li, M.; Choudhary, G.; Chou, H. T.; Lu, C.-D.; Tai, P. C.; Wang, B. Synthesis and evaluation of new antagonists of bacterial quorum sensing in vibrio harveyi. *ChemMedChem* **2009,** *4* (9), 1457-1468.

122. Rubino, M. T.; Agamennone, M.; Campestre, C.; Fracchiolla, G.; Laghezza, A.; Loiodice, F.; Nuti, E.; Rossello, A.; Tortorella, P. Synthesis, SAR, and biological evaluation of α-sulfonylphosphonic acids as selective matrix metalloproteinase inhibitors. *ChemMedChem* **2009,** *4* (3), 352-362.

123. Stephens, J.; Findlay, J.; Kinsella, G.; Martin, D.; Devine, R.; Velasco-Torrijos, T. Preparation of N-acyl-N'-phenylpiperazine derivatives as sRBP modulators for use in the treatment of

diabetes and obesity. Int. Patent WO 2013060860 A1, May 2, 2013.

124. Sun, C.-Y.; Li, Y.-S.; Shi, A.-L.; Li, Y.-F.; Cao, R.-F.; Ding, H.-W.; Yin, Q.-Q.; Zhang, L.-J.; Zheng, H.-C.; Song, H.-R. Synthesis and antiproliferative activity of novel 4-substituted-phenoxy-benzamide derivatives. *Chin. Chem. Lett.* **2015,** *26* (10), 1307-1310.